HYDRAULICS OF RIVER FLOW UNDER ARCH BRIDGES

001360

JUNE 1964
NO. 11
VOL. I

by

J. W. DELLEUR

Joint Highway Research Project
PURDUE UNIVERSITY
LAFAYETTE INDIANA

HYDRAULICS OF RIVER FLOW UNDER ARCH BRIDGES

TO: K. B. Woods, Director
Joint Highway Research Project

June 19, 1964

FROM: H. L. Michael, Associate Director
Joint Highway Research Project

Project: HPS-R-1 (36)
File: 9-8-2

The Final Report on the project "Hydraulics of River Flow Under Arch Bridges" is attached. The title of the report is the title of the project and it has been prepared by Dr. J. W. Delleur, under whose direction most of the study has been performed.

This project was initiated in April 1958 and will be terminated upon acceptance of this final report by the cooperating agencies. During the six years of the project many monthly progress reports and seven larger progress reports were submitted. The attached report summarizes all the work performed during the entire project period and is in two volumes with Volume II containing only the figures.

This research has provided information on the backwater effects and energy losses of arch bridge constrictions with rigid boundaries. The information provided should be of great value to highway engineers in evaluating the problems associated with arch bridge crossings of streams.

The report is submitted for the record and will also be sent to the Indiana State Highway Commission and the Bureau of Public Roads for their acceptance of this Final Report on this project, subject of course to their review and comments and any subsequent action required.

Respectfully submitted,

Harold L. Michael

Harold L. Michael, Secretary

HLM:bc

Attachment

Copy:

F. L. Ashbaucher
J. R. Cooper
W. L. Dolch
W. H. Goetz
F. F. Havey
F. S. Hill
G. A. Leonards
J. F. McLaughlin
R. D. Miles
R. E. Mills
M. B. Scott
J. V. Smythe
E. J. Yoder

Final Report

HYDRAULICS OF RIVER FLOW UNDER ARCH BRIDGES

Vol. I

by

J. W. Delleur
Professor of Hydraulic Engineering

Joint Highway Research Project

Project: HPS-R-1(36)

File: 9-8-2

Prepared as Part of an Investigation

Conducted by

Joint Highway Research Project
Engineering Experiment Station
Purdue University

in cooperation with

Indiana State Highway Commission

and the

Bureau of Public Roads
U S Department of

Released for Publication

Subject to Change

Purdue University

Not Reviewed by

Indiana State Highway Commission
or the
Bureau of Public Roads

Lafayette, Indiana

June 19, 1964

Digitized by the Internet Archive
in 2011 with funding from
LYRASIS members and Sloan Foundation; Indiana Department of Transportation

http://www.archive.org/details/hydraulicsofrive00dell

TABLE OF CONTENTS

I. PREFACE AND ACKNOWLEDGMENTS

This report completes a general program sponsored by the State Highway Department of Indiana and the U.S. Bureau of Public Roads at Purdue University on the hydraulics of river flow under arch bridges.

The project has been active from April, 1958, to December, 1963. From the beginning to June, 1961, and from September, 1962 to December, 1963, the project was under the direction of Professor J. W. Delleur. From June, 1961, to September, 1963, it was under the direction of Professor G. H. Toebes. Several reports on different phases of the study have been submitted. In 1958, Mr. S. T. Husain[1]* reported his work, "Preliminary Model Investigation of Hydraulic Characteristics of River Flow Under Arch Bridges". This was an investigation in a 12 foot long, 6 inches wide tilting flume with smooth boundaries which led, in 1959, to the building of a 64 foot by 5 foot by 2 foot, all steel tilting flume. The design of the 64 foot flume was undertaken by Mr. H. J. Owen. This, along with the first tests in this flume was described in the report entitled: "Design and Construction of Hydraulic Flume and Backwater Effects of Semi-circular Constrictions in Smooth Rectangular Channel", by H. J. Owen and J. W. Delleur.[2] Mr. A. A. Sooky[3] derived an equation for the discharge through a sharp edged semi-circular constriction for the case of free surface flow through the opening. He also extended Mr. S. T. Husain's preliminary tests in the 6 inch wide flume to include the effect of rough boundaries. The work of Husain, Sooky and Owen was summarized in a report entitled, "Hydraulics of River Flow Under Arch Bridges - A Progress Report".[3]

In 1960 and 1961, Mr. P. F. Biery undertook an investigation of artificial roughness in the 5 foot wide flume and studied single span arch bridge constrictions with free surface flow. The experiment did not include skew, eccentricity or entrance rounding, but tests were made with smooth and rough boundaries. A backwater equation

*Superscripts refer to references in the bibliography.

was obtained together with a bridge design procedure for free surface flow through the opening, and a procedure for indirect discharge calculation from high water marks. The work was summarized in two reports entitled: "Hydraulics of SingleSpan Arch Bridge Constrictions"[4] and "Discussion on Roughness Spacing in Rigid Open Channels"[5] and both authored by P. F. Biery and J. W. Delleur. These reports were later published in the Journal of the Hydraulics Division of the American Society of Civil Engineers.[6]

In 1961 and 1962, Messrs. S. Lippai and T. P. Cheng investigated the free surface geometry due to dual bridges, wing walls, eccentricity, skew and arch segments. No formal report was submitted on the works of Messrs. S. Lippai and T. P. Cheng. A summary of this work was presented in the monthly progress reports prepared by Professor G. H. Toebes.

In 1962 and 1963, O. Eikeri undertook the study of the effect of submergence of arch bridge constrictions on backwater superrelevation. His work was presented in a report entitled "Hydraulics of Submerged Arch Bridges"[8]. The experimental data of Messrs. P. F. Biery, S. Lippai and T. P. Cheng were reanalyzed in the fall of 1963. The necessary computer programs and plots were prepared by M. Mushtaq.

Also in 1962, a program of field verification was undertaken. Messrs. T. P. Cheng and J. T. Strange of the Indiana Flood Control and Water Resources Commission investigated over 100 arch bridge sites and selected 10 field verification sites[9]. Air photographs of 9 of these sites were made by the State Highway Department of Indiana. Topographic maps were prepared from these photographs in the Air-Photo Laboratory at Purdue University under the direction of Professor R. Miles.

The research reported herein was performed in the Hydraulics Laboratory, School of Civil Engineering at Purdue University, under the auspices of the Joint Highway Research Project, Professor K. B. Woods, Director and Professor H. Michael, Associate Director.

The present report summarizes the work done during the entire duration of the project. It includes the following parts: a literature abstract, a theoretical analysis, a description of the experimental procedure used in the testing program, and finally the presentation and analysis of the test data.

Regarding the motivation for studying the hydraulic characteristics of arch bridges, the following question could well be asked: How many arch bridges are there in the entire United States? Although this figure is probably unknown, Indiana alone has about 900 arch bridges, over 100 of these are in Marion County and adjacent counties. This explains the particular interest that has existed in Indiana regarding the hydraulics of arch bridges.

By increasing the backwater upstream from the bridge site, many of these bridge constrictions cause additional flooding during high flow; people and valuable property are endangered. In recent years, the problem of minimizing the backwater effect due to bridge constriction has become increasingly important. The highway engineers are faced with a multisided problem; not only do they have to build bridges to convey a specified traffic volume and are safe with respect to flooding, but they also must find the most economic design possible. It is common knowledge to the highway engineer that a bridge crossing will interfere with the natural flow of the stream and will result in a rise of stage upstream from the bridge and in an increase in velocity through the bridge constriction. The engineers are also aware of alternatives of the inexpensive soil fill compared to a structural span. The optimum design is the shortest span that will not cause damage due to stage increase during serious flood conditions. In order to meet these requirements, exhaustive investigations were undertaken to study the hydraulic characteristics of the water flow through different bridge constrictions.

The other motivation for the study of hydraulics of arch bridges is the indirect determination of flood discharge from high water marks. The existing methods are not applicable to the arch geometry. Due to the large number of arch bridges in Indiana, particularly on small streams, many of which are ungaged, the determination of peak discharge from backwater observation at bridge site would provide a valuable addition to the knowledge of small watershed hydrology.

The scope of the present research is limited to the study of the backwater effects and energy losses through arch bridge constrictions with rigid boundaries. In other words the effects of scour at the bridge site are not considered. This is not an excessive limitation as a correction curve for backwater with scour is available in the literature[10].

BIBLIOGRAPHY OF CHAPTER 1

1. Husain, [illegible] T., "Preliminary Model Investigations of [illegible] Characteristics of River Flow Under Arch Bridges", Masters Thesis, Purdue University, 195[illegible].

2. Owen, H. J. and Delleur, J. W., "Design [illegible] of Hydraulic [illegible] and Backwater Effects of Semi-Circular Constrictions [illegible] Channel", Joint Highway Research Project No. [illegible] [illegible]. Also submitted by H. J. Owen as M.S. Thesis, Purdue University, [illegible].

3. Sooky, A. A., Husain, [illegible] T., Owen, H. J. and Delleur, J. W., "[illegible] River Flow Under Arch Bridges - A Progress Report", Progress Report [illegible] to the Board of the Joint Highway Research Project, May [illegible], 195[illegible], Purdue University, also published in the Proceedings [illegible] No. 100, Purdue Eng. Exp. Station, Lafayette, [illegible] 19[illegible].

4. Biery, P. F., and Delleur, J. W., "Hydraulics of [illegible] Constrictions", Joint Highway Research Project Report No. [illegible], [illegible]. Also submitted by P. F. Biery as M.S. Thesis, Purdue University, 19[illegible].

5. Biery, P. F. and Delleur, J. W., "[illegible] in [illegible] Channels", Joint Highway Research Project [illegible].

6. Biery, P. F. and Delleur, J. W., Discussion of "[illegible] in [illegible] Channels", Journal Hydraulics Division, ASCE, Vol. [illegible], also in Trans. ASCE, 196[illegible], Vol. 12[illegible], Part I, p. 37[illegible].

7. Biery, P. F. and Delleur, J. W., "Hydraulics of [illegible] Bridge Constrictions", Journal Hydraulics Division, ASCE, Vol. [illegible], HY[illegible], [illegible].

8. Eikeri, O. and Delleur, J. W., "Hydraulics of [illegible] Arch Bridges", Joint Highway Research Project, Report No. [illegible], December, [illegible], also submitted by O. Eikeri as M.S. Thesis, Purdue University, 196[illegible].

9. Cheng, T. [illegible] and [illegible], "A Preliminary Field [illegible] Model-Prototype Comparison of Hydraulics of Arch Bridge Constrictions", Indiana [illegible] Control and Water Resources Commission, November, [illegible].

10. Bradley, J. N., "Hydraulics of Bridge Waterways", U. S. Bureau of Public Roads, U.S. Government Printing Office, [illegible], 19[illegible].

II. REVIEW OF LITERATURE

To the author's knowledge there is no previous systematic investigation of the hydraulic characteristics of arch bridges in particular. There is, however an extensive body of literature on the hydraulics of bridge constrictions, on open channel constrictions in general, on culverts and on the fundamental aspects of the mechanics of contracting and expanding streams.

An annotated bibliography covering some of the most recent literature is given below. This bibliography was compiled by the author as part of his activity in the Task Force on Hydraulics of Bridges of the American Society of Civil Engineers.

I. CONSTRICTION AND BACKWATER

BRADLEY, J. N. Use of Backwater in Design of Bridge Waterways. Pub. Roads Vol. 30 No. 10 Oct. 1959. pg. 221-6.

"Investigations carried out by Division of Hydraulic Research Bur. Pub. Roads centered on determination of backwater produced by bridges. Scour at bridge abutments, scour around piers, and methods for alleviating scour; research results, design information derived and application of bridge backwater to waterway design; data presented are based on experimental backwater studies using hydraulic models and field measurements", from Engr. Ind. 1960, pg. 160. For a more detailed discussion see Bradley, "Hydraulics of Bridge Waterways".

BRADLEY, J. N., Hydraulics of Bridge Waterways. U.S. Dept. of Commerce. Bureau of Public Roads. Govt. Printing Office. 1960

This report gives the hydraulic design criteria for bridge waterway design and for the computation of backwater caused by bridges, and is written for highway departments engineers. Design procedures and illustrative problems are given for normal crossing, dual bridges, skew crossing, eccentric crossing, abnormal state discharge, and backwater with scour. The methods of computing the backwater are based almost entirely on model tests conducted at Colorado State University (see Liu, Bradley and Plate)

CHOW, VEN TE, Open Channel Hydraulics. McGraw-Hill Book Company, 1959.

In addition to being the most recent and comprehensive text on hydraulics of open channels, Professor Chow's book contains a chapter on "Flow Through Nonprismatic Channel Sections", (Chapt. 17). A detailed summary (Art. 17-16) with complete set of figures of the work of Kindsvater Carter and Tracy, (reproduced from U.S.G.S. circular 284, 1959) gives all the necessary information to calculate the discharge through constrictions, or the backwater ratio due to bridge constrictions.

GRAGWALL, JR. J. Indirect Methods of Discharge Measurement. Proceedings 6th Hydraulics Conference 1955 State University of Iowa. Studies in Engineering-Bulletin 36, 1956.

The 1951 flood in the Kansas river basin is taken as an example to discuss the necessity for indirect discharge measurements. The indirect methods are classified in four groups: 1) the slope area, 2) the contracted opening, 3) the flow through culvert, 4) the flow over dam. Each method is discussed briefly.

For a more detailed discussion of indirect discharge measurement at bridge constrictions see Kindsvater, Carter, and Tracy, "Computation of Peak Discharge at Contractions".

HENRY, H. R. Discussion on "Backwater Effects on Open Channel Constrictions". Trans. ASCE, 120, 1013-1017 (1955)

By simultaneous use of the momentum equation and the specific energy relation both in dimensionless form, Mr. Henry obtains graphically a theoretical solution for the backwater ratio, thus eliminating the trial and error calculation required by the method of Tracy and Carter (see also Ven Te Chow, Open Channel Hydraulics, example 17-3). The effect of the roughness on the decrease of momentum occasioned by boundary shear in the zone of expansion downstream of the constriction is compared to the roughness effect on the loss of energy on the contracting flow upstream of the constriction.

IZZARD, C. F. Discussion on "Tranquil Flow" by C. E. Kindsvater and R. W. Carter. Trans., ASCE, Vol. 120, pg. 985-89. 1955.

The experiments of Kindsvater and Tracy on "Tranquil Flow through Open-Channel Constrictions", were limited to the case of a horizontal bed. Izzard extends the analysis to the case of sloping channels, and making use of experimental data of Tracy and Carter ("Backwater Effects of Open-Channel Constrictions") he shows that the backwater of the constriction may be expressed approximately as the product of a velocity head (velocity at normal depth in downstream section of constriction) times a coefficient which depends primarily on the contraction ratio of the constriction Whereas Kindsvater and Tracy were concerned with the problem of estimating the discharge from measurement of water levels in the vicinity of a channel constriction, Izzard is concerned with the reverse problem of estimating the backwater caused by a channel carrying a known flow at normal depth.

IZZ RD, C. F. Discussion on "Backwater Effects of Open Channel Constriction" by H. J. Tracy and R. W. Carter. Trans. ASCE Vol. 120 pg. 1008-13. 1955.

The paper by Tracy and Carter is analyzed from the highway engineer viewpoint which is that of calculating expected backwater elevations due to floods of various frequencies. As the accuracy of the flood peak estimates is seldom better than ± 20%, simplifications may be introduced in the backwater calculation. The following simplification is proposed by Izzard. Neglecting minor effects (roughness, and length of constriction) the ratio of the maximum backwater depth upstream of the constriction to the normal depth in the unconstricted channel may be correlated to the contraction ratio and the velocity head in the constricted section. The velocity head in the constricted section is based on the area at normal depth.

IZZARD, C. F. and BRADLEY, J. N. Field verification of model tests on flow through highway bridges and calverts. Proc. 7th Hydr. Conf. Iowa Inst. of Hydr. Res. June 1958, Iowa City, Iowa, State University Iowa 1959, pg. 225-43. AMR 13-4641. Sept. 1960.

The paper reports on comparison of prototype measurements with computed values, derived from model tests for backwater caused by birdges, scour at bridge abutments, and head-discharge characteristics of culverts. Computed and measured values of the drop in water level across the bridge embankment is given for ten sites, two of which are for submerged deck girder. The smallest error is 0.5%, the largest is 13%.

KINDSVATER, C. E.; CARTER, R. W.; TRACY, H. J. "Computation of Peak Discharge at Contractions. USGS - Circular 284, 1953.

This report gives a procedure for computing subcritical peak discharges at contractions based on laboratory studies. The discharge formula given includes a discharge coefficient which may be obtained from sets of curves which contain the essential geometric and hydraulic factors governing the flow at a constriction. The factors are: the contraction ratio, the relative length of the abutment, the Froude number, the entrance rounding, the abutment chamfers, the angularity of the constriction, the side depth at abutments, the side slope of the abutment, the eccentricity of the constriction, the bridge submergence, and bridge piles and piers. The primary variables are the contraction ratio and the relative length of the abutments. Standard values of the discharge coefficient as a function of the primary variables are given for four types of geometries: 1) vertical embankments and vertical abutments; 2) sloping embankment and vertical abutments; 3) sloping embankments with sloping abutments; 4) sloping embankments with vertical abutments with wing walls. The standard value of the discharge coefficient is then multiplied by adjustment coefficients, which take into account the effect of the remaining variables, to obtain the discharge coefficient. Detailed field and office procedures are given.

See also: Kindsvater and Carter, "Tranquil Flow through Open-Channel Constrictions" -, for a summary including working curves see Ven Te Chow, "Hydraulics of Open Channels".

KINDSVATER, C. E. and CARTER, R. W., "Tranquil Flow through Open-Channel Constrictions". Trans. ASCE 120, 955-992, 1955.

A practical method of solving the discharge equation for tranquil flow of water through open channel constrictions is described. The functional relationships between the coefficient of discharge and the principal independent variables (contraction ratio, length of contraction, Froude number, entrance rounding, eccentricity of opening, angularity and guide walls) is presented from experimental data. Boundary conditions considered include vertical constrictive elements, channel cross-sectional shapes and roughness pattern. Within the limits tested the proposed computation procedure yields satisfactory results. Tests were run in a horizontal flume. See also the discussion by C. F. Izzard. (adapted from author's conclusions).

LANE, E. W. "Experiments on the Flow of Water through Contractions in an Open Channel. Trans. ASCE, 83, 1149 (1919 - 1920).

This is probably the first laboratory study on open channel constriction in the U.S. The Froude numbers used are higher than those usually found in bridge waterways. There is a limited number of boundary shapes. Experiments were made in four different flow contractions, namely rounded-edge plate, sharp edge plate, short flume, Venturi flume. Coefficients of discharge were first computed using D'Aubuisson's and Weisbach's formulas. Based on the experimental data a general equation of contraction was developed. The results of flume tests were presented in detail and discussed.

LIU, H. K; BRADLEY, J. N.; PLATE, E. J. "Backwater Effects of Piers and Abutments." Rept. CER 57 HKL 10; Colorado State Univ. 1957.

This is the final report of a project undertaken at Colorado State University in cooperation with the Bureau of Public Roads, U.S. Dept. of Commerce. Maximum backwater due to bridge constriction is given for simple normal crossing, abnormal stage-discharge condition, dual bridge crossing, skew crossing, eccentric crossing piers, partially submerged bridge girders. The water surface profiles, coefficient of contraction, location of maximum backwater, are presented. This report is perhaps the most comprehensive work on hydraulics of bridge constrictions in the American technical literature.

NAGAI, S., On the two-dimensional analyses of suddenly contracted flows. Houille Blanche. Nov., 1950. Pg. 662-73. AMR 7-1849

Position of contraction in suddenly contracted flows is determined by use of the Schwarz-Christoffel theorem. Study is made for flows about a suddenly contracted pipe and about that having a round corner. The position of contraction is approximately given with determination of the stationary points of vortex center. Corner radius can be found by which vortex will vanish.

TRACY, H. J., CARTER, R. W. Backwater Effects of Open Channel Constriction. Trans. ASCE 120, 993-1018. 1955.

A method of computing the backwater due to open channel constriction is given. It is based on empirical discharge coefficients and on a laboratory investigation of channel shape, constriction geometry and influence of channel roughness. The solution involves the computation of water-surface drop through the constriction and the determination of a factor which is the ratio of backwater to water surface drop. This ratio is shown to be a function of channel roughness, per centage of channel contraction, and constriction geometry. See also the discussion by Izzard (adapted from author's synopsis).

II. EXPANSION LOSSES

ALBERTSON, M. L., JENSEN, R. A., DAI, Y. B., ROUSE, H. Diffusion of submerged jets. Trans. ASCE Vol. 115 (1950) pg. 639-697.

This paper deals with the turbulence generated at the edges of a free air jet issuing from orifices and slots. Results are given of measurements of the distribution of the longitudinal velocity and of turbulence characteristics. Of particular interest to bridge hydraulics is the discussion by H. R. Henry (1950) on flow under sluice gates.

ARCHER, W. H. Experimental Determination of Loss of Head due to Sudden Enlargement in Pipes. ASCE Trans. Vol. 76 (1913) pg. 999.

Sudden expansion head loss:

$$h = \frac{1.098\ (\bar{U}m1 - \bar{U}m2)^{1.919}}{2g}$$

where $\bar{U}m1$ and $\bar{U}m2$ are the mean velocities in the upstream and downstream conduits.

BLANCHET, C. Sur Le Probleme Des Renous Et Des Pertes De Charge Produits par Les Singularities Dans Les Canaux Et Rivers. Houille Blanche No. 1, Nov. 1945 - Jan. 1946. pg. 39-62.

"Problem of turbulence and loss of head caused by obstructions in channels and rivers; turbulence curves related to curves of specific energy; influence of sill at channel bed and of contraction of cross section area on kinetic energy; results of study can be applied only to channels or rivers of stable bottom not liable to form deposits". From Engr. Ind. 1946 pg. 428.

CHATURVEDI, M. C. Flow Characteristics of Axisymmetric Expansions. Jour. of the Hydraulics Division ASCE, Vol. 89-HY3; May 1963.

Characteristics of flow for four abrupt expansions with half angles of 15°, 30°, 45° and 90° have been determined by a combination of analytical and experimental means. The transformation of mean energy, the rate of production of turbulence, and the rate of dissipation of turbulence energy are determined. The evaluated head-loss results from the air-duct studies are checked by independent measurements in a water-pipe assembly. The kinetic energy of the mean motion, kinetic energy of turbulence, pressure distribution, turbulence production, and turbulence shear are presented in the form of their spatial distribution, for all expansion angles. Head loss in abrupt expansions is given for different angles of separation; for 90° (half angle) the head loss coefficient is practically equal to that obtained in the assumption of constant pressure at the inlet section and one-dimensional analysis (p. 80 and Fig. 13). The variation of the head loss with changing expansion ratio is considered (p. 89 and Fig. 20

DAVIDIAN, J., CARRIGAN, P. H. JR., SHEN, J. (USGS) Flow through Opening in Width Constrictions. Water Supply Paper 1369-D, 1962, p. 91-122. plate.

"Flow pattern at constrictions with 2 to 7 openings; laboratory experiments and analysis were directed toward development of methods for computing discharge through multiple opening constrictions, apportioning given total discharge among several openings and predicting backwater caused by constrictions". Engr. Index 1962.

DELORME, A. Considerations Sur Les De Bouches Des Petits Ouvrages Sous Routes. Annales Des Ponts Et Chaussees. Vol. 129. No. 2. March-April 1959. p. 141-67.

"Water passages under small road bridges; size of underpass is often over-dimensioned, because formulas of calculation use too high safety factor; it is recommended that permissible factor of incidence of submersion should be defined by considering possible damage due to submersion; calculations should be based on flood statistics, also law of large values; practical applications." Engr. Ind. 1959, p. 171.

GIBBINGS, J. C., DIXON, J. R. Two-Dimensional Contracting Duct Flow. Quart. J. Mech Appl. Math. 10, 1, 24-41, Feb. 1957. AMR 10-2954. Sept. 1957.

This paper is primarily for wind tunnel design dealing with potential flow through two-dimensional contracting channels of finite length. Method of eliminating adverse velocity gradient along channel wall was presented in great detail. A numerical example is given.

HENRY, H. R. Discussion on Submerged Jets. Transactions, ASCE, Vol. 115 (1950) p. 6..

This is a discussion to a paper by M. L. Albertson, Y. B. Dai, R. A. Jensen and H. Rouse on diffusion of submerged jets. The effect of boundary conditions different from those used in the main paper are investigated. These, for the case of the flow under a sluic gate, are the effects of the free surface i.e. gravitational effect and the presence of a solid boundary, i. e. the flume floor, instead of a plane of symmetry of a two-dimensional jet.
Hydraulic design conclusion: Experimental discharge coefficients for the flow under a sluice gate are given in terms of a dimensionless gate opening, a dimensionless tailwater depth and the orifice Froude number (Fig. 35, p. 691). The expansion of the jet (which is limited by a fixed lower boundary and by a free surface upper boundary) is reported to have a slope of 1 on 6 approximately.

KINDSVATER, G. E. Energy Loss Associated with Abrupt Enlargements in Pipes. USGS. Water Supply Paper 1369-B-1961.

In connection with the USGS study of hydraulics of bridge-waterways, an experimental investigation was made of the flow of water through abrupt concentric enlargements in circular pipes. Particular attention is paid to the influence of pipe-wall roughness and to methods of computing the energy loss resulting from enlargements. The conventional method of computing the energy loss from the Borda-Carnot equation was found adequate for practical use.

PETERS, H. Conversion of Energy in Cross Sectional Divergences Under Different Conditions of Inflow". NACA TM 737, 1934.

Hydraulic design conclusion: Super imposing a spiral motion on the flow entering an expansion increased the efficiency, as the rotational motion delays the separation.

ROUSE, H. Energy Transformation in zones of separation. Proceedings 9th IAHR Conf. Durbrounik, 1961.

The integrated equations of momentum and of mean energy are examined for the case of two-dimensional flow over a normal wall, and attention is given to the variation of the sum of the terms of Bernoulli equation along a streamline in either the primary flow or the zone of separation.
This paper establishes some of the theoretical background on the mechanism of flow separation used in the experimental studies of Chaturvedi (1963).

ROUSE, H. Repartion de l'energie dans les Zones de Decollement. La Houille Blanche No. 3, May 1960 and No. 4, June, 1960.

Distribution of energy in regions of separation
Described in the present paper is the determination of the mean and secondary patterns of axisymmetric flow for two comparable boundary forms: the abrupt inlet and the blunt shaft.
Measurements available for analysis included the distributions of mean velocity, mean pressure, longitudinal and radial intensities of turbulence, turbulent shear, and longitudinal intensity gradient. Through use of the equations of momentum and of energy for the mean and the secondary motion, the measured distributions were adjusted to yield the required balance of the essential terms in the equations, thus yielding results in general accord with physical requirements. These are presented in the form of the flow patterns. (from author's abstract)

TULTS, H., Flow expansion and pressure recovery in fluids. Transactions ASCE, Vol. 121, 1956, Pg. 65. (AMR 8-2394. Aug. '55)

Investigating the possibility of improving the pressure recovery in flow expansions, author observed visually the separation phenomena and measured the development of velocity profiles and pressure distribution in a gradual unilaterally expanding two-dimensional rectangular test canal with varied divergence from zero degrees to 20 degrees in range of Reynolds number 5×10^4 to 3×10^5.
A simple analytical dependency is established between the angle of divergence and the rate of separation at which the maximum pressure recovery in each section occurs. This permits us to predict the optimum divergence for any required rate of gradual expansion.

VALLENTINE, H.R., Flow in rectangular channels with lateral constriction plates, Houille Blanche 13, 1, 75-84, Jan.-Feb. 1958. (AMR 12-834.)

Characteristics of flow in a rectangular channel with sharp-edged lateral constriction plates placed symmetrically, normal to the flow, are examined in a small tilting channel. The flow rate Q is related to the upstream depth y_1 by means of a discharge equation $Q = Cby_1^{3/2}$, where b is the width of opening and C is an experimental coefficient which depends upon the constriction ratio and the Froude number of the unconstricted flow. The values of C are established for Froude numbers up to 2.1 and constriction ratios up to 95%.

The conditions under which insertion of constriction plates produces an increase in upstream depth are investigated and the extent of the increase is evaluated. (From author's summary)

III. SUBMERGENCE

BENJAMIN, T. B., On the flow in channels when rigid obstacles are placed in the stream, J. Fluid Mech. 1, 2, 227-243. July 56 (AMR 11-503)

Author uses three physical quantities Q, R, S introduced in a previous paper (see Benjamin, T. B., and Lighthill, "On cnoidal waves and bores", Proc. roy. Soc. (A), 224, 448-460, 1954) with the meaning

$Q = vh$, $R = \frac{1}{2} v^2 h$, $S = v^2h + \frac{1}{2} gh^2$

i.e., Q is the flow rate, R the energy for unit mass, and S the momentum flow rate for unit span (corrected for changes in horizontal pressure force due to changes in depth) and divided by density. Invariability of these quantities at different cross sections implies, respectively, conservation of flow rate, of energy, and of momentum.

This present paper is divided in five parts: 1-Introduction; 2-General theory of flow; 3-Flow under a sluice gate; 4-Flow under a planning surface; 5-Experimental tests.

Parts 1 and 2 deal with some properties of flow and waves. In the last three parts, author studies the flow under a vertical or inclined gate. This subject has also been treated in the Italian papers of Gentilini Energia elett. April and June 1941 and March Ann. Mat. pura appl. (IV) 34, 1953.

BINNIE, A.M., The flow of water under a sluice-gate, Quart. J. Mechn. appl. Math 5, Part 4, 395-407, Dec. 1952, (AMR 6-2256.)

By introducing the Froude number of the flow, author simplifies relationship between conditions upstream and downstream of sluice gate. Well-known expressions are derived for alternate depth of flow, discharge, and force in the gate. A simple explanation is presented for the absence of waves on both sides of the gate. Coefficient of contraction C_c of the issuing flow is given as a review of experimental and theoretical investigations. Actually, author does not mention C_c, but presents instead the gate opening required to produce given Froude number.

BIRKHOFF, G. Calculation of Potential Flow with Free Streamlines. ASCE Jour. Hydr. Div. Vol. 87-HY6. Nov., 1961.

The most recent survey of the methods for computing three classes of steady potential flows with free streamlines: (1) plane flows having free boundaries and curved fixed boundaries without gravity; (2) plane flows having free boundaries and straight fixed boundaries with gravity and (3) axially symmetric flow having free boundaries without gravity.

Discussion by H. Rouse (March 1962, p. 187); L. Landweber (May, 1962 p. 223); S. P. Garg, T. S. Strelkoff and Y. S. Yu (July 1962, p. 293), and the closing discussion by G. Birkhoff, (March 1963, p. 147) point out the limitations of the mathematical methods; and comparisons between theoretical calculations and experimental results are given. The paper along with its discussions provides an excellent source of references on the subject.

BLISDELL, F. W. Comparison of Sluice Gate Discharge in Model and Prototype, Trans. ASCE Vol. 102 p. 544. 1937.

"(1) Models of sluice gates can be depended upon to predict the discharge of their prototypes with reasonable accuracy, (2) Froude model law will apply to the discharge of sluice-gate, (3) Roughness of both model and prototype must be given consideration in the construction of the model; and (4) good results should not be expected for small gate-openings and low velocities". (From Authors Conclusion.)

FRANKE, P., Jet contraction in flow under sluice gates in rectangular channels. Bautechnik 32, 8, 257-259, Aug. 55. (AMR 9-2240)

Analytical study is based on energy considerations of the flow under a sluice gate in a rectangular channel. Author computes the downstream depth in the case where energy losses are neglected and in the case where they are taken into consideration. Values of the coefficient of contraction are given for different ratioes of upstream depth to gate opening. All results are expressed in dimensionless form.

FRANKE, P., Theoretical consideration of jet contraction in flows under a sluice gate. Bautechnik 33, 3, 73-77, March '56. (AMR 9-[illegible])

Author analyses the contraction of an irrotational stream issuing from the opening of a sluicegate. In the first part of the analysis use is made of the results of von Mises (who did not consider gravity) for flow from a two-dimensional opening. The computed results do not compare well with the experimental data given in the paper.

The only exact (in the sense that no assumption in addition to irrotationality is made) solution for the sluice-gate problem is that of Southwell and Vaisey Phil. Trans. (A) 240, 117-161, which yields results in better agreement with author's experimental curve than any of his curves obtained from calculation.

GENTILINI, B., Flow under inclined or radial sluice gates. W.E.S. Translation [illegible] 11 pp., Nov. 195[illegible]. (AMR 5-[illegible])

Theoretical and experimental determinations were made of coefficient of discharge for inclined and radial sluice gates. Experimental channel was 16 cm wide, and angles of inclination of 15°, 30°, 45°, 60°, 75° and 90° were used. Opening ranged from [illegible] cm to 9 cm. Results closely checked theoretical coefficients that were derived from the specific energy relation.

ROUSE, H., and ABUL-FETOUH, A. H., Characteristics of irrotational flow through axially symmetric orifices. J. Appl. Mech. 17,4, 421-426, Dec. 1950 (AMR 4-3279.)

Although an exact analytical solution of the orifice problem has not yet proved feasible, use of the relaxation method has permitted a numerical determination of flow characteristics to be made with sufficient precision for the problem to be considered solved. The coefficient of contraction is found to be practically identical with that evaluated by von Mises for two-dimensional flow from slots over the entire range of area ratio, and reasonable agreement is shown to exist between measurement and computation. Coordinates of the jet profiles are presented in tabular and graphical form, and are found to differ appreciably from those previously adapted from the two-dimensional case. A composite dimensionless chart is also provided showing the distribution of pressure along the boundary and center line and across the efflux section for the various area ratios. (From authors summary.)

CHAPTER III THEORETICAL ANALYSIS

III-1 Flow Configuration at an Open Channel Constriction

The backwater due to a constriction in an open channel depends mainly on the boundary geometry, the discharge and the regime of the flow, i.e., the Froude Number. The phenomenon is usually so complicated that the resulting flow pattern is not entirely subject to analytical solution. A practical solution is only possible through experiments.

In the natural streams, the Froude Number of the flow usually ranged from 0.1 to 0.5. In this range of Froude Numbers the constriction will induce a pronounced backwater effect that extends a long distance upstream. A critical control section may exist at the constriction. When a critical control section exists at the constriction, a hydraulic jump occurs downstream of the constriction.

When a constriction is introduced into an otherwise uniform, friction-controlled flow in a prismatic channel of mild slope (see Fig. 3-1), a backwater of the M-1 type is developed upstream of the constriction. Upstream of the backwater curve the flow is undisturbed and the flow distribution is governed by the channel characteristics. Approaching the constriction, the flow decelerates as the depth increases. The deceleration process continues until a section (designated section (1)) is reached. Farther downstream the flow begins to accelerate owing to the convergence of the flow into the contracted opening (section 2). The flow pattern between sections 1 and 2 is essentially dominated by the constriction geometry.

As the fluid passes through the opening, the live stream contracts to a width somewhat less than that of the opening and the corresponding average longitudinal profile drops sharply. At the section of minimum (section 3) the expansion process begins and continues until normal flow again is established at some distance downstream (section 4).

The boundary roughness plays an important role in the downstream pattern of motion, especially when the flow just downstream of the constriction becomes supercritical. The roughness may force the hydraulic jumps to move upstream, and may eventually reach the downstream face of the constriction.

When the constriction is submerged, the centerline profile and plan view are as shown in figures 3-2 and 3-3 respectively. In figure 3-2 the approaching water surface is shown to have a profile of an M_1 curve; Y_o or Y_n is the normal depth of the unobstructed channel flow, Y_1 is the depth at the section of maximum backwater, Y_2 is the downstream depth taken in the deadwater flow portion of the channel, and Y_3 is the depth of the live stream at the vena contracta. The flow may be fully submerged as shown by the solid line or the discharge may be free at the downstream end of the constriction. The plan view of the channel constriction flow in figure 3-3 shows the streamlines of the flow entering the opening. The velocity upstream of the constriction is low and the streamlines follow the walls very closely. The eddies sketched on the upstream side of the opening moves in a vertical plane in a screw motion towards the opening. A particle in the corner would not remain in this region but due to these eddies it moves towards the opening. The eddies downstream of the constriction, shown on both sides of the jet, are in the horizontal plane and are less active. Particles could often remain there for longer periods of time.

The three basic equations of fluid mechanics: conservation of mass, conservation of momentum, and conservation of energy are used in the following study. These are applied to a definite volume called the control volume (c.v.) and the boundary of this volume is known as the control surface (c.s.). The shape of the control volume remains constant, but the amount and identity of the fluid in it may vary in time.

The flow configurations in the problem at hand are strictly three-dimensional. However, in order to simplify the analysis, a one-dimensional flow in which the velocity and the depth of flow vary only along the path of the channel is often used. In addition, the flow is that of a real fluid, that is to say that friction is present; boundary layers exist and flow separation may occur. The flow is thus rotational. The rotationality of the flow and its three-dimensional characteristics preclude the use of potential flow theory. The free streamline theory, so ably reviewed by Birkhoff[1] (1961) is not applicable.

The errors introduced by using a one-dimensional analysis may be eliminated by using suitable correction coefficients. However, in practice these coefficients are not known exactly, and even in the laboratory, their evaluation requires time-consuming measurements and calculations. It is, therefore, often customary to use the one-dimensional analysis without correction factors, realizing the limitations of such an analysis. The approximations so-obtained are nevertheless useful for engineering design; their accuracy is consistent with that of the data of the problem. It must be recognized that in the design of a bridge waterway opening, the design flow obtained from hydrologic computation is seldom known exactly and errors of ± 20% are common. Furthermore, all the irregularities of a natural water course cannot be taken into consideration, and average values or typical cross sections of the stream are considered. In the reverse problem of calculating a flood discharge from high water marks, the several inaccuracies inherent to the high water mark measurement and changes in roughness coefficient at high stages make it difficult to evaluate the discharge closer than within 10 to 15%.

The conservation of mass is expressed by the continuity equation which for a steady incompressible flow takes the form

$$\oiint_{C.S.} \vec{V} \cdot \vec{dA} = 0 \qquad (3\text{-}2\text{-}1)$$

in which the integral of the net efflux is taken around the whole control surface (C.S.). This equation simply states the inflow into the control volume (C.V.) is equal to the outflow from the control volume, and its one-dimensional form takes the usual form

$$V_1 A_1 = V_2 A_2 \qquad (3\text{-}2\text{-}2)$$

The conservation of momentum for steady flow states that the sum of the external forces on the control surface and of the body forces (usually gravity) acting inside the control volume is equal to the net rate of efflux of momentum across the control surface:

$$\vec{F}_s + \iiint_{C.V.} \vec{B} \rho \, d v = \iint_{C.S.} \vec{V} (\rho \vec{V} \cdot \vec{dA}) \qquad (3\text{-}2\text{-}3)$$

where $\vec{F}_s$ represents the external surface forces and B is the body force per unit of mass. The one dimensional counterpart of this equation is

$$F_x = \rho Q (\beta_2 V_{x2} - \beta_1 V_{x1}) \qquad (3\text{-}2\text{-}4)$$

where β is the momentum correction factor which takes into account the non-uniformity of the velocity distribution

$$\beta = \frac{1}{A} \iint (u/V)^2 \, d A \qquad (3\text{-}2\text{-}5)$$

The momentum equation applied to a straight open channel reach is:

$$\rho Q (\beta_2 V_2 - \beta_1 V_1) = P_1 - P_2 + W \sin \theta - F_f \qquad (3\text{-}2\text{-}6)$$

where P_1 and P_2 are the resultant forces acting on the end sections of the reach

W is the weight of water between the sections

θ is the angle of inclination of the channel

F_f is the external friction force exerted by the boundaries on the fluid

The friction force F_f may be evaluated from Manning's formula written for the boundary shear stress

$$\tau_o = \frac{14.5\, n^2 \rho V^2}{R^{1/3}} \qquad (3\text{-}2\text{-}7)$$

where τ_o is the average boundary shear and R is the hydraulic radius.

The specific force equation is obtained by applying the momentum equation to a short prismatic horizontal open channel reach, neglecting the friction force and assuming a hydrostatic pressure distribution:

$$\beta_1 \frac{Q^2}{gA_1} + \bar{Y}_1 A_1 = \beta_2 \frac{Q^2}{gA_2} + \bar{Y}_2 A_2 \qquad (3\text{-}2\text{-}8)$$

or

$$F_{s1} = F_{s2}$$

where F_s is the specific force, and where $\bar{Y}$ is the head over the center of gravity of the cross section.

The conservation of energy for steady flow may be written

$$\oiint_{C.S.} (V^2/2g + Z + p/\gamma)\,(\gamma \vec{V} \cdot \vec{dA}) = \text{hydraulic losses} \qquad (3\text{-}2\text{-}9)$$

and its one dimensional counterpart is

$$\alpha_1 V_1^2/2g + Z_1 + p_1/\gamma = \alpha_2 V_2^2/2g + Z_2 + p_2/\gamma + h_f \qquad (3\text{-}2\text{-}10)$$

where α is the energy correction factor which takes into account the non-uniformity of the velocity distribution

$$\alpha = 1/A \iint (u/V)^3 \, dA \qquad (3\text{-}2\text{-}11)$$

The head loss in steady uniform flow in open channel flow may be evaluated from Manning's formula

$$V = (1.486/n)\, R^{2/3}\, S^{\frac{1}{2}} \tag{3-2-12}$$

where

$$S = h_f/L \tag{3-2-13}$$

is the head loss per unit length.

In open channel flow, it is convenient to consider the energy with respect to the bottom as a datum. Thus is the specific energy first introduced by Bakhmeteff[2]:

$$E = V^2/2g + Y \tag{3-2-14}$$

In this form it is assumed that the velocity is uniform and that the streamlines are essentially parallel, thus the pressure is hydrostatic. If the velocity is not uniform, and if the streamlines are curved, the velocity head is multiplied by the kinetic energy coefficient, and the depth y may be multiplied by a pressure coefficient (α')

$$\alpha' = 1 + 1/Qy \iint c\, V\, d\, A \tag{3-2-15}$$

where

$$c = (d/g)\, V^2/r \tag{3-2-16}$$

and is positive for concave flow and negative for convex flow, d being the depth, and r the radius of curvature of a streamline. The specific energy thus becomes in general

$$E = \alpha V^2/2g + \alpha' Y \tag{3-2-17}$$

The specific force and the specific energy equations are used to define a number of open channel flow characteristics. When the specific energy or the specific force is minimum, the flow is called critical. The following relationship for critical flow may be derived from the specific energy equation for a stream of an arbitrary cross section, with $\alpha' = 1$

$$Q^2/g = A_c^3/W_c \tag{3-2-18}$$

$$Q/\sqrt{g/\alpha} = Z; \; Z = A\sqrt{A/W} = A\sqrt{D} \tag{3-2-19}$$

$$\alpha V^2/2g = A_c/2W_c = D_c/2 \tag{3-2-20}$$

$$V = \sqrt{(g/\alpha)\,(A_c/W_c)} = \sqrt{g\,D_c/\alpha} \tag{3-2-21}$$

$$V/\sqrt{gD_c/\alpha} = F = 1 \tag{3-2-22}$$

where W is the width of the free surface, Z is the section factor for critical flow computation, D is the hydraulic depth, and F is the Froude number. For a stream of rectangular cross section, letting g be the discharge per unit width, the above relationships take the following simplified forms:

$$q = [gy_c^3/\alpha]^{\frac{1}{2}} \tag{3-2-23}$$

$$\alpha V^2/2g = y_c/2 \tag{3-2-24}$$

$$V_c = [gy_c/\alpha]^{\frac{1}{2}} \tag{3-2-25}$$

$$Y_c = [\alpha q^2/g]^{1/3} \tag{3-2-26}$$

$$E = 3/2\, Y_c \tag{3-2-27}$$

For flow in rectangular channels the specific force and the specific energy equations may be written in a dimensionless form, making use of the critical flow relationships. They are respectively

$$\frac{\bar{Y}_1}{Y_1}\left[\frac{Y_1}{Y_c}\right]^2 + \beta_1 \frac{Y_c}{Y_1} = \frac{\bar{Y}_2}{Y_2}\left[\frac{Y_2}{Y_c}\right]^2 + \beta_2 \frac{Y_c}{Y_2} \tag{3-2-28}$$

and

$$\frac{Y_1}{Y_c} + \alpha_1 \left(\frac{Y_c}{Y_1}\right)^2 = \frac{Y_2}{Y_c} + \alpha_2 \left(\frac{Y_c}{Y_2}\right)^2 \tag{3-2-29}$$

where the ratio $\bar{Y}/Y$ is a geometric characteristic of the cross section and is equal to 0.5 for rectangular channels, $\bar{y}$ being the head over the center of gravity of the section.

III-3 Types of Flow at a Bridge Constriction

Six classes of flow may exist at a bridge constriction:

Class 1 - The flow is subcritical throughout the transition

Class 2 - The flow passes from subcritical to supercritical in the transition

Class 3 - The flow is supercritical throughout the transition

Class 4 - The flow passes from supercritical to subcritical near the transition

Class 5 - The transition inlet is submerged but the outlet is free, resulting in a free orifice flow.

Class 6 - The transition inlet and outlet are submerged resulting in a submerged orific flow.

The following analysis illustrates a method of distinguishing between the first four types of free surface flow. The latter two types are not truly free surface flow. A method to discriminate between the free surface flow and the orifice flow is also given.

As the flow towards the constriction is an accelerating flow, and as the energy losses are relatively small in a converging flow, the energy equation is suitable to describe the flow between sections 1 and 3. The expanding flow between sections 3 and 4 is better described by a momentum equation.

The first four types of flow may be delineated by the following simplified analysis. Writing an energy equation between sections 1 and 2,

$$\alpha_1 \frac{V_1^2}{2g} + \alpha_1' Y_1 = \alpha_3 \frac{V_3^2}{2g} + \alpha_3' Y_3 + h_f \qquad (3\text{-}3\text{-}1)$$

Assuming $\alpha_1 = \alpha_3 = \alpha_1' = \alpha_3' = 1$ and $h_f = 0$, letting b_3 the mean width of the stream at section 3, making use of the continuity equation

$$V_1 BY_1 = V_3 b_3 Y_3$$

the equation of energy may be re-written, after dividing both sides by Y_1.

$$\frac{V_1^2}{2gY_1} + 1 = \frac{V_1^2}{2gY_1} \left(\frac{B}{b_3} \frac{Y_1}{Y_3}\right)^2 + \frac{Y_3}{Y_1} \qquad (3\text{-}3\text{-}2)$$

or

$$\tfrac{1}{2}F_1^2 \left[\left(\frac{B}{b_3} \frac{Y_1}{Y_3}\right)^2 - 1 \right] = 1 - \frac{Y_3}{Y_1} \qquad (3\text{-}3\text{-}3)$$

or

$$F_1^2 = \frac{2\left(1 - \frac{Y_3}{Y_1}\right)}{\left(\frac{B}{b_3} \frac{Y_1}{Y_3}\right)^2 - 1} \qquad (3\text{-}3\text{-}4)$$

$$= \frac{2\left(\frac{Y_3}{Y_1}\right)^2 \left(1 - \frac{Y_3}{Y_1}\right)}{\left(\frac{B}{b_3}\right)^2 - \left(\frac{Y_3}{Y_1}\right)^2} \qquad (3\text{-}3\text{-}5)$$

F_1 is plotted as a function of $\frac{Y_3}{Y_1}$ in terms of $\frac{B}{b_3}$ in Fig. 3-2. The curve for which the flow is critical at section 3 corresponds to $F_3 = 1$, and is obtained from the continuity equation:

$$V_1 \, B \, Y_1 = V_3 \, b_3 \, Y_3 \qquad (3\text{-}3\text{-}6)$$

or

$$V_1^2 \, B^2 \, Y_1^2 = V_3^2 \, b_3^2 \, Y_3^2 \qquad (3\text{-}3\text{-}7)$$

or

$$\frac{V_1^2}{gY_1} \, \frac{B^2}{b_3^2} \, \frac{Y_1^3}{Y_3^3} = \frac{V_3^2}{gY_3} \qquad (3\text{-}3\text{-}8)$$

or

$$F_1^2 \, \frac{B^2}{b_3^2} \, \frac{Y_1^3}{Y_3^3} = F_3^2 \qquad (3\text{-}3\text{-}9)$$

When the flow is critical at section 3, $F_3 = 1$ and

$$F_1^2 = \left(\frac{Y_3}{Y_1}\right)^3 \left(\frac{b_3}{B}\right)^2 \qquad (3\text{-}3\text{-}10)$$

Solving the two equations simultaneously:

$$F_1^2 = \frac{2\left(\frac{Y_3}{Y_1}\right)^2 \left(1 - \frac{Y_3}{Y_1}\right)}{F_1^2 \left(\frac{Y_3}{Y_1}\right)^{-3} - \left(\frac{Y_3}{Y_1}\right)^2} \qquad (3\text{-}3\text{-}11)$$

or
$$F_1^4 - F_1^2 \left(\frac{Y_3}{Y_1}\right)^5 - 2 \left(\frac{Y_3}{Y_1}\right)^5 \left(1 - \frac{Y_3}{Y_1}\right) = 0 \qquad (3\text{-}3\text{-}12)$$

from which
$$2 F_1^2 = \left(\frac{Y_3}{Y_1}\right)^5 \pm \sqrt{\left(\frac{Y_3}{Y_1}\right)^{10} + \left(\frac{Y_3}{Y_1}\right)^5 \left(1 - \frac{Y_3}{Y_1}\right)} \qquad (3\text{-}3\text{-}13)$$

Only the positive sign in front of the square root has a physical significance.

This equation gives the values of the Froude number at section 1 corresponding to a Froude number of unity at the vena contracta.

The plane of Fig. 3-2 is thus divided in 4 regions:

Above the line $F_1 = 1.0$ the flow is supercritical in the approach of the constriction, below the line $F_1 = 1.0$, the flow is subcritical at section 1. Above the curve $F_3 = 1$, the flow is supercritical, and below the curve $F_3 = 1$ the flow is subcritical. The four regions of the figure are labelled according to the four classes of flow listed at the beginning of this section.

III-4 Discrimination Between Free Surface Flow and Orifice Flow

Orifice flow will occur when the head over the crown of the arch exceeds the velocity head plus the head loss in the orifice.

Thus for the limiting case, calling r the semi-circular arch radius:

$$\frac{V_3^2}{2g} + \left(\frac{1}{C_v^2} - 1\right)\frac{V_3^2}{2g} = Y_1 - r \qquad (3\text{-}4\text{-}1)$$

where $\left(\frac{1}{C_v^2} - 1\right)\frac{V_3^2}{2g}$ is the orific head loss.

Then $$\frac{1}{C_v^2}\frac{V_3^2}{2g} = Y_1 - r \qquad (3\text{-}4\text{-}2)$$

By continuity $V_1 BY_1 = V_3 b_3 y_3 = V_3 C_c A_o$ where A_o is the opening area.

Then $$\frac{1}{C_v^2}\frac{V_1^2}{2g}\frac{B^2 Y_1^2}{C_c{}^2 A_o{}^2} = Y_1 - r \qquad (3\text{-}4\text{-}3)$$

$$\frac{V_1^2}{2gY_1} = \left(1 - \frac{r}{Y_1}\right) C_d^2 \left(\frac{A_o}{A_1}\right)^2 \qquad (3\text{-}4\text{-}4)$$

$$F_1^2 = 2C_d^2 \left(1 - \frac{r}{Y_1}\right)\left(\frac{A_o}{A_1}\right)^2 \qquad (3\text{-}4\text{-}5)$$

There will be submergence when

$$F_1^2 < 2\, C_d^2 \left(1 - \frac{r}{Y_1}\right)\left(\frac{A_o}{A_1}\right)^2 \qquad (3\text{-}4\text{-}6)$$

where $C_d \approx 0.55$.

or when $$F_1^2 < 1/8\, C_d^2\, \pi^2 \left(1 - \frac{1}{2}\frac{b}{Y_1}\right)\left(\frac{b}{B}\right)^2\left(\frac{b}{Y_1}\right)^2 \qquad (3\text{-}4\text{-}7)$$

and since $\frac{b}{B} = M$

when $$\frac{F_1^2}{M^2} < 1/8\, \pi^2 C_d^2 \left(1 - \frac{1}{2}\frac{b}{Y_1}\right)\left(\frac{b}{Y_1}\right)^2 \qquad (3\text{-}4\text{-}8)$$

An empirical relationship to distinguish between free surface flow and orifice flow, can be obtained, making use of the notation developed in the article on dimensional analysis, and of the results of chapter 5.

From free surface flow experiments (see chapter 5)

$$\frac{Y_1}{Y_n} = 1 + 0.47 \left(\frac{F_n}{M'}\right)^{2.26} = 1 + 0.47 \frac{1}{Cm^{2.26}} \left(\frac{F_n}{M}\right)^{2.26} \qquad (3\text{-}4\text{-}9)$$

where $C_m = M'/M$. (See Figure 3-12)

From orific flow experiments (see chapter 5)

$$\frac{Y_1}{Y_n} = 1 + 1.18\left[\frac{F_n}{\frac{A_o}{BY_n}}\right]^{1.8} = 1 + 1.18 \left(\frac{8}{\pi}\right)^{1.8} \left[\frac{Y_n}{b}\right]^{1.8} \left[\frac{F_n}{M}\right]^{1.8} \qquad (3\text{-}4\text{-}10)$$

Equating

$$\left[\frac{F_n}{M}\right]^{0.46} = 13.46 \quad C_m^{2.26} \left(\frac{Y_n}{b}\right)^{1.8} \qquad (3\text{-}4\text{-}11)$$

and since for d = 0

$$C_M = \frac{1}{2}\left\{\sqrt{1 - \left(\frac{Y_n}{r}\right)^2} + \frac{r}{Y_n} \sin^{-1} \frac{Y_n}{r}\right\} \qquad (3\text{-}4\text{-}12)$$

For the limiting case

$$\left(\frac{F_n}{M}\right)^{0.46} = 13.46 \left\{\frac{1}{2}\sqrt{1 - \left(\frac{Y_n}{r}\right)^2} + \frac{r}{Y_n} \sin^{-1} \frac{Y_n}{r}\right\}^{2.26} \left(\frac{Y_n}{2r}\right)^{1.8}$$

(3-4-13)

A plot of this relationship is given in figure 3-5, from which it is possible to predict for a given Froude, normal depth and contraction geometry, whether the flow will be free or submerged.

III-5 Flow Class 1 - Subcritical Flow through Unsubmerged Constriction

a) General considerations

This is the most common case. The flow pattern divides itself in two parts: (see fig. 3-1).

1) a zone of contracting or accelerating flow, from the section of maximum backwater (section 1) to the section of minimum area or "vena contracta" - (section 3).

2) a zone of expanding or decelerating flow, from the vena contracta (section 3) to the section where the stream has regained its normal depth (section 4).

It is, therefore, expected that the analysis of the flow pattern would be divided in two parts. An energy equation may be used for the analysis of the contracting flow, and a momentum equation for that of the expanding flow. Section 4, at which the flow occurs at normal depth is the control section. The calculation of the flow profile for a given discharge could proceed from section 4 to section 3 by means of the momentum equation, and from section 3 to section 1 by means of the energy equation, the continuity equation being used to relate the areas at the several sections. The difficulty in this approach lies in the lack of proper definition of the geometry of section 3. The geometry of section 2, at the section of separation, is defined by the water depth, as the geometry of the constriction is assumed to be known — in our case a semi-circular arch.

At section 2 the flow separates from the solid boundaries, and the three-dimensional live stream converges to the vena contracta. The geometry of the free boundary of the convergent live stream cannot be determined by means of the free streamline theory as the latter is limited to two-dimensional flow. Consequently, it is customary to make some assumption on the flow geometry between sections 2 and 3. Typical assumptions are:

a) The geometry of section 3 is assumed.

b) The depths at sections 2 and 3 are assumed to be identical.

c) The depth at section 2 is assumed to be equal to the normal depth of the uncontracted stream.

The three assumptions will be discussed.

a) Assumed geometry at section 3.

Experiments by P. F. Biery indicate (Fig. 7-2-7) that the depth at section 3 is not uniform across the section, but that in the dead water region it is only 1% larger than across the live stream. The depth Y_3 may thus be reasonably assumed constant across the section. The width of the live stream b_3 may be approximated using the two-dimensional coefficient of contraction and

$$b_3 = C_{c2}\, b \qquad (3\text{-}5\text{-}1)$$

Thus the cross section of the livestream would be

$$A_3 = C_{c2}\, b\, Y_3 \qquad (3\text{-}5\text{-}2)$$

The values of the coefficients of contraction for slots, after von Misses([illegible]) is given in the following table:

$\frac{b}{B}$	0	0.1	0.2	0.3	0.4	0.5	0.6	0.7	0.8	0.9	1.0
C_{c2}	0.611	0.612	0.616	0.622	0.631	0.644	0.662	0.687	0.722	0.781	1.00

This assumption makes it possible to relate the depth $Y_n = Y_1$ to Y_3 by means of the momentum equation, and then Y_3 to Y_1 by means of the energy equation.

b) Assumed equality of depths at sections 2 and 3.

This assumption was used by Tracy and Carter (ASCE Trans. 1955 p. 997). The experiments of P. F. Biery, (Jour. Hyd. Div. ASCE, Vol. 83 No. HY2 p. 96, Fig. 13) do not substantiate this assumption.

c) Depth at section 2 assumed equal to normal depth of uncontracted stream.

This assumption has been implied by Izzard (ASCE Trans 1955, p. 1010). Although this assumption cannot be justified theoretically, the experiments of P. F. Biery show that this assumption is approximately satisfied. It is then possible to express the head loss in the constriction as a function of the velocity head at section 2,

$$hf = K \frac{V_{n2}^2}{2g} \qquad (3\text{-}5\text{-}3)$$

The depth of flow at section 1 may then be obtained by means of an energy equation between sections laand 2 or between sections 1 and 4. This assumption has also been used with reasonable success by I. P. Wu[4] in a preliminary calculation of indirect determination of flood discharge from contracted bridge openings and high water marks.

b) Momentum equation for diverging flow

The momentum equation is written between sections 3 and 4 with the assumption that the pressure distribution is hydrostatic at t, These sections:

$$F_3 + M_3 = F_4 + M_4 + F_D - F_G \qquad (3\text{-}5\text{-}4)$$

F_3 and F_4 represent the hydrostatic forces at section 3 and 4 respectively; M_3 and M_4 are the momenta, F_D is the drag force of the expanding stream on the bottom and F_G is the component of the gravity force in the direction of the flow.

To calculate the hydrostatic force at sections 3 and 4, let $\bar{Y}_3$ and $\bar{Y}_4$ be the heads over the respective centers of gravity of the cross sections. To calculate the momentum flux through section 3 it is necessary to evaluate the cross sectional area of the live stream at section 3. It is assumed that

$$A_3 = b_3 Y_3 \qquad (3\text{-}5\text{-}5)$$

The momentum equation may then be written

$$\gamma \bar{Y}_3 B Y_3 + \rho Q V_3 = \bar{Y}_4 B \bar{Y}_4 + \rho Q V_4 + F_D - F_G \qquad (3\text{-}5\text{-}6)$$

Making use of the continuity equation, it follows that

$$\gamma \bar{Y}_3 B Y_3 + \rho \frac{Q^2}{A_3} = \gamma \bar{Y}_4 B Y_4 + \rho \frac{Q^2}{A_4} + F_D - F_G \qquad (3\text{-}5\text{-}7)$$

or

$$\bar{Y}_3 Y_3 + \frac{q^2 B}{g A_3} = \bar{Y}_4 Y_4 + \frac{q^2 B}{g A_4} + \frac{F_D - F_G}{\gamma B} \qquad (3\text{-}5\text{-}8)$$

Introducing the critical depth $Y_c^3 = q^2/g$,

$$\bar{Y}_3 Y_3 + \frac{Y_c^3 B}{Y_3 b_3} = \bar{Y}_4 Y_4 + \frac{Y_c^3}{Y_4} + \frac{F_D - F_G}{\gamma B} \qquad (3\text{-}5\text{-}9)$$

The momentum equation may be written in a dimensionless form by dividing both sides of the above equation by Y_c^2:

$$\frac{\bar{Y}_3}{Y_3}\left(\frac{Y_3}{Y_c}\right)^2 + \frac{Y_c}{Y_3}\,\frac{B}{b_3} = \frac{\bar{Y}_4}{Y_4}\left(\frac{Y_4}{Y_c}\right)^2 + \frac{Y_c}{Y_4} + \frac{F_D - F_G}{\gamma B Y_c^2} \qquad (3\text{-}5\text{-}10)$$

The quantity $\frac{\bar{Y}}{y}$ is a geometric constant for many cross sections. For example for a

rectangular section	$\frac{\bar{Y}}{y} = 0.5$
triangular section	$= 0.333$
semi-circle section	$= 1 - (4/3)\pi$
parabola section	$= 3/5$

Let $\frac{\bar{Y}}{Y} = G$ a geometric constant of the section. Then the dimensionless momentum equation becomes:

$$G_3\left(\frac{Y_3}{Y_c}\right)^2 + \frac{B}{b_3}\,\frac{Y_c}{Y_3} = G_4\left(\frac{Y_4}{Y_c}\right)^2 + \frac{Y_c}{Y_4} + \frac{F_D - F_G}{\gamma B Y_c^2} \qquad (3\text{-}5\text{-}11)$$

Neglecting for the time being the contribution of the term

$$(F_D - F_G)/\gamma B Y_c^3$$

and calling the specific force F_s

$$F_s = \gamma \bar{Y} B Y + \rho Q V \qquad (3\text{-}5\text{-}12)$$

then the generalized dimensionless momentum equation becomes:

$$G_x\left(\frac{Y_x}{Y_c}\right)^2 + \frac{B}{b_x}\,\frac{Y_c}{Y_x} = F_s/\gamma B Y_c^2 \qquad (3\text{-}5\text{-}13)$$

A plot of the relationship is given in the right hand side of figure 3-7, which may be used for an approximate solution of the depth Y_3 if the depth Y_4 is given. The width of the live stream at section 3 is usually unknown a priori, but may be taken as the width of the constriction times a contraction coefficient.

The drag force of the diverging stream on the channel bottom between the vena contracta and section 4 may be obtained by integrating the shear stress over the expansion area along the bottom. From the discussion by Henry[5] it appears that the rate of expansion of a submerged jet is approximately 1 on 6. The model is assumed for the zone of expansion is shown Fig. 3-6.

From Manning's formula, the shear stress on the bottom is

$$\tau = \frac{14.5 n^2 \rho v^2}{R^{1/3}} = \frac{14.5 n^2 \rho Q^2}{Y^{1/3} b'^2 Y^2} = \frac{14.5 n^2 \rho q^2 B^2}{Y^{7/3} b'^2} \qquad (3\text{-}5\text{-}14)$$

and the elementary drag force is

$$dF_D = \tau \, dA = \frac{14.5 n^2 \rho q^2 B^2}{Y^{7/3} b'} dx \qquad (3\text{-}5\text{-}15)$$

or

$$\frac{dF_D}{\gamma B Y_c^2} = \frac{14.5 n^2 B Y_c}{Y^{7/3} b'} dx = 14.5 \left(\frac{n}{Y_c^{1/6}}\right)^2 \left(\frac{Y_c}{y}\right)^{7/3} \frac{B}{Y_c} \frac{dx}{b'} \qquad (3\text{-}5\text{-}16)$$

The dimensionless drag force is

$$\frac{F_D}{\gamma B Y_c^2} = 14.5 \left(\frac{n}{Y_c^{1/6}}\right)^2 \frac{B}{Y_c} \int_0^{L_{3-4}} \left(\frac{Y_c}{y}\right)^{7/3} \frac{dx}{b'} \qquad (3\text{-}5\text{-}17)$$

Since $b' = C_d b + x/3$, and taking an average value of the depth, an approximate value of the drag force is given by

$$\frac{F_D}{\gamma B Y_c^2} = 14.5 \left(\frac{n}{Y_c^{1/6}}\right)^2 \frac{B}{Y_c} \left(\frac{2Y_c}{Y_n + Y_3}\right) \int_0^{3(B - bC_d)} \frac{dx}{bC_d + x/3} \qquad (3\text{-}5\text{-}18)$$

$$= 14.5 \left(\frac{n}{Y_c^{1/6}}\right)^2 \frac{B}{Y_c} \left(\frac{2Y_c}{Y_n + Y_3}\right)^3 \ln \frac{B}{bC_d} \qquad (3\text{-}5\text{-}19)$$

The gravity force is

$$F_G = B \frac{Y_3 + Y_4}{2} L_{3-4} S_o$$

$$= B \frac{Y_3 + Y_4}{2} 3 (B-bC_d) S_o \quad (3-5-20)$$

and the dimensionless gravity force is

$$\frac{F_G}{BY_c{}^2} = 3/2 \frac{Y_3 + Y_n}{Y_c} \frac{B - bC_d}{Y_c} S_o \quad (3-5-21)$$

In the actual computation, a first approximation of Y_3 is obtained by neglecting F_D and F_G. With this approximate value of Y_3, the values of F_D and F_G may be calculated from the above equations.

c) Energy Equation for Converging Flow

The energy equation between sections 1 and 3 may be written

$$S_1 L_{1-3} + Y_1 + \alpha_1 \frac{V_1^2}{2g} = Y_3 + \alpha_3 \frac{V_3^2}{2g} + h_f \quad (3-5-22)$$

where h_f is the head loss between sections 1 and 3. Making use of the continuity equation

$$V_1 A_1 = V_3 A_3$$

$$Y_1 + \alpha_1 \frac{q^2}{2gY_1{}^2} = Y_3 + \alpha_3 \left(\frac{A_1}{A_3}\right)^2 \frac{q^2}{2gY_1{}^2} + h_f - S_o L_{1-3} \quad (3-5-23)$$

Introducing the critical depth $Y_c{}^3 = q^2/g$

$$\frac{Y_1}{Y_c} + \alpha_1 \left(\frac{Y_c}{Y_1}\right)^2 = \frac{Y_3}{Y_c} + \alpha_3 \left(\frac{B}{b_3}\right)^2 \frac{Y_c}{Y_3}^2 + \frac{h_f}{Y_c} - S_o \frac{L_{1-3}}{Y_c}$$

(3-5-24)

which is the dimensionless form of the energy equation. Assuming $\alpha_1 = \alpha_3 = 1$, and neglecting the difference of the last two terms..

$$\frac{Y_1}{Y_c} + \left(\frac{Y_c}{Y_1}\right)^2 = \frac{Y_3}{Y_c} + \left(\frac{B}{b_3}\right)^2 \left(\frac{Y_c}{Y_3}\right)^2 = \frac{E_s}{Y_c} \qquad (3\text{-}5\text{-}25)$$

The plot of this equation is given in the left-hand side of figure 3-7.

The friction loss between sections 1 and 3 may be calculated from the expression

$$h_f = L_{1-2} \frac{Q^2}{K_1 K_3} + L_{2-3} \frac{Q^2}{K_3^2} \qquad (3\text{-}5\text{-}26)$$

The value of the conveyance

$$K = \frac{1.486}{n} \quad AR^{2/3} \qquad (3\text{-}5\text{-}27)$$

may be approximated as follows

$$K_1 = \frac{1.486}{n} \quad BY_1^{5/3} \qquad (3\text{-}5\text{-}28)$$

$$K_3 = \frac{1.486}{n} \quad b_3 Y_3^{5/3} \qquad (3\text{-}5\text{-}29)$$

then

$$\frac{h_f}{Y_c} = \frac{q^2 B^2 n^2}{(1.486)^2 Y_c} \left\{ \frac{L_{1-2}}{B\, b\, Y_1^{5/3}\, Y_3^{5/3}} + \frac{L_{2-3}}{b_3^2\, Y_3^{10/3}} \right\} \qquad (3\text{-}5\text{-}30)$$

$$= \frac{g\, Y_c^2\, n^2\, B}{2.2} \left\{ \frac{L_{1-2}}{b} \quad \frac{1}{Y_1^{5/3}\, Y_3^{5/3}} + \frac{L_{2-3}\, B}{b_3^2} \quad \frac{1}{Y_3^{10/3}} \right\} \qquad (3\text{-}5\text{-}31)$$

$$= \frac{g}{2.2} \quad \frac{B}{Y_c} \left(\frac{Y_c}{Y_3}\right)^{5/3} \left(\frac{n}{Y_c^{1/6}}\right)^2 \left\{ \frac{L_{1-2}}{b} \left(\frac{Y_c}{Y_1}\right)^{5/3} + \frac{L_{2-3}}{b_3^2} \left(\frac{Y_c}{Y_3}\right)^{5/3} \right\} \qquad (3\text{-}5\text{-}32)$$

The experiments of Biery show that $L_{1-2} \approx L_{1-3} \approx b$. Then

$$\frac{h_f}{Y_n} = \frac{g}{2.2} \frac{B}{Y_c} \left(\frac{Y_c}{Y_3}\right)^{5/3} \left(\frac{n}{Y_n^{1/6}}\right)^2 \left\{ \left(\frac{Y_c}{Y_1}\right)^{5/3} + \frac{Bb}{b_3^2} \left(\frac{Y_c}{Y_3}\right)^{5/3} \right\} \qquad (3\text{-}5\text{-}33)$$

In an actual computation, a first approximation of Y_1 is obtained by neglecting the difference between the head loss h_f and $S_o\ L_{1-3}$. The term neglected is the loss in addition to the normal flow head loss due to the acceleration of the flow between section 1 and 3 and the separation of the flow from the boundaries at section 2. The quantity neglected is usually negligible.

d) Graphical Solution of Backwater due to a Constriction

The dimensionless specific force and specific energy curves may be used to obtain graphically the backwater upstream of a constriction, as was first suggested by H. R. Henry[6]. Part of the specific force and specific energy diagram has been enlarged in Fig. 3-8 for the illustration of the graphical method.

As an example, the conditions of the experiment 16-S, Geometry Ia (see table 7-1-2) are illustrated. The data of the problem are:

$$Q = 2.0 \text{ cfs}, \; Y_n = 20.30 \text{ cm}; \; M = B/b = 0.491.$$

Calculate

$$Y_c = \left(\frac{Q^2}{gB^2}\right)^{1/3} = 5.24 \text{ cm}$$

and $$Yn/Yc = 3.88.$$

Enter the diagram with the value of $Y_4/Y_c = Y_n/Y_c = 3.88$ and proceed to the specific curve labeled $B/b_3 = 1.0$, corresponding to no contraction. With a coefficient of contraction $C_d = 0.64$, calculate

$$\frac{B}{b_3} = \frac{B}{bC_d} = \frac{1}{MC_d} = \frac{1}{0.491 \times 0.64} = 3.18$$

Proceed on the diagram along a vertical line, corresponding to a constant specific force, until an interpolated curve for $B/b_3 = 3.18$ is reached. Proceed to the left and read $Y_3/Y_c = 3.72$. The experimental value of Y_3/Y_c was $\frac{19.41}{3.88} = 5.0$. With the obtained value of Y_3/Y_c of 3.72, proceed to an interpolated specific energy corresponding to $B/b_3 = 3.18$. Proceed upward following a line of constant specific energy until the curve $B/b_3 = 1$ is reached, corresponding to no contraction at station 1. Read the value of $Y_1/Y_c = 4.069$ and calculate $Y_1 = 4.069 \times 5.24 = 21.30$ cms. The experimental value was 21.26 cms. A good agreement was obtained in spite of the neglect of the friction and head loss terms. However, it should be remembered that the example chosen corresponds to smooth boundaries, and consequently, the head losses are indeed small.

III-6 Flow Class 2 - The Flow Goes Through Critical in the Constriction

a) Geometric Properties of Semi-Circular and Circular Segment Channels

In this type of flow the control is in the constriction, where there exists a relationship between the depth of flow and the discharge. The depth at section 1 may be obtained directly by writing an energy equation between the control section and section 1. As the calculation of the critical depth in a conduit having a semi-circular section, or a circular segment section, is tied to the geometry of the section, this geometry is studied first. At critical stage

$$Z = \frac{Q}{\sqrt{g/\alpha}} \qquad (3\text{-}6\text{-}1)$$

where

$$Z = A\sqrt{\bar{y}} \qquad (3\text{-}6\text{-}2)$$

and $\bar{y}$ is the hydraulic depth, defined by

$$\bar{y} = \frac{A}{W} \qquad (3\text{-}6\text{-}3)$$

where W is the free surface width.

The geometric properties of the semi-circular and circular segment arches are summarized in Fig. 3-9. The top right hand side quadrant gives the relationship between the section factor for critical flow computation and the critical depth in terms of the distance from the springline to the center of curvature of the arch. The curve labeled $d/b = 0$ corresponds to the semi-circular arch. In order to obtain the critical depth in the constriction of a given diameter b for a given discharge Q, one calculates the section factor for critical flow Z by means of the relation

$$\frac{Q}{\sqrt{g/\alpha}} = Z$$

and entering the diagram with the proper value of $Z/b^{5/2}$ for the desired d/b one reads the ratio of the critical depth to the diameter Y_c/b. The value of the hydraulic depth $\bar{y}$ and of the free surface width W can be obtained by means of the sets of curves in the top and bottom left hand side of the figure respectively.

With reference to Fig. 3-9 (bottom right hand side) the area of the section of depth y is:

$$A = \frac{b^2}{8} \sec^2 \frac{\theta_2}{2} \left(\theta_1 - \theta_2 + \sin\theta_1 - \sin\theta_2\right) \tag{3-6-4}$$

the free surface is

$$W = b \frac{\cos\frac{\theta_1}{2}}{\cos\frac{\theta_2}{2}} \tag{3-6-5}$$

the hydraulic depth is

$$\bar{y} = \frac{A}{W} = \frac{b}{8} \frac{\theta_1 - \theta_2 + \sin\theta_1 - \sin\theta_2}{\cos\frac{\theta_1}{2} \cos\frac{\theta_2}{2}} \tag{3-6-6}$$

the section factor for critical flow computation is:

$$Z = A\sqrt{\bar{y}} = \frac{b^2/8}{\cos^2\frac{\theta_2}{2}} \left(\theta_1 - \theta_2 + \sin\theta_1 - \sin\theta_2\right) \sqrt{\frac{b}{8} \frac{\theta_1 - \theta_2 + \sin\theta_1 - \sin\theta_2}{\cos\theta_1 \cos\theta_2}} \tag{3-6-7}$$

or in dimensionless form:

$$Z = \frac{b^{5/2}}{8^{3/2}} \frac{\left(\theta_1 - \theta_2 + \sin\theta_1 - \sin\theta_2\right)^{3/2}}{\left(\cos\frac{\theta_2}{2}\right)^{5/2} \left(\cos\frac{\theta_1}{2}\right)^{1/2}} \tag{3-6-8}$$

$$\therefore \frac{Z}{b^{5/2}} = \frac{1}{8^{3/2}} \frac{\left(\theta_1 - \theta_2 + \sin\theta_1 - \sin\theta_2\right)^{3/2}}{\left(\cos\frac{\theta_2}{2}\right)^{5/2} \left(\cos\frac{\theta_1}{2}\right)^{1/2}} \tag{3-6-9}$$

The above relationships were used to prepare the curves of Fig. 3-9.

b) Limiting Backwater

The purpose of the following analysis is to calculate the backwater at Section 1 when the flow goes through critical in the constriction. This type of flow represents the boundary between classes 1 and 2.

Assuming that the kinetic energy coefficient and the pressure coefficients are unity, the specific energy equation is

$$Y_1 + \frac{V_1^2}{2g} = Y_2 + \frac{V_2^2}{2g} \tag{3-6-10}$$

or

$$Y_1 \left(1 + \frac{V_1^2}{2gY_1}\right) = \bar{y}_2 \left(\frac{Y_2}{\bar{y}_2} + \frac{V_2^2}{2g\bar{y}_2}\right) \tag{3-6-11}$$

or

$$Y_1 \left(1 + \frac{F_1^2}{2}\right) = \bar{y}_2 \left(\frac{Y_2}{\bar{y}_2} + \frac{F_2^2}{2}\right) \tag{3-6-12}$$

When the flow is critical at section 2, $F_2 = 1$, then

$$Y_1 \left(2 + F_1^2\right) = \bar{y}_2 \left(2\frac{Y_2}{\bar{y}_2} + 1\right) \tag{3-6-13}$$

or

$$\frac{\bar{y}_2}{Y_1} \frac{\left(2\frac{Y_2}{\bar{y}_2} + 1\right)}{\left(2 + F_1^2\right)} = 1 \tag{3-6-14}$$

The equation of continuity

$$(V_1 Y_1 B_1)^2 = (V_2 \bar{y}_2 W)^2 \tag{3-6-15}$$

may be written

$$F_1^2 B^2 Y_1^3 = F_2^2 \bar{y}_2^3 W^2 \tag{3-6-16}$$

which for $F_2 = 1$ becomes

$$\left(\frac{\bar{y}_2}{Y_1}\right)^3 = \left(\frac{B}{W}\right)^2 F_1^2 \tag{3-6-17}$$

Introducing this result into the specific energy equation (3-6-14) it follows that

$$F_1^2 \frac{B^2}{b^2} \frac{b^2}{W^2} \frac{\left(2\frac{Y_2}{\bar{y}_2} + 1\right)^3}{\left(2 + F_1^2\right)^3} = 1 \tag{3-6-18}$$

or

$$\left(\frac{b}{B}\right)^2 = M^2 = F_1^2 \frac{b^2}{W^2} \left\{\frac{2\frac{Y_2/b}{\bar{y}_2/b} + 1}{2 + F_1^2}\right\}^3 \tag{3-6-19}$$

As the value of the critical depth is a function of the critical flow factor

$$\frac{Y_c}{b} = f\left(\frac{Z}{b^{5/2}}\right) \tag{3-6-20}$$

and as the values of the free surface width W, and of the hydraulic depth $\bar{y}$ depend on Y_c, they are implicit functions of $Z/b^{5/2}$. Equation (3-6-20) may be then represented in a functional form as $M = \left(\frac{b}{B}\right) = f\left(F_1, \frac{Z}{b^{5/2}}\right)$ for a given value of d/b.

This relationship is presented in Fig. 3-10 several values of d/b ranging from 0 to 4. The values of $\frac{W}{b}, \frac{Y}{b}, \frac{\bar{y}}{b}$ necessary for the preparation of these curves were obtained from Fig. 3-9 for values of $Z/b^{5/2}$ of 0.1; 0.2; 0.3; 0.4; and 0.5. and introduced in formula (3-6-19) for M^2 for several values of F_1.

For a given discharge Q, and a trial opening ratio b/B one may calculate the dimensionless section factor for critical flow

$$\frac{Z}{b^{5/2}} = \frac{Q^2}{\sqrt{g}\; b^{5/2}}$$

This value of this parameter defines a curve in Fig. 3-10. For points located above the curve, the flow is subcritical in the constriction. Points located on the curve correspond to flow going through critical in the constriction. The limiting backwater may be obtained by reading the value of F_1 on Fig. 3-10 corresponding to given values of $Z/b^{5/2}$, b/B and d/B, then Y_1 is calculated from

$$Y_1^{\,3} = Y_n^{\,3} \left(\frac{F_1}{F_n}\right)^2 \tag{3-6-21}$$

For large discharge, the constrictions partially dam the flow, until it becomes an orifice flow.

III-7 Discharge Equations

a) The Equation of Discharge for Free Surface Flow

With reference to Fig. 3-1 and neglecting the velocity of approach, the discharge is found to be $Q = \int VdA = \int_0^{Y_1} C \sqrt{2g\,(Y_1 - h)} \times 2\sqrt{r^2 - h^2}\, dh$ (3-7-1)

An approximate value of the above integral may be obtained by expanding the integrand into a series, and integrating term by term. Making use of the fact that $2r = b$

$$Q = C_d \sqrt{2g}\, \frac{17}{24}\, Y_1^{3/2}\, b \left\{ (1 - 0.1294 \left(\frac{Y_1}{r}\right)^2 - 0.0177 \left(\frac{Y_1}{r}\right)^4 \ldots \right\} \quad (3\text{-}7\text{-}2)$$

This may be written as

$$Q = C_1 Y_1^{3/2}\, b\, T_1 \quad (3\text{-}7\text{-}3)$$

where $$C_1 = C_d \frac{17}{24} \sqrt{2g} \quad (3\text{-}7\text{-}4)$$

and $$T_1 = 1 - 0.1294 \left(\frac{Y_1}{r}\right)^2 - 0.0177 \left(\frac{Y_1}{r}\right)^4 \quad (3\text{-}7\text{-}5)$$

The above equation is valid as long as the constriction is unsubmerged and $Y_1 > r$.

The evaluation of the equation of discharge in the integral form (equation 3-7-1) can be accomplished in two ways. One by expanding into a series and integrating term by term or by evaluating the integral in terms of complete and incomplete elliptical integrals of the first and second kind. The approximate solution was given above and the exact solution follows.

The theoretical discharge may be obtained from equation 3-7-1 by making the coefficient of discharge C_d equal to unity:

$$Q_t = 2\sqrt{2g} \int_0^{Y_1} \sqrt{(Y_1 - h)\,(r^2 - h^2)}\, dh \quad (3\text{-}7\text{-}6)$$

Let $K^2 = \frac{Y_1 + r}{2r}$ or $Y_1 = 2r\,(k^2 - 1)$, $k < 1$, $Y_1 < r$ (3-7-7) and $$\mathrm{sn}^2\, u = \frac{h + r}{Y_1 + r} \qquad (3\text{-}7\text{-}8)$$

Since $$\mathrm{sn}^2\, u + \mathrm{cn}^2\, u = 1$$

then $$h = Y_1\, \mathrm{sn}^2 u - r\mathrm{cn}^2 u = 2rk^2 \mathrm{sn}^2 u - r \qquad (3\text{-}7\text{-}9)$$

and $$\frac{dh}{du} = 4 \cdot rk^2 \mathrm{snu}\ \frac{d}{du}\ \mathrm{snu} = 4rk^2 \mathrm{snu\ cnu\ dnu} \qquad (3\text{-}7\text{-}10)$$

since $$\frac{d}{du}\ (\mathrm{snu}) = \mathrm{cnu\ dnu}$$

From (3-7-8) and making use of (3-7-7)

$$\begin{aligned} Y_1 - h &= Y_1\ (1 - \mathrm{sn}^2 u) + r\mathrm{cn}^2 u \\ &= Y_1\ \mathrm{cn}^2 u + r^2\ \mathrm{cn}^2 u \\ &= 2rk^2 \mathrm{cn}^2 u \end{aligned} \qquad (3\text{-}7\text{-}11)$$

Also from 3-7-8

$$\begin{aligned} r^2 - h^2 &= 4r^2\ k^2\ \mathrm{sn}^2 u\ (1 - k^2 \mathrm{sn}^2 u) \\ &= 4r^2\ k^2\ \mathrm{sn}^2 u\ \mathrm{dn}^2\ u \end{aligned} \qquad (3\text{-}7\text{-}12)$$

since $$\mathrm{dn}^2 u + k^2 \mathrm{sn}^2 u = 1$$

Substituting (3-7-10), (3-7-11) and (3-7-12) into (3-7-6) the expression for the theoretical discharge becomes

$$Q_t = 2\sqrt{2g} \int_{u_1}^{u_2} \left[2rk^2 \mathrm{cn}^2 u \cdot 4r^2 k^2 \mathrm{sn}^2 u\ \mathrm{dn}^2 u \right]^{\frac{1}{2}} 4rk^2 \mathrm{snu\ dnu\ cnu\ du} =$$

$$= 32\sqrt{g}\, r^{5/2}\, k^4 \int_{u_1}^{u_2} \mathrm{cn}^2 u\ \mathrm{sn}^2 u\ \mathrm{dn}^2 u\ du \qquad (3\text{-}7\text{-}13)$$

The lower limit u_1 is obtained from (3-7-8) as follows:

$$\mathrm{sn}^2 u_1 = \frac{0 + r}{Y_1 + r}$$

or $$\mathrm{sn}u_1 = \sin\phi = \sqrt{\frac{r}{Y_1 + r}}$$

where $$\phi = \mathrm{am}\, u_1$$

and finally $$u_1 = F(\phi, k) = \int_0^{\phi} \frac{d\phi}{\sqrt{1 - k^2 \sin\phi}} \quad , \quad k < 1 \qquad (3\text{-}7\text{-}14)$$

$F(\phi, k)$ is the incomplete elliptic integral of the first kind.

the upper limit u_2, is obtained from (3-7-8) as follows:

$$\mathrm{sn}^2 u_2 = \frac{Y_1 + r}{Y_1 + r} = 1$$

or $$\mathrm{sn}\, u_2 = 1$$

and $$u_2 = K = \int_0^{\pi/2} \frac{d\,\phi}{\sqrt{1 - k^2 \sin\phi}} \qquad (3\text{-}7\text{-}15)$$

where K is the complete elliptic integral of the first kind

The expression for the theoretical discharge (3-4-13) becomes

$$Q_t = 32\sqrt{g}\; r^{5/2}\, k^4 \int_{F(\phi,\, k)}^{K} \mathrm{cn}^2 u\; \mathrm{dn}^2 u\; \mathrm{sn}^2\, u\; du \qquad (3\text{-}7\text{-}16)$$

Upon performing the integration, and introducing the diameter $b = 2r$

$$Q_t = \frac{4}{15}\sqrt{2g}\; b^{5/2}\Big\{ 2(1-k^2 + k^4)\left[E - E(\phi, k)\right] - (1-k^2)(2-k^2)\left[K - F(\phi, k)\right]$$
$$- k^2 \sin\phi \cos\phi\, \Delta\phi\, (3k^2 \sin^2\phi - 1 - k^2)\Big\} \qquad (3\text{-}7\text{-}17)$$

where $$E = \int_0^{\pi/2} \sqrt{1 - k^2 \sin^2\phi}\; d\,\phi \qquad (3\text{-}7\text{-}18)$$

which is the complete elliptic integral of the second kind, and

$$E(\phi, k) = \int_0^{\phi} \sqrt{1 - k^2 \sin^2\phi}\; d\,0 \qquad (3\text{-}7\text{-}19)$$

which is the incomplete elliptic integral of the second kind, and

$$\phi = \sin^{-1}\sqrt{\frac{r}{Y_1+r}} \tag{3-7-20}$$

and

$$\Delta\phi = \sqrt{1 - k^2 \sin^2 \phi} = \sqrt{0.5} \tag{3-7-21}$$

and finally

$$k = \sqrt{\frac{Y_1 + r}{b}} \tag{3-7-22}$$

Equation (3-7-17) yields the theoretical discharge for the flow through a semicircular constriction of diameter $b = 2r$ and where the maximum depth upstream of the constriction is y_1. The quantities K, E, $F(\phi, k)$, $E(\phi, k)$ may be obtained from tables. Equation (3-7-17) is somewhat similar to that for the flow through circular weirs obtained by J. C. Stevens[7] which is

$$Q_t = \frac{4}{15}\sqrt{2g}\; D^{5/2}\left\{2(1 - k^2 + k^4)\, E - (2 - k^2)(1 - k^2)\, K\right\} \tag{3-7-23}$$

where $k^2 = H/D$, H being the head over the invert, and D is the diameter of the circular weir. Stevens also gives an infinite series approximation to equation (3-7-23) which is similar to equation (3-7-2):

$$Q_t = 2\sqrt{2g}\, D^{5/2}\left(\frac{1}{8}z^2 - \frac{1}{32}z^3 - \frac{5}{1024}z^4 \ldots\ldots\right) \tag{3-7-24}$$

where $z = H/D$.

b) <u>The Equation of Discharge for Orifice Flow</u>

With reference to Fig. 3-11 and neglecting the velocity of approach, the discharge is found to be:

$$Q = \int V\, dA = 2\, C_d \sqrt{2g}\int_0^r (Y_1 - h)^{\frac{1}{2}}\,(r^2 - h^2)^{\frac{1}{2}}\, dh \tag{3-7-25}$$

An approximate solution to the above integral is found by expanding each term of the integrand into a binomial series, multiplying the two series and integrating term by term. The result, using the 5 leading terms is

$$Q = 0.4019\ C_d \sqrt{2g}\ Y^{\frac{1}{2}}\ b^2 \left[1 - 0.2136 \left(\frac{r}{Y_1}\right) - 0.03216 \left(\frac{r}{Y_1}\right)^2 - 0.0112 \left(\frac{r}{Y_1}\right)^3 - 0.005344 \left(\frac{r}{Y_1}\right)^4 \dots \right] \qquad (3\text{-}7\text{-}26)$$

or

$$Q = C_1\ Y_1^{\frac{1}{2}}\ b^2\ T \qquad (3\text{-}7\text{-}27)$$

where

$$C_1 = 0.4019 \sqrt{2g}\ \ C_d = 3.22\ C_d \qquad (3\text{-}7\text{-}28)$$

and

$$T = 1 - 0.2136 \left(\frac{r}{Y_1}\right) - 0.03216 \left(\frac{r}{Y_1}\right)^2 - 0.0112 \left(\frac{r}{Y_1}\right)^3 - 0.005344 \left(\frac{r}{Y_1}\right)^4 \qquad (3\text{-}7\text{-}29)$$

The above equation is valid as long as the constriction is submerged, which means for $Y_1 > r$.

A simpler form of the orifice discharge equation when the approach velocity is very low relative to the velocity in the discharge jet, and when the orifice is considered as a whole is:

$$Q = C_d^{\frac{1}{2}}\ \frac{\pi d^2}{4}\ \sqrt{2g\ Y_1} \qquad (3\text{-}7\text{-}30)$$

where Q = discharge through the opening

d = diameter of the opening

and Y_1 = the depth of the backwater

C_d = coefficient of discharge for type of inlet

Now rearranging equation (3-7-30):

$$\frac{Q^2}{g\ d^4} = \frac{C_d^2\ \pi^2}{32}\ Y_1 \qquad (3\text{-}7\text{-}31)$$

By dividing by d, and taking the square root of both sides of (3-7-31), the following dimensionless equation is obtained

$$\frac{Q}{g^{\frac{1}{2}}\, d^{5/2}} = \frac{C_d\, \pi}{\sqrt{32}} \left(\frac{Y_1}{d}\right)^{\frac{1}{2}} \qquad (3\text{-}7\text{-}32)$$

where $\frac{C_d\, \pi}{\sqrt{32}}$ is a constant.

The previous equation may be written in the general form

$$\frac{Q}{g^{\frac{1}{2}}\, d^{5/2}} = f\left(\frac{Y_1}{d}\right) \qquad (3\text{-}7\text{-}33)$$

which is used in plotting experimental results.

III-8 Energy Loss in the Constriction

It has been shown that a complete theoretical analysis is not possible. However, some important conclusions regarding the classification of flow types and limiting cases have been obtained from momentum and energy considerations. The applicability of the momentum and energy equations is limited principally by the difficulty of formulating the drag force and the head losses. Izzard[8] and Bradley[9] have proposed an empirical relation for the head loss in a constriction. The head loss due to the contraction and expansion of the flow may be expressed as

$$h = K \frac{V_{2n}^2}{2g} \qquad (3\text{-}8\text{-}1)$$

where V_{2n} is a reference velocity, which is given by

$$V_{2n} = \frac{Q}{A_{2n}} \qquad (3\text{-}8\text{-}2)$$

where A_{2n} is the area of section 2 corresponding to the normal depth in the unconstricted flow.

The energy equation, written between sections 1 and 4 is:

$$Y_1 + \alpha_1 \frac{V_1^2}{2g} + S_o L_{1-4} = Y_4 + \alpha_4 \frac{V_4^2}{2g} + E_{1-4} \qquad (3\text{-}8\text{-}3)$$

where E_{1-4} is the total energy loss between sections 1 and 4. This energy loss is made of two parts: the normal boundary resistance plus the additional loss due to the contraction and expansion of the flow:

$$E_{1-4} = S_o L_{1-4} + K \frac{V_{n2}^2}{2g} \qquad (3\text{-}8\text{-}4)$$

Replacing in the energy equation

$$Y_1 - Y_4 = K \frac{V_{n2}^2}{2g} + \alpha_4 \frac{V_4^2}{2g} + \alpha_1 \frac{V_1^2}{2g} \qquad (3\text{-}8\text{-}5)$$

Since at section 4 the normal depth has been regained $Y_4 = Y_n$, and making use of the continuity equation

$$V_1\, A_1 = V_4\, A_4 = V_{n2}\, A_{n2} \qquad (3\text{-}8\text{-}6)$$

$$Y_1 - Y_n = h_1^* = K\,\frac{V_{n2}}{2g} + \left[\alpha_4 \left(\frac{A_{n2}}{A_4}\right)^2 - \alpha_1 \left(\frac{A_{n2}}{A_1}\right)^2\right] \frac{V_{n2}}{2g}^2 \qquad (3\text{-}8\text{-}7)$$

from which

$$K = \frac{h_1^*}{V_{n2}^2/2g} - \left[\alpha_4 \left(\frac{A_{n2}}{A_4}\right)^2 - \alpha_1 \left(\frac{A_{n2}}{A_1}\right)^2\right] \qquad (3\text{-}8\text{-}8)$$

or approximately

$$K = h_1^*/(Y_{n2}^2/2g) \qquad (3\text{-}8\text{-}9)$$

The same results are valid for submerged constriction, when the total cross sectional area of the constriction A_o is taken as reference area instead of A_{n2}. Then the head loss due to the contraction and expansion of the flow is written as

$$h_f = K\,\frac{V_o^2}{2g} \qquad (3\text{-}8\text{-}10)$$

where

$$V_o = \frac{Q}{A_o} \qquad (3\text{-}8\text{-}11)$$

and as before

$$h_1^* = K\,\frac{V_o^2}{2g} + \left[\alpha_4 \left(\frac{V_4}{V_o}\right)^2 \frac{V_o^2}{2g} - \alpha_1 \left(\frac{V_1}{V_o}\right)^2\right] \frac{V_o^2}{2g} \qquad (3\text{-}8\text{-}12)$$

and

$$K = \frac{h_1^*}{V_o^2/2g} - \left[\alpha_4 \left(\frac{A_o}{A_4}\right)^2 - \alpha_1 \left(\frac{A_o}{A_1}\right)^2\right] \qquad (3\text{-}8\text{-}13)$$

In formulas 7-8-7, 7-8-8 and 7-8-12, 7-8-13, a simplification may be obtained by assuming $\alpha_1 = \alpha_4 = \alpha$.

An alternate simplified expression for the head loss in the contracting flow may be obtained by considering the contraction as an orifice, and by assuming that the depth at the orifice is the normal depth. With these assumptions, and neglecting the velocity head of approach $V_{n1}^2/2g$, the energy equation yields

$$\frac{V_{n2}^2}{2g} = Y_1 - Y_n \qquad (3\text{-}8\text{-}14)$$

Introducing a coefficient of velocity

$$C_v = C_v\,(M', F) \qquad (3\text{-}8\text{-}15)$$

where M' is the channel opening ratio, then

$$V_{n2}^2 = C_v^2\, 2g\, (Y_1 - Y_n) \qquad (3\text{-}8\text{-}16)$$

Introducing an orifice Froude number defined by

$$F_o^2 = \frac{V_{n2}^2}{gY_n} = 2C_v^2 \left(\frac{Y_1}{Y_n} - 1\right) \qquad (3\text{-}8\text{-}17)$$

then

$$\frac{Y_1}{Y_n} - 1 = \frac{1}{2}\left(\frac{F_o}{C_v}\right)^2 \qquad (3\text{-}8\text{-}18)$$

But as

$$\left(\frac{F_o}{F_1}\right)^2 = \left(\frac{V_{n2}}{V_{n1}}\right)^2 = \left(\frac{A_{n2}}{A_{n1}}\right)^2 = \left(\frac{1}{M'}\right)^2 \qquad (3\text{-}8\text{-}19)$$

then

$$\frac{Y_1}{Y_n} - 1 = \frac{1}{2C_v^2}\left(\frac{F_1}{M'}\right)^2 \qquad (3\text{-}8\text{-}20)$$

The head loss through an orifice is given by

$$h_f = \left(\frac{1}{C_v^2} - 1\right)\frac{V^2}{2g} \qquad (3\text{-}8\text{-}21)$$

so that the head loss in the contracting flow is, in dimensionless form,

$$\frac{h_f}{y_n} = \left(\frac{1}{C_v^2} - 1\right)\frac{V_n^2}{2gY_n} = \frac{1}{2}\left(\frac{1}{C_v^2} - 1\right)\left(\frac{F_n}{M_1}\right)^2 \qquad (3\text{-}8\text{-}22)$$

But, by meansof (3-8-20)

$$\frac{1}{C_v^2} = 1 + \frac{2\left(\frac{Y_1}{Y_n} - 1\right)}{\left(\frac{F_n}{M}\right)^2} - 1 \qquad \text{([illegible])}$$

and (7-8-[illegible]2) becomes:

$$\frac{h_f}{Y_n} = \left(\frac{Y_1}{Y_n} - 1\right) - \frac{1}{2}\left(\frac{F_n}{M}\right)^2 \qquad \text{([illegible])}$$

As experiments have shown that in general

$$\frac{Y_1}{Y_n} = f\left(\frac{F_n}{M}\right)^2$$

then, in general

$$\frac{h_Y}{Y_n} = f\left(\frac{F_n}{M}\right)^2 \qquad \text{(7-8-[illegible])}$$

III-9 Backwater Ratio Equations

The backwater ratio is defined as the ratio of the maximum centerline water depth to the normal depth of flow.

Expressions for the backwater ratio may be obtained from the energy equation or from the discharge equation. The use of the energy equation will be considered first.

The energy equation is written in dimensionless form by dividing both sides by Y_n:

$$\frac{h_1^*}{Y_n} = \frac{1}{2}\left(\frac{F_n}{M'}\right)^2 \left[\alpha_4 M'^2 - \alpha_1 M'^2 \left(1 - 2\frac{h_1^*}{Y_n}\right) - K\right] \qquad (3\text{-}9\text{-}6)$$

Assuming $\alpha_1 = \alpha_4 = \alpha$ it follows that

$$\frac{h_1^*}{Y_n} = \frac{1}{2}\left(\frac{F_n}{M'}\right)^2 \left[2\ M' \frac{h_1^*}{Y_n} + K\right] \qquad (3\text{-}9\text{-}7)$$

or

$$\frac{h_1^*}{Y_n}\left[1 - \alpha F_n^2\right] = \frac{1}{2}\left(\frac{F_n}{M'}\right)^2 K \qquad (3\text{-}9\text{-}8)$$

whence

$$\frac{h_1^*}{Y_n} = \left(\frac{F_n}{M'}\right)^2 \frac{\frac{1}{2}K}{1 - (F_n)^2\alpha} \qquad (3\text{-}9\text{-}9)$$

In general, the expression for the backwater ratio for free surface flow is:

$$\frac{h_1^*}{Y_1} = D\left(\frac{F_n}{M'}\right)^2 \qquad (3\text{-}9\text{-}10)$$

where

$$D = \frac{1/2\ K}{1 - (F_n)^2\alpha} \qquad (3\text{-}9\text{-}11)$$

is a factor related to the head loss in the constriction.

This result is valid only when the flow is subcritical through the constriction and when $h_1^*/Y_n < 1$.

Experimental results have yielded the empirical relation (for single span semi-circular arches, see Chapter V).

$$\frac{h_1^*}{Y_n} = 0.45 \left(\frac{F_n}{M'}\right)^2 \qquad (3\text{-}9\text{-}12)$$

with this result

$$D = \frac{1/2\ K}{1 - F_n^2 \alpha} = 0.45 \qquad (3\text{-}9\text{-}13)$$

or

$$K = 0.90\ (1 - \alpha F_n^2) \qquad (3\text{-}9\text{-}14)$$

or with $\alpha = 1$

$$K = 0.90\ (1 - F_n^2) \qquad (3\text{-}9\text{-}15)$$

The test results are presented in the form of plots of $\frac{h_1^*}{Y_1}$ vs $\left(\frac{F_n}{M'}\right)^2$ and least square curves of the form

$$\frac{h_1^*}{Y_n} = C \left(\frac{F_n^2}{M'^2}\right)^n \qquad (3\text{-}9\text{-}16)$$

are obtained. As from equation (3-9-10), D is the slope of the curve of h_1^*/Y_n vs $(F_n/M')^2$, it follows from equation (3-9-16) that

$$\frac{d\left(\frac{h_1^*}{Y_n}\right)}{d\left(\frac{F_n}{M'}\right)^2} = nc \left(\frac{F_n^2}{M'^2}\right)^{n-1} = D \qquad (3\text{-}9\text{-}17)$$

Alternate expressions for the backwater ratio may be obtained from the discharge equation for free surface and for orifice flow separately.

Consider the free surface flow case first. The equation for the discharge through the constriction is (from equ. 3-7-3)

$$Q = C_1\ Y_1^{3/2}\ b\ T_1 \qquad (3\text{-}9\text{-}18)$$

where

$$C_1 = Cd\ \frac{17}{24}\ \sqrt{2g} \qquad (3\text{-}9\text{-}19)$$

and

$$T_1 = 1 - 0.1294 \left(\frac{Y_1}{r}\right)^2 - 0.0177 \left(\frac{Y_1}{r}\right)^4 \qquad (3\text{-}9\text{-}20)$$

The discharge in the approach channel is

$$Q = V_n A_n = F_n \sqrt{g} \quad B Y_n^{3/2} \tag{3-9-21}$$

Equating the two expressions for the discharge one obtains

$$\frac{Y_1}{Y_n} = \left[\frac{12\sqrt{2}\,F_n}{17 C_d\,MT_1}\right]^{2/3} \tag{3-9-22}$$

or in general

$$\frac{Y_1}{Y_n} = C\left(\frac{F_n}{M'}\right)^{2/3} \tag{3-9-23}$$

where

$$C = \frac{12 \quad 2 \quad C_m}{17\ C_d \quad T}^{2/3} \tag{3-9-24}$$

Since $M = M'/C_m$ (see equation 3-10-8)

Experimental results for free surface flow have yielded the following relation (see chapter VII)

$$\frac{Y_1}{Y_n} = 1 + 0.47\left[\left(\frac{F_n}{M'}\right)^{2/3}\right] 3.39 \tag{3-9-25}$$

It has been observed that the equations derived by several different investigators for the backwater ratio produced by various constriction geometries seem to have a basic similarity. As an example, equation (23) in the present text for y_1/y_n appears to be a function of $(F/M')^{2/3}$.

$$y_1/y_n = g_1\ (F_n/M')^{2/3} \tag{3-9-26}$$

An equation for the backwater ratio given by Valentine[8] for lateral constriction plates is

$$y_1/y_n = (g\ F_n/\ C\ M)^{2/3} = g_2\ (F_n/M')^{2/3} \tag{3-9-27}$$

where C = a discharge coefficient

and $M = b/B = M'$ since $C_M = 1$

Also Liu et al[11] present an empirical formula for a two dimensional vertical board model

$$(h_1^*/h_n)^3 = 4.483\ F_n^2\ (\frac{1}{M^2} - \frac{2}{3}(2.5 - M)) - 1 \qquad (3\text{-}9\text{-}28)$$

where $M = b/B = M'$ since $C_M = 1$

Considering only the leading term $1/M^2$ of the quantity in brackets, equation (3-9-28) becomes

$$h_1^*/y_n = g_3\ (F_n/M')^{2/3} \qquad (3\text{-}9\text{-}29)$$

It appears that with the proper interpretation of the variables, namely M' and F_n, the results of tests performed on different geometric shapes of bridge openings should produce the same results. For instance, a vertical abutment deck type bridge may physically appear completely different than a semicircular arch bridge. However, hydraulically speaking if they have the same opening ratio M', they should produce the same backwater ratio. The limitations of the assumption must necessarily lie in the fact that both bridges must have the same eccentricity, skewness and entrance rounding conditions. It is believed that this concept applies equally as well to multiple span bridges. An attempt has been made to compare the two dimensional semi-circular test results of the author, the segment data obtained by A. A. Sooky, and the Vertical Board (VB) data as given by Liu[11]. The results of this comparison will be shown and discussed in a later section.

A similar expression for the backwater ratio may be obtained from the theoretical discharge equation for orifice flow. The equation for the discharge through the constriction was found to be: (see equ. 3-7-27)

$$Q = C_1\ Y_1^{\frac{1}{2}}\ b^2\ T \qquad (3\text{-}9\text{-}30)$$

The discharge in the approach channel is:

$$Q = V_n\ A_n = F_n\ \sqrt{g}\ \ B\ Y_n^{3/2} \qquad (3\text{-}9\text{-}31)$$

Equating the two discharge equations (3-9-30 and 3-9-31):

$$C_1\ Y_1^{\frac{1}{2}}\ b^2\ T = F_n \sqrt{g}\ \ Y_n^{3/2}\ B \qquad (3\text{-}9\text{-}32)$$

and

$$C_1 = \left(\frac{Y_n}{Y_1}\right)^{\frac{1}{2}} \frac{F_n BY_n}{b^2 T} = \left(\frac{Y_n}{Y_1}\right)^{\frac{1}{2}} \left(\frac{B}{b} \cdot \frac{Y_n}{b}\right) F_n \frac{1}{T} \qquad (3\text{-}9\text{-}33)$$

but

$$\frac{B}{b} \cdot \frac{Y_n}{b} = \frac{A_n}{k A_o} = \frac{1}{k M'}$$

where

$$k = \frac{8}{\pi}$$

Now rearranging the equation (3-9-33):

$$\frac{Y_1}{Y_n} = \left(\frac{1}{k M'} F_n \cdot \frac{1}{C_1} \cdot \frac{1}{T}\right)^2 \qquad (3\text{-}9\text{-}34)$$

or in general a relation of the following form would be expected

$$\frac{Y_1}{Y_n} = C \left(\frac{F_n}{M'}\right)^2 . \qquad (3\text{-}9\text{-}35)$$

It has been found empirically that, instead of equation (3-9-35), the experimental results can conveniently be represented by a function of the form:

$$\frac{h_1^*}{Y_n} = \frac{Y_1}{Y_n} - 1 = f \left(\frac{F_n}{M'}\right)^2 \qquad (3\text{-}9\text{-}36)$$

where h_1^* is the backwater superelevation.

Experimental results for the orifice flow have yielded the following relation (see Chapter VII)

$$\frac{Y_1}{Y_n} = 1 + 1.18 \left[\left(\frac{F_n}{M'}\right)^2\right]^{0.90} \qquad (3\text{-}9\text{-}37)$$

or

$$\frac{Y_1}{Y_n} = 1 + 1.18 \left(\frac{F_n}{M'}\right)^{1.80} \qquad (3\text{-}9\text{-}38)$$

The experimental result for the backwater ratio equation for free surface was developed by P. F. Biery and found to yield the relation (see chapter V)

$$\frac{Y_1}{Y_n} = 1 + 0.47 \left[\left(\frac{F_n}{M'}\right)^{2/3} \right]^{3.39} \qquad (3\text{-}9\text{-}39)$$

or

$$\frac{Y_1}{Y_n} = 1 + 0.47 \left(\frac{F_n}{M'}\right)^{2.26} \qquad (3\text{-}9\text{-}40)$$

III-10 Dimensional Consideration

a) Dimensional Analysis

Figure 3-1 shows a definition sketch of the effects of a channel constriction on the water surface profile. Section view B illustrates the type of centerline profile obtained with a Class I flow. This is the most generally occurring situation that appears in actual practice. In the figure Y_o or Y_n is the normal depth of the unobstructed channel. Y_1 is the depth at the point of maximum backwater elevation. Y_2 is the depth at the section of minimum jet area or the vena contracta. Y_3 is the minimum water depth of the regain curve, and Y_4 is at a point sufficiently downstream from the contraction where the flow returns to the normal depth.

For any physical problem such as this, a dimensional analysis is convenient for the purpose of guidance and interpretation of a testing program. In this manner, the basic variables can be grouped into dimensionless quantities and their relationships investigated. In the problem at hand, it is desired to determine the maximum water depth upstream of the constriction. It is assumed that the variables which govern the backwater superelevation may be grouped into three categories as follows: the fluid properties, the kinematic and dynamic variables, and the dimensions defining the boundary geometry. Due to the two dimensional character of the constriction, the latter is expressed in terms of flow areas rather than the usual linear dimensions. (See figure 3-1 for an illustration of the terminology.)

The variables are:

a) Fluid Properties

1) ν , the kinematic viscosity of the fluid

2) ρ , density of the fluid

b) Kinematic and Dynamic Flow Variables

1) g, acceleration of gravity

2) Y_1, maximum water depth upstream of the constriction

3) Y_n, the normal depth of flow in the approach channel.

4) V_n, the velocity of flow at normal depth

5) n, Manning's roughness coefficient of the approach channel

c) Properties of the Constriction Geometry (see figures 2, 4, and 24 for definition of symbols).

1) A_{n1}, the total normal depth flow area at section 1.

2) A_{n2}, the normal depth flow area in the opening of the constriction (see Fig. 4). $A_{n2} = A_o$ for submerged bridges.

3) L/b, thickness factor, where L is the length of bridge in direction of flow, b is the width of opening at the bottom.

4) bL_d/A_{n2}, distance factor where L_d is the distance between two parallel identical bridges.

5) ϕ_1, wing wall angles

6) ϕ_2, skew angle

7) β, segment factor defined by = d/r where d is the distance between the channel bottom and the center of the circular segment.

8) N, number of spans

9) e, eccentricity defined by $e = 1 - c/a$, where c and a are the width on either sides of the bridge openings.

From the above list of variables,

$$Y_1 = f_1 \left(Y_n, V_n, n, \nu, h, V, \rho, g, A_{n1}, A_{n2}, L/b, \frac{bL_d}{A_{n2}}, \phi_1, \phi_2, e, \beta, N\right)$$

Buckingham's theorem states that in a physical problem including n quantities in which there are m dimensions, the quantities may be arranged into (n-m) dimensionless parameters. With the mass, length and time system of units, the n-m or 14 dimensionless parameters are as follows:

$$\frac{Y_1}{Y_n} = f_2 \left(\frac{V_n^2}{Y_n g}, \frac{V_n Y_n}{\nu}, \frac{n}{Y_n^{1/6}}, \frac{A_{n1}}{Y_n^2}, \frac{A_{n2}}{Y_n^2}, \frac{h}{Y_n}, \frac{L}{b}, \frac{bL_d}{A_{n2}}, \phi_1, \phi_2, e, \beta, N\right)$$

where $\frac{V_n^2}{Y_n g}$ is the square of the Froude number F_n and $\frac{V_n Y_n}{\nu}$ is the Reynolds number R. It is known that:

1) Viscous forces play a negligible role in open channel flow. So the term R can be neglected. Furthermore, by combining the ratio A_{n2}/Y_{n2} and A_{n1}/Y_n^2 into $A_{n2}/A_{n1} = M'$, and letting n be constant, which means that the boundary roughness in the flume is kept the same, then the above equation simplifies to:

$$\frac{Y_1}{Y_n} = f\left(Fn,\ M',\ \frac{L}{b},\ \frac{bLd}{An2},\ \phi_1,\ \phi_2,\ e,\ \beta,\ N\right) \qquad (3\text{-}10\text{-}1)$$

Of the nine variables only two, the Froude number and the contraction ratio describe the flow field. The other seven variables in the dimensionless analysis describe the different model geometries that could be tested separately. For a definition of the separate geometries see section on Definition of Test Geometries.

b) Definition of Channel Opening Ratio and Channel Width Ratio

The channel opening ratio (M') is defined as that portion of the total normal depth flow that can pass through the bridge waterway without contraction. By definition it is equivalent to the ratio A_{n2}/A_{n1} obtained from the dimensional analysis. Along with the normal depth Froude number, the opening ratio is perhaps the most critical variable in the problem.

Referring to figure 3-12-a for the rectangular case, the total flow is that flow in area ADEH, and the flow that passes through the bridge opening without contraction is that represented by the area BCFG. Therefore the opening ratio M' is

$$M' = q/Q \qquad (3\text{-}10\text{-}2)$$

If we assume that there is a constant uniform velocity V_n across the entire normal depth section, equation (3-10-2) becomes

$$M' = q/Q = A_{n2}V_n/A_{n1}V_n = A_{n2}/A_{n1} = by_n/By_n = b/B \qquad (3\text{-}10\text{-}3)$$

However, for an arch bridge, as shown also in figure (3-12-b), the surface width will be different for each and every normal depth y_n. Therefore in the same manner:

$$M' = q/Q = A_{n2}V_n/A_{n1}V_n = A_{n2}/A_{n1} \qquad (3\text{-}10\text{-}4)$$

The ratio of the two areas is clearly not equivalent to b/B. (for simplicity, b/B is hereafter defined by the symbol M)

For the portion GIKF of a semicircular arch with radius r and depth y_n the area becomes

$$A_{n2} = \int_0^{y_n} 2\sqrt{r^2 - y^2}\, dy = 2\left[\tfrac{1}{2}\left\{ y_n\sqrt{r^2 - y_n^2} + r^2 \sin^{-1} y_n/r \right\}\right] \qquad (3\text{-}10\text{-}5)$$

The segment of arch GECF shown in figure 3-12-b has a radius r and springline width b. The arch has been superimposed upon the flow area of depth y_n. The center of curvature is at a distance d below the springline of the arch. The flow area (A_{n1}) of the rectangular channel is By_n, while the area GECF is given by

$$A_{n2} = \int_0^{D} 2\sqrt{r^2 - y^2}\, dy - \int_0^{d} 2\sqrt{r^2 - y^2}\, dy \qquad (3\text{-}10\text{-}6)$$

and the corresponding channel opening ratio is

$$M' = A_{n2}/A_{n1} = \frac{D\sqrt{r^2 - D^2} + r^2 \sin^{-1} D/r}{By_n} - \frac{d\sqrt{r^2 - d^2} + r^2 \sin^{-1} d/r}{By_n} \qquad (3\text{-}10\text{-}7)$$

The channel opening ratio M' can be expressed in terms of three other dimensionless ratios: the ratio of span to channel width M = b/B, the ratio of depth of the arch center below the streambed to the arch radius $\eta = d/r$ and the ratio of normal depth to arch radius $\zeta = y_n/r$. The channel opening ratio of equation (3-10-7) may thus be expressed as:

$$M' = MC_M$$

in which

$$M = b/B \qquad (3\text{-}10\text{-}8)$$

and the channel opening ratio coefficient is

$$C_M = \frac{1}{2}\left[\left\{\frac{\sqrt{1-(\eta+\zeta)^2} + \frac{1}{\eta+\zeta}\sin^{-1}(\eta+\zeta)}{\frac{\zeta}{\eta+\zeta}\,(1-\eta^2)^{1/2}}\right\} - \left\{\frac{\sqrt{1-\eta^2} + \frac{1}{\eta}\sin^{-1}\eta}{\frac{\zeta}{\eta}\,(1-\eta^2)^{1/2}}\right\}\right] \qquad (3\text{-}10\text{-}9)$$

with $\eta = d/r$

and $\zeta = y_n/r$

In the form of equation (3-10-8) the value of $M = b/B$ is adjusted for the particular arch by an amount equivalent to C_M such that M' is the same as the ratio of A_{n2} to A_{n1}. In the more general case, the values of ζ and η can take on numbers within certain limits, before the normal depth will submerge the crown of the arch. The limits are as follows:

For $\zeta = y_n/r$ $\quad 0/r \leq y_n/r \leq (r-d)/r$ (3-10-10)

or

$0 < \zeta < (1 - \eta)$

For $\eta = d/r$ $\quad 0 < \eta < 1$ (3-10-11)

When $\eta = 0$, the case of a semicircular arch with the center of curvature at the springline exists. When $\eta = 1$, the contraction reduces to two parallel abutments.

The values of C_M have been calculated for several values of ζ and η and are summarized in the graph of figure 3-13. The submergence limit represents the upper limits of both ζ and η. The segment arch which is a constant radius arch with its center of curvature below the springline of the arch (i.e. $\eta > 0$) can be used as an arch in its own right or as an approximation to an elliptical or a multiple radius arch. The value of M' for the elliptic and multiple radius arch could be determined directly from equation (3-10-4).

III-11 Definition of Test Geometries - Selection of Tests

Nine independent variables were considered in the dimensional analysis to determine the dependent variable Y_1/Y_n. Of these nine variables, seven describe different types of constriction geometries, the other two, the Froude number and the contraction ratio describe the flow field and the amount of contraction. These seven geometric variables were used to define seven types of geometries that were tested separately. These types of geometries are defined below.

Geometry I-a

Two-Dimensional Semicircle Arch Bridge Constrictions:

(Figure 3-14) The characteristics of this type of geometry are the following:

a) Since the model is two-dimensional, $\frac{L}{b} = 0$

b) Single bridge case, $L_d = 0$ and $\frac{bL_d}{An2} = 0$

c) No wingwalls, according to definition of ϕ_1, $\phi_1 = 90^\circ$

d) None-skew case, according to definition of ϕ_2, $\phi_2 = 0^\circ$

e) Semicircular case, $d' = 0$ and $\beta = \frac{d'}{r} = 0$

f) One span case, $N = 1$

g) No eccentricity, $e = 0$

h) Froude number, $F_n = \frac{V_n}{(gY_n)^{\frac{1}{2}}}$ designated as an independent variable.

i) Constriction opening ratio M', designated as an independent channel opening ratio M'

Hence, seven independent descriptive variables, $\frac{L}{b}$, $\frac{bL_d}{An2}$, e, ϕ_1, ϕ_2, β and N in the dimensionless equation (3-10-1), $\frac{Y_1}{Y_n} = f\,(F_n, M', \frac{L}{b}, \frac{bL_d}{An2}, \phi_1, \phi_2, e, \beta)$ are designated as constants and we get the relation:

$$\frac{Y_1}{Y_n} = f\,(F_n, M')$$

Geometry I-b

Three-Dimensional Semicircular Arch Bridges:

This geometry differs from the previous one only in that L is varied, thus
e parameter $\frac{L}{b}$ describing the length of the model in the direction of the flow
a variable and the dimensionless equation (3-10-1) for this case becomes

$$\frac{Y_1}{Y_n} = f\left(F_n, M', \frac{L}{b}\right)$$

Geometry II

Dual Parallel Three-Dimensional Arch Bridge Constrictions:

This geometry consists of two identical bridges of geometry I-b, placed at
listance L_d apart, measured center to center. One new variable, L_d, is introduced,
ich is characterized by the parameter $\frac{BL_d}{A_{n2}}$ (Note: For submerged bridge constric-
ns, $A_{n2} = A_o$, see Chapter III). Equation (3-10-1) simplifies for this case to:

$$\frac{Y_1}{Y_n} = f\left(F_n, M', \frac{bL_d}{A_{n2}}\right)$$

Geometry III

Three-Dimensional Arch Bridge Constriction with Wingwalls:

The geometric characteristics were as follows:

a) $\frac{L}{b} = 0.25$

b) $\frac{bL_d}{A_{n2}} = 0$

c) ϕ_1 is a variable $O_1 = 90°, 60°, 45°,$ or $30°$

d) $\phi_2 = 0°$

e) $\beta = 0$

f) $N = 1$

g) $e = 0$

h) F_n is a variable

i) M' is a variable

Hence, equation (3-10-1) can be simplified to:

$$\frac{Y_1}{Y_n} = f\,(F_n, M^\circ, \phi_1)$$

Geometry IV

Two-Dimensional Semicircular Arch Bridge Constrictions with Eccentricity:

The geometric characteristics were as follows:

a) $\frac{L}{b} = 0$

b) $\frac{bL_d}{A_{n2}} = 0$

c) $\phi_1 = 90^\circ$

d) $\phi_2 = 0^\circ$

e) $\beta = 0$

f) $N = 1$

g) e is a variable

h) F_n is a variable

i) M° is a variable

And the equation (3-10-1) can be reduced to:

$$\frac{Y_1}{Y_n} = f\,(F_n, M^\circ, e)$$

Geometry V-a

Two-Dimensional Semicircular Arch Bridge Constrictions with Skew:

The geometric characteristics were as follows:

a) $\frac{L}{b} = 0$

b) $\frac{bL_d}{A_{n2}} = 0$

c) $\phi_1 = 90^\circ$

d) ϕ_2 is a variable

e) $\beta = 0$

f) $N = 1$

g) $e = 0$

h) F_n is a variable

i) M° is a variable

And the equation (3-10-1) can be reduced to:

$$\frac{Y_1}{Y_n} = f\,(F_n, M^\circ, \phi_2)$$

Geometry V-b

Three-Dimensional Semicircular Arch Bridge Constrictions with Skew:

This geometry is the same as the previous one, except that the length of the nstriction is allowed to vary, the parameter $\frac{L}{b}$ is thus a variable and the dimen- onless equation (3-10-1) can be simplified to:

$$\frac{Y_1}{Y_n} = f\left(F_n, M', \phi_2, \frac{L}{b}\right)$$

Geometry VI

Three-Dimensional Two-Span Semicircular Arch Bridge Constrictions:

The geometric characteristics were as follows:

a) $\frac{L}{b} = 0.50$

b) $\frac{bL_d}{A_{n2}} = 0$

c) $\phi_1 = 90^o$

d) $\phi_2 = 0^o$

e) $\beta = 0$

f) $N = 2$, Two-span case

g) $e = 0$

h) F_n is a variable

i) M' is a variable

j) $p = \frac{b}{10}$ (for submerged tests)

$p = \frac{b}{3}$ (for free surface tests)

The equation (3-10-1) can be reduced to:

$$\frac{Y_1}{Y_n} = f\left(F_n, M'\right)$$

Geometry VII

Two-Dimensional Segment Arch Bridge Constrictions:

The geometric characteristics were as follows:

a) $\frac{L}{b} = 0$

b) $\frac{bL_d}{A_{n2}} = 0$

c) $\phi_1 = 90^o$

d) $\phi_2 = 0^o$

e) β is a variable

f) $N = 1$

g) $e = 0$

h) F_n is a variable

i) M' is a variable

Hence, equation (3-10-1) reduces to:

$$\frac{Y_1}{Y_n} = f\,(F_n,\ M',\ \beta)$$

BIBLIOGRAPHY OF CHAPTER III

1. Birkhoff, G., "Calculation of Potential Flow with Free Stream Lines", ASCE, Jour. Hydr. Div. Vol. 87, HY6, November, 1961.

2. Bakhmeteff, B. A., "Hydraulics of Open Channels", McGraw-Hill, 1932.

3. von Misses, R., "Berechnung von Ausfluss and Ueberfallzahlen", Zeitschrift VDI, Vol. 61, 1917, p. 447.

4. Wu, I. P. "Preliminary Study of the Indirect Determination of Flood Discharge from Contracted Bridge Openings and High Water Marks", Memorandum from I. P. Wu to Mr. J. I. Perrey, Indiana Flood Control and Water Resources Commission, August 15, 1962.

5. Henry, H. R., Discussion on "Submerged Jets" Transactions ASCE, Vol. 115, 1950, p. 687.

6. Henry, H. R., Discussion on "Open Channel Constrictions", Transactions ASCE, Vol. 120, 1955, p. 1013.

7. Stevens, J. C., "Flow Through Circular Weirs", Journal of the Hydraulics Division, ASCE, Vol. 83, No HY6, December 1957.

8. Izzard, C. F., "Discussion on Open Channel Constrictions", Trans, ASCE, 1955, Vol. 120, p. 985.

9. Bradley, J. N., "Hydraulics of Bridge Waterways", U. S. Bureau of Public Roads, U. S. Government Printing Office, August, 1960.

10. Valentine, "Flow in Rectangular Channels with Lateral Constriction Plates", La Houille Blanche, Jan. - Feb. 1953, p. 75.

11. Lui, H. K., Bradley, J. N., Plate, E. J., "Backwater Effects of Piers and Abutments". Civil Engineering Section, Colorado State University, Fort Collins, Colorado, Rept. CER57HKL10, Oct. 1957.

IV PRELIMINARY INVESTIGATION

A preliminary investigation was conducted in a small flume for the purpose of evaluating the design requirements for a larger testing flume and of establishing the testing procedure. The small flume also provided a facility where some preliminary tests could be run with scales and relative roughnesses different from those used in the large flume.

IV-1 Small Flume, Models and Test Conditions

For the purpose of preliminary testing, a small variable slope flume 6" wide and 12' long was used. The channel sides and bottom were constructed of lucite and carefully aligned by means of adjusting screws. (Fig. 4-1) The slope of the flume was controlled by a hand operated scissor jack at the lower end of the flume. An aluminum I-beam mounted horizontally above the flume served as a track for the mechanical and electric point gages used in obtaining the water surface measurements. The electric point gage consisted of two metal points of slightly different length that were wired to a set of batteries and a galvanometer. When the shorter metal point would make contact with the water surface, the longer one being already submerged, the circuit would close and the galvanometer would deflect. The flow was metered by a 1 inch orifice plate in a 2 inch supply line. Two and three dimensional tests were run with both smooth and rough boundaries. For the rough tests, the bottom and the walls were lined with copper wire mesh of 16 meshes per inch.

The two dimensional semicircular models were constructed with diameters of 3, 4 and 5 inches (see fig. 4-2). The material used was brass. The edges were machined to 1/32 of an inch and then beveled to a 45 degree angle. The two dimensional segment models were of the same type of construction as the semicircular models and had a value of $\eta = d/r$ equal to 0.5. Three three-dimensional models were built for the purpose of this preliminary testing.

The material used was "Lucite". The dimensions of the three-dimensional models are the following:

Lucite Model	Length of Model Along Stream in Inches	Arch Diameter in Inches	Rise Inches
1	9.7	7.7	1.4
2	24	5	2.5
3	24	4	2

A photograph of the models is given in Figure 4-2. Model No. 1 is a reproduction to a scale of 1/60 of the Arch Bridge in Clay County, Indiana, on State Road 246c over Branch Connley Ditch. For measuring the water surface under the bridge, vertical glass tubes were installed on the models as shown in Figure 4-4. Through these tubes the probe of an electrical point gauge could be introduced.

In all cases, an adjustable weir was used at the and of the flume. This permitted to increase the depth of flow, and to reduce the length of the M-2 curve at the free overfall so as to obtain a long test section with uniform flow. The weir height varied for the different tests. The weir heights used are indicated for the several tests.

The three-dimensional model tests were conducted for the following variable conditions:

1. Wall roughness: The channel sides and bottom were either smooth or rough, as described in the previous paragraph.
2. Slope: Three different slopes were used: $S_o = 0$, $S_o = 0.0003$, $S_o = 0.0005$.
3. Discharges The discharges used in cubic feet per second are:

Q = 0.0114	(with 0.413 in orifice meter)
0.0138	"
0.015	"
0.017	(with 1.034 in orifice meter)
0.023	"
0.028	"
0.031	"
0.0379	"
0.042	"
0.0519	"
0.0525	"

4. Models: Three models were used, designated as Nos. 1, 2, 3 and as described in previous paragraphs.

The steps of the test routine were the following:

1. Adjustment of horizontality of beam on which the point gauges travel. This was done by maintaining a pool of water in the flume, and taking the point gauge readings of the water surface at several points. The beam position was adjusted so that the point gauge readings were the same all along the beam.

2. Control of the channel slope. This was accomplished by adjusting the scissor jack until the difference between the point gauge readings of the bottom of the flume at two points 10 feet apart would be equal to ten times the desired slope.

3. Establishment of the flow. The flow was adjusted by means of a control valve so as to obtain the desired reading on the orifice meter manometer. The desired readings were obtained from the calibration curves.

4. Establishment of uniform flow. The adjustable weir at the downstream end of the flume was set so as to obtain uniform flow through most of the flume. The flow was considered uniform in a reach when constant depths were observed in that reach. Depth was measured at one foot intervals. The section of the flume with uniform flow was the test section.

5. Installation of model in flume. The models were installed in the test section so as to show the complete regain curve and as much as possible of the backwater curve. In the case of the tests with rough channel walls, no roughness was installed on the model. The bottom of the flume under the arch was covered with artificial roughness for models 2 and 3 only. For model 1 the roughness was not installed on the bottom under the bridge, but was installed along the rest of the flume.

6. Observation of the water surface profile. The water surface elevation was first measured with a mechanical point gauge along the center line of the flume upstream and downstream of the model. At a later time vertical glass tubes were installed on the models. The water surface elevation was then measured with an electrical point gauge along the centerline of the arch. The test data are tabulated in the Appendix. (Table 4-1)

-2 Test Results

The observations of the water surface profiles observed are tabulated in Table . of the Appendix.

Col. 1 is the station as read from the tape on the horizontal beam. The tape is graduated to .01 foot from downstream (station 4) to upstream (station 14).

Col. 2 is the distance along the flume in the direction of the flow. Station 14 corresponds to zero and station 4 to 10.

Col. 3 is the flume bottom point gauge reading. At each 1 foot or 2 foot interval the bottom elevation was observed with the mechanical point gauge.

Col. 4 is the water surface reading obtained with the mechanical point gauge before fixing the model, i.e., with uniform flow.

Col. 5 is the water surface reading upstream and downstream of the model obtained with the mechanical point gauge and the water surface under the bridge obtained with the electrical point gauge.

Col. 6 is the difference between Col. 4 and Col. 3, namely the normal water depth.

Col. 7 is the difference between Col. 5 and Col. 3, namely the depth of water with model in place.

Col. 8 is used for general remarks such as: slope, diameter, rise, length of model, tail weir height that were used in the particular set of readings were noted in this column.

The data pertaining to the rough boundary, two dimensional, segment arch tests he small flume and the calculations necessary for the analysis of the segment are given in Table 4-2.

The results of the two-dimensional weir tests were put in graphical form by ting the coefficient of discharge vs the Froude Number with the channel width o as the parameter. The channel width ratio M is defined as the ratio of the weir diameter b to the flume width B. This graph is shown in the upper left corner of Figure 4-5. The lower graph shows the relation of the Froude Number and the ratio of depth upstream of the weir to the normal depth.

A typical water surface profile for the three-dimensional arch bridge models is shown in Figure 4-5. In that case, the flume walls were lined with copper wire mesh of 16 meshes per inch. This gave a Manning's roughness coefficient of approximately 0.025, which is typical of many canals and natural streams. Figure 4-7 shows the results of the three-dimensional tests with smooth boundaries using bridge models of width L = 24 inches. The coefficients of discharge C_d and the ratio of the backwater depth Y_1 to the normal depth Y_o are plotted vs the Froude Number for several values of the channel width ratio M. The results of the two- and three-dimensional tests with smooth boundaries are compared in Figure 4-8. It is interesting to notice that for small Froude Numbers, say less than 0.5, C_d and the ratios $\frac{Y_1}{Y_o}$ are approximately the same for the two cases. For higher Froude Numbers, the three-dimensional tests exhibit smaller values of C_d and larger values of $\frac{Y_1}{Y_o}$.

As part of the preliminary testing, a series of 93 tests were run in the small flume on two dimensional segment weirs (Geometry VII) with a η = d/r value of 0.5 (See Table 4-2) The data obtained were reanalyzed in terms of the channel opening ratio M'. These tests were run in the small channel with rough boundaries which had a Manning's n of 0.0201. Results were plotted in the same manner as the large flume rough tests and are shown in Figure 4-8a.

V EXPERIMENTAL EQUIPMENT

V-1 Design and Construction of the Testing Flume

Before the design of the flume itself could proceed, it was necessary to determine whether the backwater and regain phenomena could be represented to a convenient and easily measurable scale in the space available in the hydraulics laboratory.

Several sets of arch bridge plans provided by the Indiana State Highway Department were analyzed for the values of backwater. The theory of varied flow and the equations and tables presented by Bakhmeteff(1) and by the U.S. Bureau of Public Roads(2) were used. It was possible to make only an approximate calculation of the backwater because of the unknown effect of an arch-type constriction.

One criterion for the selection of the flume size was that it had to be sufficiently long to accommodate the full length of the regain curve downstream of the constriction, the bridge width and part of the backwater curve upstream of the constriction within the test section of the flume. The test section of the flume includes only that part of the flume where uniform flow can be obtained. The upstream end of the flume where the flow is developing, and the downstream end which is affected by the curvature of the free surface are not suitable for testing. The limitations on the flume size were imposed by the space available and by the capacity of the water supply.

A calculation was made for bridge S79 in Clay County in Indiana. This bridge has a span of 30 feet and the stream has a width of 46 feet. The backwater curve and the regain curve were calculated assuming a velocity of 6 ft/sec in the constriction. The prototype bridge had a width of 48 feet and the calculated length of the regain curve was 146 feet. At a scale of 1:10 this would represent a length of 19.4 feet. In a test section of 30 feet in length, it would be possible to reproduce a 100 foot section of the upstream backwater.

Taking into account the boundary layer growth at the entrance of the flume and the drop-off curve at the downstream end, a total length of about 60 feet was required. A width of 5 feet and a depth of 2 feet was consistent with the scale of 1/10 for this bridge crossing. These flume dimensions required a pumping capacity which was close to the maximum supply available of 2100 GPM.

From this and similar computations and from the small flume tests,(1) it appeared that a flume length of 64 feet utilizing all of the available space in the laboratory would be satisfactory.

The width of the flume was fixed at 5 feet. This was based on a consideration of the scale ratios and the space available. The cross section of the flume was to be rectangular since this configuration lent itself well to both ease of construction and adaption.

In order to test the flows under varying slope conditions, the flume was to be tiltable about one end. Screw jacks were selected for the slope control because of accuracy and ease of operation, as well as permanence and appearance.

In order to keep the deflections due to the variable weight of water within the same order of magnitude of the smallest readings of the point gage for depth measurement, 0.1 mm, the flume bottom was designed of 1/4 inch steel plate supported at 2 foot intervals on channels. The channels in turn were to be supported by two main beams riding on the jacks. The side plates were designed of 1/4 inch steel plate supported by vertical angles resting on the channel members. A longitudinal horizontal angle mounted on the vertical angles served as a support for the guide rails. The guide rails, which serve as a reference plane from which measurments are based, were to be polished stainless steel to minimize corrosion and scale.

The design was based on a possible water depth of 2 feet. The distance between beam supports was set as 20 feet. Simply supported connection was assumed. The beams were selected so that their deflections would be negligible. The beam first selected was an 18 I 54.7 which gave a calculated deflection of 0.00225 feet under the design loading. Contacts with the fabricator and erector were made at a later date and it was found that a 20 I 65.4 would be available at a cost less than that of the lighter beam. The use of the heavier beam was accepted and the design proceeded based on this beam. The deflection due to the variable water weight was approximately 0.002 feet for a depth of one foot. Adjustment bolts were provided for transverse leveling. These adjustment bolts were placed between the channels and the main beams. This arrangement gave the bottom plate full support across its width at 2 foot intervals.

The bottom plate was designed slightly wider than the flume width. This permitted attaching an angle to hold the bottom edge of the vertical plate fixed. The upper edge of the vertical plate had nuts welded on at the two foot points. Studs were attached between the nuts and the vertical angles to support the plate and provide an adjustment for its longitudinal alignment. The inside of the flume was finished with an epoxy resin applied with a hand roller. The flume construction is shown in figure 5-1.

Tailgate

Control over the depth was exercised by a gate mounted at the end of the flume. The gate was manually operated from the side of the flume. Figure 5-3 shows the gate. The gate was made in such a way that it could be used either as a sluice or as a weir. Throughout the tests, the gate was used exclusively as a weir.

Forebay

The forebay, 8 feet wide and 10 feet long, was constructed of plywood and lined with sheet metal, and is shown in figure 5-4. The 3 inch and 6 inch pipes entered the rear of the forebay at the top. The 6 inch line was centered and the 3 inch line was placed slightly off center. The diffusing mechanism for each supply line consisted of a tee and cross pipe of the same size as the line at the bottom of the forebay. The turbulence level of the entering water was controlled by a 4 inch gravel baffle and three wire mesh screens of 13 mesh per inch. The transition section continuing into the bottom and side walls of the flume was made of quarter ellipses in the horizontal and vertical planes respectively with a ratio of major to minor axes of 1.5 to 1.0. The joint between the flume and the forebay was sealed with a flexible rubber gasket mounted so as not to interfere with the flow.

Slope Control Mechanism

The flume rests upon six screw jacks and a hinge. The hinge is located at the joint of the flume and the forebay. The jacks are similar in all respects with the exception of the gear ratio. The jacks are divided into three pairs with rates of raise of one, two, and three inches for 96 turns of the shaft. Since the hinge was a fixed point and the opposite end of the flume was the point of maximum movement, the jacks were arranged such that the pair nearest the hinge moved the least and the pair at the opposite end of the flume had largest displacement per revolution. This maintained the bottom of the flume as a plane while it was being raised and lowered. The jacks on each side of the flume were driven by a common 1 inch shaft line connected at one end to a 90° miter gear. The miter gears on either side in turn were connected to a single 60:1 ratio gear reducer. The power to operate all the jacks was supplied by a 1-1/2 horsepower, 1750 revolutions per minute, reversible, electric motor connected directly to the gear reducer. This provides a rate of vertical displacement at the downstream jack station of approximately 1 inch per minute.

The jacks were arranged in such a way that the downstream end of the flume may move from 12 inches below horizontal to 3 inches above horizontal, resulting in a maximum positive slope of 1/60 and a maximum adverse slope of 1/240. The motor was controlled by a raise, lower, and stop control switch. Safety switches were located both near the motor and near the control switch. It was necessary to unlock these before the control circuit could be completed. In addition, automatic limit switches were provided to prevent running the jacks beyond their limits. The general arrangement of jacks and gears is shown in figure 5-5.

In order to connect the ends of the jacks (which move in a vertical line) to the flume (which moves in an arc), it was necessary to use a pinned linkage. A photograph of the linkage is shown in figure 5-2. (Appendix C) Due to the ark of the linkage, the relation between the rise of the flume and the revolutions, turned by the jack shafts, was not linear. Therefore, it was necessary to make a calibration of the slope rather than computing it.

At the time of erection, the jacks were leveled at .001 foot before the flume was erected. During the alignment procedure, the jacks were raised or lowered individually as needed to obtain a level base. The shaft couplings were then installed and no further individual movements were made.

V-2 Water Supply and Measurement System

The water available in the laboratory is recirculated through the system by two pumps rated at 300 Gpm and 2000 Gpm. This 3 inch line contained a 3 x 2.25 inch venturi accurate to 0.5% over the range from 30 Gpm to 300 Gpm. A 60 inch differential manometer reading to 0.01 inch was connected to the venturi and filled with tetrabromo-ethane (specific gravity 2.95) which gave a monometer deflection of 51 inches with a flow of 336 Gpm.

The 2000 Gpm pump was connected to a 6 inch line which contained a 6 x 4.176 inch venturi accurate to 0.5% over the range 200 Gpm to 2000 Gpm. A 30 inch differential manometer reading to 0.01 inch was connected to the venturi and filled with mercury (specific gravity 13.6). This manometer gave a deflection of 14.9 inches for a maximum flow of 1790 Gpm. In both cases the venturis were fitted with air vents to insure proper measurements.

In order that the calibration of the venturi meters should have no error larger than that of the venturi meter, the scale to be used for the calibration was checked against standard weights by the Indiana State Board of Health, Division of Weights and Measures. The scale error was less than 0.2% or 2 pounds per 1000 pounds. For the purpose of calibrating of the venturi meters, branch lines led to a baffled concrete channel located above the weighing tank.

At the point immediately before the 3 inch and inch lines entered the forebay, valves and valve bypasses were installed. The 6 inch line had a 2 inch bypass and valve and the 3 inch line was fitted with a 1 inch bypass and valve. The manometers were mounted in a position easily visible to the person adjusting the valves. The overall apparatus arrangement in the laboratory is shown in figure 5-4.

The calibration curves of the venturi meters are given in figures 5-6 and 5-7.

V-3 Measuring Equipment

a) Instrument Carriage

An aluminum instrument carriage, mounted on two stainless steel guide rails running the length of the flume, was installed so that the bottom of the flume could serve as a reference plane. The four wheels of the carriage were grooved to give a precision fit on the rails. One of the wheels had a set screw to keep the carriage from moving when an experiment was conducted. A surveyors tape was mounted along the whole length of the flume and an indicating point on the carriage served as a reference point for all longitudinal measurements. Another surveyors tape was installed in the transverse direction of the flume on a grooved rail of the instrument carriage. This rail served as a guide for the slide on which a point gage and Prandtl tube were mounted. This slide also had an indicating point serving as reference point for transverse measurements. By means of these two tapes any point in the flume could be located in the horizontal plane. The instrument carriage was also equipped with a fluorescent lamp, several electrical outlets and a wide 3/4 inch plywood strip on one side to serve as a desk for notekeeping etc. The carriage could easily be moved to any location along the flume and locked in a specific position with an accuracy of 0.005 ft. (Figure 5-8 shows a top view of the carriage.)

b) Point Gage

All water surface elevation measurements were obtained by means of an electric indicating point gage. It was mounted on the instrument carriage slide which could be positioned with an accuracy of ± 0.002 ft. in the transverse direction of the flume. The staff of the point gage was marked in millimeters and was equipped with a vernier which allowed a reading accuracy of ± 0.05 mm in the vertical direction. The accuracy of the water surface elevation measurements varied between 0.1 mm to 2.0 mm depending on the smoothness of the free surface.

c) Prandtl Tube

The flow velocity measurements were obtained by means of a 1/8" O.D. Prandtl tube of standard design. The Prandtl tube was mounted on a vertical staff which was marked in 0.2 cm and had a vernier allowing a vertical positioning within ± 0.01 cm of accuracy. A set screw prevented the position to change during test measurements. The support of the Prandtl tube permitted, in addition to vertical and traverse motions, a rotation so that the horizontal portion of the probe could be aligned according to the direction of the flow indicated by a freely swinging stiffened tuft attached to the tube. The amount of rotation was measured as an angle by means of an indicator sliding along a fixed protractor. For measurement of large velocities, the Prandtl tube was connected to an inverted U manometer which had a fluid of specific gravity 0.810.

) Variable-Reluctance Pressure Transducers

The small magnitude of the pressure differentials to be measured with the Prandtl tube in zones of small velocities made it necessary to employ a Variable-Reluctance Differential Pressure Transducer (model P7D, Pace Eng. Comp.) instead of the conventional liquid manometer. In the low velocity regions a pressure transducer having a range of ± 0.1 psid. was used. In the higher velocity regions - as in the discharge jet of the models - range at ± 0.5 psid. was needed. Figure 5-10 shows sketch of velocity pressure transducer system.

) Calibration of Velocity Probe

By using the relation between the dynamic and static head $\frac{V^2}{2g} = h$ (where V is velocity in fps., h is feet of water and g is the acceleration of gravity) a static calibration could be performed.

Two reservoirs were connected to the stagnation and static openings of the Prandtl tube respectively. The reservoirs were connected through a valve. A datum level was measured by an electric point gage when the connecting valve was open, and the voltmeter needle was adjusted to the zero mark. The pressure was then equal on both sides of the diaphragm in the pressure transducer. The valve connecting the reservoirs was closed and distilled water was added to increase the level in the reservoir connected to the stagnation opening. The water level was recorded for even increments in the voltmeter reading. Figure 5-11 shows the calibration setup. Calibration curves are shown in Figure 5-12.

V-4 Boundary Roughness Analysis in the Large Flume

a) Smooth Boundaries

The actual testing program in the large flume was run under two different boundary roughness patterns. The first roughness which will be referred to as the smooth boundary consisted of the steel flume walls finished with an epoxy resin paint.

It was necessary to define the region of uniform flow prior to testing the models so that their effects on the flow pattern could be evaluated. The models and the affected flow reach must be contained within a uniform flow region. Special tests were run to determine the characteristics of uniform flow. The values of Manning's n, the Darcy-Weisbach friction coefficient and the length required for the full boundary layer development were calculated as discussed below.

The section used for model testing was the portion of the flume between 20.00 ft. and 50.00 ft. from the entrance. With the known uniform depth within the test equation, the discharge, channel geometry and slope, the Manning's equation could be used to determine a value of Manning's n. Throughout the testing program, it was felt necessary to maintain good control of uniform depths. Based upon an average of all the calculations of Manning's n for the smooth boundaries, a value of 0.0110 was determined. The range of n was from 0.009 to 0.0130 for discharges and Froude numbers from 1 cfs to 4 cfs and 0.05 to 1.00 respectively.

Darcy-Weisbach Coefficient

In addition, the Darcy-Weisbach friction factor was calculated according to the following equation.

$$f = 8 g R_n S/V^2_n \qquad (5\text{-}4\text{-}1)$$

where f = Darcy-Weisbach friction factor

V_n - Average velocity

R_n - Hydraulic radius

S - slope

The friction factor was plotted against the Reynolds number and compared to the Blasius and Prandtl Von-Karman curves for smooth surfaces. The resulting plot is shown in figure 5-13. The Reynolds number is that defined by Chow[3] as VR/ν, where ν is the kinematic viscosity of the water. Some of the scatter of the smooth data points is due to the fact that the surfaces were so smooth that relatively flat slopes were necessary. As a result, the slopes and surface profiles were very difficult to measure and they introduce experimental errors in the calculations.

Turbulent Boundary Layer Growth

To ensure that the model tests were being run in a regime of fully developed turbulent flow, the distance downstream from the entrance of the flume to the point at which the boundary layer thickness δ was equal to the normal depth y_n was computed. The equation used for the development of the turbulent boundary layer for smooth surfaces was that developed for flow over a flat plate. This equation is based upon the Blasius 1/7th power law. (See for example Daugherty and Ingersoll[4])

$$\delta/X = 0.377/\, Re_x^{1/5} \qquad (5\text{-}4\text{-}2)$$

where δ = the thickness of the turbulent boundary layer

X = distance downstream from the point where $\delta = 0$

$Re_x = V_n X/\nu$

V_n = average uniform velocity

Solving (27) for X

$$X = (\delta / 0.377)^{5/4} (V_n/\nu)^{1/4} \qquad (5\text{-}4\text{-}3)$$

Although this formula is restricted to flow over a flat plate, it will serve as a first approximation in the problem at hand. If δ is made equal to the uniform depth Y_n, then the value of X will estimate the distance to the point at which the turbulent boundary layer becomes fully developed.

Test results showed that the values of X ranged from about 8 feet for small discharges and steep slopes to about 40 feet at high discharges and steep slopes.

For the majority of the runs, the values of X were well within the first 20 feet of the flume, indicating that the flow could be considered fully developed within the test section.

b) Rough Boundaries

It has been shown that Manning's n value for the smooth boundaries was 0.0110. This value was not representative of any natural stream condition. It was decided to run a second series of tests with a boundary roughness which would simulate a more natural condition, and would permit the use of steeper slopes in the flume.

For natural streams, Daugherty and Ingersoll[4] give the following values of Manning's n.

	Minimum n	Maximum n
Smooth Natural Streams	0.025	0.033
Roughest Natural Streams	0.045	0.060

Based upon a scale ratio of 1/10 between model and prototype, a roughness with n = 0.020 in the model would correspond approximately to an n = 0.030 in a natural stream. Also a Manning's n of 0.030 in the model would be approximately 0.045 in the field. Therefore, it would be desirable to select a roughness pattern for model testing purposes that would have a Manning's n between 0.020 and 0.030.

Referring to the work done at Colorado State University[5], the following roughness pattern was selected. The roughness along the bottom consisted of two layers of 1/4 inch aluminum rods; a bottom layer of longitudinal bars placed 12 inches on center and a top layer of transverse bars 6 inches on center. Along the side walls, there was one layer of vertical bars 6 inches on center placed 1/4 inch from the wall. The bottom layers of bars were tied together with screen wire. The vertical bars were tied at the bottom to the transverse bars and clamped to the walls above the free surface. This roughness pattern can be seen in figure 5-14.

Figure 5-15 is a diagram of two velocity profiles. One profile was taken 0.03 feet downstream of a roughness element and the other at a point midway between two adjacent bars. It may be concluded that a significant amount of flow was beneath the elements.

Manning's n and Darcy-Weisbach f

As in the case of the smooth boundaries, several uniform flow tests were made. The tests were conducted for discharges of 1, 2 and 3 cfs and for 24 different slopes ranging from 0.000010 to 0.00450. Results show that the Froude numbers ranged from 0.05 to 0.56. An average value of Manning's n was computed as 0.0238. The actual value of n ranged from 0.022 to 0.025.

Darcy-Weisbach friction factors were calculated for the rough boundaries and plotted in figure 5-13. The data for rough boundaries was broken down according to constant discharge and constant hydraulic radius. The raw data for the 24 normal depth tests in the rough channel are listed in table 5-1 of the Appendix.

Equivalent Sand Roughness

Nikuradse's equivalent sand roughness was determined from an equation given by Chow[3] for uniform flow in rough open channels. (page 204)

$$V_n = V_f \left(6.25 + 5.75 \log (R_n/k)\right) \qquad (5\text{-}4\text{-}1)$$

where

V_n = average uniform velocity

$V_f = \sqrt{g R_n S}$ - shear velocity

R_n = hydraulic radius

k = Nikuradse's equivalent sand roughness

Results showed the average k to be 0.095 ft. with a range from 0.05 ft. to 0.12 ft.

Turbulent Boundary Layer Growth

As for the smooth boundary, the growth of the turbulent boundary layer was investigated. For the rough flow, an approximate method proposed by Bauer and presented in Chow[4] (page 198) was used. Although this method was primarily developed for steep slopes, it was found applicable to channels of small slope provided the flow was uniform. The equation proposed by Bauer was

$$\delta / X = 0.024 \, / \, (X/k)^{0.13} \qquad (5\text{-}4\text{-}5)$$

where δ = thickness of the turbulent boundary layer

X = distance from the point where $\delta = 0$

k = Nikuradse's equivalent sand roughness

Having already evaluated k for the rough boundaries, the distance to the point where the boundary layer thickness was equal to the normal depth Y_n could be evaluated. For the maximum depth, the value of X determined from equation 5-4-5 was 80 ft. However, for the majority of tests, the value of X was equal to or less than 25 feet, in which cases the flow was fully developed in the test section.

Sayre and Albertson[7] have presented a comprehensive report on the effect of roughness elements in rigid open channels. They state that a roughness parameter χ (chi) which depends "on the size, shape and spacing of the roughness elements", should completely describe the boundary roughness. The true value of χ depends on whether or not 1) the boundary is hydrodynamically rough -- negligible viscous effects, and 2) the channel is sufficiently wide such that any appreciable side wall effects are essentially eliminated.

According to Robinson, Koloseus and Sayre, the friction coefficient for fully rough turbulent flow may be expressed as a function of the relative roughness and a parameter representing the roughness spacing. In terms of Chezy C, as given by Sayre and Albertson[7]

$$C / \sqrt{g} = A \log (Y_n/a) + C_2 \qquad (5\text{-}4\text{-}6)$$

C_2 = a roughness parameter representing the roughness spacing and independent of roughness size.

a = parameter describing the actual roughness height

A = slope of the plotted line

The constant C_2 may be found by graphical extrapolation in a $C/\sqrt{g}$ vs Y_n/a plot as the value of $C\sqrt{g}$ at which $y_n/a = 1$. The value of Y_n extrapolated to $C/\sqrt{g} = 0$ defines the roughness parameter χ. The properties of a and C_2 in equation (5-4-6) are combined in χ according to the relationship

$$C_2 = -A \log (\chi / a) \quad (5\text{-}4\text{-}7)$$

Sayre deomonstrated that by describing the boundary roughness by a single parameter the data would group about a single curve described by the equation

$$C / \sqrt{g} = 6/06 \log (y_n/\chi) \quad (5\text{-}4\text{-}8)$$

Extensive comparisons to the work of Sayre and Albertson were made. Since the true value of χ depends on having fully rough flow, the testing flume was set to its maximum slope of 0.0125 and a series of six tests at various discharges were run. The data for these tests are given in Table 5-2 of the Appendix.

Figure 5-16 shows a plot of the resistance function $C/\sqrt{g}$ against the value of log y_n/a in equation (5-4-6). This plot was made by assuming the value of a to be 1/2 inch for the particular pattern of 1/4 inch aluminum rods. The value of the slope was 6.06 as in equation (5-4-8) and the extrapolated value of C_2 was 3.15. With the values of C_2, A, and a the value of χ was determined to be 0.0126 feet. Figure 5-17 gives a plot of equation (5-4-8). The determined χ value was used to plot this curve.

Velocity Distribution

Sayre also demonstrated that equation (5-4-8) can be used to represent velocity profiles. The resistance function $C/\sqrt{g}$ is equivalent to $V_n/\sqrt{\tau_o/\rho}$ where the shear velocity $\sqrt{\tau_o/\rho}$ is equal to $\sqrt{g\, y_n\, S}$ for open channel flow. Along with the normal depth tests to determine the χ parameter, a centerline velocity profile was taken at a slope of 0.0125 and a discharge of 3.714 cfs. The profile is shown in dimensionless form in figure 5-18. It is compared to the similar profile presented by Sayre. The equation obtained was

$$v / \sqrt{\tau_o/\rho} = 6.06 \log (y/\chi) + 4.6 \quad (5\text{-}4\text{-}9)$$

The noticable difference in the constants (i.e. 4.6 and 2.6) was probably due to the different type of roughness used. The roughness baffles used by Sayre were placed in such a way that there was no flow beneath the elements. The numerical value of a in equation (5-4-6) was assumed to be 1/2 inch. In actuality an effective value of a less than the assumed value could probably have been used. If a smaller value of a less than 1/2 inch had been used, then the value of χ would decrease and the numerical values of y/χ in figure 5-18 would increase causing the velocity profile to shift to the left. The constants would then be approximately equal.

General Resistance Diagram

Figure 5-19 shows a portion of the general resistance diagram for uniform flow in rigid open channels as presented by Sayre. The equations shown are those derived in his original paper. Added on this graph are the six special tests for rough boundaries and the value corresponding to the uniform flow depths used in both the smooth and rough boundary model testing program. In a later section of this report, the concepts presented in the paper of Sayre and Albertson have been extended to apply to field conditions. Although their work pertained only to rigid open channels, it is shown that the χ parameter could possibly be applied to natural rivers and streams.

BIBLIOGRAPHY OF CHAPTER V

1. Bakhmeteff, B. A., "Hydraulics of Open Channels", Engineering Societies Monograph", McGraw-Hill, 1932.

2. U. S. Bureau of Public Roads, "Computation of Backwater Caused by Bridges", October, 1958.

3. Chow, Ven te, "Open Channel Hydraulics", McGraw-Hill, 1959.

4. Daugherty, R. L., and Ingersoll, A. C. "Fluid Mechanics", McGraw-Hill, 1954.

6. Liu, H. K., Bradley, J. N., Plate, E. J., "Backwater Effects of Piers and Abutments", Colorado State University, Report CER57HKL10, October, 1957.

10. Sayre, W. W., and Albertson, M. L., "Roughness Spacing in Rigid Open Channels", Trans. ASCE, 1963, Vol. 128, Part I, p. 343.

VI PROCEDURE AND DATA PROCESSING FOR FREE SURFACE FLOW TESTS

VI-1 Selection of Variables

For each geometry, several models were built to cover the practical range of the geometric and flow variables. The principal geometric variable is M = b/B. Models were built to cover 3 to 5 different values of M. A listing of the range of all the geometric variables tested for the seven basic geometries is given in the table, page 93.

The principal flow variable that was varied was the Froude number. Tests were generally made for a range of values of the Froude number between 0.1 and 0.5. Each value of the Froude number could be obtained with different values of the discharge. The discharges used varied between 1 and 4 cfs.

Once the Froude number and the discharge were selected, the normal depth, the tail gate elevation and the flume slope could be calculated. A nomograph prepared for this purpose is given in Figs. 6-1 and 6-2. Entering this diagram with the selected value of the Froude number and using the chosen discharge, one may read directly the slope and the corresponding revolution counter setting, the tail gate height and the normal depth.

For definition of the Geometries see Fig. 3-14.

TABLE - SELECTION OF VARIABLES FOR FREE

SURFACE FLOW TESTS

Geometry / Variable	Ia	Ib	II	III	IV	Va	Vb	VI	VII
F	.04-1.25	.04-.804	.05-0.4	0.1 0.15 0.25 0.3 0.4 0.5	0.1 0.15 0.2 0.25 0.3 0.4 0.5-0.25	0.1 0.14 0.2-0.3 0.4-0.5	0.09-0.5	0.1-0.475	0.1-0.5
M	.3-.9	0.3-0.9	0.3 0.5 0.7 0.9	0.3 0.5 0.7	0.3 0.5 0.7	0.3 0.5 0.7 0.9	0.2 0.5	0.3 0.5 0.7	0.35 0.5 0.75
$\frac{L}{b}$	0	0 0.5 1.0	0.25	0.25	0	0	0.5	0	0
$\frac{ld\ b}{An2}$	0	0	0 0-7.5 7.5-15 15-25 25-30	0	0	0	0	0	0
ϕ_1	90	90	90	30 45 60 90	90	90	90	90	90
ϕ_2	0	0	0	0	0	0 15 30 45	15 30	0	0
β	0	0	0	0	0	0	0	0	0 0.3 0.5
N	1	1	1	1	1	1	1	1	1
n	.011 .0238	.0238	.0238	.0238	.0238	.0238	.0238	.0238	.0238
e	0	0	0	0	0.0 0.8 0.85 0.9 0.95 1.0	0	0	0	0

VI-2 Obtention of Uniform Flow

Once the Froude number and the discharge have been selected and the normal depth slope and tail gate setting have been calculated, the discharge is adjusted to the proper value, the slope and the tail gate are set to the calculated values.

The depth of flow is then measured at several stations along the flume, usually at 10 foot intervals from station 10 to station 50. If the depth at these stations varies by more than 1 mm the tail gate position is adjusted until uniform flow is obtained.

VI-3 Free Surface Measurements

Usually the water surface measurements were taken along the centerline of the arch opening. Additional measurements of the free surface were taken for two-span arch bridge models, for two-dimensional segment models, for three-dimensional skewed models. The upstream face of the model was located at station 30. The maximum backwater depth occurredusually between stations 20 and 30. Water surface measurements were usually taken from station 15 to the end of the regain curve downstream of the bridge. The interval of the measurements varied with the slope and the curvature of the free surface, but in the vicinity of the point of maximum backwater depth, measurements were made at intervals of 0.5 to 1 foot.

The water surface measurements were taken by means of an electric point gage, which could be read to the nearest 0.1 mm.

VI-4 Data Processing

In the theoretical development it has been shown (see equ. 3-9-29 and 3-9-35) that the ratio of the backwater depth Y_1 to the normal depth Y_n could be expressed as a function of the ratio of the Froude number F_n (which is the governing flow parameter) to the channel opening ratio M' (which is the governing geometric parameter) of the types:

$$\frac{Y_1}{Y_n} = f_1 \left(\frac{F_n}{M'}\right)^{2/3} \qquad (6\text{-}4\text{-}1)$$

or

$$\frac{Y_1}{Y_n} = f_2 \left(\frac{F_n}{M'}\right)^{2} \qquad (6\text{-}4\text{-}2)$$

It was found from the experimental data analysis that it was more convenient to present the backwater superelevation ratio h_1^*/Y_n as a function of F_n/M' in the forms

$$\frac{Y_1}{Y_n} - 1 = \frac{h_1^*}{Y_n} = f_3 \left(\frac{F_n}{M'}\right)^{2/3} \qquad (6\text{-}4\text{-}3)$$

$$\frac{Y_1}{Y_n} - 1 = \frac{h_1^*}{Y_n} = f_4 \left(\frac{F_n}{M'}\right)^{2} \qquad (6\text{-}4\text{-}4)$$

The general form of equ. 6-4-3 was used in the presentation of the results in the several progress reports. This presentation of the results is given in the following chapter.

In addition, a new analysis of the data was made according to the form of equ. 6-4-4. This presentation is given for the first time in this report. The value of constriction head loss coefficients have been calculated for all seven geometries by means of the formula (see equ. 3-8-13).

$$K = \frac{h_1^*}{V_{n2}^2/2g} - \alpha\left[\left(\frac{A_{n2}}{A_4}\right)^2 - \left(\frac{A_{n2}}{A_1}\right)^2\right] \qquad (6\text{-}4\text{-}5)$$

The value of α used in the computations was 1.20, which was obtained from velocity distribution measurements. (See chapter VII).

It has been shown (see equ. 3-9-10) that the backwater ratio $\frac{h_1^*}{Y_n}$ is proportional to the square of the ratio of Froude number F_n and the contraction ratio:

$$\frac{h_1^*}{Y_n} = D \left(\frac{F_n}{M'}\right)^2 \qquad 6$$

The value of D was calculated from equ. 3-9-17, namely

$$D = n\, C \left[\left(\frac{F_n}{M'}\right)^2 \right]^{n-1} \qquad (6\text{-}4\text{-}7)$$

and plotted vs. $\frac{h_1^*}{Y_n} / \left(\frac{F_n}{M'}\right)^2$ for the purpose of evaluating the consistency of the results.

A geographical multiple correlation technique was used for the presentation of the data of geometries II to VII. This technique is described in the following paragraphs. The remaining calculations were performed on the digital computer. Figure 6-3 shows the program flow chart for data analysis using Fortran II on the IBM 7090 computer.

VI-5 Four Variables Graphical Multiple Correlation

(I) Principles of correlation

A. The coaxial method of graphical correlation is based on the premise that if any important factor is omitted from a relation, the scatter of the points in a plotting of the observed values of the dependent variable vs. the values computed from the relation will be at least partly explained by the omitted factor. In other words, if the points on such a plotting are labeled with the corresponding values of the new factor, a family of curves can be drawn to modify the values computed from the original relation. For example:

B. For 2-D segment arch bridge model test, the following relation resulted from dimension analysis for the unsubmerged case

$$\frac{Y_1}{Y_n} = f\,(F_n, M, \beta)$$

(II) Procedures for Correlation

(1) Tabulate the required data: F_n, β, M, Y_1/Y_n for each run

(2) Consider $\frac{Y_1}{Y_n}$ as the dependent variable, plotted along the final axis. (See fig. 6-4)

The F values vary in all tests and should be used as the first correlating variable. The values of β and M are fixed for a given model; it will be convenient to consider them in the second and third steps (quadrants A and B).

(3) Assume $\frac{Y_1}{Y_n} = f_1\,(F, \beta)$ and neglect the variable M.

(III) Remark:

The reading sequence in Fig. 6-10 should follow the sequence of correlation. For example, given F_n, β, M, to find Y_1/Y_n. The sequence of reading must follow the sequence $F_n \rightarrow \beta \rightarrow M \rightarrow Y_1/Y_n$. The sequence $F_n \rightarrow M \rightarrow \beta \rightarrow Y_1/Y_n$ does not yield the correct answer.

F_n is used as the abscissa and $\frac{Y_1}{Y_n}$ as the ordinate, as shown in Fig. 6-5.

A point $P_1(F_n, Y_1/Y_n)$ can be located in the quadrant A and the β value of this point is shown by an assigned symbol. For example, in Fig. 6-5 symbol O shows that the value of β is 0.5.

In Fig. 6-5, the points are scattered because the essential factor M has not been considered. However, an average line for each β can be found through the average positions of the points.

(4) Add the factor M (see Fig. 6-6), $\frac{Y_1}{Y_n} = f_2 (F_n, \beta, M)$

With given values of F_n, β and Y_1/Y_n, a point P_2 may be located and the value of M is labeled or shown by an assigned symbol. An average line for M is plotted through the average position of the points.

(5) Check the accuracy of the above correlation. See Fig. 6-7.

With given values of F_n, β and M, a computed Y_1/Y_n can be found from Fig. 6-6. Then the computed Y_1/Y_n and the measured Y_1/Y_n define a point in quadrant C of Fig. 6-7. Draw a line through the origin bisecting the quadrant C. Then the degree of scatter of the points around the line will show the degree of accuracy of the above correlation.

(6) The β-lines and the M-lines in quadrants A and B are adjusted to improve the correlation, see Fig. 6-8.

a. With the given values of F_n, M, Y_1/Y_n and using the M-lines obtained in the previous step, the points are adjusted in quadrant A. The scatter is reduced, and a better fit of the points is obtained.

b. In the same way with given values of F_n, β, Y_1/Y_n and the newly obtained β-lines, new M-lines are obtained and their accuracy is improved.

c. Then check the accuracy of the correlation in quadrant C. The points will be closer to the bisecting line than before. This means that the accuracy has been improved.

d. Try the procedures (a to c) a number of times until the points in quadrant no longer change their position, then the accuracy of the correlation has reached its maximum possible value.

e. The β-lines and M-lines may also be presented as shown in Fig. 6-9.

(7) Change Fig. 6-9 to a more convenient form, Fig. 6-10, by combining quadrants and B together.

VII ANALYSIS OF TEST RESULTS

I-1 Geometry I

a) Introduction

The results discussed in this chapter pertain to the large flume model tests. r the two dimensional model tests in smooth and rough boundaries, the backwater tio and the discharge coefficient are given in terms of the channel opening tio and the normal depth Froude Number. For model tests in rough boundaries, the ations of the points of maximum and minimum depths are given. A method of [illegible] ing the minimum depth is presented. The effects of different channel roughnesses different bridge lengths on the backwater ratio and on the discharge coefficient compared. Finally, surface topography and velocity profiles at [illegible] sections obtained and the kinetic energy and momentum correction [illegible] should be restated that all the curves and conclusions presented are limited to metric single span arches without entrance rounding of [illegible] (see , 3-14).

b) Smooth Boundaries -- Tests by H. J. Owen

The test data and the calculated values of the discharge coefficient C_d, of [illegible] tion coefficient f, and of the Reynolds number are presented in table [illegible]. ratio of the backwater depth to the normal depth h_1/h_0 is plotted versus the o of the velocity head to normal depth with the contraction ratio M as a parameter igure 7-1-1. The ratio of the velocity head to the normal depth is a measure of kineticity of the flow, it is exactly half of the kineticity as defined by Bakhmeteff alf the square of the Froude number. The discharge coefficient C_d calculated from tion 3-7-2 is plotted versus the ratio of the velocity head to the normal depth the channel width ratio M as a parameter in figure 7-1-2.

The consistency of the data is well illustrated by the lack of scatter of the experimental points as plotted in figures 7-1-1 and 7-1-2. These test results may be compared with the small scale tests done as part of the Preliminary Tests (see Chapter IV) for the contraction ratio of 0.5 which is common to both test series. Inspection of figure 4-8 and figure 7-1-1 and 7-1-2 shows that the values are almost identical. For example, at a Froude number of 0.2, the value of the discharge coefficient C_d from the small scale tests (figure 4-8) is 0.38 and the superelevation ratio Y_1/Y_n is 1.1. Compared to this, the large small tests, (figures 7-1-1 and 7-1-2) give C_d as 0.375 and Y_1/Y_n as 1.119 for a kineticity of 0.08 which corresponds to the Froude number of 0.2. At a Froude number of 0.4 the results of the small scale tests indicated C_d was equal to 0.53 and Y_1/Y_n was 1.4. Similarly, at a corresponding kineticity of 0.08, the large scale tests showed C_d to be 0.483 and Y_1/Y_n to be 1.432. The reliability of the data may be better discussed in terms of the values of the friction coefficient and of the backwater ratio.

The Darcy-Weisbach friction factor and the Reynolds number for the uniform flow established before each test were calculated in table 7-1-1 as follows:

$$R = \frac{VR}{\nu}$$

$$f = \frac{8gRS}{V^2}$$

The experimental friction factors were compared to the theoretical values obtained by adapting the Blasius and Prandtl formulas for flow in smooth pipes to the rectangular open channel.

The formulas for smooth pipe flow are:

$$\text{Blasius} \quad f = 0.3164 \left(\frac{VD}{\nu}\right)^{-\frac{1}{4}} \quad R_e \leq 10^5$$

$$\text{Prandtl-Von Karman} \quad \frac{1}{\sqrt{f}} = 2.0 \log \left(\frac{VD}{\nu}\sqrt{f}\right) - 0.8$$

Replacing D by 4R and simplifying, the equations become:

$$\text{Blasius:} \quad f = 0.223 \left(\frac{[illegible]}{R}\right)^{\frac{1}{4}}$$

$$\text{Prandtl-Von Karman} \quad \frac{1}{\sqrt{f}} = 2.[illegible] \log \left(\frac{[illegible]R}{\nu} \sqrt{f}\right) - [illegible]$$

Powell and Posey [2], working with a triangular flume found the formula governing their friction factor to be

$$\frac{1}{\sqrt{f}} = 2.074 \log [illegible] \sqrt{f} [illegible]$$

for tranquil flow in a smooth channel. The comparison [illegible] values [illegible] the theoretical formulas is shown in figures [illegible] and 7-1-[illegible]. In figure [illegible] experimental values of the Darcy-Weisbach coefficient f are [illegible] Reynolds number. Both f and R are [illegible] defined [illegible] based [illegible]. Also plotted on the same figure are the Blasius and Von Karman [illegible] as the general range of experimental values obtained by [illegible] and [illegible][3] for smooth triangular channels.

In figure 7-1-[illegible] the friction coefficient f and the Reynolds number [illegible] on the normal depth, assuming two dimensional flow. Although this assumption is not completely true for the depth to [illegible] used in the [illegible] this [illegible] to compare the data with the experiments [illegible][4] which [illegible] a [illegible].

In general, as shown in figure 7-1-4 the data fall above the [illegible] lines which are a lower limit for a perfectly smooth boundary. The average friction coefficient is f = 0.021 which corresponds to an absolute roughness of approximately $\varepsilon = f(f) = 0.0025$ feet. This corresponds to the irregularities of the [illegible] of the channel finish.

The backwater ratio $h_1^*/\Delta h$ for each model test was compared to the values obtained by Tracy and Carter[5] for rectangular constrictions. This comparison is shown in figure 7-1-5 which shows that the backwater ratios are of the same order of magnitude although different as may be expected with different boundary geometries.

c) Smooth Boundaries - Tests by P. F. Biery

The experimental results of the two-dimensional semi-circular arch model tests in the large flume with smooth boundaries were plotted as the backwater ratio Y_1/Y_n vs. the channel opening ratio M' with the normal depth Froude number F_n as the parameter. This plot is shown in Fig. 7-1-6. As would be expected, the ratio Y_1/Y_n would decrease to unity for all Froude numbers as the value of M' approaches 1.00. Also, it goes to infinity as M' goes to zero. In a similar manner, the discharge coefficient C_d was plotted vs. M' for F_n and is shown in figure 7-2-7. The value of C_d tends to 0.611 at M' = 0 and approaches the same value as the parameter F_n when M' = 1.

The curves of figure 7-1-6 and 7-1-7 have actually been interpolated for constant Froude numbers. Although the results covered the entire range of variables, the Froude number of normal depth was never exactly equal to 0.5, 0.6 or any other value of the parameter on the figure. The amount of error produced during the interpolating process was found in most cases to be less than one percent. The raw data and calculations are given in tables 7-1-2 and 7-1-3 respectively.

The data of P. F. Biery for smooth boundaries have been processed and analyzed as described in section VI-4. The backwater superelevation ratio h_1^*/Y_n is plotted as a function of $(F_n/M')^2$ in Fig. 7-1-8; the head loss coefficient K is given in terms of M' in Fig. 7-1-9, and the backwater ratio coefficient D is given in Fig. 7-1-10.

VII-2 Geometries Ia and Ib - Rough Boundaries - Tests by P. F. Biery
(See Fig. 3-14 for definitions of geometries Ia and Ib).

a) Selection of Rough Boundary Model Tests

From the nomographic chart, (Fig. 6-2) the conditions for the rough boundary model tests were selected. The X's in the table below indicate the selected normal depth conditions for each of which the following values of M and L/b were tested.

For M = b/B = 0.3, 0.5, 0.7, 0.9

and L/b = 0.0, 0.5, 1.0

Flow Rate	Froude Number													
	0.05	...	0.15	0.20	0.25	0.30	0.35	0.40	0.45	0.50	0.60	0.70	0.80	0.90
1 cfs	X			X			X			X			X	
2 cfs		X			X			X			X			X
3 cfs			X			X			X			X		

b) Test Data

Table 7-2-1 presents the raw measurements of all of the large flume, rough boundary, semicircular tests. Included are both the two and three dimensional results. The designation of the run numbers is as follows. The first number represents the normal depth set-up. The second number represents the particular model being tested. The pertinent data and calculations are summarized in Table 7-2-2.

The particular measurements that were taken on each of the smooth and rough tests in the large flume were those required to calculate the following quantities: the hydraulic radius, the Reynolds number, the Froude number, the Darcy-Weisbach friction factor, the channel opening ratio M', the discharge coefficient, the backwater ratio (Y_1/Y_n), the backwater superelevation (h_1^*), the surface profile ratio ($h_1^*/\Delta h$), the length to the maximum backwater (L_{1-2}), the length to the point of minimum depth (L_{2-3}), the length L_{1-3}, and the Manning's n. (See figure 3-1 for the definition of terms.)

In view of the large amount of data that was to be analyzed and the repetitive character of the calculations, a program was prepared for processing the data on the Royal McBee LGP-30 digital computer.

In Table 7-2-3, the surface topography measurements for run number 4-4 are listed. It was felt that this run was indicative of average natural stream conditions. For the same run, the velocity measurements at the uniform depth, maximum depth, vena contracta and minimum depth are given in Table 7-2-4. In addition to the uniform depth isovel diagram of run number 4-4 above, velocity measurements of uniform flow were also taken for normal depth runs number 2 and 10. This data is also listed in Table 7-2-4.

With the isovel diagrams for uniform flow, the kinetic energy correction factor α and the momentum correction factor β were determined. This was accomplished by obtaining the areas between two adjacent constant velocity lines with an area planimeter. Once the areas were determined, the equations for α and β were solved in the following form.

$$\alpha = \frac{\int v^3 \, da}{V^3 A} \qquad \frac{\sum_{i=1}^{n} v_i^3 \, \Delta a_i}{V^3 A} \tag{7-2-1}$$

and

$$\beta = \frac{\int v^2 \, da}{V^2 A} \qquad \frac{\sum_{i=1}^{n} v_i^2 \, a_i}{V^2 A} \tag{7-2-2}$$

where n = number of sub-areas

$$V = \sum_{i=1}^{n} v_i \, \Delta a_i \tag{7-2-3}$$

$$A = \sum_{i}^{n} \Delta a_i \tag{7-2-4}$$

c) Test Results

α) Backwater ratio and discharge coefficient

The backwater ratio is plotted vs. the channel opening ratio with the normal depth Froude number as a parameter for the two-dimensional semicircular arch models as observed in the large flume with rough boundaries. In view of the importance of these curves, the scale was expanded and the results are shown in two parts. Figure

7-2-1a gives the results of Y_1/Y_n vs. M' for the range of backwater ratios less than 1 1.50. For the ratios greater than 1.50, figure 7-2-1b should be used.

As for the smooth boundaries, the experimental values of the discharge coefficient for the same test conditions are presented in figure 7-2-2. This figure and figures 7-2-1a and b have been interpolated for constant Froude numbers. The hump that appears in the Froude number lines of 0.25 to 0.60 was a phenomena which appeared in all of the curves of C_d. This was true for the smooth, rough and all L/b plots.

When compared to the preliminary test results of Fig. 4-8, the values of the backwater ratio for a given Fn and M' are almost identical.

β) Location of the points of maximum backwater, and minimum depth

In order to describe the centerline profile, it is desirable to have an estimate of the distance from the upstream face of the constriction to the point of maximum backwater elevation. This distance is referred to as L_{1-2}. Because of the flatness of the surface profile in the vicinity of the maximum point, it was extremely difficult to get an exact measurement of L_{1-2}. The actual measurements taken could have been in error by as much as ± 0.5 feet. However, with the large amount of data which was available, it was possible to study L_{1-2} on an average basis. Average values of L_{1-2} were calculated for several combinations of b/B, L/b, L/B, etc. In this manner, it appeared that the effect of the variable bridge length and the change in M' were of the same order of magnitude as the experimental error. The most consistent relationship was found by plotting the dimensionless ratio L_{1-2} vs. the Froude number F_n with M = b/B as the parameter. This relationship is shown in figure 7-2-3a. The values of L_{1-2} obtained from the smooth boundary tests also compared favorably with figure 7-2-3a. In a similar manner it was found that the length L_{1-3} (distance from the maximum depth point to the minimum depth point) varied only with the constriction geometry. The values of L_{1-3}/b are plotted vs. M = b/B with L/b as a parameter in figure 7-2-3b. These curves are good for both two and three dimensional semicircular arch bridges.

γ) Determination of the minimum depth

Several other investigators have used the Froude number at section 3 ($F_3 = V_3/\sqrt{gy_3}$; see figure 3-1) as an estimator of the maximum backwater. Others have used F_3 as a controlling parameter in making indirect measurements of flood discharges. Due to the extremely irregular flow pattern at the minimum point, it would seem that the use of F_3 may be misleading. In the present research, the normal depth Froude number F_n was found to be a very reliable estimator of Y_1/Y_n. In order to test the variability of F_3 with F_n, a correlation curve of F_3/F_n vs. F_n was prepared. This curve is shown in figure 7.2-4. Below a Froude number of 0.5, the correlation was good. However, above $F_n = 0.5$, the depth y_3 was often below the critical depth and the correlation of F_3/F_n to F_n was very poor. The scatter seemed to increase with increasing values of L/b. Therefore, only the test results of the L/b = 0 tests are shown. If used with caution, these curves can be used to estimate the minimum depth y_3. It appears from this curve that F_n is a much more reliable estimator than F_3.

δ) Regain Curve Length

The regain curve was measured for a few runs. This was done in order to establish the fact that the water surface profile returns to normal depth before the end of the testing flume was reached. The tests selected were those which would have the longest regain curve. The results are summarized below.

Run No.	M	L/b	F_n	L_{2-4}
1-4	0.491	0.0	0.0489	20 ft.
2-7	0.693	0.0	0.1005	9 ft.
4-4	0.491	0.0	0.1984	5 ft.

In all cases the regain curve was within the test section.

ε) Comparisons of roughness effects

Comparisons between the model tests in the smooth and rough channel were made by plotting the backwater ratio and the discharge coefficient against the normal depth Froude number F_n for constant channel opening ratios. Similar comparisons were made between the several three-dimensional model tests in the rough flume.

The values of the backwater ratio Y_1/Y_n and the discharge coefficient C_1 in the smooth and rough channel boundaries are compared in figures 7-2-5a and 7-2-5b. It appears that the values are essentially the same for both smooth and rough conditions at Froude numbers F_n less than 0.5. Since the practical range of Froude numbers for natural channels are those less than 0.5, these curves show that for all practical purposes the effect of roughness can be ignored.

ζ) Comparison of bridge length effects

Similarly, all of the L/b results were compared at constant values of the channel opening ratio M'. Figures 7-2-6a and b illustrate these comparisons. Again it appears from the plots that for the practical range of field conditions ($L/b \leq 1.0$ and $F_n \leq 0.5$) the effect of bridge length is negligible. The effect of length did seem to increase with a decrease in the channel opening ratio. However, as the value of M' gets small, the physical proportions are closer to those of a culvert rather than a bridge opening.

η) Surface topography

In order to complete the analysis of the maximum backwater, additional studies were made of the velocity distributions and the surface profiles. These studies were made for the condition of a sharp-crested semicircular constriction with $M = b/B = 0.5$ and F_n approximately 0.20.

A detail of the surface topography both upstream and downstream of the model was observed. The results of this study are shown in figure 7-2-7. The numbers shown indicate the depths in centimeters. Only a detail of one half of the surface is given since the pattern is essentially symmetrical. The graph shows lines of equal surface elevation. The centerline profile is also given in the figure. It is interesting to note that the actual maximum water surface elevation is not along the centerline, but on the upstream face of the abutment. Although this may be expected, since there is a stagnation point at the abutment, the actual magnitude of the difference in elevation between the centerline maximum elevation and the actual maximum is the important question. The actual maximum shoreline elevation was found to exceed the maximum centerline elevation by as much as 5% of the centerline depth. This fact was verified in the surface topographies taken at other conditions. Liu[6], as well as Herbich[9] gave similar surface topographies of other geometric constrictions, and the differences in water surface elevations was again found to be about 5% of the centerline depth.

i) Velocity profiles

Traverses were run with the Prandtl Tube at four sections with the M = 0.5, L/b = 0.0 and F_n approximately 0.20 model tests. The first section was in the normal depth flow without the model. The second was at the section of maximum backwater, the third at the upstream face of the bridge and the fourth at the section of minimum depth. At the section of normal depth and maximum depth, vertical velocity traverses were taken at the centerline and 1 ft. and 2 ft. left and right. At the vena contracta, they were taken at the centerline, 0.5 ft. and 1 ft. left and right. Finally at the section of minimum depth, traverses were taken at the centerline, 1 ft., 1.5 ft., and 2.2 ft. left and right. In general a more detailed traverse was taken at the centerline of each section. From these measurements, plots of equal velocity lines were prepared for each section. This was done first by plotting the velocity profiles at each location within each section on arithmetic graph paper. Typical are the profiles shown in figure 7-2-8 at the maximum depth condition. From these curves, points of equal velocity were found and plotted in the appropriate location on a cross-section view of the channel. A composite picture of the isovel diagrams is shown in figure 7-2-9. Only half of the diagram is given due to symmetry. All of the diagrams were integrated with an area planimeter and the discharge so obtained was checked against the venturi meter discharge. In all cases they checked within 1%.

In addition to the isovel diagrams for uniform flow in figure 7-2-9, two other uniform flow velocity profiles were plotted. The test conditions were similar to those of a natural stream. All of the diagrams were integrated and the values of the discharge, the kinetic energy correction factor and the momentum correction factor were computed. Listed below are the determined values of α and β for each profile.

Q	Slope	y_n	Approx. F_n	α	β
2 cfs	0.000131	0.799 ft.	0.10	1.145	1.055
1 cfs	0.000584	0.319 ft.	0.20	1.216	1.084
1 cfs	0.004080	0.173	0.50	1.250	1.090

k) The generalized backwater equation and head loss coefficients

With the introduction of the channel opening ratio M', the assumption was made that if properly interpreted, the backwater produced by constrictions of the same M' would be equal, regardless of its geometry (i.e., a semi-circle, or a circular segment, or a rectangle etc.) as long as the constriction effects are not modified by skew, chamfers, eccentricity, wingwalls, etc.

To test this hypothesis, the results of this section (VII-2) are compared with the circular segment data obtained in the preliminary investigation (Fig. 4-8) and with the vertical board data given by Liu[7]. The latter tests were run in a flume which was wider than the large flume used in this investigation. The roughness pattern used by Liu was also different. It produced a Manning's n of 0.024. It is felt extremely interesting to note that the test data taken by three investigators in three different flumes and under three completely different constriction geometries produced almost identical results. This clearly verifies that, as defined, the channel opening ratio M' is the governing geometric parameter. Of course, the data compared were those where the eccentricity was zero, the skew was zero, and the entrance was sharp. It is still necessary to apply correction terms for these conditions.

As mentioned previously in the analysis, a similarity was noticed between the several different backwater equations. The term $(F_n/M')^{2/3}$ appeared in several solutions of y_1/y_n. In general it appeared that

$$y_1/y_n = C\left[(F_n/M')^{2/3}\right]^{\gamma} \qquad (7\text{-}2\text{-}5)$$

where C is a coefficient which would take into account the effects of the discharge coefficient, approach velocity, and non-uniform velocity distributions and other empirically determined factors. Equation 7-2-5 is actually the equation of a straight line on logarithmic paper with a slope of γ. A total of 50 semicircular L/b = 0 test values, 44 vertical board values (Colorado) and 50 segment values were plotted in the form of $Y_1/Y_n - 1$ vs $(F_n/M')^{2/3}$ and are shown in figure 7-2-10. The value of $Y_1/Y_n - 1$ was used instead of the backwater ratio. It is quite apparent that the data tends to collapse into one straight line relationship.

The method of least squares was applied to a random sample of the 144 test points to determine the empirical straight line relationship. After solving for γ and C, equation 7-2-5 became

$$Y_1/Y_n = 1 + 0.47 \left[(F/M')^{2/3}\right]^{3.39} \qquad (7\text{-}2\text{-}6)$$

Equation 7-2-6 is a very simple and easy solution for the backwater produced by any type of constriction. In actual practice, this equation will give as good an estimate of the maximum backwater y_1 as any previously suggested method.

It has been suggested by C. F. Izzard that equation 7-2-6 could be approximated by

$$Y_1/Y_n = 1 + 0.45\ (F/M')^2 \qquad (7\text{-}2\text{-}7)$$

and still fit the data very closely.

The data were also reanalyzed in terms of the simpler equation

$$\frac{h_1^*}{Y_n} = \frac{Y_1}{Y_n} - 1 = f\ \left(\frac{F}{M'}\right)^2$$

Figures 7-2-11 to 7-2-13 give plots of this relation for values of L/b = 0; 0.5; and 1.0. Fig. 7-2-14 summarizes the backwater ratio information for geometry I, for smooth and rough boundaries. The curves shown in this figure are the same as those previously obtained in figures 7-1-3 and 7-2-11 to 7-2-13. In addition, a least square fitting of all the data (smooth and rough) taken by P. F. Biery is given.

The head loss coefficient K is given as a function of M' for L/b = 0; 0.5; 1.0 in figures 7-2-15 to 7-2-18. A summary of the head loss coefficient curves is given in fig. 7-2-18. The backwater ratio coefficient D is given in Fig. 7-2-19 to 7-2-21 corresponding to values of L/b = 0; 0.5 and 1.0.

VII-3 Geometry II Tests by S. Lippai and T. P. Chang

Dual Parallel Three Dimensional Semi-Circular Arch Bridge Constrictions: (See Fig. 3-14 for definition of Geometry II)

For simplicity, only the case of two identical arch bridges placed parallel to each other and normal to the direction of flow, was considered. The effect of Froude Number (F_n), the channel opening ratio (M'), and the distance between the centerlines of dual parallel bridges (L_d), on the backwater ratio (Y_1/Y_n) has been determined.

The raw and calculated data for the 117 tests are given in table 7-3. Typical surface profiles are shown in Fig. 7-3-0. Figures 7-3-1 to 7-3-5 were obtained by plotting backwater ratio Y_1/Y_n against the dimensionless bridge spacing bL_d/A_{n2} with the channel opening ratio M' as parameter for F_n = 0.10, 0.15, 0.20, 0.25, 0.30 and 0.40.

It was found that for low Froude Numbers ($F_n \leq 0.25$) the backwater due to closely placed dual parallel bridges ($bL_d/A_{n2} \leq 5$) was less than what it would have been for a single bridge. The lower part of the graphical correlation of Fig. 7-3-6 shows clearly this effect.

It was also found that for higher Froude Numbers ($F_n \geq 0.25$) and small channel opening ratios ($M' = 0.3$), the placing of models at $bL_d/A_{n2} \cong 8$ to 9 resulted in strong wave action between the models and an abrupt increase in backwater ratio was observed as can be seen in Figures 7-3-3 to 7-3-5. For the latter conditions, the jet expansion below the upper bridge was unstable. It oscillated from the left to right and back with a period of about 2 sec. The backwater upstream of the upper bridge was minimum when the jet was symmetrical along the centerline. The backwater increased as the jet was deflected sideways. The values plotted were the maximum backwater elevations observed.

Figure 7-3-6 shows the graphical multiple correlation for 4 variables (F_n, M', Y_1/Y_n, bL_d/A_{n2}). Knowing any three of them, the fourth one may be determined from Fig. 7-3-6.

A straight line relationship between Y_1/Y_n and $(F_n/M')^{2/3}$ on log-log paper was obtained for dual parallel bridges placed at $bL_d/A_{n2} = 0$, 10, 20, and 30. Figure 7-3-7 was arrived at through the following steps:

1. Fig. 7-3-6 was used to obtain values of Y_1/Y_n for $bL_d/A_{n2} = 0$, 10, 20, 30 $M' = 0.3$, 0.5, 0.7 and 0.9, $F_n = 0.10$, 0.20, 0.30 and 0.40.

2. This data was processed and an arithmetic plot of Y_1/Y_n vs. $(F_n/M')^{2/3}$ for $bL_d/A_{n2} = 0$, 10, 20 and 30 was constructed.

3. To obtain a straight line relationship between Y_1/Y_n vs. $(F_n/M')^{2/3}$ for $bL_d/A_{n2} = 0$, 10, 20 and 30 on log-log paper, appropriate values of c were determined by using the method described in reference 8.

4. The curve of figure 8 doesn't apply to the unstable flow condition with heavy wave action between the dual bridges.

In addition the data were reanalyzed making use of the computer program. The backwater superelevation ratio h_1^*/Y_n is plotted as a function of $(F_n/M')^2$ in figures 7-3-8 to 7-3-13, for the following values of the parameter $L_d b/A_{n2}$:

Fig. 7-3-8	$L_d b/A_{n2} = 0$
Fig. 7-3-9	0 to 7.5
Fig. 7-3-10	7.5 to 15
Fig. 7-3-11	15 to 25
Fig. 7-3-12	25 to 30

The equation of a least square fitting is given for each range of the parameter $L_d b/A_{n2}$. A summary of these curves is given in Fig. 7-3-13.

The head loss coefficient K is given in the channel opening ratio M' for the following values of the parameter $L_d b/A_{n2}$:

Fig. 7-3-14	$L_d b/A_{n2} = 0$
Fig. 7-3-15	0 to 7.5
Fig. 7-3-16	7.5 to 15
Fig. 7-3-17	15 to 25
Fig. 7-3-18	25 to 30

Whenever a good least square curve fitting could be obtained its equation is given on the graph. In the other cases, the average values of the several groups of test for a given value of M' was obtained, and a line was fitted by eye through these points. Figure 7-3-19 is a summary of the head loss coefficient curves. Figure

7-3-20 gives the values of the backwater ratio coefficients D. The raw and calculated data for Geomety II are given in Table 7-3.

VII-4 Geometry III Tests by T. P. Chang

Three Dimensional Semi-Circular Arch Bridge Constriction with Wingwalls
(See Fig. 3-14 for definition of Geometry III)

The influence of wingwalls on the backwater ratio (Y_1/Y_n) has been tested for wingwall angles $\phi_1 = 30^\circ, 45^\circ, 60^\circ$ and 90, using a model with L/b ratio of 0.25. The raw and calculated data are listed in table 7-4. Figures 7-4-1 to 7-4-4 were obtained by plotting the backwater ratio, (Y_1/Y_n) against the channel opening ratio, (M') with the Froude Number (F_n) as parameter for wingwall angles $\phi_1 = 30^\circ$, 45°, 60° and 90°.

Fig. 7-4-5 is obtained by graphical multiple correlation. Knowing any three of four variables, Y_1/Y_n, F_n, M', and ϕ_1, the fourth one may be determined by this chart.

Fig. 7-4-6 shows the relation between the backwater ratio (Y_1/Y_n) and $(F_n/M')^{2/3}$ with ϕ_1 as parameter. It was based on the graphical correlation of Fig. 7-4-5. Due to the indirect plotting method, the accuracy of Figure 7-4-6 is less than that of Figures 7-4-1 to 7-4-4.

The data were reanalyzed making use of the computer program. The results are presented in the form of plots of the backwater superelevation ratio h_1^*/Y_n vs. the square of the ratio of the Froude number to the channel opening ratio $(F_n/M')^2$ for wingwall angle of 30°, 45°, 60° and 90° in Figures 7-4-7 to 7-4-10.

For each value of the parameter ϕ_1, the equation of the least square curve fitting is given on the figure. A summary of these results is given in Fig. 7-4-11.

The head loss coefficient K has been calculated for each of the wingwall angles. The results are presented in the form of plots of K vs. the channel opening ratio. Wherever possible a least square fitting of the data was obtained, and the equation of the line is given. In the other cases, average values of the coefficient K for grouping of points with the same value of M' was obtained, and a straight line was fitted by eye through these average points. These results are presented in Fig. 7-4-12 to 7-4-15 for wingwall angles of 30°, 45°, 60° and 90°. A summary of the curves is presented in Fig. 7-4-16.

Finally, the values of the backwater ratio coefficient D are presented in

ig. 7-4-17 to 7-4-20 for the four wingwall angles.

The raw and calculated data for Geometry XXI are given in Table 7-4.

VII-5 Geometry IV Two-Dimensional Semi-Circular Arch Bridge Constrictions with Eccentricity - Tests by T. P. Chang

(The eccentricity is defined as one minus the ratio of the small embankment to the larger embankment. (See Fig. 3-14 for definition of Geometry IV)

The influence of eccentricity on the backwater ratio along the centerline (Y_1/Y_n) has been determined for eccentricities e = 0; 0.80; 0.85; 0.90; 0.95; and 1.00. Figures 7-5-1 to 7-5-6 give the backwater ratio (Y_1/Y_n) plotted vs. the channel opening ratio (M') with the Froude Number as a parameter for each of the six eccentricities tested. Figure 7-5-7 shows the relation between the backwater ratio (Y_1/Y_n) and $(F_n/M')^{2/3}$ with the eccentricity as a parameter. Figure 7-5-7 was obtained by graphical multiple correlation.

The results of the re-analysis of the same data making use of the computer program is given in the following figures. The backwater superelevation ratio (h_1^*/Y_n) is plotted vs. $(F_n/M')^2$ for the six eccentricities tested in figures 7-5-8 to 7-5-13. For each eccentricity the equation of the least square curve fitting the data is given. A summary of the results is given in Fig. 7-5-14.

The values of the head loss coefficient K are plotted against the channel opening ratio M' for each of the six eccentricities tested in figures 7-5-15 to 7-5-20. The straight lines were obtained by obtaining average values for K for groups of points having the same value of M'. A straight line was fitted by eye through these average points. A summary of the head loss coefficient K is given in Fig. 7-5-21.

The values of the backwater ratio coefficient are given in Fig. 7-5-22 to 7-5-27.

The raw and calculated data for Geometry IV are given in Table 7-5.

VII-6 Geometry Va

o Dimensional Semi-Circular Arch Bridge Constrictions with Skew Tests by T. P. Chang
(See Fig. 3-14 for definition of Geometry Va)

The influence of skew on the backwater ratio along the centerline, (Y_1/Y_n) has en determined for skew angles of $\theta_2 = 0°$, $15°$, $30°$ and $45°$. The raw and calculated ta are given in Table 7-6.

Fig. 7-6-1 to 7-6-4 were obtained by plotting the backwater ratios (Y_1/Y_n) against e channel opening ratio, (M') with Froude No. (F_n) as parameter for skew angles = $0°$, $15°$, $30°$ and $45°$.

Fig. 7-6-5 was obtained through graphical multiple correlation. Knowing any three four variables, Y_1/Y_n, F_n, M', and θ_2 the fourth variable may be determined from the rrelation chart.

Fig. 7-6-6 shows a relation between Y_1/Y_n and $(F_n/M')^{2/3}$ with θ_2 as parameter. was based on the graphical correlation of Figure 7-6-5. Due to the indirect plotting thod the accuracy of Fig. 7-6-6 is less than that of Figures 7-6-1 to 7-6-4.

The same data were reanalyzed making use of the computer program. The backwater perelevation ratio (h_1^*/Y_n) is plotted vs. $(F_n/M')^2$ for the four skew angles tested figures 7-6-7 to 7-6-10. The equation of the least square fit is given on each gure. A summary of these results is given on Fig. 7-6-11. The values of the head ss coefficient K were plotted against the channel opening ratio M for each of the ur skew angles tested in figures 7-6-12 to 7-6-15. The best fit lines were obtained the least square method, and the equations of these lines are given in the respective gures. A summary of the head loss coefficients is given in Figure 7-6-16. Finally values of the backwater ratio coefficient D are given in figures 7-6-17 to 7-6-20.

The raw and calculated data for Geometry Va are given in Table 7-6.

VII-7 Geometry Vb

Three-Dimensional Semi-Circular Arch Bridges Constrictions with Skew Tests by T.P. Chang
(See Fig. 3-14 for definition of Geometry Vb)

The influence of the skew on the backwater superelevation ratio along the center-line (h_1^*/Y_n) has been investigated for skew angles of $\phi_2 = 15^\circ$ and 30°. Figures 7-7-1 and 7-7-2 give the backwater superelevation h_1^*/Y_n as a function of $(F_n/M')^2$ for the two skew angles tested. A summary of these results is given in Fig. 7-7-3.

The raw and calculated data for Geometry Vb are given in Table 7-7.

VII-8 Geometry VI Two-Span Semi-Circular Arch Bridge Constrictions Tests by [illegible]
(See Fig. 3-14 for definition of Geometry VI)

The pier width, P, used in the models was equal to one third of the span or [illegible]. (A different pier width was used for submerged tests.) The influence of this type of constriction on the backwater superelevation ratio has been investigated for 3 values of the channel width ratio M = 0.3, 0.5 and 0.7.

The backwater superelevation ratio h_1^*/Y_n was plotted vs. $([illegible])^2$ in Fig. [illegible] and the equation of the least square fit line is given in the figure. The values of the head loss coefficient K are plotted vs. the channel opening ratio M' in fig. 7-[illegible] and the equation of the line obtained by the least square method is given in the figure. The values of the backwater ratio coefficient [illegible] are given in Fig. 7-8-b.

The raw and calculated data for Geometry VI are given in Table 7-8.

VII-9 Geometry VII-Two-Dimensional Circular Segment Arch Bridge Constrictions
Tests by T. P. Chang
(See Fig. 3-14 for definition of Geometry VII)

The influence of the amount of depression of the center of the arch with respect to the bottom of the stream, (as given by $\beta = d/r$, where d the distance between the channel bottom and the center of the circular segment of radius r) on the backwater superelevation ratio has been investigated for 3 values of the depression parameter $\beta = 0$; 0.3 and 0.5.

The values of the backwater superelevation ratio h_1^*/Y_n have been plotted vs. $(F_n/M')^2$ in figures 7-9-1 to 7-9-3 for the three values of the depression parameter. In each figure the equation of the least square fit has been given. A summary of the results is given in fig. 7-9-4.

Values of the head loss coefficient K are plotted vs. the channel opening ratio M', for the three values of the depression parameter tested, in figures 7-9-5 to 7-9-7. In each figure the equation of the least square fit straight line is given. A summary of the head loss coefficient values is given in fig. 7-9-8.

The values of the backwater ratio coefficient are given in figures 7-9-9 to 7-9-11.

VII-10 Bibliography of Chapter 7

1. Bakhmeteff, B., "Hydraulics of Open Channels", McGraw-Hill 1932.

2. Powell, R. W. and Posey, C. J., "Resistance Experiments in a Triangular Channel", Journal of the Hydraulics Division, Proceedings ASCE, May 1959.

3. Lansford, W. M., Robertson, J. M., Discussion, Trans., ASCE, Vol. 123, 1958, p. 707.

4. Owen, W. M., "Laminar to Turbulent Flow in Wide Open Channel", Trans. ASCE, vol. 119, 1954.

5. Tracy, H. J., Carter, R. W., "Backwater Effects of Open Channel Constrictions", Trans. ASCE 120, 1955.

6. Henry, H. R., Discussion on 'Diffusion of Submerged Jets", Trans. ASCE, vol. 115, 1950, p. 687-694.

7. Liu, H. K., Bradley, J. N. and Plate, E. J., "Backwater Effects of Piers and Adjustments", Colorado State University, CER57HKL10, Oct. 1957.

8. Lipka, J. "Graphical and Mechanical Computation", p. 140-141.

VIII SUBMERGED FLOW TESTS RESULTS - Tests by O. Eikeri

VIII-1 Test Selection

The selected models were to be tested in the 64 foot long flume, first with smooth and then with rough boundaries. The large number of variables involved made it necessary to establish a systematic procedure for selecting the quantities allowed to vary and those held constant in the several tests so that the possible range of the variables could be covered uniformly and completely. This was of concern because the range of discharges and slopes for which submergence could be attained was very limited. The procedure followed was based on the theoretical analysis and on the testing of simple geometries.

The channel width ratios, M' = b/B for which submergence was possible with the flow available in the laboratory was determined from preliminary tests. The testing of geometry I-a with the selected channel width ratios gave the flow rates necessary for submergence for each model. The dimensionless discharge $\frac{Q}{g^{\frac{1}{2}} b^{5/2}}$, which according to equ. 3-7-33 is related to the backwater ratio Y_1/b, was calculated for several discharges and channel width ratios to be tested as indicated in the following table.

Q	$\frac{Q}{g^{\frac{1}{2}} b^{5/2}}$				
cfs	M = 0.15	M = 0.20	M = 0.25	M = 0.275	M = 0.30
2.0	0.7[illegible]95	0.353	0.202	0.159	0.128
2.5	0.885	0.441	0.2525	0.199	0.160
3.0	1.062	0.529	0.303	0.238	0.19[illegible]
3.5	-	-	0.354	0.278	0.224
4.0	-	-	0.405	0.318	0.256

By choosing flow rates in the test runs that give different values of $Q/g^{\frac{1}{2}}b^{5/2}$, grouping of data in the graphs could be prevented. The seven tables that follow this section show the test runs made for the different geometries. The conditions selected n Table I through VII were chosen in part from the table developed in this section.

Table I - Smooth Boundary Tests

$n = 0.0110$

Geometry I-a

Flow Rate cfs.	Froude Number F_n			Channel Width Ratio (b/B)			
	0.10	0.15	0.20	0.20	0.25	0.275	0.30
2.0	X			X	X	X	X
2.0		X		X	*	*	*
2.0			X	X	*	*	*
2.5	X			0	X	X	X
2.5		X		X	X	X	X
2.5			X	X	X	X	X
3.0	X			0	X	X	X
3.0		X		0	X	X	X
3.0			X	0	X	X	X
3.5							
3.5		X		0	X	X	X
3.5			X	0	X	X	X

X Regular test measurements obtained

0 The flow overtopped the model and channel walls

* Submergence was not possible for these flow conditions

Table II - Smooth Boundary Test

n = 0.0110

Geometry 1-b

Flow Rate cfs.	Froude Number F_n .10	.15	.20	Channel Width Ratio b/B 0.20 — Thickness Factor L/b .25	.50	.75	1.0	0.25 .25	.50	.75	1.0	0.30 .25	.50	.75	1.0
2.0	X			X	X	X	X	X	X	X	X	X	X	X	X
2.0		X_i		*	*	*	*	*	*	*	*	*	*	*	*
2.0			X_i	*	*	*	*	*	*	*	*	*	*	*	*
2.5	X			0	0	0	0	X	X	X	X				
2.5		X		X	X	X	X	X	X	X	X	X	X	X	X
2.5			X					X			X	X	X	X	X
3.0	X_i			0	0	0	0								
3.0		X		0	0	0	0	X	X	X	X	X	X	X	X
3.0			X	0	0	0	0				X				
3.5	X_i			0	0	0	0	0	0	0	0				
3.5		X		0	0	0	0	X	X	X	X	X	X	X	X
3.5			X	0	0	0	0			X	X				
4.0	X_i			0	0	0	0	0	0	0	0				
4.0		X		0	0	0	0	0	0	0	0			[illegible]	[illegible]
4.0			X_i	0	0	0	0								

X Regular test measurements obtained

0 The flow overtopped the model and channel walls

* Submergence was not possible for these flow conditions

X_i Experimental condition investigated

Table III - Rough Boundary Tests

n = 0.0238

Geometry I

Flow Rate cfs.	Froude Number F_n			Channel Width Ratio b/B			
	0.10	.015	0.20	0.20	0.25	[illegible]	0.30
2.0	X			X	X	X	X
2.0		X_1			*	*	*
2.0			X	X	*	*	*
2.5							
2.5		X		X	X	X	X
2.5			X	X	X	X	X
3.5							
3.5		X		O	X		
3.5			X	O			

X Regular test measurements obtained

O The flow overtopped the model and channel wall

* Submergence was not possible for these flow conditions

X_1 Experimental condition investigated

Table IV - Rough Boundary Tests

n = 0.0238

Geometry I-b

Flow Rate cfs.	Froude Number F_n .10	.15	.20	Channel Width Ratio (b/B) 0.20 Thickness Factor (T/b) .25	.50	.75	1.0	0.25 .25	.50	.75	1.0	0.30 .25	.50	.75	1.0
2.0	X			X			X	X			X			X	
2.0		X_i						*	*	*	*	*	*	*	*
2.0			X	X	X		X	*	*	*	*	*	*	*	*
2.5	X_i			O	O	O	O								
2.5		X		X		X	X	X		X	X	X	X	X	
2.5			X	X		X	X				X			X	
3.5	X_i			O	O	O	O	O	O	O	O				
3.5		X		O	O	O	O	X	X		X				
3.5			X_i	O	O	O	O								

X Regular test measurements obtained

O The flow overtopped the model and channel walls

* Submergence was not possible for these flow conditions

X_i Experimental condition investigated

Table V - Rough Boundary Tests

$n = 0.0238$

Geometry V-b

Flow Rate cfs.	Froude Number F_n			Thickness Factor L/b = 0.50, Channel Width Ratio (b/B) 0.20, Angles of Skew O_2			0.30		
	.10	.15	.20	15°	22½°	30°	15°	22½°	30°
2.0	X			X	X	X		X	X
2.0		X		X	X	X	X	*	*
2.0			X	X	[illegible]	X	*	*	*
3.0	X			X		X	X		X
3.0		X		X		X	X		X
3.0			X	X		X	X		X

X Regular test measurements obtained

O The flow overtopped the model and channel walls

* Submergence was not possible for these flow conditions

Table VI - Rough Boundary Tests

$n = 0.0233$

Geometry VI

Flow Rate cfs.	Froude Number F_n .10	.15	.20	Thickness Factor L/b = 0.50, Channel Width Ratio b/B .15	.20	.25
2.0	X			X	X	X
2.0		X		X	X	*
2.0			X	X	X	*
2.5	X			X	X	X
2.5		X		X	X	X
2.5			X	X	X	[illegible]
3.0	X			X	X	X
3.0		X		X	X	X
3.0			X	X	X	X

X Regular test measurements obtained

O The flow overtopped the model and channel walls

* Submergence was not possible for these flow conditions

Table VII - Rough Boundary Tests

$n = 0.0238$

Geometry VII

Flow Rate cfs.	Froude Number F_n .1	.2	.3	.4	.5	Channel Width Ratio b/B 0.35 $\sigma = 0$	0.35 $\sigma = .3$	0.35 $\sigma = .5$	0.50 $\sigma = 0$	0.50 $\sigma = .3$	0.50 $\sigma = .5$
1.0	X					*		X	*	*	
2.0	X					*	X		*	*	X
2.0		X				*	X		*	*	X
2.0			X			*	X		*	*	X
2.0				X		*			*	*	X
2.0					X	*			*	*	X
2.5	X					X			*		
2.5				X		*	X		*	*	
2.75					X	*	X		*	*	
3.0	X									X	
3.0		X				X				*	X
3.85	X							O	X		
3.85		X						O	*	X	
3.85			X			X		O	*	*	X
3.85				X		X		O	*	*	X
3.85					X	X		O	*	*	X

X Regular test measurements obtained

O The flow overtopped the model and channel walls

* Submergence was not possible for these flow conditions

II-2 Definitions: Fully Submerged and Partly Submerged Flow

The terms free outflow, fully submerged and partly submerged outflow are fre-
uently used in this chapter and are defined as follows. Free outflow exists when
he jet discharging from the downstream face of the bridge opening is surrounded,
xcept for the channel bottom, only by air and a hydraulic jump occurs further down-
tream. Fully submerged outflow exists when the jet discharges into a stream that
as a depth equal to or greater than the downstream height of the bridge opening.
partly submerged outflow is the case when the jet discharges into a stream that
as a depth less than the height of the bridge opening and no downstream jump occurs.

VIII-3 Geometry Ia - Smooth Boundaries
(See fig. 3-14 for definition of Geometry Ia)

a) Coefficients of Contraction, of Discharge and of Velocity for Free Jet Outflow

In order to investigate the coefficients of velocity, contraction and discharge for submerged bridge inlets, 67 test runs were made (see Table I - VII). The coefficients are defined as follows: Coefficient of contraction, C_c, is the ratio of jet area at vena contracta A_v to the area of the orifice A_o.

$$C_c = \frac{A_v}{A_o}$$

Coefficient of discharge, C_d, is the ratio of the actual discharge Q_a, obtained from the Venturimeter reading, to the theoretical Q_t, as calculated by formula

$$C_d = \frac{Q_a}{Q_t}$$

Coefficient of velocity is the ratio of actual velocity V_a to the theoretical velocity V_t

$$C_v = \frac{V_a}{V_t}$$

It is customary to combine the three coefficients as follows: From continuity equation the following can be written:

$$\frac{Q_a}{Q_t} = \frac{A_v}{A_o} \cdot \frac{V_a}{V_t}$$

from which it follows that:

$$C_d = C_c \, C_v$$

To find the coefficient of contraction the vena contracta had to be located and the cross-sectional area measured. This was done by means of the electronic point gage.

A sufficient number of readings were taken at the vena contracta to plot the cross sectional area on graph paper. By use of a planimeter the area A_v was obtained and the coefficient of contraction could be calculated, as the area of the model opening was known.

The coefficient of contraction was plotted versus the ratio b/Y_1 of the model opening width to the backwater depth using the channel width ratio b/B, as parameter (see Figure 8-3-1).

To obtain values for the calculation of the coefficient of discharge C_d, a theoretical discharge equation was developed. The development of this equation (3-7-26) was presented in the theoretical analysis in Chapter III. The actual rate of flow through the constriction was obtained from the manometer readings and the venturi meter calibration curves. Curves were plotted for the coefficient of discharge C_d versus the ratio b/Y_1 and the channel width ratio was again used as parameter (see Figure 8-3-1). The coefficient of velocity was then found from the relationship between the three coefficients, $C_d = C_c\ C_v$ and plotted versus b/Y_1 in Figure 8-3-1.

The C_d curves seem to converge toward the value 0.61 as the $\frac{b}{Y_1}$ ratio tends to zero. The curves are closely spaced straight lines and the C_d values decrease with increasing channel width ratios. The C_c curves also tend towards the 0.61 value as the $\frac{b}{Y_1}$ ratio decreases. Values of C_c decrease for increasing channel width ratios. For increasing C_c values, within the test range, the C_c curves tend to increase toward the value 0.71 and then stabilize at this value. The C_v curves have the same relative spacing as the C_c and C_d curves as to the $\frac{b}{B}$ ratio but tend toward the value 1.0 as a limiting value when the $\frac{b}{Y_1}$ ratio decreases toward zero.

The test data are recorded in test runs 1 - 67 shown in Table 8-1. The calculated values to find C_c, C_d and C_v are found in Table 8-4.

b) Velocity Distribution at Vena Contracta for Free Jet Outflow

Extensive velocity measurements were taken in the jet downstream of constriction at the vena contracta in order to observe the velocity distribution. The Prandtl tube together with the pressure transducer were used. The readings were taken in a grid system to obtain full coverage over the cross section. The borderline of the area at the cross-section was also measured and plotted on graph paper together with the velocity grid values. From this the isovelocity curves were drawn. Figure

8-3-2 shows one of the typical isovelocity curves drawn from such grid measurements. Figure 8-3-3 shows the result obtained by following the individual isovelocity curves in the water cross-section itself. This was done by moving the Prandtl tube through the cross-section and mapping the path for the individual isovelocity curves obtained by means of the horizontal and vertical traversing devices. The data of Figures 8-3-2 and 8-3-3 correspond to discharges 3.75 cfs and 2.62 cfs, normal depth Froude number 0.142 and 0.108 and opening ratios 0.30 and 0.30 respectively.

In Figure 8-3-4 the values of the velocities are plotted at different depths and a mean velocity curve is drawn. The data for Figure 8-3-4 are the same as those for Figure 8-3-3. Figure 8-3-4 shows the velocity variation over the opening width at different depths. A similar study was made for other flow conditions as recorded in Table 8-3. All the recorded values when plotted, show the same characteristic velocity distribution as shown in Figures 8-3-2 to 8-3-4.

c) The Generalized Backwater Equation -- Outflow Fully and Partly Submerged

From the theoretical analysis done in Chapter III it is expected that the general relation between the backwater and normal depth is of the form

$$\frac{Y_1}{Y_n} = C \left[\left(\frac{F_n}{M'} \right)^2 \right]^{\gamma} \qquad (8\text{-}3\text{-}1)$$

where C is a coefficient that would take into account the effects of the approach velocity, discharge coefficient, non-hydrostatic pressure distribution, non-uniform velocity distribution and other empirically determined factors. In a logarithmic plot of Y_1/Y_n versus $(F_n/M')^2$, the slope of the line is γ. A total of 3? tests were made on geometry I-a and processed on the IBM 1620 computer to obtain plotting values of $(Y_1/Y_n - 1)$ versus $(F_n/M')^2$. The graph is shown on Figure 8-3-5. From this graph the values γ and C were found to be 0.90 and 1.18 respectively, and equation 8-3-1 can be written for the submerged conditions of geometry I-a in the following way:

$$\frac{Y_1}{Y_n} = 1 + 1.18 \left[\left(\frac{F_n}{M'} \right)^2 \right]^{0.90} \qquad (8\text{-}3\text{-}2)$$

or

$$\frac{Y_1}{Y_n} = 1 + 1.18 \left(\frac{F_n}{M'}\right)^{1.80} \qquad (8\text{-}3\text{-}3)$$

The test data taken to obtain this generalized backwater equation 8-3-3 are recorded in test runs 102-134 which are located in Table 8-2. The calculated values from the data are presented in Table 8-3. A least square fitting of the backwater ratio points for fully submerged flow is given in Fig. 8-10-1. The values of the head loss coefficient K are given in Fig. 8-9-1.

A general backwater equation was not obtainable for the free jet outflow. This is because the Froude numbers for test runs 1-67 are all in the range of 0.550 - 0.587 which results in one group of numbers, and a line could not be defined.

d) Discharge Coefficient for Free, Submerged and Partly Submerged Outflow

A graph was made of the discharge coefficient, C_d, versus the channel opening ratio, M', for the submerged smooth bridge opening, Geometry I-a (Figure 8-3-6). The curves obtained are for the submerged discharge jet except for the two upper most curves which are for partly submerged jets. These curves are similar to those estimated by P. F. Biery (see Art. VII-1-c) for the unsubmerged case and for channel opening ratios of 0.29 and up. The present values for the submerged case were obtained for the range of M' between 0.10 and 0.35. Figure 8-3-6 shows the C_d versus M' curves for submerged and partly submerged flow as well as Biery's discharge coefficient curves for the unsubmerged case which have been superposed for the purpose of comparison. The test data taken to obtain the curves in Figure 8-3-6 are recorded in test runs 102 to 134 which are located in Table 8-2. The calculated values are presented in Table 8-4.

The values of the discharge coefficient are summarized in Figure 8-3-7. For the submerged jet, two sets of curves are given, one uses the Froude number as a parameter, the other uses the ratio $Y_n/\frac{b}{2}$ of the normal depth to the arch radius. The free jet discharge coefficient curves previously presented in Figure 8-3-1 have been reproduced here for completeness. The calculations are shown in Table 8-4.

VIII-4 Geometry I-b - Smooth Boundaries

As can be seen from the definition of test geometries, (fig. 8-1) geometry I-a is a special case of geometry I-b. By setting the variable $\frac{L}{b}$ equal to zero in the definition of geometry I-b, the geometry I-a is obtained. Geometry I-a therefore represents the limiting case of geometry I-b, and can be treated together with I-b.

In the theoretical analysis made in Chapter III the dimensionless relation

$$\frac{Q}{g^{\frac{1}{2}} b^{5/2}} = f\left(\frac{L}{b}\right) \qquad (8-4-1)$$

was developed for the orifice type flow through a submerged arch constriction. A total of 92 test runs were conducted for submerged conditions in the smooth channel. Three sets of dimensionless curves were plotted. To save space and make it easier to compare the curves, they were all plotted in one figure. The $\frac{L}{b}$ ratio is used as parameter, and the Froude number is constant for each set of curves. To be able to show all three sets of curves clearly on one graph, the vertical coordinate axis was broken into three parts each starting from zero. The curves are shown in Figure 8-4-1. For higher Froude numbers the curves get closely spaced. This means that the L/b ratio becomes insignificant for all practical purposes when the Froude number reaches a value of about 0.20 for the smooth ($n = 0.0110$) boundary case of geometry I-b. The data from the 92 test runs are listed in run number 101-192 and recorded in Table 8-2. The calculated values of the plotted points are shown in Table 8-4.

The backwater superelevation ratio h_1^*/Y_n is plotted vs. $(F_n/M')^2$ for values of the length parameter L/b = 0.25; 0.50; 0.75 and 1.0 in figures 8-10-2 to 8-10-5. The equations of the lines obtained by least squares are given in the figure. Figure 8-10-6 summarizes the backwater superelevation data for geometries Ia, and Ib with smooth boundaries. The values of the head loss coefficient K and the lines obtained by least square fitting are given in figures 8-9-2 to 8-9-5 for the same values of the length parameter L/b. A summary of the head loss coefficients for geometries Ia and Ib with smooth boundaries is given in Fig. 8-9-6.

VIII-5 Geometries I-a and I-b - Rough Boundaries

a) Test Data

A total of 38 test runs were made in order to plot the dimensionless curves shown in Figure 8-5-1. These three sets of curves were also based on the dimensionless equation 3-7-33 developed in Chapter III. The data are recorded in test runs 193-231 and can be found in table 7-2. The calculated values from the data are listed in Table 8-4.

The values of the backwater superelevation ratio h_1^*/Y_n were plotted vs. $(F_n/M)^2$ for the five values of the length parameter tested (L/b = 0; 0.25; 0.50; 0.75; 1.00) in figure 8-10-7. The lines were fitted by eye, and their equations are given in the figure. The values of the discharge coefficient were plotted vs. the channel opening ratio in fig. 8-9-7 for the same values of the length parameter. The equations of the lines fitted by eye are given in the figure.

The investigation shows that the width of the constriction in the direction of flow, L, influences the backwater to a certain degree when the Froude number is low. The wider the bridge in the direction of flow, the lower is the backwater depth obtained. For a Froude number of 0.15 the backwater ratio for an L/b ratio of 1.0 was as much as 30% lower than for a L/b ratio of 0.00. For the more practical cases where the Y_1/b ratio is in the order of about 0.50 to 1.00, a lowering of about 10-20% in the backwater ratio is usual when the L/b ratio is increased from 0.00 to 1.00. Flow through three dimensional arch bridges is very similar in behavior to the flow through short culverts. For short culverts, the flow characteristics are relatively independent of the slope and the factors that involve the length are comparatively unimportant. The control section for square edge openings, such as investigated here, is at the inlet.

Separation of flow around the opening, at the inlet section, was frequently observed. The flow contracted towards vena contracta section in the first part of the barrel expanded in a spiral motion as shown in Figure 8-5-2 and ended in a slug flow at the submerged outlet. Figure 8-5-3 shows the case where slug flow occurs at

ne exit of the barrel. Figure 8-5-4 presents the free jet case for geometry I-a
th rough boundaries and the same flow.

Vortex action was also often observed. This air-vortex occurs from the surface
ight above the crest of the inlet and introduces air through the opening. This
ecreases the water area of the opening and hence the flow through the constriction,
nd as a result the backwater increases.

An important effect upon the separation phenomena, that controls the change of
low from a sluice type to full conduit flow, is the existence of a negative pressure
n the barrel. This is caused by the relative magnitudes of air inflow from the
utlet and from the vortex action over the inlet. The outflow of air due to entrain-
ent at the air-water surface also has an effect upon the separation phenomena, the
ore air entrained the less separation will occur and the barrel will tend towards
ull conduit flow.

) Comparison Between Smooth and Rough Boundary Tests

A comparison between the limiting curves of Figures 8-4-1 and 8-5-1 for the
mooth and rough boundary conditions respectively are made in Figure 8-5-5. These
urves show that a rough boundary condition is of advantage for higher Froude numbers
$F_n > 0.15$) as could be expected from observing the flow behavior. For higher Froude
umbers the approach velocities will increase and consequently give a higher turbulence
evel due to the natural roughness. This will improve the ability of the barrel to
roduce full conduit flow, because it increases the air entrainment in the barrel
t the air-water surface and hence reduces the separation at the inlet.

VIII-6 Geometry V-b Three-Dimensional Skewed Bridges - Rough Boundaries
(See Fig. 3-14 for definition of geometries)

The discharge jet shoots to the side of the flume in a direction [illegible] perpendicular to the face of the bridge.

The test results are [illegible] in the dimensionless [illegible] curves in Figure 8-6-1, based on the theoretical [illegible] 3-7-33 [illegible] in Chapter III. Three sets of curves are plotted [illegible] the Froude number and the angle of [illegible], ϕ_2, as parameters. The [illegible] ratio [illegible] is kept constant [illegible]. The performance curves show that a variation in the angle [illegible] $\phi_2 = 15°$ and $\phi_2 = 30°$ is a relatively [illegible] compared [illegible] the effect of a change in the Froude number. To be noted is also [illegible] performance of [illegible] constrictions for low Froude numbers [illegible] compared to the ϕ_2 [illegible] of Geometry I-b. The explanation [illegible] non-[illegible] constriction [illegible] in the [illegible] and [illegible] condition closer to conduit flow [illegible] Froude number [illegible] and both Geometries, I-b and V-b [illegible] about the same [illegible] flow, the difference in the performance curves [illegible]. [illegible] having a Y_1/b ratio less than [illegible] but are merely an expected [illegible]. [illegible] 24 test runs were made [illegible] run numbers 232 to 255. [illegible] 8-4. The values of the [illegible] ratio [illegible] in Figure 8-10-3. [illegible] values of the discharge coefficient K are plotted vs. the channel opening ratio in Fig. 8-9-8. The equation of a visual fit line is given on the figure.

VIII-7 Geometry VI - Two Span Semicircular Arch Bridge Constriction Rough Boundaries
(See Fig. 3-14 for definition of geometries)

This geometry represents about 11% of all existing arch bridges in the state of Indiana. The great majority of these bridge constrictions have a thickness factor, L/b, of about 0.50 which was chosen for the experimental models of Geometry VI.

The test results are presented in the dimensionless graphs shown in Figure 8-7-1. To be noted is that the opening width of the models, b, is the width of one of the openings. The performance of the modes in Geometry VI is approximately the same as for Geometry I-b of same thickness factor.

A total of 27 test runs were made and the data taken are recorded in test runs no. (256-282) as shown in Table 8-2. The calculated values are presented in Table 8-5. The values of the backwater superelevation ratio h_1^*/Y_n were plotted vs. $(F_n/M)^2$ in fig. 8-10-9. The equation of a visual fit line is given on the figure. The values of the discharge coefficient K are plotted vs. the channel opening ratio M in Fig. 8-9-8. The equation of a visual fit line is given on the figure.

VIII-8 Geometry VII - Segment Arch Bridge Rough Boundaries
(See Fig. 3-14 for definition of geometries)

With reference to Figure 3-12, it is readily seen that the dimensionless relationship of the discharge as a function of the backwater depth and the width of the constriction holds true also for the segment arch openings. The curves shown in Figure 8-8-1 are based on this relationship as expressed in Equation 3-7-2[illegible], derived in Chapter III. A total of 22 test runs (No, 285 to 307) were done and recorded in Table 8-2. The calculated values are found in Table 8-5.

Figure 8-8-1 shows that the spacing between the curves becomes very small as the Froude number increases beyond 0.3. This means that the Froude number becomes insignificant as a parameter when the degree of turbulence increases beyond a certain value ($F_n > 0.3$).

The values of the backwater superelevation ratio h_1^*/Y_n were plotted vs. [illegible] in fig. 8-10-10. The equation of a visual fit line is given in the figure. The values of the discharge coefficient K are plotted vs. the channel opening ratio M' in Fig. 8-9-10. The equation of a visual fit line is given in the figure.

VIII-9 Head Loss due to Submerged Arch Bridge Constrictions

In the theoretical analysis in Chapter III an expression for the additional head loss coefficient due to the bridge constriction was found, equation (3-8-13). Assuming $\alpha_1 = \alpha_4 = \alpha$, then

$$K = \frac{h_1^*}{V_o^2/2g} - \alpha\left[\left(\frac{A_o}{A_y}\right)^2 - \left(\frac{A_o}{A_1}\right)^2\right] \qquad (8\text{-}8\text{-}[illegible])$$

This equation, which holds for submerged bridge constrictions is similar to the one for free surface flow through a bridge constriction, and K varies primarily with

a) The channel opening ratio M'

b) Type and shape of bridge constriction such as inlet shape, wing wall angle [illegible], skewness angle ϕ_2 and thickness factor, L/b

c) Number of bridge spans, N

d) Eccentricity of bridge opening, e

e) Froude number F_n

The head loss coefficient K was computed on the IBM 7090 from equation 8-8-[illegible]. The corresponding value of the channel opening ratio, M', was also computed, and by a least mean square routine the slope of the line of the plot K versus M' was found in arithmetic scale. A significant value such as L/b, ϕ_2 and [illegible] was used as parameters both for smooth and rough boundary tests. The plot of these curves are shown in Figures 8-9-1 to 8-9-10.

For the smooth boundaries a sufficient number of data was available to use the least square method on the computer. In the case of rough boundaries, however, the data available for each parameter were not always sufficient and some of the lines had to be fitted by eye.

The data used for the calculations are listed in runs 101-306 presented in Table 8-2. The calculated values from the computer are listed in tables 8-4 and 8-5.

VIII-10 General Backwater Equations for Geometries I-a, I-b, VI and VII - Smooth and Rough Boundaries

The theoretical developement of these equations was done in Chapter III. The generalized backwater equation is of the form

$$\frac{Y_1}{Y_n} = C\left[\left(\frac{F_n}{M'}\right)^2\right]^{\gamma} \qquad (8\text{-}10\text{-}1)$$

However, it was found more convenient to plot the test results for the fully submerged discharge jet in the form

$$\frac{Y_1}{Y_n} - 1 = C\left[\left(\frac{F_n}{M'}\right)^2\right]^{\gamma} \qquad (8\text{-}10\text{-}2)$$

If h_1^* is substituted for $Y_1 - Y_n$, equation 8-10-2 can be written in the following form:

$$\frac{h_1^*}{Y_n} = C\left[\left(\frac{F_n}{M'}\right)^2\right] \qquad (8\text{-}10\text{-}3)$$

This is the presentation used in the graphs at the end of this section. Figures 8-10-1 to 8-10-10 present the generalized backwater equations for the geometries considered. Significant values of the geometries are used as parameters.

Values for $\frac{h_1^*}{Y_n}$ and $\left(\frac{F_n}{M'}\right)$ were calculated in the same computer program as used for the head loss considerations in the previous section. These points were to be plotted on a log log scale, so the computer program was also written to determine the slope of the best fitting line through these points. A least mean square routine for log log plots was used. For the smooth boundaries a sufficient number of data was available to use the least square method in finding the slope of the line. In the case of rough boundaries, however, it was sometimes necessary to fit the lines by eye from the few data available.

The data used for the calculations are listed in runs 101-306, presented in table 8-2. The calculated values are listed in tables 8-4 and 8-5.

There are some advantages in doing all these calculations in one computer program. Only one set of data has to be prepared and the computer stores the values in the memory once. The computer time used, therefore, becomes a minimum. For all the calculations pertaining to the figures 8-9-1 to 8-10-10, the time used by the IBM 7090 was less than 10 minutes.

VIII-11 Conclusions - Submerged Tests

The results of this report are applicable to bridges with submerged inlet and geometries I-a, I-b, V-b, VI and VII (see definition of geometries in Chapter III and figure 3-14.) No eccentricity, entrance rounding or wing walls are counted for.

Findings are the following:

1. Equation of discharge for orifice type flow through a semi-circular submerged arch bridge constriction.

2. Semi-empirical expression for the occurrence of free surface flow and orifice type flow through the bridge opening.

3. Graphs presenting the discharge as a function of the ratio of the backwater depth to the arch span.

4. Graphs showing the ratio of the backwater to the normal depth as a function of the normal depth Froude number and the channel opening ratio.

5. Empirical generalized backwater equations derived for the several geometries from the graphs in point 4.

6. Graphs giving the values of the constriction head loss coefficient as a function of the channel opening ratio for the different test geometries.

Conclusions

1. The backwater at submerged arch bridge constrictions perpendicular to the stream decreases as the length of the bridge in the direction of flow increases.

2. For equal bridge length the backwater due to submerged arch bridges is further decreased when the constriction is skewed with respect to the direction of flow, at least for skew angles up to 30°.

3. The value of the head loss coefficient due to a submerged arch bridge constriction is independent of the normal depth Froude number as long as both inlet and outlet of the bridge are submerged.

4. For hydraulically short submerged arch bridges (that is where the barrel is not sufficiently long to allow the expanding depth of flow below the contraction to raise and fill the barrel), the backwater depth increases for an increase in the normal depth Froude number.

5. To obtain a minimum backwater depth at a submerged arch bridge constriction the barrel should flow full (full conduit flow).

IX FIELD WORK

IX-1 A Preliminary Field Survey of Sites for Model-Prototype Comparison of the Hydraulics of Arch Bridge Constrictions

by T. P. Chang and J. T. Strange

INDIANA FLOOD CONTROL AND WATER RESOURCES COMMISSION
INDIANAPOLIS, INDIANA

Introduction

A series of model-testing studies of the hydraulics of semicircular arch constrictions have been made during the past four years at the Hydraulic Laboratory of Purdue University, under the guidance of Professor Delleur and Professor Toebes. The Indiana Flood Control and Water Resources Commission has been requested to make a field check of some of the arch bridges in Indiana so that a suitable arch bridge, either one-span or two-span, may be selected in order to make model-prototype comparisons by taking field measurements during a flood.

The preliminary field reconnaissance work started in the middle of October of this year. More than 100 arch bridges, both one-span and two-span, have been examined. Ten of these bridges; eight one-span and two two-span, have been chosen for further investigation. Preliminary surveys and photographs have been taken for these ten arch bridges.

Criteria Used for the Selection of Bridge Sites

1. Location:

   For the convenience of future field measurements during a flood, the bridges should be as close to Indianapolis as possible. The [illegible] season, the field reconnaissance was limited to Marion, Hendricks, Morgan, Johnson, Shelby, Hancock, Hamilton and Boone Counties.

2. Channel Condition:

   (a) The channel reach close to the bridge site, both upstream and downstream, should be as clear as possible so that the flow during the flood will not be unduly disturbed.

(b) The cross sections of the channel reach, both upstream and downstream from the bridge, should be uniform in order to avoid the effect of head loss due to enlargement and contraction, and the water should be confined within the stream banks during the flood.

(c) The channel reach should be nearly straight. There should be no confluence close to the bridge.

(d) The shape of the channel cross sections should have as few irregularities as possible.

(e) There should be no structures, such as other bridges, dams, wiers, etc., near the bridge site.

(f) Bridge skew should not be excessive. Skewed bridges, in which the center line of the openings are not parallel with the direction of the channel, should be avoided.

3. Arches of the Bridges:

(a) The shape of the arch should be close to semicircular or a part of a circular arch.

(b) The opening ratio of the arch should be small enough to produce an appreciable backwater effect.

(c) Excessive eccentricity should be avoided. The arch opening should be symmetrical with respect to the center line of the channel.

4. Flow Condition:

(a) Flow velocity during a flood should be great enough to create a relatively high Froude number, $F = \frac{V_n}{\sqrt{gy_n}}$.

(b) The drainage basin should be relatively large (about 15 square miles or more) and topographic relief within the basin relatively small in order to produce a flood of sufficient duration so that desired data may be obtained.

scription of the Field Situation

As far as the purpose of this report is concerned, all of the arch bridges ich have been inspected can be put into three general classifications. These e; Highway bridges, City bridges and County Road bridges. Each has its general atures and problems.

1. Highway Arch Bridges:

(a) Arch shape is excellent, but almost all of them have a very large opening. Flood waters will probably never reach the middle part of the arch. Hence, the arch effect is negligible.

(b) Usually the road side drainage ditches are near the faces of the bridge, both upstream and downstream. These drainage ditches suddenly enlarge the channel cross section.

(c) Channels are not very clear or uniform. Channel and bank conditions are such that if flood levels were high enough to produce the desired arch effect, water would spill out into the fields; thereby, greatly changing the shape of the channel cross sections.

(d) Since the traffic is usually heavy, working conditions on the bridge are not good.

(e) Usually the length of the arch constriction is relatively long.

2. City Arch Bridges:

(a) Channel conditions are fairly good, especially in the park areas.

(b) Flood water is confined within the banks. Flood water levels are high enough to produce an arch effect.

(c) The shape of the arches are not good, either too flat or not semicircular.

(d) [illegible] are in the channel reach close to the bridge or under the bridge. This is a common and serious problem with the city bridges.

3. County Road Arch Bridges:

(a) The openings of the arch are usually small.

(b) Channels are not uniform and are sometimes choked by brush and small trees.

(c) Farm fences across the channel near the bridge catch logs and debris which seriously affect the flood flow under the bridge.

(d) The channel and bridge size is usually smaller than the highway arch bridge or the city arch bridge.

Conclusion

After three weeks of field inspection of the arch bridges in the eight counties near Indianapolis, the writers are of the opinion that it is extremely difficult to find an arch bridge for the purpose of model-prototype comparison without any defects. However, ten of the most suitable bridge sites have been selected for further investigation. Each one has some good features and some defects. The list of the bridges are as follows:

1. Olney Street, Indianapolis, crossing Pogues Run (Bridge No. 2a)
2. Brookside Parkway, Indianapolis, crossing Pogues Run (Bridge No. 2b)
3. Jefferson Avenue, Indianapolis, crossing Pogues Run (Bridge No. 2c)
4. South Belmont Avenue, Indianapolis, crossing Little Buck Creek (Bridge No. 8a)
5. State Road 100, crossing Williams Creek (Bridge No. 13)
6. Villa Avenue, Indianapolis, crossing Pleasant Run (Bridge No. 15a)
7. Linden Avenue, Indianapolis, crossing Pleasant Run (Bridge No. 15b)
8. State Road 44, crossing HurricaneCreek (Bridge No. 51)
9. White Lick Creek near State Boys School, Plainfield (Bridge No. 59a)
10. Dean Road, Indianapolis, crossing Howland Ditch (Bridge No. 66a)

The complete information for each of the above bridges are compiled on a separate form. A suggestion given by the writers has been made for each of those bridges.

X-2 Summary of Information on Bridge Sites

For each of the ten bridge sites a resume sheet, one plan view and four cross ections were prepared by the Indiana Flood Control and Water Resources Commission. ereal photographs were made by the State Highway Department of Indiana for nine f these sites. Topographic maps were prepared from these aerial photographs in the irphoto Laboratory, School of Civil Engineering, Purdue University, under the upervision of Professor R. Miles.

I. OLNEY STREET, INDIANAPOLIS, CROSSING POGUES RUN

RESUME

(1) Compiled number of bridge: No. 2a.
(2) Location: Lat. 39°47'25", Long. 86°06'26", Indianapolis east Indiana, quadrangle sec. 32, T. 16 N., R. 4 E., at bridge on Olney Street, Indianapolis, crossing Pogues Run, eastern central part of Indianapolis.
(3) Drainage area: 8.7 square miles.
(4) Tributary to: Tributary to West Fork White River, Wabash River basin.
(5) Slope of channel: 3.1/1000.
(6) Bridge type: One-span concrete arch bridge.
(7) Skew toward upstream: 2° L.
(8) Skew toward downstream: 25° L.
(9) Width of Bridge: 50 feet.
(10) Clearance of arch opening: 12.7 feet.
(11) Width between banks of channel: 90 feet.
(12) Width of channel bottom: 24 feet.
(13) Eccentricity: Low flow part of channel located at left side of channel. Center line of arch is about 7 feet right of center line of low flow channel, but the arch center line nearly coincides with the center line between the two banks.
(14) High water mark: 3 feet below top of arch opening but date is uncertain.
(15) Channel condition:
    (a) Bend about 175 feet upstream from upstream face of bridge. Bend about 180 feet downstream from downstream face of bridge.
    (b) Trees and brush distributed along right banks both upstream and downstream.
    (c) Two 1-foot diameter sewers in upstream side.
    (d) Channel bottom is irregular.
    (e) A bridge on Sherman Drive located 1,500 feet upstream from this site. A bridge on Brookside Parkway (Bridge No. 2b) located 1,700 feet downstream from this site.
(16) Arch condition: In upper part, arch is in good shape, but lower part is straight wall.

Suggestion: The opening ratio is small. For a very high flood the channel irregularity and the straight part of the opening could be neglected.

Figures 9-1-1 to 9-1-5 show the plan view and cross sections at the bridge site. Figure 9-1-6 is a topographic map prepared from aereal photographs.

II. BROOKSIDE PARKWAY, INDIANAPOLIS, CROSSING POGUES RUN

RESUME

(1) Compiled number of bridge: No. 2b.
(2) Location: Lat. 39°47'26", Long. 86°06'41", Indianapolis east, Indiana, quadrangle, sec. 32, T. 16 N., R. 4 E., at bridge on Brookside Parkway, Indianapolis, crossing Pogues Run, eastern central part of Indianapolis.
(3) Drainage area: 9.2 square miles.
(4) Tributary to: Tributary to White River, Wabash River basin.
(5) Slope of channel: 2.9/1000.
(6) Bridge type: One-span concrete arch bridge.
(7) Skew toward upstream: 15°L.
(8) Skew toward downstream: 5°L.
(9) Width of bridge: 20 feet.
(10) Clearance of arch opening: 16 feet.
(11) Width between banks of channel: 127 feet.
(12) Eccentricity: No.
(13) High water mark: 4.8 feet below top of arch, date is uncertain.
(14) Channel condition:
   (a) Bend at 170 feet upstream from upstream face of bridge.
   (b) Bushes distributed along banks both upstream and downstream.
   (c) Channel bottom is regular but parabolic shape.
   (d) 18-inch diameter sewer in downstream side.
   (e) A bridge on North Rual Street located 2,200 feet downstream from the bridge No. 2b.
(15) Arch condition: It is a good shape arch.

Suggestion: The channel condition is very good, only one sewer in downstream side. Skew is small. It is recommended to be used for a common flood. However, the influence of 80° bend in upstream is uncertain.

Figures 9-2-1 to 9-2-5 show the plan view and cross sections of the bridge site. Aereal photographs of this site are not available.

III. JEFFERSON AVENUE, INDIANAPOLIS, CROSSING POGUES RUN

RESUME

(1) Compiled number of bridge: No. 2c.
(2) Location: Lat. 39°47'11", Long. 86°07'28", Indianapolis east, Indiana quadrangle, sec. 31, T. 16 N., R. 4 E., at bridge on Jefferson Avenue, Indianapolis, crossing Pogues Run, eastern central part of Indianapolis.
(3) Drainage area: 10.3 square miles.
(4) Tributary to: Tributary to West Fork of White River, Wabash River basin.
(5) Slope of channel: 2.4/1000.
(6) Bridge type: One span concrete arch bridge.
(7) Skew toward upstream: 5° R.
(8) Skew toward downstream: 5° L.
(9) Width of bridge: 45 feet.
(10) Clearance of arch opening: 11 feet.
(11) Width between banks of channel: 70 feet.
(12) Width of channel bottom: 35 feet.
(13) Eccentricity: None.
(14) High water mark: Two high water marks, lower one is about 6.7 feet below the top of arch opening, the higher one is about 1.4 feet below top of arch opening. Dates are uncertain.
(15) Channel condition:
  (a) No bend close to the bridge site both upstream and downstream side. Channel is straight.
  (b) Trees and bushes distributed along both side banks of downstream channel.
  (c) Two sewers upstream side, one 2-foot 6-inch diameter, another one 3-foot 6-inch diameter.
  (d) Channel bottom is very good, regular and flat.
(16) Arch condition: Upper part of opening is arch shape, but lower part is straight wall.

Suggestion: The two big sewers are major defect, but the influence is uncertain, otherwise, this is a good site.

Figures 9-3-1 to 9-3-5 show the plan view and crossections at the bridge site. Figure 9-3-6 is a topographic map of the briage site prepared from aereal photographs.

IV. SOUTH BELMONT AVENUE, INDIANAPOLIS, CROSSING LITTLE BUCK CREEK

RESUME

(1) Compiled number of bridge: No. 8a.
(2) Location: Lat. 39°40'00", Long. 86°11'47", Maywood, Indiana, quadrangle, on east line sec. 9, T. 14 N., R. 3 E., at bridge on south Belmont Avenue, Indianapolis, crossing Little Buck Creek, southwestern corner of Indianapolis.
(3) Drainage area: 16.7 square miles.
(4) Tributary to: Tributary to West Fork White River, Wabash River Basin
(5) Slope of channel: 1.5/1000.
(6) Bridge type: One-span concrete arch bridge.
(7) Skew toward upstream: 10° L.
(8) Skew toward downstream: 15° R.
(9) Width of bridge: 40 feet.
(10) Clearance of arch opening: 16.5 feet.
(11) Width between banks of channel: 109 feet.
(12) Width of channel bottom: Not clear.
(13) Eccentricity: The low flow part is located in the left side of the channel. The center line of arch is about the same position as the center line between banks.
(14) High water mark: Flood of 1955, 7.5 feet below top of arch.
(15) Channel condition:
    (a) The bridge site is just on a 25° curve.
    (b) The channel is clear.
    (c) Banks are high enough to confine the flood.
    (d) Channel bottom is irregular.
    (e) No sewers nearby.
(16) Arch condition: It is in good shape but too flat.

Suggestion: The channel is clear and uniform, banks confine the flood flow very well. It is recommended to be used during very high flood, 4 feet or more than the flood of 1955.

Figures 9-4-1 to 9-4-5 show a plan view and cross sections at the bridge site. Figure 9-4-6 is a topographic map of the bridge site prepared from aereal photographs.

V. STATE ROAD 100, CROSSING WILLIAMS CREEK

RESUME

(1) Compiled number of bridge: No. 13.
(2) Location: Lat. 39°54'44", Long. 86°10'28", Carmel, Indiana, quadrangle, on north line sec. 22, T. 17 N., R. 3 E., at bridge on State Road 100 crossing Williams Creek, 2 1/2 miles northwest of Augusta, Marion County, and 3.8 miles upstream from mouth.
(3) Drainage area: 17.4 square miles.
(4) Tributary to: Tributary to West Fork White River, Wabash River basin.
(5) Slope of channel: about 2/1000.
(6) Bridge type: One-span concrete arch bridge.
(7) Skew toward upstream: 15° R.
(8) Skew toward downstream: No skew.
(9) Width of bridge: 42 feet.
(10) Clearance of arch opening: 22 feet.
(11) Width between banks of channel: About 160 feet.
(12) Width of channel bottom: About 30 feet.
(13) Eccentricity of arch opening: Center line of arch opening is 10 feet left of the center line of stream.
(14) High water mark: Flood of April 25, 1961, 14.5 feet below top of arch opening.
(15). Channel condition:
- (a) No bend both upstream and downstream within 1,000 feet.
- (b) Trees and bushes distributed on banks both upstream and downstream.
- (c) Right banks both upstream and downstream are very low so that the flood water levels were limited to the lower part of arch opening.
- (d) No sewer nearby.

Suggestion: The arch shape is very good. It is recommended to be used for very high flood.

Figures 9-5-1 to 9-5-5 show a plan view and cross sections at the bridge site. Figure 9-5-6 is a topographic map of the bridge site prepared from aereal photographs.

VI. VILLA AVENUE, INDIANAPOLIS, CROSSING PLEASANT RUN

RESUME

(1) Compiled number of bridge: No. 15a.
(2) Location: Lat. 39°44'53", Long. 86°07'35", Maywood, Indiana, quadrangle, northeastern corner of sec. 18, T. 15 N., R. 4 E., at bridge on Villa Avenue, Indianapolis, crossing Pleasant Run, south part of Indianapolis.
(3) Drainage area: 12.9 square miles
(4) Tributary to : Tributary to West Fork White River, Wabash River basin.
(5) Slope of Channel: 2.5/1000.
(6) Bridge type: One span concrete arch bridge.
(7) Skew toward upstream: 15° R.
(8) Skew toward downstream: 20° R.
(9) Width of bridge: 40 feet.
(10) Clearance of arch opening: 14.5 feet.
(11) Width between banks of channel: 116 feet.
(12) Width of channel bottom: 65 feet.
(13) Eccentricity of arch opening: Center line of arch opening is at 7 feet right of center line of low flow channel.
(14) High water mark: Flood of April 1961, 7 feet below top of arch opening.
(15) Channel condition:
  (a) Bend at 150 feet downstream from downstream face. Bend at 150 feet upstream from upstream face.
  (b) Channel is relatively clear and fairly uniform.
  (c) The banks are high enough to confine the flood water.
  (d) Bottom is very regular.
  (e) A fairly large tree near upstream face may obstruct flood flow.
  (f) Two 1-foot diameter sewers in upstream side.
(16) Arch condition:
  (a) Upper part is too flat.
  (b) Two ends of the arch are elliptic shape.

Suggestion: The channel is clear and uniform but the arch seems too flat. It is recommended to be used for segment arch bridge model - prototype comparison. On the other hand, the degree of disturbances due to bends and sewers are uncertain.

Figures 9-6-1 to 9-6-5 show a plan view and cross sections at the bridge site. Figure 9-6-6 is a topographic map of the bridge site prepared from aereal photographs.

VII. LINDEN AVENUE, INDIANAPOLIS, CROSSING PLEASANT RUN

RESUME

(1) Compiled number of bridge: No. 15b.
(2) Location: Lat. 39°44'45", Long. 86°08'14", Maywood, Indiana quadrangle, west of sec. 18, T. 15 N., R. 4 E., at bridge on Linden Avenue, Indianapolis, crossing Pleasant Run, south part of Indianapolis.
(3) Drainage area: 13.3 square miles.
(4) Tributary to: Tributary to West Fork White River, Wabash River basin.
(5) Slope of channel: 1.5/1000.
(6) Bridge type: One span concrete arch bridge.
(7) Skew toward upstream: 5° L.
(8) Skew toward downstream: 15° L.
(9) Width of bridge: 40 feet.
(10) Clearance of arch opening: 11.5 feet.
(11) Width between banks of channel: 107 feet.
(12) Width of channel bottom: 55 feet.
(13) Eccentricity: None.
(14) High water mark:
  (a) Flood of April 1961, 5.8 feet below top of arch.
  (b) Highest water mark; uncertain date, 1 foot below top of arch.
(15) Channel condition:
  (a) Bend at about 200 feet upstream from upstream face.
  (b) At arch bridge on Shelby Street crossing Pleasant Run at 1000 feet downstream from the bridge.
  (c) The channel is uniform and clear.
  (d) The banks are high enough to confine the flood.
  (e) Channel bottom is very regular.
  (f) Three 8 inch diameter sewers, one in downstream side and two in upstream side. One 12 inch diameter sewer in right bank of downstream side.
(16) Arch condition: It seems too flat.

Suggestion: The channel is uniform and clear, but the arch seems too flat. It is recommended to be used for segment arch bridge model - prototype comparison. On the other hand, the degree of disturbances due to upstream bend, downstream bridge and sewers are uncertain.

Figures 9-7-1 to 9-7-5 show a plan view and cross sections at the bridge site. Figure 9-7-6 is a topographic map of the bridge site prepared from aereal photographs.

VIII. STATE ROAD 44 CROSSING HURRICANE CREEK

RESUME

(1) Compiled number of bridge: No. 51
(2) Location: Lat. 39°28' 51", Long. 86°02' 53", Franklin, Indiana, quadrangle, sec. 14, T. 12 N., R. 4 E., at bridge on State Road 44, crossing Hurricane Creek, eastern part of Franklin.
(3) Drainage area: 27 square miles.
(4) Tributary to: Tributary to Youngs Creek.
(5) Slope of channel: 1.3/1000.
(6) Bridge type: Two-span stony arch bridge.
(7) Skew toward upstream: 35° R.
(8) Skew toward downstream: 35° R.
(9) Width of bridge: 45 feet.
(10) Clearance of arch opening:
  7.5 feet for left side arch.
  9 feet for right side arch.
(11) Width between banks of channel: 43 feet.
(12) Width of channel bottom: 38 feet.
(13) Eccentricity: The left part of channel is about 2 feet higher than right side. A part of the right side arch is obstructed by the right bank.
(14) High water mark: 2.4 feet below the top of arches. Date is uncertain.
(15) Channel condition:
  (a) The channel is perfectly straight and uniform.
  (b) Two sewers, one 3.5 feet diameter and one 2 feet diameter are under the right side arch opening.
  (c) An obstacle, a 2 feet diameter sewer, is at 25 feet downstream from downstream face of bridge.
  (d) The bank slopes are vertical, both upstream and downstream.
(16) Arch condition:
  (a) The shape of the arch is very good.
  (b) A part of the right side arch is obstructed by the right bank.

Suggestion: The channel is uniform and straight. Since the skew is considerable, it is recommended to be used for skew arch bridge model-prototype comparison. However, the influence of sewers are uncertain.

Figures 9-8-1 to 9-8-5 show a plan view and cross sections at the bridge site. Figure 9-8-6 is a topographic map of the bridge site prepared from aereal photographs.

IX. WHITE LICK CREEK NEAR STATE BOYS SCHOOL, PLAINFIELD

RESUME

(1) Compiled number of bridge: No. 59a.
(2) Location: Lat. 39°41'35", Long. 86°23'53", Plainfield, Indiana, quadrangle, sec. 35, T. 15 N., R. 1 E., at bridge near State Boys School, Plainfield, crossing White Lick Creek, southern edge of Plainfield.
(3) Drainage area: 101 square miles.
(4) Tributary to: Tributary to West Fork White River, Wabash River basin.
(5) Slope of channel: 1.4/1000.
(6) Bridge type: Two-span concrete arch bridge.
(7) Skew toward upstream: 5° R.
(8) Skew toward downstream: 5° R.
(9) Width of bridge: 18 feet.
(10) Clearance of arch opening: 16 feet for right side arch, 12 feet for left side arch.
(11) Width between banks of channel: 172 feet.
(12) Width of channel bottom: Not very clear.
(13) Eccentricity: Low flow part of channel is close to right bank.
(14) High water mark: Flood of 1957, just about the same height as the top of arch opening.
(15) Channel condition:
   (a) Bend about 250 feet upstream from the bridge.
   Bend about 300 feet downstream from the bridge.
   (b) Sand heaps distributed along the left part of channel.
   (c) Left part of channel is 4 feet, average, higher than right side.
   (d) The banks are able to confine the flood 4 feet lower than the flood of 1957.
(16) Arch condition: The arches are in good shape except the ends close to the pier.

Suggestion: This is the best two-span arch bridge under inspection. The defects are the non-symmetric channel cross section and the low bank on left side. So it is recommended to be used for a medium flood.

Figures 9-9-1 to 9-9-5 show a plan view and cross sections at the bridge site.
Figure 9-9-6 is a topographic map of the bridge site prepared from aereal photographs.

X. DEAN ROAD, INDIANAPOLIS, CROSSING HOWLAND DITCH

RESUME

(1) Compiled number of bridge: No. 66a.
(2) Location: Lat. 39°53'33", Long. 86°05'54". Fishers, Indiana, quadrangle, sec. 29, T. 17 N., R. 4 E., at bridge on Dean Road, Indianapolis, crossing Howland Ditch, northern part of Indianapolis.
(3) Drainage area: 4.5 square miles.
(4) Tributary to: Tributary to West Fork White River.
(5) Slope of channel: 3.5/1000.
(6) Bridge type: Original bridge is a one-span concrete arch. Roadway was widened by addition of a one-span concrete flat decked structure on the downstream side of original bridge.
(7) Skew toward upstream: 15° L.
(8) Skew toward downstream: 15° L.
(9) Width of bridge: Arch part, 18 feet.
flat part, 13 feet.
(10) Clearance of arch opening: 7 feet.
(11) Width between banks of channel: 46 feet.
(12) Width of channel bottom: 30 feet.
(13) Eccentricity: None.
(14) Highwater mark: None.
(15) Channel condition:
 (a) The cross section near the upstream face is larger than cross sections 10 feet upstream.
 (b) Channel cross sections are regular.
 (c) Small bend at 120 feet downstream from bridge.
 (d) Channel is clear.
(16) Arch condition:
 (a) Arch opening is in good shape.
 (b) Flat deck part of this bridge is high enough to be free from disturbing the flow.

Suggestion: Arch is good, channel is clear and regular. Perhaps the drainage area is not big enough to avoid the flash flood.

Figures 9-10-1 to 9-10-5 show a plan view and cross sections at the bridge site. Figure 9-10-6 is a topographic map of the bridge site prepared from aereal photographs.

IX-3 Preliminary Study of the Indirect Determination of Flood Discharge from Contracted Bridge Openings and High Water Marks, by I. P. Wu, Indiana Flood Control and Water Resources Commission

As soon as a bridge is constructed across a natural stream, it serves in at least some degree as a contracted opening to confine the stream flow, particularly in the higher ranges of discharge. Under suitable conditions, such contracted openings provide opportunity for the indirect determination of the flood discharge passing through the bridge opening.

This office has for some years been engaged in a program for the field establishment of high water marks along a number of streams in the State following major floods, including the setting of such marks at and in the vicinity of bridges. The purpose of this study is to develop relationships whereby the high water mark data collected by this office at various bridges may be used to estimate the flood discharge at that point.

The experimental data used herein was obtained from a study by Purdue University on arch bridges and by the University of Colorado on simple normal crossings with a vertical-sided model.

Basic Hydraulics and Assumptions for Deriving the Relationship Between the Flood Discharge and High Water Marks

When the flow is contracted by the bridge opening, the flow profile along the center line of the stream can be plotted roughly as follows:

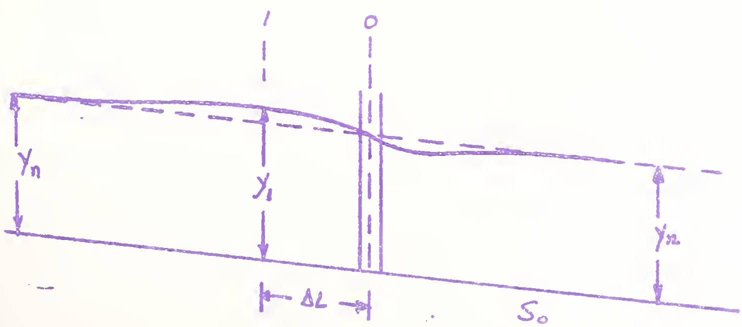

where section 1 is the section of the highest heading up, the depth is y_1

section o is the section right at the opening, the depth is y_o

y_n = normal depth

Δy = the maximum heading up = $y_1 - y_n$

v_n = normal velocity

v_1 = velocity at section 1

v_o = velocity at section o

S_o = channel bottom slope

L = length from the bridge opening to the section of maximum heading up.

by conservation of energy, we have the relation

$$\frac{v_1^2}{2g} + y_1 + S_o \Delta L = \frac{v_o^2}{2g} + y_o + h_f$$

where h_f is the friction loss from section 1 to section o.

If S_o is small, so that the term $S_o \Delta L$ may be neglected, and assuming $y_o = y_n$,

Eq. 1 becomes:

$$\frac{v_1^2}{2g} + y_1 = \frac{v_o^2}{2g} + y_o + h_f$$

$$\frac{v_1^2}{2g} + \Delta y + y_n = \frac{v_o^2}{2g} + y_n + h_f$$

$$\frac{v_1^2}{2g} + \Delta y = \frac{v_o^2}{2g} + h_f$$

Since the high water marks are located on the banks of the stream, the elevation of the marks will be higher than the elevation of the water at the center line of the stream, due to differences in velocity. Assuming that the velocity of flow near the banks is very low or approaching zero, it might be said that Δy_E, which is defined as the difference in elevation between the high water marks on the banks and the depth of normal stream flow y_n, is Δy plus its velocity head, that is $\Delta y_E = y + \frac{v_1^2}{2g}$

then $\Delta y_E = \frac{v_o^2}{2g} + h_f$

if $h_f = K \frac{v_o^2}{2g}$

where K = friction loss coefficient

then $\Delta y_E = (1 + K)\frac{v_o^2}{2g}$

or $\frac{\Delta y_E}{y_n} = (1 + K) \frac{v_o^2}{2gy_n}$

and $\frac{\Delta y_E}{y_n} = \frac{1 + K}{2} F_o^2$

where F_o^2 is the Froude number at the bridge opening.

This gives the relation that Δy_E is a function of the velocity head at the bridge opening and $\frac{\Delta y_E}{y_n}$ is a function of the Froude number of that opening.

Study of Experimental Data

Data from the experimental tests of flow through contracted openings made by the University of Colorado and Purdue University were collected. Since the actual field conditions investigated show that the opening ratio M' is large and the ratio of Δy and y_n is small, only those experimental data were selected which met the criteria that $M' > 0.6$ and $\frac{\Delta y}{y_n} < 0.1$. The relations of $\frac{\Delta y_E}{y_n}$ and F_o^2 can be seen in Figure 11-1, which shows that the data holds the relation:

$$\frac{\Delta y_E}{y_n} = \frac{1}{2} F_o^2$$

or $\Delta y_E = \frac{v_o^2}{2g}$

Indirect Determination of Flood Discharge for Indiana Streams

Since the above study shows the relations of high water marks and the velocity at the opening, this will serve as a tool to estimate the peak flood discharge which passed the bridge opening during the particular high water event. Several bridges which are located on a relatively straight and uniform stream, and where the high water mark data is considered to be reliable were selected for this study. There are also U.S.G.S. gaging stations nearby at which the flood discharge was measured directly.

Information as to high water marks, computed discharge, and the actual discharge for the eight bridges selected for study is as follows:

Bridge Location	Date of Flood	Δy_E ft.	Computed Q cfs	Measured Q cfs
Eagle Creek, B&O RR Bridge at Speedway	June 1957	1.37	27,850	25,200
Sugar Creek, at Edinburg	May 1956	0.90	23,000	27,600
Sugar Creek, Hwy. 231 near Crawfordsville	May 1956	0.81	23,700	18,200
Sugar Creek, Hwy. 231 near Crawfordsville	June 1957	1.12	31,400	26,300
Sugar Creek, Hwy. 41 near Byron	May 1956	0.34	19,600	20,600
Raccoon Creek, Hwy. 59 near Mansfield	1957	1.00	37,400	38,400
Flat Rock River, Hwy. 421 near St. Paul	Jan. 1959	0.274	13,300	14,500
Flat Rock River, Hwy. 421 near St. Paul	Nov. 1955	0.265	9,600	10,800

There is shown in Figure 11-2 a plot of Δy_E against the velocity head. Data from the eight bridges shown in the above tabulation, and the experimental study from the University of Colorado and Purdue agree well with the theoretical line $\Delta y_E = \frac{V_o^2}{2g}$. It appears that this theoretical line can be used for a rough estimate of the peak flood discharge which passed through the bridge opening.

Discussion

Theoretically, the flood discharge passed through the bridge opening is a function of the normal depth of stream flow, the cross section of the channel, the size of the bridge opening, the friction loss in the channel and the bridge opening, and the energy coefficient.

Since the normal depth of the natural channel is difficult to determine, the assumption was made that normal depth occurs at the bridge opening. This was based on the results of the experimental study made by Purdue University, which showed from the flow profiles that normal depth occured somewhere close to the opening under the condition that the opening ratio $M' > 0.6$ and that the Froude number is smaller than 0.5. The other major assumption was that the velocity of flow close to the bank is very small or approaching zero, such that the elevation of the high water mark on the bank is equal to the elevation of the flow profile along the center line plus its velocity head. Neither of these assumptions can be proved at this time and hence, constitute the weak points of this study.

As the velocities used in this study are all mean velocities, the velocity head actually is not $\frac{v^2}{2g}$ but $\alpha\frac{v^2}{2g}$. The energy coefficient α is a little larger than one for large uniform channels, but is far greater than one for the section close to a contracted opening. Since it is assumed to be unity in this study, a loss of accuracy undoubtedly results.

As shown in Figure 11-1 data from the experimental tests by the University of Colorado and Purdue agree well with the relation $\frac{\Delta y_E}{y_n} = \frac{1}{2}F_o^2$, or $\Delta y_E = \frac{v_o^2}{2g}$. This does not mean that the friction coefficient K is zero, but rather indicates that this factor may be cancelled by the energy coefficient α, or that there are other undetermined effects as a result of the two basic assumptions.

By studying the relation $\Delta y_E = \frac{v_o^2}{2g}$, it will be noted that this is nothing more than the simple statement that the velocity head at the bridge opening is just equal to the maximum heading upstream from the contracted opening. Inasmuch as assumptions made in this study are not quite correct and since the friction loss coefficient K and energy coefficient α are not precisely determined, the results of this study can only be used as a rough estimate of the flood discharge or as a check on the flood discharge as determined by other methods.

Further work is necessary to use the experimental data in conjunction with that from actual natural streams to evaluate all the specific factors involved.

APPENDIX A

NOTATIONS

SYMBOL	DIMENSIONS	DEFINITION
A	L^2	Area
A_1	L^2	Total depth water area at section 1, $A_1 = BY_1$
A_c	L^2	Critical flow area
A_{n1}	L^2	Normal depth water area, $A_{n1} = BY_n$
A_{n2}	L^2	Total depth flow area at section 2
A_o	L^2	Area of bridge opening
B		Rectangular channel width; Body force per unit of mass
b'	L	Diameter of circle of which the arch segment is a part
b	L	Span width at the springline of the arch
C		A coefficient
C	$L^{\frac{1}{2}}/T$	The Chezy roughness coefficient$=V_n/\sqrt{R_n S}$
C_1		Coefficient, see equation 3-7-4
C.V.		Control volume
C_c		Coefficient of contraction
C.S.		Control surface
C_d		Coefficient of discharge
C_m		Correction factor = M'/M (see Fig. 3-13)
C_v		Coefficient of velocity
d	L	Diameter of a circle, distance between center of circular arch segment and channel bottom (Fig. 3-12), depth of flow measured perpendicularly to the bottom.
D	L	Hydraulic depth as defined by A/W; pipe diameter

SYMBOL	DIMENSIONS	DEFINITION
d'	L	Distance from the springline to the center of curvature of the arch
d	L	Orifice diameter
E_{1-4}		Energy loss between section 1 and 4
e		Eccentricity
F		Denotes a mathematical function, Froude number
F_f		Friction force
F_n		Normal depth Froude number $= V_n/\sqrt{gY_n}$
F_s	F	Surface force on control volume
f		Denotes a mathematical function, friction coefficient
G		Denotes a mathematical function
g		Denotes a mathematical function
g	L/T^2	Acceleration of gravity
H	L	Total energy head
h_1^*	L	$Y_1 - Y_n$
h		Static head
h_f	L	Headloss
K		Weir coefficient as defined in Francis weir formula
K		Head loss due to bridge constriction alone
k		Nikuradse's equivalent sand roughness
L	L	Length of the bridge in the direction of flow
L_d	L	Distance between bridges
L_{1-3}	L	Distance between sections 1 and 3

SYMBOL	DIMENSIONS	DEFINITION
L_{1-4}	L	Distance between sections 1 and 4
M		Channel width ratio, b/B
M'		Channel opening ratio, A_o/A_n for submerged opening; A_{n2}/A_{n1} for unsubmerged opening.
M_1		Mild slope backwater curve in an open channel
N		Number of spans
n	$L^{1/6}$	Manning's roughness coefficient
n		Subscript which refers to the normal depth for uniform flow
p	F/L^2	Pressure intensity; pier width (See Fig. 3-14)
P	F	Pressure force
Q_a	L^3/T	Actual discharge through opening
Q_t		Theoretical calculated discharge through opening
Q	L^3/T	Total flow
q	L^3/T	That portion of the total flow which could pass through the bridge without contraction
R	L	Hydraulic radius
R, R_e		Reynolds number $V_n R_n/\nu$
r	L	Radius of curvature of the arch, radius of curvature of streamline
S		Slope; head loss per unit length
S_o		Slope for normal depth flow in unconstricted channel

SYMBOL	DIMENSIONS	DEFINITION
T		A series defined in Art. IV-7a
t	T	Time
V	L/T	Average velocity
V_o	L/T	Average velocity through constriction, Q/A_o
V_n	L/T	Average velocity when uniform, normal flow occurs, Q/BY_n
V		Volt
W	L	Free surface width; weight of water within a control volume
X		Distance along flume
$\bar{y}$	L	Hydraulic depth $\bar{y} = A/W$
Y	L	Depth of flow
$\bar{Y}$	L	Head over the center of gravity of a section
Y_1	L	Depth of flow at section of maximum backwater
Y_c	L	Critical depth
Y_n or Y_o	L	Depth of the normal unconstricted flow
Y_t	L	Tailgate height
Z		Section factor for critical flow computation $Z^2 = A^3/W$; elevation head
α		Kinetic energy coefficient
α'		Pressure coefficient
β		Segment factor d/r, Momentum coefficient
γ	F/L^3	Specific weight of water
δ		Boundary layer thickness

SYMBOL	DIMENSIONS	DEFINITION
ε		Roughness size
η		d/r (See fig. 3-12)
ν	L^2/T	Kinematic viscosity of the fluid
ρ	FT^4/L^4	Fluid mass density
τ	F/L^2	Shear stress
ϕ_1	degrees	Wingwall angle (See Fig. 3-14)
ϕ_2	degrees	Skew angle (See Fig. 3-14)
θ	degrees	Angle of inclination of channel

LIST OF TABLES

*Tables 4-1 and 4-2 refer to the small flume preliminary investigations. The remaining tables refer to the large flume tests.

[illegible] 4-1 [illegible] P. 1

STA[illegible]	[illegible] ALONG FLUME	FLUME [illegible]	WATER SURFACE WITH [illegible]	WATER SURFACE M[illegible]	NORMAL DEPTH	[illegible] IN [illegible]	
1	2	3	4	5	6	7	8
4.0	10	.420	.515	.515	.095	.095	[illegible] 0
4.5							[illegible] .0114
5.0	9	.420	.515	.515	.095	.095	[illegible] 4"
5.5	8.5			.515		.095	
5.6	8.4			.514		.094	[illegible] 2"
5.7	8.3			.514		.094	[illegible] 24"
5.8	8.2			.514		.094	
5.9	8.1			.513		.093	[illegible] 6/8"
6.0	8		.515	.513	.095	.093	[illegible]
6.1	7.9			.513		.093	
6.2	7.8			.513		.093	[illegible] .002'
6.3	7.7			.513			[illegible] .005'
6.4	7.6			.513		.093	
6.5	7.5			.513			[illegible] 4.035'
6.6	7.4			.513		.093	[illegible] to
6.8	7.2			.512		.092	[illegible] 6.035'
7.0	7	.420	.515	.512	.095	.092	
7.065	6.935			.512		.092	
7.72	6.28			.513E		.093	.047
8	6		.515		.095		~~32~~
8.24				.514E		.094	
9	5		.515		.095		
9.065	4.035			.515		.095	
9.1	4			.515		.095	
9.3	4.7			.516		.096	
9.5	4.5			.516		.096	
10.0	4	.420	.515	.517	.095	.097	
10.5				.517			
11.0	3		.515	.517	.095	.097	
11.5				.517			
12.0	2		.515	.517	.095	.097	
13.0	1		.515	.517	.095	.097	
14.0	0	.420	.515	.517	.095	.097	

4-1

P2

STATION					NORMAL			
4.0	10	.425	.538	.538	.113	.113		0
4.5	9.5							.0114
5.0	9		.538	.538	.113	.113		
5.5	8.5							4"
6.0	8		.538	.538	.113	.113		2"
6.5	7.5							24"
7.0	7		.538	.538	.113	.113		
7.5	6.5				.113			1"
7.75	6.25			.538		.113		
8.00	6		.538	.537	.113	.112		
8.1	5.9			.537		.112		.001
8.2	5.8			.537		.112		
8.3	5.7			.535		.110		.005
8.4	5.6			.534		.109		3.5'
8.5	5.5			.535		.110		to
9.0	5		.538		.113			5.5'
9.21				.536E		.111		
9.5	4.5							
9.725				.537E		.112		.035
10.0	4		.538		.113			
10.23				.538E		.113		
10.5	3.5			.538		.113		
10.6	3.4			.539		.114		
10.7	3.3			.539		.114		
10.8	3.2			.539		.114		
10.9	3.1			.539		.114		
11.0	3		.538	.539	.113	.114		
11.5	2.5			.539		.114		
12.0	2		.538	.539	.113	.114		
12.5	2.5							
13.0	1		.538	.539	.113	.114		
13.5	.5							
14.0	0	.425	.538	.539	.113	.114		

2-1 P.3

STATION	[illegible]	FLUME [illegible]	WATER [illegible]	[illegible]	NORMAL [illegible]	[illegible]	
	2	3	4	5	6	7	8
4.0	10	.420	.515	.515	.095	.095	S_0 = 0
4.5	9.5						Q_T = .0114
5.0	9		.515	.515	.095	.095	Dia 5"
5.5	8.5			.514		.094	R = 2.5"
5.9	8.1			.514		.094	
6.0	8	.420	.515	.513	.095	.093	L = 24"
6.1	7.9			.513		.093	Z = 6/8"
6.2	7.8			.513		.093	Weir
6.3	7.7			.513		.093	Height =
6.4	7.6			.513		.093	
6.5	7.5			.513		.093	h* = .001
6.6	7.4			.513		.093	Δh = .003
6.7	7.3			.513		.093	
6.8	7.2			.513		.093	Bridge = 5'
6.9	7.1			.513		.093	Position to
7.0	7		.515	.513	.095	.093	Along Flume 7'
7.24	6.76			.514E		.094	[illegible]
8.0	6	.420	.515		.095		.047
8.24				.515E		.095	
9.0	5		.515	.516	.095	.096	[illegible] 31
9.1	4.9			.516		.096	
9.2	4.8			.516		.096	
9.3	4.7			.516		.096	
9.4	4.6			.516		.096	
9.5	4.5			.516		.096	
10.0	4	.420	.515	.516	.095	.096	
10.5				.516		.096	
11.0	3		.515	.516	.095	.096	
11.5							
12.0	2		.515	.516	.095	.096	
12.5							
13.0	1		.515	.516	.095	.096	
13.5							
14.0	0	.420	.515	.516	.095	.096	

L-1 P.4

4.0	10	.425	.538	.538	.113	.113	0
4.5	9.5						.0114
5.0	9		.537	.538	.113	.113	5"
5.5	8.5					.113	
6.0	8		.538	.538	.113	.113	2.5"
6.5	7.5						24"
7.0	7.0		.538	.538	.113	.113	
7.5	6.5						1"
8.0	6.0		.538	.538	.113	.113	
8.1	5.9			.537		.112	
8.2	5.8			.536		.111	.001
8.3	5.7			.535		.110	.005
8.4	5.6			.534		.109	
8.5	5.5			.534		.109	3.5'
8.695	5.315			.533E		.108	to
9.0	5.0		.538		.113		5.5'
9.19				.534E		.109	
9.5	4.5						
9.693				.535E		.110	.035
10.0	4.0		.538		.113		
10.183				.536E		.111	
10.5	3.5		.538	.537	.113	.112	
10.6	3.4			.537		.112	
10.7	3.3			.538		.113	
10.8	3.2			.539		.114	
10.9	3.1			.539			
11.0	3.0		.538	.539	.113	.114	
11.5	2.5			.539			
12.0	2.0		.538	.539	.113	.114	
12.5	1.5			.539			
13.0	1.0		.538	.539	.113	.114	
13.5	.5						
14.0	0	.425	.538	.539	.113	.114	

4-1 P. 5

STATION			WATER SURFACE			IN PLACE	
			MODEL	MODEL IN PLACE			
			4			7	8
4.0	10	.420	.515	.515	.095	.095	S0= 0
4.5	9.5						Q .0114
5.0	9	.420	.515	.515	.095	.095	7.7"
5.5	8.5						1.4"
6.0	8	.420	.515	.515	.095	.095	
6.5	7.5						9.7"
7.0	7		.515	.515	.095	.095	
7.5	6.5						Z 6/8"
7.7	6.3		.515	.515		.095	
7.8	6.2			.514		.094	
7.9	6.1			.514		.094	.001
8.0	6	.420	.515	.514	.095	.094	.003
8.1	5.9			.514		.094	
8.2	5.8			.514		.094	4.45'
8.5	5.5			.514		.094	to
8.75	5.25			.513		.093	5.25'
9.0	5		.515		.095		
9.55	4.45			.515		.095	
9.60	4.4		.515	.516	.095	.096	
9.7	4.3			.516		.096	~~30~~
9.8	4.2		.515	.516	.095	.096	
9.90	4.1			.516		.096	
10.0	4	.420	.515	.516	.095	.096	
10.5							
11.0	3		.515	.516	.095	.096	
11.5							
12.0	2	.420	.515	.516	.095	.096	
12.5							
13.0	1		.515	.516	.095	.096	
13.5							
14.0	0	.420	.515	.516	.095	.096	

TABLE 4-1 WATER SURFACE MEASUREMENTS P. 6

STATION	DISTANCE ALONG FLUME	POINT GAGE READING			NORMAL DEPTH	DEPTH MODEL IN PLACE	
		FLUME BOTTOM	WATER SURFACE				
			WITHOUT MODEL	MODEL IN PLACE			
1	2	3	4	5	6	7	8
4.0	10	.420	.520	.520	.10	.10	S_o = 0
5.0	9		.520	.520	.10	.10	Q_m = .0138
5.5	8.5						Dia = 4"
6.0	8	.420	.520	.520	.10	.10	Rise = 2"
7.0	7		.520	.520	.10	.10	L = 24"
7.5	6.5			.520	.10	.10	
7.6	6.4			.519		.099	Z- Weir Height = 6/8"
7.7	6.3			.518		.098	
7.8	6.2			.518		.098	
7.9	6.1			.518		.098	h^* = .001'
8.0	6	.420	.520	.518	.10	.098	
8.1	5.9			.518		.098	Δh = .004'
8.2	5.8			.518		.098	Bridge Position Along Flume = 3' to 5'
8.3	5.7			.518		.098	
8.4	5.6			.518		.098	
8.5	5.5			.517		.097	
8.6	5.4			.517		.097	E.P.G.-M.P.G.= .047
8.7	5.3			.517		.097	
8.8	5.2			.517		.097	FIG. NO.
8.9	5.1			.517		.097	
9.0	5		.520	.517	.10	.097	
9.71	4.29			.518E		.098	
10	4	.420	.520		.10		
10.22	3.78			.519E		.099	
11.0	3		.520	.520	.10	.10	
11.1	2.9			.521		.11	
11.3	2.7			.522		.12	
11.5	2.5			.522		.12	
12.0	2		.520	.522	.10	.12	
13.0	1		.520	.522	.10	.12	
14.0	0	.420	.520	.522	.10	.12	

TABLE 4-1 WATER SURFACE MEASUREMENTS P. 7

STATION	DISTANCE ALONG FLUME	POINT GAGE READING			NORMAL DEPTH	DEPTH MODEL IN PLACE	
		FLUME BOTTOM	WATER SURFACE				
			WITHOUT MODEL	MODEL IN PLACE			
1	2	3	4	5	6	7	8
4.0	10	.420	.520	.520	.100	.10	S_o= 0
4.5							Q_m= .0138
5.0	9	.420	.520	.520	.10	.10	Dia = 5"
5.5							Rise = 2.5"
6.0	8	.420	.520	.520	.10	.10	L = 24"
6.5							
7.0	7		.520	.520	.10	.10	
7.3	6.7			.519		.099	Z- Weir Height = 6/8"
7.4	6.6			.519		.099	
7.5	6.5			.519		.099	
7.6	6.4			.519		.099	h^*= .001'
7.7	6.3			.519		.099	Δh= .003'
7.8	6.2			.519		.099	
8.0	6	.420	.520	.519	.10	.099	Bridge Position Along Flume = 3' to 5'
8.2	5.8						
8.4	5.6			.519		.099	
8.5	5.5			.518		.098	E.P.G.-M.P.G.= .047
8.7	5.3			.518		.098	
9.0	5			.518		.098	
9.23	4.67			.519E		.099	FIG. NO.
10.0	4						
10.23	3.67			.519E		.099	
11.0	3	.420	.520	.520	.10	.10	
11.1	2.9			.520		.10	
11.2	2.8			.521		.101	
11.3	2.7			.521		.101	
11.4	2.6			.521		.101	
11.5	2.5			.521		.101	
11.75	2.25			.521		.101	
12.0	2	.420	.520	.521	.10	.101	
12.5				.521		.101	
13.0	1			.521		.101	
13.5				.521		.101	
14.0	0	.420	.520	.521	.10	.101	

TABLE 4-1 WATER SURFACE MEASUREMENTS P.8

STATION	DISTANCE ALONG FLUME	POINT GAGE READING			NORMAL DEPTH	DEPTH MODEL IN PLACE	
		FLUME BOTTOM	WATER SURFACE				
			WITHOUT MODEL	MODEL IN PLACE			
1	2	3	4	5	6	7	8
4.0	10	.420	.520		.10	.10	S_0 = 0
5.0	9		.520		.10	.10	Q_m = .0138
6.0	8		.520		.10		Dia = 7.7"
7.0	7.0		.520	.520	.10	.10	Rise = 1.4"
7.25	6.75			.520			L = 9.7"
7.7	6.3						
7.9	6.1		.520	.520	.10	.10	
8.0	6.0	.420	.520	.519	.10	.099	Z- Weir Height = 6/8"
8.3	5.7			.518		.098	
8.5	5.5			.518		.098	
8.75	5.25			.518		.098	h* = .001'
9.0	5.0		.520		.10		Δh = .003'
9.50							
9.55	4.45			.519		.099	Bridge Position Along Flume = 4.45' to 5.25'
9.60	4.4			.520		.100	
9.70	4.3			.520		.100	
9.8	4.2			.520		.100	EPG-MPG =
10.0	4.0	.420	.520	.520	.10	.100	
10.25	3.75			.521		.101	
10.50	3.5			.521		.101	FIG NO. ~~33~~
11.0	3.0		.520	.521	.10	.101	
11.5	2.5			.521		.101	
11.75	2.25			.521		.101	
12.0	2.0			.521	.10	.101	
13.0	1.0		.520	.521	.10	.101	
14.0	0	.420	.520	.521	.10	.101	

TABLE 4-1 WATER SURFACE MEASUREMENTS P. 9

STATION	DISTANCE ALONG FLUME	POINT GAGE READING: FLUME BOTTOM	POINT GAGE READING: WATER SURFACE WITHOUT MODEL	POINT GAGE READING: WATER SURFACE MODEL IN PLACE	NORMAL DEPTH	DEPTH MODEL IN PLACE	
1	2	3	4	5	6	7	8
4.0	10	.425	.542	.542	.117	.117	S_0 = 0
4.1	9.9			.541		.116	Q_m = .0138
4.2	9.8			.540		.115	Dia = 7.7"
4.3	9.7			.539		.114	Rise = 1.4"
4.4	9.6			.538		.113	L = 9.7"
4.5	9.5			.537		.112	
4.655	9.345			.539E		.114	
5.0	9		.542		.117		Z- 1"
5.14	8.86			.540E		.115	Weir Height =
5.3	8.7			.541		.116	
5.4	8.6			.541		.116	h^* = .001
5.5	8.5			.542		.117	Δh = .006
5.6	8.4			.542		.117	
6.0	8.0	.425	.542	.543	.117	.118	Bridge Position Along Flume = 8.7' to 9.5'
6.5	7.5			.543		.118	
7.0	7			.543		.118	
7.5	6.5			.543		.118	
8.0	6	.425					EPG-MPG =
8.5	5.5			.543	.117	.118	.042
9.0	5						FIG NO. ~~29~~
9.5	4.5			.543		.118	
10.0	4	.425	.542		.117		
10.5	3.5			.543	.117	.118	
11.0	3						
11.5	2.5			.543		.118	
13.0	1			.543		.118	
13.5							
14.0	0	.425	.542	.543	.117	.118	

TABLE 4-1 WATER SURFACE MEASUREMENTS P. 12

STATION	DISTANCE ALONG FLUME	POINT GAGE READINGS			NORMAL DEPTH	DEPTH, MODEL IN PLACE	
		FLUME BOTTOM	WATER SURFACE				
			WITHOUT MODEL	MODEL IN PLACE			
1	2	3	4	5	6	7	8
4	10	.425	.542	.542	.117	.117	S_0 = 0
4.5							Q = .0139
5.0	9		.542	.542	.117	.117	Dia = 4"
5.5							Rise = 2"
6.0	8	.425	.542	.542	.117	.117	L = 24"
6.5	7.5						
7.0	7.0		.542	.542			
7.4	6.6		.542	.542	.117	.117	Z- 1"
7.5	6.5			.541		.116	Weir Height
7.6	6.4			.540		.115	
7.7	6.3			.539		.114	h^* = .001
7.8	6.2			.539		.113	Δh = .005
7.9	6.1			.537		.112	
8.0	6.0	.425	.542	.538	.117	.113	Bridge Position Along Flume = 4' to 6'
8.70	5.30			.537E			
9.0	5.0		.542	.538E	.117		
9.72				.541E			ERG-M.E.G.
10.0	4.0	.425	.542	.542	.117	.117	.035
10.1	3.9			.543		.118	
10.2	3.8			.543		.118	FIG. NO. ~~20~~
10.3	3.7			.543		.118	
10.4	3.6			.543		.118	
10.5	3.5			.543			
11.0	3.0		.542	.543	.117	.118	
11.5				.543			
12.0	2.0	.425	.542	.543	.117	.118	
12.5				.543		.118	
13.0	1.0		.542	.543	.117	.118	
13.5				.543		.118	
14.0	0	.425	.542	.543	.117	.118	

TABLE 4-1 WATER SURFACE MEASUREMENTS P. 13

STATION	DISTANCE ALONG FLUME	POINT GAGE READING			NORMAL DEPTH	DEPTH MODEL IN PLACE	
		FLUME BOTTOM	WATER SURFACE				
			WITHOUT MODEL	MODEL IN PLACE			
1	2	3	4	5	6	7	8
4	10	.425	.542	.542	.117	.117	S_o = 0
4.5							Q_m = .0139
5.0	9	.425		.542	.117	.117	Dia = 5"
5.5							Rise = 2½"
6.0	8	.425	.542	.542	.117	.117	L = 24"
6.5							
7.0	7	.425	.542	.542	.117	.117	Z- Weir Height = 1"
7.5	6.5		.542	.542	.117	.117	
7.6	6.4			.540		.115	
7.7	6.3			.539		.114	
7.8	6.2			.539		.114	h^* = .001
7.9	6.1			.539		.114	Δh = .004
8.0	6.0	.425		.539		.114	Bridge Position Along Flume = 4' to 6'
8.19				.540E			
8.5	5.5		.542		.117		
8.69				.541E			
9.0	5	.425					EPG-MPG = .035
9.185				.541E			
9.69				.541E			
10	4	.425	.542		.117		FIG. NO. ~~19~~
10.1	3.9		.542	.542	.117	.117	
10.2	3.8			.543		.118	
10.3	3.7			.543		.118	
10.4	3.6			.543		.118	
10.5	3.5			.543		.118	
11.0	3	.425	.542	.543	.117	.118	
11.5				.543		.118	
12.0	2	.425	.542	.543	.117	.118	
12.5				.543		.118	
13.0	1	.425	.542	.543	.117	.118	
13.5				.543		.118	
14.0			.542	.543	.117	.118	
14.5	0	.425	.542	.543	.117	.118	

[illegible] 4-1 [illegible] P. 14

STATION	DISTANCE ALONG FLUME	FLUME BOTTOM	WATER SURFACE: W[illegible] MODEL	WATER SURFACE: [illegible]CE	NORMAL DEPTH	[illegible]	
1	2	3	4	5	6	7	
4.0	10.0	.423	.541	.541	.118	.118	0
5.0	9.0			.541		.118	.015
5.5	8.5			.541		.118	4"
5.75	8.25			.540		.117	2"
6.0	8.0	.423	.541	.540	.118	.117	24"
6.5	7.3			.539		.116	
6.8	7.2			.538		.115	1"
7.0	7.0			.538		.115	
7.72	6.28			.539E		.116	
8.0	6.0	.423	.541		.118		
8.24	5.76			.540E		.117	.002'
9.0	5	.423	.541	.541	.118	.118	.005'
9.1	4.9			.542		.119	5'
9.3	4.7			.543		.120	to
9.5	4.5			.543		.120	7'
10.0	4	.423	.541	.543	.118	.120	
11.0	3	.423	.541	.543	.118	.120	
11.5	2.5			.543	.118	.120	.047
12.0	2	.423	.541	.543	.118	.120	
13.0	1	.423	.541	.543	.118	.120	
14.0	0	.423	.541	.543	.118	.120	

TABLE 4-1 WATER [illegible] P.15

STATION	DISTANCE ALONG FLUME	POINT GAGE READING			NORMAL DEPTH	DEPTH MODEL IN PLACE	
		FLUME BOTTOM	WATER SURFACE				
			WITHOUT MODEL	MODEL IN PLACE			
1	2	3	4	5	6	7	8
4	10.0	.423	.541	.541	.118	.118	S_0 = 0
5	9.0	.423	.541	.541	.118	.118	Q = .015
5.5	8.5						Dia = 5"
5.7	8.3			.541		.118	Rise = 2.5"
5.8	8.2			.540		.117	L = 24"
6.0	8.0	.423	.541	.540	.118	.117	
6.2	7.8			.539		.116	Z = 1"
6.5	7.5			.539		.116	Weir
6.8	7.2			.539		.116	height =
7.0	7.0	.423	.541	.539	.118	.116	h* = .001'
7.24	6.76			.540E		.117	
7.75	6.25			.540E		.117	Δh = .003'
8.24	5.76			.541E		.118	Bridge 5'
8.75	5.25			.541E		.118	Position to
9.0	5	.423	.541	.542	.118	.119	Along 7'
9.2	4.8			.542		.119	Flume
9.5	4.5			.542		.119	EPG-N
9.75	4.25			.542		.119	.047
10.0	4	.423	.541	.542	.118	.119	
10.5	3.5			.542			FIG NO
11.0	3			.542		.119	
12.0	2	.423	.541	.542	.118	.119	
13.0	1			.542		.119	
14	0	.423	.541	.542	.118	.119	

TABLE 4-1 P. 16

STATION	DISTANCE ALONG FLUME	FLUME BOTTOM	WATER SURFACE WITHOUT MODEL	WATER SURFACE WITH MODEL	NORMAL DEPTH	DEPTH MODEL IN	
	2	3			5		
4	10.0	.423	.541	.541	.118	.119	
6.0	8.0	.423	.541	.541	.118	.118	S_0 = 0
6.5	7.5			.540		.117	.015
6.75	7.25			.540		.117	7.7"
7.0	7	.423	.541	.540	.118	.117	1.4"
7.25	6.75			.540		.117	9.7"
7.5	6.5			.539		.116	
7.8	6.2			.539		.116	1"
8.0	6	.423	.541	.539	.118	.116	Weir Height
8.8	5.2			.543		.120	
9.0	5	.423	.541	.543	.118	.120	h^* = .002'
9.3	4.7			.543		.120	
9.5	4.5			.543		.120	Δh = .004'
10.0	4	.423	.541	.543	.118	.120	Position = 5.2'
11.0	3			.543		.120	Along to
12.0	2	.423	.541	.543	.118	.120	Flume 6.0'
12.5	1.5						
13.0	1	.423	.541	.543	.118	.120	EF
14.0	0	.423	.541	.543	.118	.120	.047

			4		6	7	8
4.0	10	.421	.495	.495	.074	.074	S_0 - 0
5.0	9	.421	.495	.495	.074	.074	.017
6.0	8	.421	.495	.495	.074	.074	7.7"
7.0	7	.421	.495	.495	.074	.074	1.4"
8.0	6	.421	.495	.495	.074	.074	
9.0	5	.421	.495	.495	.074	.074	9.7"
10.0	4		.495	.495	.074	.074	
10.10	3.9			.494		.073	3/8"
10.2	3.8			.494		.073	
10.3	3.7			.493		.072	
10.4	3.6			.493		.072	.001'
10.5	3.5			.492		.071	.004'
10.685	3.315			.492		.071	
11.0	3	.421	.495		.074		2.65'
11.485	2.515						to
11.57	2.43			.494		.073	3.25'
11.6	2.4			.495		.074	
11.65	2.35			.495		.074	
12.0	2	.421	.495	.496	.074	.075	
12.5	1.5			.496		.075	
13.0	1	.421	.495	.496	.074	.075	
13.5	.5			.496		.075	
14.0	0	.421	.495	.496	.074	.075	

TA[illegible] 4-1 [illegible] P. 18

STATION	DISTANCE ALONG FLUME	FLUME BOTTOM	WATER SURFACE WITHOUT MODEL	WATER SURFACE MODEL IN PLACE	NORMAL DEPTH	DEPTH MODEL IN PLACE	
1	2	3	4	5	6	7	[illegible]
4.0	10	.421	.512	.512	.091	.091	S_0 = 0
5.0	9		.512	.512	.091	.091	Q_m .028
6.0	8		.512	.512	.091	.091	7.7"
7.0	7		.512	.512	.091	.091	1.4"
8.0	6		.512	.512	.091	.091	
9.0	5		.512	.512	.091	.091	9.7"
10.0	4		.512	.512		.091	3/8"
10.1	3.9		.512	.511		.090	
10.2	3.8			.510		.089	
10.3	3.7			.509		.088	
10.6	3.4			.508		.087	h .005'
10.77	3.23						.009'
11.0	3		.512		.091		
11.55	2.45						2.45'
11.7	2.3			.514		.093	to
11.8	2.2			.515		.094	Flume 3.23'
11.9	2.1			.516		.095	
12.0	2		.512	.517	.091	.096	
12.5				.517		.096	
13.0	1		.512	.517	.091	.096	~~35~~
13.5				.517		.096	
14.0	0	.421	.512	.517	.091	.096	

TABLE 4-1 WATER SURFACE MEASUREMENTS P. 19

STATION	DISTANCE ALONG FLUME	POINT GAGE READING: FLUME BOTTOM	POINT GAGE READING: WATER SURFACE WITHOUT MODEL	POINT GAGE READING: WATER SURFACE MODEL IN PLACE	NORMAL DEPTH	DEPTH MODEL IN PLACE	
1	2	3	4	5	6	7	8
4.0	10	.423	.571	.571	.148	.148	S_o = 0
5.0	9		.571	.571	.148	.148	Q_m = .031
6.0	8		.571		.148		Dia = 4"
6.5	7.5		.571		.148		
7.0	7		.571	.571	.148	.148	Rise = 2"
7.1	6.9			.570		.147	L = 24"
7.3	6.7			.569		.146	
7.5	6.5			.568		.145	Z- Weir Height = 6/8"
7.8	6.2			.568		.145	
8.0	6			.567		.144	
8.2	5.8			.565		.142	h^* = .005'
8.3	5.7			.565		.142	Δh = .011'
8.6	5.4			.565		.142	
8.7	5.3			.565		.142	Sludge Position Along Flume = 3' to 5'
8.9	5.1			.565		.142	
9.0	5			.565	.148	.142	
10.0	4		.571		.148		EPG-MPG.
11.0	3			.572	.148	.149	
11.1	2.9			.573		.150	
11.2	2.8			.574		.151	FIG NO ~~37~~
11.3	2.7			.575		.152	
11.4	2.6			.576		.153	
12.0	2			.576		.153	
12.5	1.5			.576		.153	
13.0	1			.575		.153	
13.5				.576		.153	
14.0	0	.423	.571	.576	.148	.153	

TABLE 4-1 WATER SURFACE MEASUREMENTS 20

STATION	DISTANCE ALONG FLUME	POINT GAGE READING			NORMAL DEPTH	DEPTH MODEL IN PLACE	
		FLUME BOTTOM	WATER SURFACE				
			WITHOUT MODEL	MODEL IN PLACE			
1	2	3	4	5	6	7	8
4.0	10	.421	.611	.611	.190	.190	S_0 = 0
5.0	9	.421	.611	.611	.190	.190	Q_m = .0519
6.0	8						
7.0	7.0			.611		.190	Dia = 5"
8.0	6.0	.421	.611	.611	.190	.190	Rise = 2.5"
8.8	5.2		.611	.611	.190	.190	= 24"
9.0	5.0			.611	.190	.190	
9.1	4.9			.610		.189	Z = 6/8"
9.3	4.7			.609		.188	Weir Height =
9.5	4.5			.607		.187	
9.532	4.468			.606		.186	h* = .006'
10.0	4.0	.421	.611		.190		Δh = .011'
10.5	3.5						
11.0	3.0						Bridge Position Along Flume = 2.468' to 4.468'
11.5	2.5						
11.532	2.468			.612		.191	
11.6	2.4			.615		.194	
11.7	2.3			.616		.195	R.P.M. =
12.0	2.0	.421	.611	.617	.190	.196	
12.5	1.5			.617		.196	FIG NO ~~36~~
13.0	1.0			.617		.196	
13.5	.5			.617		.196	
14.0	0	.421	.611	.617	.190	.196	

					NORMAL DEPTH	DEPTH MODEL	
4.0	10	.422	.531	.531	.109	.109	.0003
4.5	9.5						.0113
5.0	9	.422	.531	.531	.109	.109	4"
5.5	8.5						2"
6.0	8	.423	.532	.532	.109	.109	
6.5	7.5						24"
7.0	7	.423	.532	.532	.109	.109	
7.1	6.9			.531		.108	1"
7.2	6.8			.531		.108	
7.3	6.7			.531		.108	
7.4	6.6			.531		.108	.002
7.5	6.5			.530	.109	.107	.005
7.93	6.02			.530E			
8.19	5.81			.530E			4.5'
8.70	5.30			.531E			to
9.20	4.80			.532E			6.5'
9.5	4.5		.532	.534		.112	
9.6	4.4			.534			.042
9.7	4.3			.535			
9.8	4.2			.535			~~22~~
9.9	4.1			.53		.112	
10.0	4	.424	.533	.535	.109	.112	
10.5	3.5			.535			
11.0	3			.535			
11.5				.535			
12.0	2			.535			
12.5		.425	.534	.534	.109	.109	
13.0	1						
13.5							
14.0	0	.425	.534	.534	.109	.109	

TABLE 4-1 [illegible] P. 22

STATION	DISTANCE ALONG FLUME	FLUME BOTTOM	WATER SURFACE WITHOUT MODEL	WATER SURFACE MODEL IN PLACE	NORMAL DEPTH	DEPTH MODEL IN PLACE	
1	2	3	4	5	6	7	8
4.0	10	.422	.538	.538	.116	.116	S = .0003
4.1	9.9			.537		.115	[illegible] .0138
4.2	9.8			.537	.116	.115	[illegible] 7.7"
4.3	9.7			.536		.114	[illegible] 1.4"
4.4	9.6			.535		.113	
4.5	9.5			.535	.116	.113	[illegible] 9.7"
4.68	9.32			.536E		.114	
4.93				.537E		.115	[illegible] 1"
5.0	9						
5.3	8.7			.539		.117	
5.4	8.6			.539		.117	h* = .001
5.5	8.5			.539		.117	[illegible] .004
5.6	8.4			.539		.117	
5.7	8.3						Bridge = 8.7'
5.8	8.2						Position to
5.9	8.1						Along Flume 9.5'
6.0	8	.423		.540		.117	
6.5	7.5						
7.0	7	.423	.539	.540	.116	.117	.042
7.5	6.5						~~28~~
8.0	6			.540		.117	
8.5	5.5			.541		.117	
9.0	5			.541		.117	
9.5	4.5			.541		.117	
10.5	3.5			.541		.117	
11.0	3	.424	.540	.541	.116	.117	
12.0	2			.541		.117	
12.5	1.5						
13.0	1	.425		.542		.117	
14.0	0	.425	.541	.542	.116	.117	

[illegible] 4-1 WATER SURFACE [illegible] P.23

STATION	DISTANCE ALONG FLUME	POINT GAGE READINGS: FLUME BOTTOM	WATER SURFACE WITHOUT MODEL	WATER SURFACE MODEL IN PLACE	NORMAL DEPTH	DEPTH MODEL IN PLACE	
1	2	3	4	[illegible]	[illegible]	7	[illegible]
4	10	.420	.531	.531	.111	.111	S_0 = .0003
4.5	9.5			.531		.111	Q_m = .0114
4.6	9.4			.530	.111	.110	[illegible] - 4"
4.7	9.3			.530		.110	[illegible] - 2"
4.8	9.2			.529		.109	[illegible] 24"
4.9	9.1			.529		.109	
5.0	9	.420	.531	.529	.111	.109	[illegible] 1"
5.76	8.24			.530E		.110	Weir Height =
6.0	8		.531		.111		
6.28	7.78			.530E		.110	[illegible] .001'
6.78	7.22			.530E		.110	
7.0	7		.531	.531	.111	.110	[illegible] .003'
7.1	6.9			.531		.111	
7.2	6.8			.531		.111	Bridge Position Along Flume - 7' to 9'
7.3	6.7			.532		.112	
7.4	6.6			.532		.112	
7.5	6.5	.421	.532	.533	.111	.112	[illegible]
7.6	6.4			.533		.112	.045
7.7	6.3			.533		.112	[illegible]
7.8	6.2			.533		.112	
7.9	6.1			.533		.112	
8.0	6		.532	.533	.111	.112	
9.0	5		.532	.532	.111	.111	
10.0	4		.532	.532	.111	.111	
11.0	3	.422	.533	.533	.111	.111	
12.0	2		.533	.533	.111	.111	
13.0	1		.533	.533	.111	.111	
14.0	0	.423	.534	.534	.111	.111	

TABLE 4-1 WATER SURFACE MEASUREMENTS P. 24

STATION	DISTANCE ALONG FLUME	POINT GAGE READINGS: FLUME BOTTOM	WATER SURFACE: WITHOUT MODEL	WATER SURFACE: MODEL IN PLACE	NORMAL DEPTH	DEPTH MODEL IN PLACE	
	2	3	4	5	6	7	8
4	10	.420	.531	.531	.111	.111	S = .0003
4.25	9.75			.531	.111	.111	Q_{m} .0114
4.6	9.4			.531	.111	.111	Dia = 5"
4.7	9.3			.530	.111	.110	Rise 2.5"
4.8	9.2			.530	.111	.110	L = 24"
4.9	9.1			.530		.110	
5.0	9.0	.420	.531	.530	.111	.110	Z 1"
5.22	8.78			.530E		.110	Weir Height
6.0	8.0		.531		.111		
6.22	7.78			.530E		.110	
7.0	7.0		.531	.529	.111	.109	k* = .001'
7.1	6.9			.530		.110	Δ' .002'
7.2	6.8			.531		.111	
7.3	6.7			.532		.112	Range of 7'
7.4	6.6			.532			Station to
7.5	6.5	.420	.531	.532	.111	.112	Along Flume 9'
7.6	6.4			.532			
7.7	6.3			.532			MANNING
7.8	6.2			.532			.045
7.9	6.1			.532			FIG No.
8.0	6	.421	.532	.532	.111	.111	
9.0	5		.532	.532			
10.0	4		.532	.532			
11.0	3	.422	.533	.533	.111	.111	
12.0	2		.533	.533		.111	
13.0	1		.533	.533	.111	.111	
14.0	0	.423	.534	.534	.111	.111	

4.0	10	.422	.532	.532	.110	.110	.0003
4.1	9.9			.531		.109	.0114
4.2	9.8			.531		.109	7.7 "
4.3	9.7			.531		.109	
4.4	9.6			.531	.110	.109	1.4"
4.5	9.5			.529		.107	9.7"
4.68	9.32			.530E		.108	
4.93				.532E		.110	1"
5.0	9	.422	.532		.110		
5.3	8.7			.532		.110	
5.4	8.6			.533	.110	.111	.001
5.5	8.5			.534		.111	.005
5.6	8.4			.534		.111	
5.8	8.2				.110		8.7'
5.9	8.1						to
6.0	8.0	.423		.534		.111	9.5'
6.5	7.5			.534			
7.0	7.0	.423	.533	.534	.110	.111	.042
7.5	6.5			.534		.111	
8.0	6.0			.534		.111	~~27~~
8.5	5.5			.534		.111	
9.0	5.0			.534	.110	.111	
9.5	4.5			.534			
10.5				.535			
11.0	3.0	.424	.534	.535	.110	.111	
12.0	2.0			.535		.111	
13.0	1.0		.535	.535	.110	.110	
14.0	0	.425	.535	.535	.110	.110	

TABLE 4-1 WATER SURFACE MEASUREMENTS P.26

STATION	DISTANCE ALONG FLUME	POINT GAGE READING			NORMAL DEPTH	DEPTH MODEL IN PLACE	
		FLUME BOTTOM	WATER SURFACE WITHOUT MODEL	WATER SURFACE MODEL IN PLACE			
1	2	3	4	5	6	7	8
4	10	.420	.531	.531	.111	.111	S_o - .0003
4.1	9.9			.531	.111	.111	Q_{pr} - .0114
4.2	9.8			.531	.111	.111	Dia. - 7.7"
4.3	9.7			.530	.111	.110	Rise - 1.4"
4.4	9.6			.530		.110	L - 9.7"
4.5	9.5			.530		.110	
5.0	9		.531		.111		1"
5.3	8.7		.531	.531	.111	.111	Weir =
5.4	8.6			.531	.111	.111	Height
5.5	8.5			.532	.111	.112	n^x = .001'
5.6	8.4			.532	.111	.112	
5.7	8.3			.532	.111	.112	Δh = .002'
5.8	8.2			.532	.111	.112	Bridge 8.7'
6.0	8			.532	.111	.112	Position to
6.5	7.5			.532	.111	.112	Along Flume 9.5'
7.0	7			.532	.111	.112	
7.5		.420	.531	.532	.111	.112	[illegible]
8.0	6	.421	.532	.532	.111	.111	.045
9.0	5			.532	.111	.111	[illegible]
10.0	4			.532			
11.0	3	.422	.533	.533	.111	.111	
12.0	2			.533	.111	.111	
13.0	1			.533			
14.0	0	.423	.534	.534	.111	.111	

4.0	10	.422	.534	.534	.112	.112	.0003
4.5	9.5						.0115
5.0	9		.534	.534	.112	.112	5"
5.5	8.5						
6.0	8						2.5"
6.7			.534	.534	.112	.112	24"
6.8	7.2		.534	.534	.112	.112	
6.9	7.1	.423	.534	.534			1"
7.0	7	.423	.535	.534	.112	.111	
7.1	6.9			.534		.111	
7.2	6.8			.533	.112	.110	.001
7.3	6.7			.533	.112	.110	.006
7.4	6.6			.533	.112	.110	
7.5	6.5	.423	.535	.531	.112	.108	4.5'
7.12	6.12			.531E		.108	to
8.13	5.87			.530E		.107	6.5'
8.50	5.5						
8.63				.532E		.109	.042
9.0				.534E		.111	
9.5	4.5	.423	.535	.536	.112	.113	~~21~~
9.6	4.4			.537	.112	.113	
9.7	4.3			.537			
9.8	4.2			.537	.112	.113	
9.9	4.1			.537			
10.0	4	.424	.536	.537	.112	.113	
10.5	3.5			.537			
11.0	3	.425	.537	.537	.112	.112	
11.5	2.5			.537			
12.0	2			.537			
12.5	1.5			.537	.112	.112	
13.0	1		.537	.537			
14.0	0	.425	.537	.537	.112	.112	

P. 28

4.0	10	.422	.541	.541	.119	.119	.0003
4.5	9.5		.541	.541	.119	.119	.015
5.0	9		.541	.541		.119	6"
5.5	8.5		.541	.541		.119	2"
5.6	8.4		.541	.540		.118	24"
5.7	8.3			.540		.118	
5.8	8.2			.540		.118	1"
5.9	8.1			.540		.118	
6.0	8			.540		.118	
6.1	7.9			.539		.117	
6.2	7.8			.538		.116	.002
6.3	7.7			.538		.116	.008
6.4	7.6			.537		.116	
6.5	7.5	.423	.542	.536	.119	.116	5.5' to 7.5'
7.0	7						
7.22	6.78			.536E			
7.5							
7.735	6.265			.537E			
8.0	6			.539E			.042
8.5	5.5			.541		.118	~~26~~
8.6	5.4			.542		.119	
8.7	5.3			.543		.120	
8.8	5.2			.543		.120	
8.9	5.1			.543		.120	
9.0	5			.544		.120	
9.5	3.5			.544		.121	
10.0	4			.544		.121	
10.5	3.5			.544		.121	
11.0	3	.424	.543	.544	.119	.120	
11.5	2.5			.544		.120	
12.0	2			.544		.120	
12.5	1.5			.544		.120	
13.0	1			.544		.120	
13.5	.5	.425		.545		.120	
14.0	0	.425	.544	.545	.119	.120	

TABLE 4-1 WATER [illegible] P.29

STATION	DISTANCE ALONG FLUME	POINT GAGE [illegible] FLUME BOTTOM	POINT GAGE [illegible] WATER SURFACE WITHOUT MODEL	POINT GAGE [illegible] WATER SURFACE [illegible]	NORMAL DEPTH •	DEPTH [illegible]	[illegible]
	2	3	4	5	6	7	
4.0	10	.420	.534	.534	.114	.114	[illegible] .0003
4.1	9.9			.533		.113	[illegible] .0130
4.2	9.8			.533		.113	[illegible] 4"
4.3	9.7			.532		.112	[illegible] 2"
4.4	9.6			.532		.112	[illegible] 24"
4.5	9.5			.532	.114	.112	
5.30	8.70		.534	.532			[illegible] 1"
5.81	8.19			.532E		.112	
6.0	8		.534				
6.32	7.68			.532E		.112	[illegible] .001'
6.50	7.5		.534	.532		.112	
6.6	7.4			.532		.112	[illegible] .003'
6.7	7.3			.533		.113	
6.8	7.2			.533		.113	
6.9	7.1			.534		.114	
7.0	7		.534	.535		.115	
7.1	6.9			.535		.115	
7.2	6.8			.535		.115	.045
7.3	6.7			.536		.115	
7.4	6.6			.536		.115	
7.5	6.5	.421	.535	.536	.114	.115	
7.6	6.4			.536		.115	
8.0	6		.535	.536	.114	.115	
8.5	5.5		.536	.536	.114	.114	
9.0	5	.422	.536	.536	.114	.114	
10	4	.422	.536	.536	.114	.114	
11.0	3	.422	.536	.536	.114	.114	
12.0	2		.536	.536	.114	.114	
13.0	1		.537	.536	.114	.114	
14	0	.423	.537	.536	.114	.114	

4-1 P. 30

4.0	10	.422	.533	.538	.116	.115	.0003
5.0	9			.538	.116	.116	.0138
5.7	8.3		.533	.538	.116	.116	
5.8	8.2			.537		.115	4"
5.9	8.1			.537		.115	2"
6.0	8.0			.537		.115	24"
6.1	7.9			.537		.115	
6.2	7.8			.537		.115	1"
6.3	7.7			.537		.115	
6.4	7.6			.536		.114	
6.5	7.5	.422		.535		.113	.002
7.0	7	.423	.539	.534	.116	.112	.007
7.22	6.78			.535E			
7.73	6.37			.536E			5.5'
8.25	5.75			.537E			to
8.5	5.5			.538		.116	7.5'
8.6	5.4			.539		.117	
8.7	5.3			.540		.117	
8.8	5.2			.541		.118	.042
8.9	5.1			.541		.118	~~24~~
9.0	5			.541		.118	
9.5	4.5	.423		.541		.118	
10.0	4	.424		.541		.117	
10.5	3.5			.541		.117	
11.0	3	.424	.540	.541	.116	.117	
11.5	2.5			.541		.117	
12.0	2		.540	.541		.117	
12.5		.425	.540	.541		.117	
13.0	1		.541	.541	.116	.116	
13.5							
14.0	0	.425	.541		.116	.116	

TABLE 4-1 WATER SURFACE MEASUREMENTS P. 31

STATION	DISTANCE ALONG FLUME	POINT GAGE READING			NORMAL DEPTH	DEPTH MODEL IN PLACE	
		FLUME BOTTOM	WATER SURFACE				
			WITHOUT MODEL	MODEL IN PLACE			
1	2	3	4	5	6	7	8
4.0	10	.422	.538	.538	.116	.116	S_0= .0003
5.0	9			.538	.116	.116	Q_m= .0138
6.0	8			.538	.116	.116	
6.1	7.9						Dia = 5"
6.2	7.8			.537		.115	Rise = 2.5"
6.3	7.7			.536		.114	L = 24"
6.4	7.6			.534		.113	
6.5	7.5			.534		.113	Z = 1"
6.74	7.26			.535E			Weir Height =
7.0	7	.423	.539		.116		
7.24	6.76			.537E			h^*= .001
8.24	5.76			.539E			Δh= .007
8.5	5.5			.540		.117	
8.6	5.4			.540		.117	Bridge 5.5'
8.7	5.3			.540		.117	Position to
8.8	5.2			.540		.117	Along 7.5'
9.0	5			.540		.117	Flume
9.5		.424		.541		.117	EHG-MHG=
10.0	4			.540		.117	.042
10.5				.541		.117	FIG NO ~~23~~
11.0	3	.424	.540	.541	.116	.117	
11.5				.541		.117	
12.0	2		.540	.541		.117	
12.5		.425	.541	.541	.116	.116	
13.0	1						
13.5							
14.0	0	.425	.541		.116	.116	

TABLE 4-1 WATEF S.JRFACE MEASUREMENTS P. 32

STATION	DISTANCE ALONG FLUME	POINT GAGE READING			NORMAL DEPTH	DEPTH MODEL IN PLACE	
		FLUME BOTTOM	WATER SURFACE				
			WITHOUT MODEL	MODEL IN PLACE			
1	2	3	4	5	6	7	8
4.0	10	.420	.535	.535	.115	.115	S_0= .0003
4.10	9.9			.534		.114	Q_m= .0138
4.20	9.8			.534		.114	Dia = 5"
4.30	9.7			.534		.114	Rise = 2.5"
4.40	9.6			.534		.114	L = 24"
4.50	9.5		.535	.534	.115	.114	
4.72	9.28			.534E		.114	
5.23	8.77			.534E		.114	Z-Weir Height: 1"
5.5	8.50						
6.22	7.78			.534E		.114	
6.5	7.5	.420	.535	.535	.115	.115	n^*= .002'
6.6	7.0			.536		.116	Δh = .005'
6.7	7.3			.537		.117	
7.0	7.0			.537		.117	Bridge Position Along Flume = 7.5' to 9.5'
7.1	6.9			.537		.117	
7.2	6.8			.537		.117	
7.3	6.7			.537		.117	EPG-MFG
7.5	6.5	.421	.536	.538	.115	.117	.045
7.6	6.40	.421	.536	.538	.115	.117	
7.75	6.25		.536	.538	.115		FIG NO
8.0	6		.537	.539	.115	.117	
9.0	5	.422	.537	.539		.117	
10.0	4	.422	.537	.539	.115	.117	
11.0	3						
12.0	2	.422	.537	.539	.115	.117	
13.0	1	.423	.538	.539	.115	.116	
14.0	0	.423	.538	.539	.115	.116	

TABLE 4-1 WATER SURFACE MEASUREMENTS P. 33

STATION	DISTANCE ALONG FLUME	POINT GAGE READING: FLUME BOTTOM	POINT GAGE READING: WATER SURFACE: WITHOUT MODEL	POINT GAGE READING: WATER SURFACE: MODEL IN PLACE	NORMAL DEPTH	DEPTH MODEL IN PLACE	
	2	3	4	5	6	7	8
4.0	10	.422	.541	.541	.119	.119	S_o .0003
5.0	9						Q_T .015
5.5	8.5	.422	.541	.541	.119	.119	
5.8	8.2			.540		.118	Dia = 5"
5.9	8.1			.540		.118	Rise 2½"
6.0	8			.540		.118	L 24"
6.1	7.9			.540		.118	
6.2	7.8			.539		.117	Z- 1"
6.3	7.7			.538		.116	Weir
6.4	7.6			.537		.115	Height
6.5	7.5	.423	.542	.537	.119	.116	.002
6.74				.536E		.113	.007
7.26				.537E		.116	
7.5							5.5'
7.73				.538E		.115	to
8.24	5.76			.539E		.116	7.5'
8.5	5.5			.540		.118	
8.6	5.4			.540		.118	
8.7	5.3			.541		.110	.042
8.8	5.2			.542		.119	~~25~~
8.9	5.1			.542		.119	
9.0	5.0			.543	.119	.120	
9.5				.543		.120	
10.0	4.0			.544		.121	
10.5				.544		.121	
11.0	3.0	.424	.543	.545	.119	.121	
11.5				.545		.121	
12.0	2.0			.545		.121	
12.5				.545		.121	
13.0	1.0			.545		.121	
13.5			.544	.545		.121	
14.0	0	.425	.544	.546	.119	.121	

TABLE 4-1 WATER SURFACE MEASUREMENTS P.34

STATION	DISTANCE ALONG FLUME	POINT GAGE READING			NORMAL DEPTH	DEPTH MODEL IN PLACE	
		FLUME BOTTOM	WATER SURFACE				
			WITHOUT MODEL	MODEL IN PLACE			
1	2	3	4	5	6	7	8
4.0	10	.420	.550	.550	.130	.130	S_o = .0003
4.1	9.9			.549		.129	C_{mf} .017
4.2	9.8			.548		.128	
4.3	9.7		.550	.548	.130	.128	Dia = 4"
4.4	9.6			.548		.128	Rise = 2"
4.5	9.5			.547		.127	L = 24"
4.55	9.45			.547		.127	
5.0	9		.550		.130		Z = 6/8"
6.0	8		.550		.130		Weir Height
6.55	7.45			.549		.129	
6.6	7.4			.550		.130	n^* = .001'
6.7	7.3			.551		.131	Δh = .005'
6.8	7.2			.551		.131	
6.9	7.1			.551		.131	Bridge = 7.45'
7.0	7	.421	.551	.552	.130	.131	Position to
7.1	6.9						Along 9.45' Flume
7.25	6.75			.552		.131	EPG-MPG-
7.5	6.5			.552		.131	
7.77	6.23			.552			
8.0	6		.551	.553	.130	.131	FIG NO.
8.5	5.5			.553		.131	
9.0	5			.553			
10.0	4		.551	.554	.130	.132	
11.0	3	.422	.552	.554	.130	.132	
12.0	2		.552	.554	.130	.132	
13.0	1			.554			
14.0	0	.423	.553	.555	.130	.132	

TABLE 4-1 WATER SURFACE MEASUREMENTS P. 35

STATION	DISTANCE ALONG FLUME	POINT GAGE READING: FLUME BOTTOM	WATER SURFACE: WITHOUT MODEL	WATER SURFACE: MODEL IN PLACE	NORMAL DEPTH	DEPTH MODEL IN PLACE	
1	2	3	4	5	6	7	8
3.7	10.3	.420	.555	.555	.135	.135	S_o= .0003
3.8	10.2			.554		.134	Q_m= .023
3.9	10.1			.553		.133	Dia= 4"
4.0	10	.420	.555	.552	.135	.132	
4.1	9.9						Rise - 2"
4.2	9.8			.552		.132	L- 24"
4.3	9.7			.552		.132	
5.0	9						Z- 6/8"
6.0	8						Weir Height =
6.3	7.7			.554		.134	
6.4	7.6			.555		.135	h^*= .002'
6.5	7.5			.556		.136	Δh= .005'
6.6	7.4			.557		.136	
6.75	7.25			.557		.136	Bridge Position
7.0	7	.421	.556		.135		Along
7.5				.557		.136	Flume
8.0	6.0			.557		.136	EPG-MPG-
8.5				.558		.137	
9.0	5.0			.558		.137	
10.0	4.0	.422	.557	.559	.135	.137	FIG NO
11.0	3.0						
11.5	2.5			.559		.137	
12.0	2.0			.559		.137	
13.0	1.0						
13.7	.3	.423	.558		.135	.137	
14.0	0	.423	.558	.560	.135	.137	

TABLE 4-1 WATER SURFACE MEASUREMENTS P. 36

STATION	DISTANCE ALONG FLUME	POINT GAGE READING			NORMAL DEPTH	DEPTH MODEL IN PLACE	
		FLUME BOTTOM	WATER SURFACE				
			WITHOUT MODEL	MODEL IN PLACE			
1	2	3	4	5	6	7	8
4.0	10	.420	.561	.561	.141	.141	S_0 = .0003
4.1	9.9			.560		.140	Q_m = .028
4.3	9.8			.559		.139	Dia = 5"
4.5	9.5			.559		.139	
4.6	9.4			.558		.138	Rise - 2.5"
4.7	9.3			.558	.141	.138	L = 24"
5.0	9						
5.5							Z- 6/8"
6.0	8						Weir Height =
6.5	7.5						
6.7	7.3			.559		.139	h^* = .002'
6.8	7.2			.560		.140	Δh = .006'
6.9	7.1			.561		.141	
7.0	7	.421	.562	.562	.141	.141	Bridge = 7.3'
7.25				.563		.142	Position to
7.50				.563		.142	Along Flume 9.3'
8.0	6			.564		.143	[illegible]
8.5				.564		.143	
9.0	5			.564	.141	.143	
9.5				.564		.143	FIG NO
10.0	4			.564		.143	
10.5		.422		.564		.142	
11.0	3	.422	.563	.563	.141	.141	
11.5							
12.0	2	.423	.564	.564		.141	
12.5							
13.0	1		.564	.564		.141	
13.5							
14.0	0	.423	.564	.564	.141	.141	

TABLE 4-1 WATER SURFACE MEASUREMENTS P.37

STATION	DISTANCE ALONG FLUME	POINT GAGE READING			NORMAL DEPTH	DEPTH MODEL IN PLACE	
		FLUME BOTTOM	WATER SURFACE				
			WITHOUT MODEL	MODEL IN PLACE			
	2	3	4	5	6	7	8
4.0	10	.420	.564	.564	.144	.144	S_0= .0003
4.20	9.8			.563		.143	Q_m .031
4.3	9.7			.563		.143	L = 5"
4.4	9.5			.562		.142	Rise = 2.5"
4.6	9.4			.561		.141	L = 24"
4.70	9.3			.561		.141	
5.0	9				.144		Z 6/8"
5.5	8.5						Weir Height =
6.0	8						
6.5	7.5						k = .001'
6.70	7.3			.563		.143	
6.8	7.2			.564		.143	Δh = .005'
6.9	7.1			.564		.143	Bridge = 7.3'
7.0	7	.421	.565	.564	.144	.143	Position to
7.1	6.9			.566		.145	Along
7.2	6.8			.566		.145	Flume 9.3'
7.3	6.7			.566		.145	FFG-M.P.-
7.5	6.6			.566		.145	
8.0	6			.566		.145	FIG NO
8.5	5.5			.566		.145	
9.0	5			.567		.145	
9.5	4.5			.567		.145	
10.0	4	.422	.566	.567	.144	.145	
10.5	3.5			.567		.145	
11.0	3		.567	.567		.145	
11.5	2.5			.567		.145	
12.0	2		.567	.567		.145	
12.5	1.5						
13.0	1		.567	.567		.145	
13.5							
14.0	0	.423	.567	.567	.144	.144	

TABLE 4-1 WATER SURFACE MEASUREMENTS P. 38

STATION	DISTANCE ALONG FLUME	POINT GAGE READING			NORMAL DEPTH	DEPTH MODEL IN PLACE	
		FLUME BOTTOM	WATER SURFACE				
			WITHOUT MODEL	MODEL IN PLACE			
1	2	3	4	5	6	7	8
4.0	10	.420	.530	.530	.110	.110	S_o= .0005
4.1	9.9			.529		.109	Q_m= .0114
4.2	9.8			.529		.109	
4.3	9.7			.529		.109	Dia - 7.7"
4.4	9.6			.529		.109	Rise = 1.4"
4.5	9.5	.421	.531	.531	.110	.110	L = 9.7"
5.0	9	.421	.531		.110		
5.3	8.7			.531		.110	Z- 1"
5.4	8.6			.531		.110	Weir
5.5	8.5			.532		.111	Height =
5.6	8.4			.532		.111	h^*= .001'
5.7	8.3			.532		.111	Δh= .003'
5.8	8.2						
5.9	8.1			.533		.111	Bridge - 8.7'
6.0	8	.422	.532	.533	.110	.111	Position to
6.5	7.5		.532	.532	.110	.110	Along Flume 9.5'
7.0	7	.422	.532	.532	.110	.110	
8.0	6		.532	.532			DRG. NO.
9.0	5	.423	.533	.533	.110	.110	
10.0	4	.423	.533	.533	.110	.110	FIG. NO.
11.0	3	.424	.534	.534	.110	.110	
12.0	2	.424	.534	.534	.110	.110	
13.0	1	.424	.534	.534	.110	.110	
14.0	0	.425	.535	.535	.110	.110	

4-1 [illegible] P.39

[illegible]	[illegible]	[illegible]	[illegible]	[illegible]	[illegible] DEPTH	DEPTH MODEL IN PLACE	
1						7	
4.0	10	.420	.528	.528	.108	.108	So= .0005
4.1	9.9			.527		.107	.0115
4.2	9.8			.527		.107	Dia=4"
4.3	9.7			.527		.107	Rise - 2"
4.4	9.6			.527		.107	24"
4.5	9.5		.528	.527	.108	.107	
5.0	9.00		.528		.108		
5.21	8.79			.527E		.107	1"
5.5	8.5						
5.72	8.28			.527E		.106	
6.0	8.0	.421	.529		.108		.002
6.22				.526E		.105	.005
6.5	7.5		.529	.528	.108	.107	
6.6	7.4			.528	.108	.107	= 7.5'
6.7	7.3			.528		.107	to
6.8	7.2			.527		.108	9.5'
6.9	7.1			.530		.109	
7.0	7.0	.421	.529	.531	.108	.110	
7.1	6.9			.531			.040
7.2	6.8			.532			
7.3	6.7			.532	.108		
7.4	6.6			.532	.108		
7.5	6.5			.532	.108	.110	
8.0	6.0	.422	.530	.532	.108	.110	
8.5	5.5						
9.0	5.0	.422	.530	.532	.108	.1100	
9.5	4.5		.531	.532			
10.0	4.0	.423	.531	.532	.108	.109	
10.5	3.5			.532			
11.0	3.0	.423	.531	.531	.108	.108	
11.5	2.5						
12.0	2.0	.426	.532	.532	.108	.108	
12.5	1.5						
13.0	1.0	.424	.532	.532	.108	.108	
13.5	.5						
14.0	0	.425	.533	.532	.108	.108	

TABLE 4-1 WATER SURFACE MEASUREMENTS P. 36 A

STATION	DISTANCE ALONG FLUME	POINT GAGE READING			NORMAL DEPTH	DEPTH MODEL IN PLACE	
		FLUME BOTTOM	WATER SURFACE WITHOUT MODEL	WATER SURFACE MODEL IN PLACE			
1	2	3	4	5	6	7	8
4	10	.420	.528	.528	.108	.108	S_o= .0005
4.2	9.8			.528		.108	Q_m= .0115
4.3	9.7			.527		.107	Dia= 5"
4.4	9.6			.527		.107	Rise= 2.5"
4.5	9.5		.528	.527		.107	L= 24"
4.75	9.25			.527E		.107	
5.0	9	.420	.528	.528E	.108		Z= 1"
5.25				.528E		.107	Weir
5.5	8.50			.528E			Height =
5.74	8.26			.529E		.107	h^*= .002
6.0	8	.421	.529		.108		
6.465	7.76			.528E		.107	Δh= .004
6.5	7.5		.529	.529	.108	.108	Bridge = 7.5
6.6	7.4			.530	.108	.109	Position to
6.7	7.3			.531	.108	.110	Along 9.5
6.8	7.2			.531	.108	.110	Flume
6.9	7.1			.531	.108	.110	EPG-MPG=
7.0	7.0	.421	.529	.531	.108	.110	.040
7.1				.531			
7.2				.531			FIG. NO
7.3				.531			
7.4				.531			
7.5				.531			
8.0	6.0	.422	.530	.531	.108	.109	
8.5			.530	.531			
9.0	5.0	.422	.530	.531	.108	.109	
9.5							
10.0	4.0	.423	.531	.531	.108	.108	
10.5							
11.0	3.0	.423	.531	.531	.108	.108	
11.5							
12.0	2.0	.424	.532	.532	.108	.108	
12.5							
13.0	1.0	.424	.532	.532	.108	.108	
13.5							
14.0	0	.425	.523	.533	.108	.108	

[illegible] C-1 [illegible] P. 37A

STATION	[illegible] ALONG FLUME	[illegible]	WATER SURFACE [illegible]	[illegible]	[illegible]	DEPTH [illegible] IN [illegible]	
4.0	10	.420	.534	.534	.116	.114	S_0 = .0005
4.1	9.9			.533		.113	[illegible] .0137
4.2	9.8			.533		.113	4"
4.3	9.7			.533		.113	2"
4.4	9.6			.532		.112	24"
4.5	9.5			.531		.111	
5.0	9						1"
5.21	8.79			.530E		.110	
5.5	8.5						
5.72	8.28			.531E		.110	
6.0	8	.421	.535		.114		.002
6.22				.533E		.112	.006
6.5	7.5			.535		.114	
6.6	7.4			.536		.115	7.5'
6.7	7.3			.537		.117	to
6.8	7.2			.537		.117	9.5'
6.9	7.1			.537		.117	
7.0	7			.537		.117	.04
7.2	6.8			.537		.117	
7.5	6.5			.537		.117	
8.0	6.0	.422	.536	.537	.114	.115	
8.5	5.5			.537		.115	
9.0	5.0	.423		.538		.115	
9.5	4.5			.538		.115	
10.0	4.0	.423	.537	.538	.114	.115	
10.5	3.5			.538		.115	
11.0	3.0	.424	.538	.539	.114	.115	
11.5	2.5						
12.0	2.0	.424	.538	.539	.114	.115	
12.5	1.5						
13.0	1.0	.425	.538	.539	.114	.115	
13.5	.5						
14.0	0	.425	.539	.539	.114	.114	

TABLE 4-1 WATER SURFACE MEASUREMENTS P. 38 A

STATION	DISTANCE ALONG FLUME	POINT GAGE READING			NORMAL DEPTH	DEPTH MODEL IN PLACE	
		FLUME BOTTOM	WATER SURFACE				
			WITHOUT MODEL	MODEL IN PLACE			
1	2	3	4	5	6	7	8
4.0	10	.420	.534		.114	.114	[illegible] .0005
4.1	9.9		.534	.534		.114	[illegible] .0137
4.2	9.8			.533		.113	[illegible] 5"
6.3	9.7			.533		.113	[illegible] 2.5"
6.4	9.6			.533		.113	[illegible] 24"
6.5	9.50			.533		.113	
4.75	9.25			.533E		.113	[illegible] 1"
5.0	9			.532E		.112	[illegible] =
5.25				.533E		.113	Height
5.5	8.5						
5.74				.533E		.113	[illegible] .001
6.0	8	.421	.535		.114		Δh= .004
6.24	7.79			.534		.113	[illegible] = 7.5'
6.5	7.5			.534		.113	Position to
6.6	7.4			.534		.113	Along
6.7	7.3			.535		.114	Flume 9.5'
6.8	7.2			.536		.115	[illegible]
6.9	7.1			.536		.115	.04
7.0	7			.536		.115	
7.3	6.8			.536		.115	[illegible]
7.5	6.5			.536		.115	
8.0	6	.422	.536	.537	.114	.115	
8.5	5.5			.537		.115	
9.0	5	.423	.537	.537	.114	.114	
9.5	4.5						
10.0	4	.423	.537	.537	.114	.114	
10.5	3.5						
11.0	3			.537		.114	
11.5	2.5						
12.0	2	.424	.538	.538	.114	.114	
12.5	1.5						
13.0	1			.538		.114	
13.5	.5						
14.0	0	.425	.539	.539	.114	.114	

TABLE 4-1 WATER SURFACE MEASUREMENTS P. 39

STATION	DISTANCE ALONG FLUME	POINT GAGE READING			NORMAL DEPTH	DEPTH MODEL IN PLACE	
		FLUME BOTTOM	WATER SURFACE				
			WITHOUT MODEL	MODEL IN PLACE			
1	2	3	4	5	6	7	8
4.0	10	.420	.535	.535	.115	.115	S_o = .0005
4.1	9.9			.534		.114	Q_m = .0138
4.2	9.8			.534		.114	Dia = 4"
4.3	9.7			.534		.114	Rise = 2"
4.4	9.6			.534		.114	L = 24"
4.5	9.5			.534		.114	
5.0	9		.535		.115		Z 1"
5.22	8.78			.534E		.114	Weir Height =
5.73	8.27			.534E		.114	
6.0	8	.421	.536		.115		h^* = .002'
6.23	7.77			.534E		.113	Δh = .003'
6.5	7.5			.534		.113	
6.6	7.4			.535		.114	Bridge Position Along Flume = 7.5' to 9.5'
6.7	7.3			.536		.115	
6.8	7.2			.538		.117	
6.9	7.1						
7.0	7			.538	.115	.117	EPG-MPG = .053
7.1	6.9						
7.2	6.8						FIG NO
7.3	6.7						
7.4	6.6						
7.5	6.5			.538	.115	.117	
8.0	6	.421	.536	.538		.117	
8.5	5.5			.538			
9.0	5	.422	.537	.538		.116	
9.5	4.5			.538			
10.0	4	.422	.537	.538		.116	
10.5	3.5			.538			
11.0	3	.422	.537	.538	.115	.116	
12.0	2	.423	.538	.538	.115	.115	
13.0	1	.423	.538	.538	.115	.115	
14.0	0	.425	.540	.540	.115	.115	

TABLE 4-1 WATER SURFACE MEASUREMENTS P.40

STATION	DISTANCE ALONG FLUME	POINT GAGE READING: FLUME BOTTOM	POINT GAGE READING: WATER SURFACE WITHOUT MODEL	POINT GAGE READING: WATER SURFACE MODEL IN PLACE	NORMAL DEPTH	DEPTH MODEL IN PLACE	
1	2	3	4	5	6	7	8
4.0	10	.420	.535	.535	.115	.115	S_o = .0005
4.2	9.8			.535		.115	Q_{mf} = .0138
4.3	9.7			.534		.114	Dia = 5"
4.4	9.6			.534		.114	Rise = 2.5"
4.50	9.5			.534		.114	L = 24"
4.71	9.29			.534E		.114	
5.0	9		.535		.115		Z 1"
5.21	8.79			.534E		.114	Weir Height =
6.0	8	.421	.536		.115		
6.21	7.79			.534E		.114	h^* = .001'
6.5	7.5			.534		.113	
6.6	7.4			.535		.114	Δh = .002'
6.7	7.3			.536		.115	Bridge Position = 7.5'
6.8	7.2			.537		.116	to
6.9	7.1			.537			Along
7.0	7.0	.421		.537		.116	Flume 9.5'
7.1	6.9			.537			[illegible]
7.2	6.8			.537			.053
7.3	6.7	.421	.536	.537	.115	.116	FIG NO.
7.5	6.5		.536	.537			
8.0	6.0		.536	.537	.115	.116	
8.5	5.5	.422	.537	.537	.115	.115	
9.0	5	.422	.537	.537	.115	.115	
10.0	4	.423	.538	.538	.115	.115	
11.0	3		.538	.538	.115	.115	
12.0	2	.424	.539	.539	.115		
13.0	1			.539	.115	.115	
14.0	0	.425	.540	.540	.115	.115	

4.0	10	.420	.536	.536	.116	.116	.0005
4.5	9.5						.015
5.0	9			.536		.116	4"
5.5	8.5						2"
5.6	8.4		.536	.536	.116	.116	24"
5.7	8.3			.535	.115	.115	
5.8	8.2			.535		.115	
5.9	8.1			.534		.114	1"
6.0	8	.421	.537	.534	.116	.113	
6.5	7.5						
6.75	7.25			.534E		.114	.002
7.0	7						.007
7.27	6.73			.534E		.115	
7.5	6.5						6'
7.72	6.28			.537E		.116	to
8.0	6	.422	.538	.538	.116	.116	8'
8.1	5.9			.539		.117	
8.2	5.8			.540		.118	.04
8.3	5.7			.540		.118	
8.4	5.6			.540		.118	
8.5	5.5			.541		.119	
8.6	5.4			.541		.119	
8.7	5.3						
9.0	5	.423		.541		.118	
9.5	4.5			.541		.118	
10.0	4	.423	.539	.541	.116	.118	
10.5	3.5			.541		.118	
11.0	3			.541		.118	
11.5	2.5			.541			
12.0	2	.424	.540	.541	.116	.117	
12.5	1.5			.541		.117	
13.0	1			.541		.117	
13.5	.5	.425	.541	.541	.116	.116	
14.0	0	.425	.541		.116	.116	

4-1 P-42

STATION	DISTANCE ALONG	[illegible]	[illegible]	F	[illegible]	V	
4	10	.420	.536	.536	.116	.116	.0005
4.5	9.5		.536	.536	.116		.015
5.0	9		.536	.536	.116	.116	5"
5.5	8.5		.536	.536	.116	.116	2.5"
5.6	8.4		.536	.536	.116	.116	
5.7	8.3			.535		.115	24"
5.8	8.2			.535		.115	
5.9	8.1			.534		.114	1"
6.0	8	.421	.537	.534	.116	.114	
6.21	7.79			.530E		.109	
6.5	7.5						.001
6.715	7.285			.532E		.112	.006
7.0	7						
7.435	6.565			.533E		.112	6'
7.5	6.5						to
8.0	6	.422		.535		.113	8'
8.1	5.9			.535		.113	
8.2	5.8			.536		.114	.04
8.3	5.7			.538		.116	
8.4	5.6						
8.5	5.5		.538	.539	.116	.117	
8.75	5.25	.423		.540		.117	
9.0	5			.540		.117	
9.5	4.5			.540		.117	
10.0	4	.423	.539	.540	.116	.117	
10.5	3.5			.541			
11.0	3			.541		.117	
11.5	2.5	.424		.541		.117	
12.0	2	.424	.540	.541	.116	.117	
12.5	1.5			.541			
13.0	1	.425	.541	.541	.116	.116	
13.5	.5						
14.0	0	.425	.541	.541	.116	.116	
14.5							

TABLE 4-1 [illegible] PROFILE MEASUREMENTS P. 43

STATION	DISTANCE ALONG FLUME	POINT GAGE READING			NORMAL DEPTH	DEPTH MODEL IN PLACE	
		FLUME BOTTOM	WATER SURFACE WITHOUT MODEL	WATER SURFACE MODEL IN PLACE			
1	2	3	4	5	6	7	8
							S = .0005
4.0	10	.421	.548	.548	.127	.127	Q = .017
4.1	9.9		.548	.548		.127	
4.2	9.8			.548		.127	Dia 7.7"
4.3	9.7			.547		.126	Rise=1.4"
4.5	9.50			.546		.125	L = 9.9"
4.75	9.25			.546		.125	
5.0	9						1"
5.55	8.45			.548		.126	Weir Height
5.60	8.40			.548		.126	
5.65	8.35			.548		.126	n* = .002'
5.70	8.3			.548		.126	Δh = .004'
5.80	8.2			.548		.126	
5.90	8.1			.549		.127	Bed Position Along Flume 8.45'
6.0	8	.422	.549	.549	.127	.127	to
6.5	7.5			.550		.128	9.25'
7.0	7			.550		.128	
7.5	6.5			.551		.129	[illegible]
8.0	6	.423	.550	.552	.127	.129	
9.0	5		.550	.552		.129	[illegible]
10.0	4	.424	.551	.553	.127	.129	
11.0	3			.553		.129	
12.0	2	.425	.552	.554	.127	.129	
12.5							
13.0	1			.554		.129	
14.0	0	.426	.553	.555	.127	.129	

4-1 P.44

STATION	DISTANCE	[illegible]	[illegible]	[illegible]	NORMAL	[illegible]		
		3			5			
4.0	10	.421	.562	.562	.141	.141	S	.0005
4.5								.031
5.0	9							5"
5.5								
6.0	8	.422	.563	.563	.141	.141		2.5"
6.1	7.9			.563		.141		24"
6.3	7.7			.562		.140		
6.5	7.5			.562		.140		6/9"
6.8	7.2			.562		.140		
7.0	7			.561		.139		
7.2	6.8			.560		.138	h	.002'
8.0	6	.423	.564		.141			.006'
9.0	5							
9.2	4.8			.565	.141	.142		4.8'
9.3	4.7			.566		.143		to
9.4	4.6			.566		.143		6.8'
9.5	4.5			.567		.144		
9.6	4.4			.566				
10.0	4	.424	.565	.566	.141	.142		
10.5	3.5			.566		.142		
10.8	3.2			.566				
11.0	3			.566		.142		
12.0	2	.425	.566	.566	.141	.141		
13.0	1	.425	.566	.566	.141	.141		
14	0	.426	.567	.567	.141	.141		

TABLE 4-1 [illegible] P.45

STATION	DISTANCE ALONG FLUME	FLUME BOTTOM	WATER SURFACE WITHOUT MODEL	WATER SURFACE MODEL IN PLACE	NORMAL DEPTH	MODEL IN PLACE	
	2	3	4	5	6	7	8
4.0	10	.421	.571	.571	.150	.150	S_o .0005
4.5				.571			C_m .0379
5.0	9						
5.5	8.5	.422		.572		.150	Dia = 5"
6.0	8	.422	.572	.572	.150	.150	Base 2.5"
6.1				.572		.150	24"
6.2	7.8			.572	.150	.150	
6.3	7.7			.571		.149	Z 6/8"
6.4	7.6			.570		.148	Weir =
6.5	7.5			.569		.147	Height
6.8	7.2					.147	h^* = .002'
7.0	7			.568		.146	Δh = .006'
7.2	6.8			.568		.146	
8	6	.423	.573				Bridge 4.8'
8.5	5.5						Position to
9.0	5						Along Flume 6.8'
9.2	4.8			.573	.150	.150	EPG-VPG
9.3	4.7			.574		.151	
9.4	4.6						
9.5	4.5			.575		.152	FIG No.
9.75	4.25	.424		.576		.152	
10.0	4	.424	.575	.576	.150	.152	
11.0	3	.424		.576	.150	.152	
12.0	2	.425	.575	.576	.150	.151	
13.0	1	.426	.576	.576		.150	
14.0	0	.426	.576		.150	.150	

TABLE 4-1 WATER SURFACE MEASUREMENTS P. 46

STATION	DISTANCE ALONG FLUME	POINT GAGE READING			NORMAL DEPTH	DEPTH MODEL IN PLACE	
		FLUME BOTTOM	WATER SURFACE				
			WITHOUT MODEL	MODEL IN PLACE			
1	2	3	4	5	6	7	8
4.0	10	.421	.580	.580	.159	.159	S_0= .0005
5.0	9		.580	.580	.159	.159	Q_m= .042
6.0	8	.422	.581	.581	.159	.159	Dia = 5"
6.6	7.4			.580		.158	
6.8	7.2			.579		.157	Rise = 2.5"
7.0	7			.578		.156	L = 24"
7.2	6.8			.578		.156	
7.5	6.5						Z = 6/8"
8.0	6	.423	.582		.159		Weir Height =
8.5							
9.0	5						h^* = .002'
9.2	4.8						Δh = .005'
9.225	4.775			.580		.157	
9.3	4.7			.581		.158	Bridge Position Along Flume = 4.8' to 6.8'
9.4	4.6			.582		.159	
9.5	4.5			.583		.160	
10.0	4	.424	.583	.584	.159	.160	
10.5				.585		.161	E.P.G.-M.P.G.=
11.0	3			.585		.161	
11.5				.585		.161	FIG NO
12.0	2	.425	.584		.159		
12.5				.585		.160	
13.0	1			.585		.160	
14.0	0	.426	.585	.585	.159	.159	

TABLE 4-1 WATER SURFACE MEASUREMENTS P. 47

STATION	DISTANCE ALONG FLUME	POINT GAGE READINGS			NORMAL DEPTH	DEPTH MODEL IN PLACE	
		FLUME BOTTOM	WATER SURFACE				
			WITHOUT MODEL	MODEL IN PLACE			
1	2	3	4	5	6	7	8
4.0	10	.421	.590	.590	.169	.169	S_o= .0005
4.1	9.9			.589		.168	Q_m= .0525
4.2	9.8			.589		.168	
4.3	9.7			.589			Dia= 5"
4.4	9.6			.588		.167	Rise= 2.5"
4.5	9.5			.587		.166	L= 24"
4.7	9.3			.587			
4.8	9.2			.505		.164	Z= 6/8"
5.0	9			.583		.162	Weir Height -
6.0	8	.422	.591		.169		
7.0	7			.589	.169	.167	h^*= .003'
7.1	6.9			.592		.170	[illegible]= .01'
7.2	6.8			.592		.170	
7.3	6.7						Bridge Position Along Flume - 7' to 9'
7.4	6.6	.423		.593		.170	
7.5	6.5			.593			
8.0	6	.423	.592	.593	.169	.170	[illegible]
8.5	5.5			.594		.171	
9.0	5			.595		.172	
9.5	4.5			.595		.172	[illegible]
10.0	4	.424	.593	.596	.169	.172	
10.5	3.5						
11.0	3			.596			
12.0	2	.425	.594	.597	.169	.172	
13.0	1			.598		.172	
14.0	0	.426	.595	.598	.169	.172	

Geometry VII

TABLE 4-2 - SMALL FLUME - SEGMENT TESTS - ROUGH BOUNDARIES

(All model tests are two dimensional)

Measured Data | Calculations

(1) Run No.	(2) Q	(3) Slope	(4) y_n	(5) y_1	(6) F_n	(7) M	(8) M'	(9) C_d	(10) y_1/y_n	(11) $(F_n/M')^{2/3}$
1	0.010	0.00005	0.1116	0.1398	0.0957	.4364	-	.208	1.251	-
2	"	"	"	0.1190	"	.5820	-	.112	1.067	-
3	"	"	"	0.1135	"	.7270	-	.080	1.018	-
4	"	0.0001	0.0848	0.1081	0.1441	.4365	-	.206	1.275	-
5	"	"	"	0.0899	"	.5820	-	.142	1.060	-
6	"	"	"	0.0861	"	.7270	-	.104	1.017	-
7	"	0.0003	0.0672	0.0906	0.2035	.4364	-	.228	1.350	-
8	"	"	"	0.0736	"	.5820	.4650	.171	1.095	0.576
9	"	"	"	0.0697	"	.727	.5194	.129	1.039	0.476
10	"	"	0.0792	0.1050	0.15[illegible]	.4364	-	.210	1.325	-
11	"	"	"	0.0841	"	.5820	.4266	.151	1.063	0.518
12	"	"	"	0.0806	"	.7270	.5936	.108	1.019	0.415
13	"	0.0010	0.0580	0.0792	0.2544	.4364	.3247	.254	1.367	0.850
14	"	"	"	0.0653	"	.5820	.4883	.192	1.125	0.648
15	"	"	"	0.0605	"	.7270	.6354	.147	1.042	0.543
16	"	0.0020	0.0526	0.0786	0.2950	.4364	.3421	.254	1.496	0.906
17	"	"	"	0.0623	"	.5820	.4988	.202	1.182	0.704
18	"	"	"	0.0556	"	.7270	.6448	.162	1.059	0.594
19	"	0.0040	0.0467	0.0744	0.3510	.4364	.3592	.266	1.591	0.985
20	"	"	"	0.0583	"	.5820	.5087	.216	1.249	0.781
21	"	"	"	0.0510	"	.7270	.6543	.175	1.091	0.661
22	"	0.0070	0.0380	0.0700	0.4790	.4364	.3766	.280	1.841	1.174
23	"	"	"	0.0548	"	.5820	.5232	.228	1.441	0.943
24	"	"	"	0.0462	"	.7270	.6688	.194	1.217	0.801
25	"	0.0085	0.0343	0.0695	0.5600	.4364	.3827	.282	2.026	1.289
26	"	"	"	0.0536	"	.5820	.5290	.232	1.565	1.039
27	"	"	"	0.0445	"	.7270	.6754	.202	1.299	0.883
28	"	0.0100	0.0311	0.0690	0.6470	.4364	.3680	.286	2.219	1.406
29	"	"	"	0.0523	"	.5820	.5349	.242	1.681	1.135
30	"	"	"	0.0425	"	.7270	.6797	.211	1.368	0.968
31	"	0.0120	0.0290	0.0682	0.7190	.4364	.3910	.287	2.352	1.500
32	"	"	"	0.0521	"	.5820	.5378	.242	1.799	1.214
33	"	"	"	0.0422	"	.7270	.6834	.211	1.457	1.034
34	"	0.0150	0.0277	0.0671	0.7700	.4364	.3932	.292	2.424	1.565
35	"	"	"	0.0510	"	.5820	.5401	.246	1.841	1.267
36	"	"	"	0.0411	"	.7270	.6856	.221	1.485	1.080
37	"	0.0180	0.0265	0.0666	0.8220	.4364	.3954	.295	2.517	1.630
38	"	"	"	0.0504	"	.5820	.5418	.248	1.900	1.321
39	"	"	"	0.0400	"	.7270	.6877	.223	1.510	1.125
40	"	0.0210	0.0251	0.0659	0.8910	.4364	.3976	.296	2.622	1.714
41	"	"	"	0.0495	"	.5820	.5442	.253	1.971	1.389
42	"	"	"	0.0385	"	.7270	.5892	.233	1.533	1.187
43	"	0.0240	0.0236	0.0612	0.9780	.4354	.4006	.322	2.595	1.813
44	"	"	"	0.0470	"	.5820	.5465	.268	1.991	1.475
45	"	"	"	0.0362	"	.7270	.6921	.247	1.533	1.259

(1) Run No.	(2) Q	(3) Slope	(4) y_n	(5) y_1	(6) F_n	(7) M	(8) M'	(9) C_d	(10) y_1/y_n	(11) $(F_n/M')^{2/3}$
46	0.020	-	0.1526	0.2782	0.1193	.4364	-	-	1.825	-
47	"	-	"	0.1847	"	.5820	-	.207	1.250	-
48	"	-	"	0.1654	"	.7270	-	.121	1.086	-
49	"	0.00005	0.1463	0.2738	0.1269	.4364	-	-	1.870	-
50	"	"	"	0.1847	"	.5820	-	.200	1.260	-
51	"	"	"	0.1589	"	.7270	-	.123	1.084	-
52	"	0.0006	0.1185	0.2444	0.1741	.4364	-	-	2.062	-
53	"	"	"	0.1529	"	.5820	-	.197	1.290	-
54	"	"	"	0.1284	"	.7270	-	.145	1.084	-
55	"	0.0010	0.0974	0.2160	0.2340	.4364	-	-	2.218	-
56	"	"	"	0.1298	"	.5820	-	.212	1.331	-
57	"	"	"	0.1045	"	.7270	.5365	.174	1.072	0.575
58	"	0.0014	0.0811	0.1987	0.3080	.4364	-	-	2.444	-
59	"	"	"	0.1116	"	.5820	.4190	.236	1.374	0.815
60	"	"	"	0.0899	"	.7270	.5874	.199	1.108	0.650
61	"	0.0030	0.0688	0.1876	0.3950	.4364	-	-	2.724	-
62	"	"	"	0.1004	"	.5820	.4604	.256	1.460	0.903
63	"	"	"	0.0803	"	.7270	.6158	.233	1.168	0.744
64	"	0.0050	0.0629	0.1860	0.4510	.4364	-	-	2.960	-
65	"	"	"	0.0964	"	.5820	.4772	.266	1.532	0.963
66	"	"	"	0.0770	"	.7270	.6274	.233	1.224	0.802
67	"	0.0070	0.0567	0.1820	0.5290	.4364	.3295	.972	3.208	1.371
68	"	"	"	0.0937	"	.5820	.4900	.275	1.651	1.052
69	"	"	"	0.0734	"	.7270	.6383	.245	1.291	0.884
70	"	0.0090	0.0500	0.1803	0.6380	.4364	.3500	.866	3.606	1.485
71	"	"	"	0.0921	"	.5820	.5034	.261	1.842	1.172
72	"	"	"	0.0723	"	.7270	.6485	.248	1.447	0.989
73	"	0.0110	0.0459	0.1792	0.7230	.4364	.3609	.824	3.908	1.588
74	"	"	"	0.0912	"	.5820	.5104	.280	1.989	1.261
75	"	"	"	0.0706	"	.7270	.6550	.252	1.540	1.068
76	"	0.0140	0.0416	0.1796	0.8360	.4364	.3692	.850	4.310	1.725
77	"	"	"	0.0900	"	.5820	.5174	.284	2.162	1.378
78	"	"	"	0.0697	"	.7270	.6623	.259	1.678	1.168
79	"	0.0180	0.0382	0.1796	0.9510	.4364	.3762	.850	4.700	1.975
80	"	"	"	0.0888	"	.5820	.5226	.286	2.323	1.490
81	"	"	"	0.0670	"	.7270	.6681	.268	1.752	1.265
82	"	0.0220	0.0362	0.1774	1.0320	.4364	.3797	.769	4.900	1.949
83	"	"	"	0.0862	"	.5820	.5255	.296	2.382	1.568
84	"	"	"	0.0625	"	.7270	.6717	.286	1.729	1.332
85	"	0.0240	0.0360	0.1751	1.0410	.4364	.3801	.708	4.870	1.955
86	"	"	"	0.0864	"	.5820	.5267	.294	2.398	1.575
87	"	"	"	0.0614	"	.7270	.6717	.292	1.702	1.340
88	"	0.0260	0.0351	0.1762	1.0800	.4364	.3810	.735	5.026	2.000
89	"	"	"	0.0863	"	.5820	.5279	.296	2.458	1.612
90	"	"	"	0.0625	"	.7270	.6732	.286	1.781	1.370

TABLE 5-1. DATA FOR NORMAL DEPTH TEST RUNS - ROUGH BOUNDARIES

Run No.	Q cfs	Slope ft./ft.	y_n cm.	y_t cm.	Temp. F
1	1.0	0.000010	22.91	19.50	71
2	"	0.000075	16.49	12.70	70
3	"	0.000200	13.55	9.70	70
4	"	0.000400	10.90	7.00	70
5	"	0.000700	9.27	5.40	69
6	"	0.001200	7.95	4.20	69
7	"	0.002000	6.96	3.60	69
8	"	0.003500	5.97	3.30	68
9	2.0	0.000025	30.80	25.00	64
10	"	0.000100	23.35	17.00	64
11	"	0.000250	18.60	12.50	66
12	"	0.000500	15.26	9.00	66
13	"	0.000800	13.17	7.00	67
14	"	0.001400	11.17	5.00	67
15	"	0.002500	9.45	3.80	67
16	"	0.004000	8.18	3.00	68
17	3.0	0.000050	39.16	31.00	71
18	"	0.000150	30.90	22.50	70
19	"	0.000300	24.02	15.50	70
20	"	0.000600	19.04	10.60	70
21	"	0.001000	15.99	7.70	72
22	"	0.001600	13.73	5.70	72
23	"	0.003000	11.41	4.00	72
24	"	0.004500	10.07	3.10	72

TABLE 5-2 - TESTS FOR THE ROUGHNESS PARAMETER χ

A) Normal Depth Tests

Run No.	y_n cm.	Q cfs	S	$C/\sqrt{g}$	y_n/a	y_n/χ
1	8.66	3.714	0.0125	8.169	6.829	22.548
2	8.44	3.574	"	8.162	6.650	21.976
3	8.05	3.273	"	8.005	6.348	20.960
4	7.72	3.066	"	7.982	6.086	20.095
5	7.07	2.586	"	7.646	5.574	18.405
6	6.06	1.969	"	7.283	4.779	15.778

B) Velocity Profile Data (y measured from the bottom)

Q = 3.714 cfs ; y_n = 0.275 ft. ; S = 0.0125 :

y ft.	y/χ	v fps	$v/\sqrt{\tau_o/\rho}$
0.010	0.794	1.89	5.985
0.015	1.190	1.94	6.143
0.020	1.587	2.00	6.333
0.025	1.984	2.17	6.872
0.030	2.381	2.25	7.125
0.035	2.778	2.31	7.315
0.040	3.175	2.42	7.663
0.045	3.571	2.59	8.2[illegible]1
0.050	3.968	2.69	8.518
0.055	4.365	2.74	8.676
0.060	4.762	2.83	8.961
0.065	5.159	2.94	9.310
0.070	5.556	2.99	9.468
0.080	6.349	3.10	9.816
0.090	7.143	3.27	10.355
0.100	7.937	3.38	10.703
0.110	8.730	3.48	11.020
0.120	9.524	3.57	11.305
0.130	10.317	3.65	11.558
0.140	11.111	3.68	11.653
0.160	12.698	3.75	11.875
0.180	14.286	3.86	12.223
0.200	15.873	3.94	12.476
0.220	17.460	4.00	12.666
0.240	19.048	4.06	12.856

GEOMETRY I_a

TABLE 7 - 1 - 1

OBSERVED AND CALCULATED DATA

Contraction Ratio	Slope x10⁻⁶ ft/ft	Q cfs	y_o cm	y_1 max cm	y_1 min cm	R ft	$\mathbb{R} = \frac{VR}{\nu}$	Cd Appendix 2 Equation 2	f	n x10	$h_1^*/\Delta h$	$V^2/2gy_o$
0.5	0	2	23.78	24.53	22.97	.5934	25,147	.2087	----	----	.48	.0053
		3	33.97	35.18	32.97	.7688	34,213	.1962	----	----	.55	.0041
	25	2	22.88	23.70	22.03	.5762	25,377	.2190	.0128	.0957	.49	.0060
		3	32.15	33.33	31.17	.7400	34,795	.2095	.0145	.1060	.55	.0048
	50	2	22.02	22.90	21.11	.5584	25,606	.2294	.0231	.1276	.49	.0067
		3	29.83	31.10	28.60	.7017	35,565	.2282	.0236	.1341	.51	.0060
	100	2	19.86	20.90	18.73	.5160	26,188	.2607	.0347	.1544	.48	.0091
		3	21.70	23.66	20.19	.5531	38,533	.3288	.0197	.1177	.56	.0158
		4	30.73	32.73	28.82	.7167	47,008	.2892	.0288	.1489	.51	.0099
	185	3.5	20.45	23.43	17.70	.5280	50,555	.4318	.0227	.1255	.52	.0407
	250	2	12.07	14.72	9.61	.3415	28,516	.4329	.0212	.1127	.52	.0397
		3	15.94	19.45	12.14	.4319	40,959	.3807	.0208	.1161	.48	.0419
		4	18.97	23.53	13.00	.4975	52,860	.4860	.0191	.1138	.43	.0904
	350	3.5	15.40	20.51	8.34	.4197	56,385	.4803	.0194	.1115	.42	.0842
	500	2	9.25	13.57	3.50	.2704	29,459	.5026	.0197	.1046	.43	.1233
		3	12.38	18.09	7.67	.3490	42,615	.3888	.0202	.1107	.55	.0256
		4	13.24	21.45	4.04	.3696	56,270	.4685	.0138	.0920	.47	.0600
0.7	0	2	23.78	23.93	23.46	.5934	25,147	.1506	----	----	.32	.0053
		3	33.97	34.18	33.57	.7688	34,213	.1357	----	----	.34	.0041
		4	41.46	41.76	40.93	.8783	42,697	.1385	----	----	.36	.0040
	25	2	22.88	23.08	22.58	.5762	25,377	.1562	.0128	.0957	.40	.0060
		3	32.15	32.34	31.72	.7400	34,795	.1466	.0145	.1060	.31	.0048
		4	40.14	40.41	39.63	.8600	43,180	.1446	.0148	.1144	.35	.0044
	50	2	22.02	22.22	21.71	.5594	25,606	.1668	.0231	.1276	.39	.0067
		3	29.75	30.06	29.31	.7003	35,590	.1625	.0235	.1319	.41	.0075
		4	37.50	37.82	36.97	.8222	44,197	.1579	.0246	.1406	.38	.0054
	100	2	19.86	20.07	19.43	.5160	26,188	.1934	.0347	.1544	.33	.0091
		3	21.70	22.18	20.98	.5531	38,533	.2560	.0197	.1177	.40	.0158
		4	30.69	31.13	29.95	.7161	47,025	.2062	.0287	.1484	.37	.0099
	185	3.5	20.45	21.19	19.13	.5280	50,555	.3765	.0227	.1281	.36	.0407
	250	2	12.07	12.78	10.84	.3415	28,516	.3737	.0212	.1127	.37	.0397
		3	15.94	16.89	14.19	.4319	40,959	.3870	.0208	.1161	.35	.0419
		4	18.97	20.06	16.80	.4975	52,860	.4913	.0191	.1138	.33	.0904
	350	3.5	15.40	16.84	13.20	.4197	56,385	.4858	.0194	.1078	.40	.0848
	500	2	9.25	10.68	6.94	.2704	29,459	.3127	.0197	.1046	.38	.0256
		3	12.38	14.14	8.75	.3490	42,615	.4377	.0202	.1107	.33	.0600
0.9	0	3	33.97	33.99	33.81	.7688	34,213	.1038	----	----	.11	.0041
	25	2	22.85	22.86	22.79	.5756	25,385	.1233	.0128	.0955	.14	.0060
		4	40.14	40.17	39.97	.8600	43,180	.1095	.0148	.1144	.15	.0044
	50	2	22.02	22.06	21.92	.5594	25,606	.1299	.0231	.1276	.29	.0067
		3	29.75	29.78	29.65	.7003	35,590	.1257	.0235	.1319	.23	.0075
		4	37.50	37.57	37.37	.8222	44,197	.1202	.0246	.1406	.35	.0054
	100	3	21.70	21.78	21.57	.5531	38,533	.1984	.0197	.1177	.38	.0158
		4	30.73	30.78	30.51	.7167	47,008	.1597	.0288	.1489	.19	.0099
	185	3.5	20.45	23.43	20.22	.5280	50,555	.3139	.0227	.1255	.—	.0407
	250	2	12.07	12.17	11.92	.3415	28,516	.3116	.0212	.1127	.40	.0397
		3	15.94	16.05	15.68	.4319	40,959	.3239	.0208	.1161	.30	.0419
		4	18.97	18.99	18.52	.4975	52,860	.4599	.0191	.1138	.04	.0903
	350	3.5	15.40	15.56	14.96	.4197	56,385	.4490	.0194	.2855	.27	.0848
	500	2	9.25	9.42	8.87	.2704	29,459	.5282	.0197	.1046	.31	.1244
		3	12.38	12.56	11.81	.3490	42,615	.2526	.0202	.1107	.24	.0256
		4	13.20	13.66	1.21	.3867	56,295	.3808	.0137	.1006	.38	.0600

GEOMETRY I_a

TABLE 7-1-2 RAW DATA - LARGE FLUME - SMOOTH BOUNDARIES P. 1

(Semicircular Model Tests)

Run No. 1S
Q - 1 cfs
y_n - 15.64 cm.
M - b/B - 0.300
L/b - 0.0
Slope - 0.0000281
Temp. - 62F
Model Sta. - 34.39

Cent. Sta. (ft.)	Depth (cm.)
20.0	17.58
24.0	17.58
28.0	17.58
30.0	17.58
31.0	17.58
32.0	17.58
32.5	17.56
33.0	17.51
35.0	15.25
35.5	15.07
36.0	14.68
36.5	14.98
37.0	15.10

Run No. 2S
Q - 1 cfs
y_n - 9.82 cm.
M - b/B - 0.300
L/b - 0.0
Slope - 0.000119
Temp. - 63F
Model Sta. - 35.79

Cent. Sta. (ft.)	Depth (cm.)
20.0	13.78
24.0	13.78
28.0	13.77
30.0	13.78
32.0	13.78
33.0	13.78
33.5	13.78
34.0	13.75
34.5	13.70
36.5	8.10
37.0	7.79
37.5	7.87

Run No. 3S
Q - 1 cfs
y_n - 7.50 cm.
M - b/B - 0.300
L/b - 0.0
Slope - 0.000286
Temp. - 64F
Model Sta. - 35.85

Cent. Sta. (ft.)	Depth (cm.)
20.0	13.02
24.0	13.02
28.0	13.03
32.0	13.08
32.5	13.07
33.0	13.07
33.5	13.07
34.0	13.04
34.5	12.98
37.5	3.40
38.0	3.09
38.5	3.15
39.0	3.23

Run No. 4S
Q - 1 cfs
y_n - 6.10 cm.
M - b/B - 0.300
L/b - 0.0
Slope - 0.000530
Temp. - 64F
Model Sta. - 31.19

Cent. Sta. (ft.)	Depth (cm.)
20.0	12.60
24.0	12.63
26.0	12.67
27.5	12.67
28.0	12.68
28.5	12.67
29.0	12.65
29.5	12.63
30.0	12.58
34.0	1.94
35.0	1.65
35.5	1.53
36.0	1.50
36.5	1.55
37.0	1.61

Run No. 5S
Q - 1 cfs
y_n - 5.11 cm.
M - b/B - 0.300
L/b - 0.0
Slope - 0.000853
Temp. - 64F
Model Sta. - 32.24

Cent. Sta. (ft.)	Depth (cm.)
20.0	12.46
24.0	12.49
26.0	12.57
28.0	12.60
29.0	12.61
29.5	12.61
30.0	12.61
30.5	12.59
31.0	12.55
38.0	0.97
39.0	0.94
39.5	0.85
40.0	0.88
41.5	0.91

Run No. 6S
Q - 1 cfs
y_n - 4.31 cm.
M - b/B - 0.300
L/b - 0.0
Slope - 0.001260
Temp. - 66F
Model Sta. - 31.87

Cent. Sta. (ft.)	Depth (cm.)
20.0	12.29
24.0	12.40
28.0	12.57
28.5	12.57
29.0	12.59
29.5	12.60
30.0	12.59
30.5	12.54
38.0	0.92
38.5	0.92
39.0	0.90
39.5	0.85
40.0	0.87

Run No. 7S
Q - 1 cfs
y_n - 4.06 cm.
M - b/B - 0.300
L/b - 0.0
Slope - 0.001790
Temp. - 66F
Model Sta. - 34.50

Cent. Sta. (ft.)	Depth (cm.)
20.0	11.88
24.0	12.07
28.0	12.28
30.0	12.40
31.0	12.45
31.5	12.46
32.0	12.48
32.5	12.48
33.0	12.46
33.5	12.39
40.0	1.00
41.0	0.85
41.5	0.83
42.0	0.81
42.5	0.80
43.0	0.82
43.5	0.84

Run No. 8S
Q - 1 cfs
y_n - 3.60 cm.
M - b/B - 0.300
L/b - 0.0
Slope - 0.00229
Temp. - 67F
Model Sta. - 33.91

Cent. Sta. (ft.)	Depth (cm.)
20.0	11.55
24.0	11.79
28.0	12.07
30.0	12.20
31.0	12.25
31.5	12.27
32.0	12.30
32.5	12.27
33.0	12.19
41.9	0.90*

Run No. 9S
Q - 1 cfs
y_n - 3.03 cm.
M - b/B - 0.300
L/b - 0.0
Slope - 0.00308
Temp. - 67F
Model Sta. - 33.95

Cent. Sta. (ft.)	Depth (cm.)
20.0	11.27
24.0	11.62
28.0	12.00
30.0	12.19
31.0	12.26
31.5	12.30
32.0	12.33
32.5	12.32
33.0	12.26
41.77	0.90*

Run No. 10S
Q - 1 cfs
y_n - 2.89 cm.
M - b/B - 0.300
L/b - 0.0
Slope - 0.00389
Temp. - 68F
Model Sta. - 34.19

Cent. Sta. (ft.)	Depth (cm.)
20.0	10.92
24.0	11.38
28.0	11.87
30.0	12.13
31.0	12.23
31.5	12.28
32.0	12.32
32.5	12.34
33.0	12.34
33.5	12.19
42.0	0.82*

Run No. 11S
Q - 2 cfs
y_n - 38.65 cm.
M - b/B - 0.693
L/b - 0.0
Slope - 0.00000712
Temp. - 67F
Model Sta. - 34.43

Cent. Sta. (ft.)	Depth (cm.)
20.0	38.72
28.0	38.72
30.0	38.72
31.0	38.71
32.0	38.72
32.5	38.71
33.0	38.70
36.0	38.52
36.5	38.51
37.0	38.54

Run No. 12S
Q - 2 cfs
y_n - 38.65 cm.
M - b/B - 0.889
L/b - 0.0
Slope - 0.00000712
Temp. - 67F
Model Sta. - 34.10

Cent. Sta. (ft.)	Depth (cm.)
20.0	38.68
24.0	38.66
28.0	38.65
30.0	38.65
31.0	38.65
31.5	38.64
32.0	38.64
33.0	38.63
35.0	38.62
36.0	38.60
36.5	38.59
37.0	38.61

Run No. 13S
Q - 2 cfs
y_n - 25.32 cm.
M - b/B - 0.491
L/b - 0.0
Slope - 0.000025
Temp. - 66F
Model Sta. - 33.41

Cent. Sta. (ft.)	Depth (cm.)
24.0	25.94
28.0	25.95
30.0	25.94
30.5	25.94
31.0	25.93
31.5	25.90
32.0	25.88
34.0	25.10
34.5	24.90
35.0	24.86
35.5	24.82
36.0	24.84
36.5	24.85

Run No. 14S
Q - 2 cfs
y_n - 25.32 cm.
M - b/B - 0.693
L/b - 0.0
Slope - 0.000025
Temp. - 66F
Model Sta. - 33.46

Cent. Sta. (ft.)	Depth (cm.)
20.0	25.50
24.0	28.46
28.0	25.48
30.0	25.45
31.0	25.45
31.5	25.43
32.0	25.43
32.5	25.41
34.0	25.23
34.5	25.18
35.0	25.13
36.0	25.11
36.5	25.09
37.0	25.11

Run No. 15S
Q - 2 cfs
y_n - 25.32 cm.
M - b/B - 0.889
L/b - 0.0
Slope - 0.000025
Temp. - 66F
Model Sta. - 33.08

Cent. Sta. (ft.)	Depth (cm.)
20.0	25.36
24.0	25.32
28.0	25.32
30.0	25.32
31.0	25.32
32.0	25.31
32.5	25.30
34.0	25.28
35.0	25.27
36.0	25.28
37.0	25.29

Run No. 16S
Q - 2 cfs
y_n - 20.3 cm.
M - b/B - 0.491
L/b - 0.0
Slope - 0.000050
Temp. 65F
Model Sta. - 32.66

Cent. Sta. (ft.)	Depth (cm.)
20.0	21.30
24.0	21.29
26.0	21.30
28.0	21.25
29.0	21.25
30.0	21.26
30.5	21.21
31.0	21.15
34.0	19.62
35.0	19.41
35.5	19.35
36.0	19.42

Run No. 17S
Q - 2 cfs
y_n - 20.3 cm.
M - b/B - 0.693
L/b - 0.0
Slope - 0.000050
Temp. - 66F
Model Sta. - 34.35

Cent. Sta. (ft.)	Depth (cm.)
20.0	20.58
24.0	20.55
28.0	20.55
30.0	20.53
30.5	20.54
31.0	20.55
32.0	20.54
32.5	20.54
33.0	20.49
33.5	20.43
35.0	20.19
36.0	20.03
36.5	20.00
37.0	19.97
37.5	19.98
38.0	20.00

Run No. 18S
Q - 2 cfs
y_n - 20.3 cm.
M - b/B - 0.889
L/b - 0.0
Slope - 0.000050
Temp. - 66F
Model Sta. - 34.90

Cent. Sta. (ft.)	Depth (cm.)
20.0	20.38
24.0	20.33
28.0	20.34
30.0	20.34
32.0	20.34
33.0	20.34
33.5	20.33
34.0	20.33
34.5	20.31
35.5	20.26
36.0	20.25
37.0	20.25
38.0	20.26

TABLE 7-1-2 RAW DATA - LARGE FLUME - SMOOTH BOUNDARIES (continued) P. 2

(Semicircular Model Tests)

Run No. 19S
Q - 2 cfs
y_n - 16.46cm.
M - b/B - 0.491
L/b - 0.0
Slope - 0.00010
Temp. - 67F
Model Sta. - 32.42

Cent. Sta. (ft.)	Depth (cm.)
20.0	17.82
24.0	17.81
28.0	17.80
29.0	17.81
30.0	17.79
30.5	17.77
34.0	15.31
34.5	15.11

Run No. 20S
Q - 2 cfs
y_n -16.46cm.
M - b/B - 0.693
L/b - 0.0
Slope - 0.00010
Temp. - 67F
Model Sta. - 31.58

Cent. Sta. (ft.)	Depth (cm.)
20.0	16.80
24.0	16.75
28.0	16.75
29.0	16.76
29.5	16.72
30.0	16.71
32.0	16.28
33.0	16.01
34.0	15.90
34.5	15.85
35.0	15.88
35.5	15.93

Run No. 21S
Q - 2 cfs
y_n -16.46cm.
M - b/B - 0.889
L/b - 0.0
Slope - 0.00010
Temp. - 66F
Model Sta. - 33.10

Cent. Sta. (ft.)	Depth (cm.)
20.0	16.49
24.0	16.47
28.0	16.46
30.0	16.47
31.0	16.47
32.0	16.44
32.5	16.42
33.0	16.40
33.5	16.37
34.0	16.35
34.5	16.33
35.0	16.34
35.5	16.36

Run No. 22S
Q - 2 cfs
y_n - 9.71cm.
M - b/B - 0.300
L/b - 0.0
Slope - 0.000486
Temp. - 66F
Model Sta. - 33.87

Cent. Sta. (ft.)	Depth (cm.)
24.0	20.68
28.0	20.73
30.0	20.77
31.0	20.70
31.5	20.70
32.0	20.68
37.12	2.25*

Run No. 23S
Q - 2 cfs
y_n - 9.71cm.
M - b/B - 0.491
L/b - 0.0
Slope - 0.000486
Temp. - 66F
Model Sta. - 34.40

Cent. Sta. (ft.)	Depth (cm.)
20.0	13.69
24.0	13.70
28.0	13.74
30.0	13.74
31.0	13.76
32.0	13.72
31.5	13.75
37.0	4.92
37.5	4.65
38.0	4.72
38.5	4.72
39.0	5.05

Run No. 24S
Q - 2 cfs
y_n -9.71 cm.
M - b/B - 0.693
L/b - 0.0
Slope - 0.000486
Temp. - 66F
Model Sta. - 33.86

Cent. Sta. (ft.)	Depth (cm.)
20.0	10.90
24.0	10.91
28.0	10.92
30.0	10.95
30.5	10.95
31.0	10.96
31.5	10.90
32.0	10.80
36.0	8.23
36.5	8.23
37.0	8.09
37.5	8.09
38.0	8.34

Run No. 25S
Q - 2 cfs
y_n - 9.71cm.
M - b/B - 0.889
L/b - 0.0
Slope - 0.000486
Temp. - 66F
Model Sta. - 33.87

Cent. Sta. (ft.)	Depth (cm.)
20.0	9.86
24.0	9.85
28.0	9.87
30.0	9.87
31.0	9.87
31.5	9.87
32.0	9.85
32.5	9.81
35.0	9.47
36.0	9.45
37.0	9.53

Run No. 26S
Q - 2 cfs
y_n - 8.86cm.
M - b/B - 0.491
L/b - 0.0
Slope - 0.000628
Temp. - 67F
Model Sta. - 33.65

Cent. Sta. (ft.)	Depth (cm.)
24.0	13.44
28.0	13.52
30.0	13.52
31.0	13.52
31.5	13.48
32.0	13.42
37.5	3.18
38.0	3.11
38.5	2.85

Run No. 27S
Q - 2 cfs
y_n - 8.86cm.
M - b/B - 0.693
L/b - 0.0
Slope - 0.000628
Temp. - 66F
Model Sta. - 33.34

Cent. Sta. (ft.)	Depth (cm.)
24.0	10.46
28.0	10.50
30.0	10.50
30.5	10.48
31.0	10.46
36.0	6.18
36.5	6.04
37.0	6.76

Run No. 28S
Q - 2 cfs
y_n - 8.86cm.
M - b/B - 0.889
L/b - 0.0
Slope - 0.000628
Temp. - 66F
Model Sta. -33.44

Cent. Sta. (ft.)	Depth (cm.)
20.0	9.02
24.0	9.03
28.0	9.05
30.0	9.05
31.0	9.05
32.0	9.00
34.5	8.47
35.0	8.45
35.5	8.46
36.0	8.51

Run No. 29S*
Q - 2 cfs
y_n -8.29 cm.
M - b/B -0.300
L/b -0.0
Slope - 0.000779
Temp. - 66F
Model Sta. - 33.83

Cent. Sta. (ft.)	Depth (cm.)
20.0	20.65
28.0	20.77
30.0	20.77
31.0	20.83
31.5	20.83
32.0	20.81
32.5	20.73
42.15	1.15*

Run No. 30S
Q - 2 cfs
y_n -8.29 cm.
M - b/B - 0.491
L/b -0.0
Slope -0.000779
Temp. - 66F
Model Sta. - 34.17

Cent. Sta. (ft.)	Depth (cm.)
20.0	30.34
28.0	30.46
30.0	30.48
31.0	30.51
31.5	30.50
32.0	30.45
32.5	30.41
37.58	2.79*

Run No. 31S
Q - 2 cfs
y_n -8.29 cm.
M - b/B - 0.693
L/b - 0.0
Slope -0.000779
Temp. - 66F
Model Sta. -33.62

Cent. Sta. (ft.)	Depth (cm.)
20.0	10.10
28.0	10.19
30.0	10.21
30.5	10.23
31.0	10.21
31.5	10.15
36.0	5.53
36.5	5.53
37.0	5.23
37.5	5.35

Run No. 32S
Q - 2 cfs
y_n -8.29 cm.
M - b/B -0.889
L/b -0.0
Slope - 0.000779
Temp. - 66F
Model Sta. -34.85

Cent. Sta. (ft.)	Depth (cm.)
20.0	8.48
28.0	8.53
30.0	8.53
31.0	8.54
31.5	8.54
32.0	8.54
32.5	8.54
33.0	8.51
33.5	8.47
36.0	7.90
36.5	7.82
37.0	7.85

Run No. 33S
Q - 2 cfs
y_n -7.35 cm.
M - b/B - 0.300
L/b -0.0
Slope -0.00115
Temp. - 66F
Model Sta. -34.35

Cent. Sta. (ft.)	Depth (cm.)
20.0	20.55
28.0	20.79
30.0	20.85
31.0	20.87
31.5	20.88
32.0	20.88
32.5	20.84
33.0	20.78
42.63	1.18*

Run No. 34S
Q - 2 cfs
y_n -7.35 cm.
M - b/B -0.491
L/b -0.0
Slope -0.00115
Temp. - 67F
Model Sta. -34.56

Cent. Sta. (ft.)	Depth (cm.)
20.0	12.98
28.0	13.21
30.0	13.30
31.0	13.30
31.5	13.31
32.0	13.32
32.5	13.28
33.0	13.19
41.56	1.57*

Run No. 35S
Q - 2 cfs
y_n -7.35 cm.
M - b/B -0.693
L/b -0.0
Slope -0.00115
Temp. - 67F
Model Sta. - 34.23

Cent. Sta. (ft.)	Depth (cm.)
20.0	9.75
28.0	9.95
30.0	10.01
31.0	10.02
31.5	10.03
32.0	9.99
32.5	9.93
37.76	3.04*

Run No. 36S
Q - 2 cfs
y_n -7.35 cm.
M - b/B - 0.889
L/b -0.0
Slope - 0.00115
Temp. - 67F
Model Sta. -34.02

Cent. Sta. (ft.)	Depth (cm.)
20.0	7.73
28.0	7.73
30.0	7.81
30.5	7.83
31.0	7.78
31.5	7.77
35.5	6.82
36.0	6.79
36.5	6.80
37.0	7.05

TABLE 7-1-2 RAW DATA - LARGE FLUME - SMOOTH BOUNDARIES (continued) P. 3

(Semicircular Model Tests)

Run No. 37S
Q - 2 cfs
y_n - 6.77cm.
M - b/B - 0.300
L/b - 0.0
Slope - 0.00161
Temp. - 66F
Model Sta. - 34.27

Cent. Sta. (ft.)	Depth (cm.)
20.0	20.32
28.0	20.67
30.0	20.78
30.5	20.80
31.0	20.80
31.5	20.81
32.0	20.83
32.5	20.79
33.0	20.75
42.10	1.20*

Run No. 38S
Q - 2 cfs
y_n -6.77 cm.
M - b/B -0.491
L/b - 0.0
Slope - 0.00161
Temp. - 67F
Model Sta. - 34.54

Cent. Sta. (ft.)	Depth (cm.)
20.0	12.85
28.0	13.20
30.0	13.32
31.0	13.35
32.0	13.37
32.5	13.33
33.0	13.22
41.2	1.55*

Run No. 39S
Q - 2 cfs
y_n -6.77 cm.
M - b/B - 0.693
L/b -0.0
Slope - 0.00161
Temp. - 66F
Model Sta. - 34.47

Cent. Sta. (ft.)	Depth (cm.)
28.0	9.81
30.0	9.90
31.0	9.92
31.5	9.94
32.0	9.94
32.5	9.88
39.71	2.18*

Run No. 40S
Q - 2 cfs
y_n -6.77 cm.
M - b/B -0.889
L/b - 0.0
Slope - 0.00161
Temp. - 66F
Model Sta. - 34.11

Cent. Sta. (ft.)	Depth (cm.)
29.0	7.00
29.5	7.18
30.0	7.20
30.5	7.10
35.5	5.43
36.0	5.15
36.5	5.10
37.0	6.30

Run No. 41S
Q - 2 cfs
y_o -6.15 cm.
M - b/B -0.300
L/b - 0.0
Slope - 0.00216
Temp. - 66F
Model Sta. - 34.28

Cent. Sta. (ft.)	Depth (cm.)
20.0	20.07
28.0	20.54
30.0	20.68
31.0	20.72
31.5	20.73
32.0	20.75
32.5	20.75
33.0	20.68
42.22	1.18*

Run No. 42S
Q - 2 cfs
y_n -6.15 cm.
M - b/B -0.491
L/b - 0.0
Slope -0.00216
Temp. - 65F
Model Sta. - 33.82

Cent. Sta. (ft.)	Depth (cm.)
20.0	12.65
28.0	13.14
30.0	13.26
31.0	13.29
31.5	13.29
32.0	13.24
40.66	1.58*

Run No. 43S
Q - 2 cfs
y_n -6.15 cm.
M - b/B -0.693
L/b - 0.0
Slope - 0.00216
Temp. - 66F
Model Sta. - 33.82

Cent. Sta. (ft.)	Depth (cm.)
20.0	9.18
28.0	9.71
30.0	9.81
30.5	9.83
31.0	9.85
31.5	9.85
32.0	9.79
39.34	2.15*

Run No. 44S
Q - 2 cfs
y_n -6.15 cm.
M - b/B -0.889
L/b - 0.0
Slope -0.00216
Temp. - 66F
Model Sta. - 34.25

Cent. Sta. (ft.)	Depth (cm.)
20.0	6.55
28.0	6.75
30.0	6.92
30.5	7.07
31.0	7.07
31.5	7.05
32.0	7.15
32.5	7.07
33.0	7.00
33.5	6.90
37.15	4.10*

Run No. 45S
Q - 2 cfs
y_o -5.70 cm.
M - b/B -0.300
L/b - 0.0
Slope -0.00276
Temp. - 66F
Model Sta. - 34.38

Cent. Sta. (ft.)	Depth (cm.)
20.0	19.78
28.0	20.43
30.0	20.58
31.0	20.76
32.0	20.76
32.5	20.77
33.0	20.76
33.5	20.57
42.40	1.19*

Run No. 46S
Q - 2 cfs
y_n -5.70 cm.
M - b/B -0.491
L/b - 0.0
Slope - 0.00276
Temp. - 66F
Model Sta. - 33.30

Cent. Sta. (ft.)	Depth (cm.)
20.0	12.34
28.0	12.97
30.0	13.15
30.5	13.20
31.0	13.21
31.5	13.25
32.0	13.25
32.5	13.24
33.0	13.14
41.21	1.53*

Run No. 47S
Q - 2 cfs
y_n -5.70 cm.
M - b/B -0.693
L/b - 0.0
Slope - 0.00276
Temp. - 66F
Model Sta. - 34.16

Cent. Sta. (ft.)	Depth (cm.)
20.0	8.85
28.0	9.57
30.0	9.73
30.5	9.75
31.0	9.76
31.5	9.82
32.0	9.81
32.5	9.77
33.0	9.65
39.58	2.10*

Run No. 48S
Q - 2 cfs
y_n -5.70 cm.
M - b/B - 0.889
L/b -0.0
Slope -0.00276
Temp. - 66F
Model Sta. -33.81

Cent. Sta. (ft.)	Depth (cm.)
20.0	5.05
28.0	7.07
30.0	7.15
30.5	6.99
31.0	7.19
31.5	7.15
32.0	7.10
35.0	6.10
35.5	5.29
36.0	5.85

Run No. 49S
Q - 2 cfs
y_n-5.24 cm.
M - b/B -0.300
L/b -0.0
Slope - 0.003495
Temp. - 66F
Model Sta. - 33.88

Cent. Sta. (ft.)	Depth (cm.)
20.0	19.35
28.0	20.18
30.0	20.39
31.0	20.49
31.5	20.51
32.0	20.55
32.5	20.53
33.0	20.32
42.02	1.12*

Run No. 50S
Q - 2 cfs
y_n -5.24 cm.
M - b/B - 0.491
L/b -0.0
Slope - 0.003495
Temp. - 66F
Model Sta. -33.15

Cent. Sta. (ft.)	Depth (cm.)
20.0	12.02
28.0	12.91
30.0	13.06
30.5	13.11
31.0	13.12
31.5	13.11
32.0	12.98
39.77	1.55*

Run No. 51S
Q - 2 cfs
y_n -5.24 cm.
M - b/B - 0.693
L/b -0.0
Slope -0.003495
Temp. - 66F
Model Sta. -33.33

Cent. Sta. (ft.)	Depth (cm.)
20.0	8.35
28.0	9.43
30.0	9.50
30.5	9.59
31.0	9.55
31.5	9.60
32.0	9.60
32.5	9.45
38.93	2.06*

Run No. 52S
Q - 2 cfs
y_n -5.24 cm.
M - b/B - 0.889
L/b -0.0
Slope - 0.003495
Temp. - 66F
Model Sta. -33.41

Cent. Sta. (ft.)	Depth (cm.)
28.0	5.20
30.0	6.45
30.5	6.85
31.0	6.35
31.5	7.20
32.0	6.25
32.5	7.25
33.0	5.85
35.5	4.55
36.0	3.90
36.5	3.50
37.0	3.65

Run No. 53S
Q - 3 cfs
y_n -33.01cm.
M - b/B - 0.491
L/b -0.0
Slope - 0.000025
Temp. - 67F
Model Sta. -34.08

Cent. Sta. (ft.)	Depth (cm.)
20.0	34.11
24.0	34.10
28.0	34.00
30.0	34.10
31.0	34.09
31.5	34.07
32.0	34.04
32.5	33.99
35.0	32.41
35.5	32.20
36.0	33.41

Run No. 54S
Q - 3 cfs
y_n -33.01cm.
M - b/B -0.693
L/b -0.0
Slope -0.000025
Temp. - 68F
Model Sta. -34.10

Cent. Sta. (ft.)	Depth (cm.)
20.0	33.07
24.0	33.05
28.0	33.06
30.0	33.06
31.0	33.05
31.5	33.05
32.0	33.06
32.5	33.03
33.0	33.02
35.0	32.96
36.0	32.97
36.5	32.95
37.0	32.94
37.5	32.98
38.0	33.00

TABLE 7-1-2 RAW DATA - LARGE FLUME - SMOOTH BOUNDARIES (continued) P.4

(Semicircular Model Tests)

Run No. 55S	Run No. 56S	Run No. 57S	Run No. 58S	Run No. 59S	Run No. 60S	Run No. 61S
Q - 3 cfs	Q - 3 cfs	Q - 3 cfs	Q - 3 cfs	Q - 3.5 cfs	Q - 3.5 cfs	Q - 3.5 cfs
y_n - 33.01cm.	y_n - 29.65cm.	y_n - 29.65cm.	y_n - 29.65cm.	y_n - 19.44cm.	y_n - 19.44cm.	y_n - 19.44cm.
M - b/B - 0.889	M - b/B - 0.491	M - b/B - 0.693	M - b/B - 0.889	M - b/B - 0.491	M - b/B - 0.693	M - b/B - 0.889
L/b - 0.0	L/b - 0.0	L/b - 0.0	L/b - 0.0	L/b - 0.0	L/b - 0.0	L/b - 0.0
Slope - 0.000025	Slope - 0.000050	Slope - 0.000050	Slope - 0.000050	Slope - 0.000185	Slope - 0.000185	Slope - 0.000185
Temp. - 67F	Temp. - 68F	Temp. - 68F	Temp. - 68F	Temp. - 70F	Temp. - 65F	Temp. - 70F
Model Sta. - 34.20	Model Sta. - 34.07	Model Sta. - 33.82	Model Sta. - 33.98	Model Sta. - 34.17	Model Sta. - 34.56	Model Sta. - 33.04

Cent. Sta. (ft.)	Depth (cm.)	Cent. Sta. (ft.)	Depth (cm.)	Cent. Sta. (ft.)	Depth (cm.)	Cent. Sta. (ft.)	Depth (cm.)	Cent. Sta. (ft.)	Depth (cm.)	Cent. Sta. (ft.)	Depth (cm.)	Cent. Sta. (ft.)	Depth (cm.)
20.0	33.09	20.0	30.87	20.0	29.93	20.0	29.69	20.0	22.70	20.0	20.27	20.0	19.58
24.0	33.06	24.0	30.87	24.0	29.91	24.0	29.67	24.0	22.68	24.0	20.27	24.0	19.56
28.0	33.06	28.0	30.87	28.0	29.91	28.0	29.66	28.0	22.75	28.0	20.27	28.0	19.55
30.0	33.06	30.0	30.90	30.0	29.91	30.0	29.66	30.0	22.71	30.0	20.27	30.0	19.53
31.0	33.06	30.5	30.89	30.5	29.90	31.0	29.66	31.0	22.72	31.0	20.26	31.0	19.54
31.5	33.04	31.0	30.85	31.0	29.89	32.0	29.66	31.5	22.66	32.0	20.24	31.5	19.50
32.0	33.05	31.5	30.80	32.0	29.87	32.5	29.64	32.0	22.62	36.0	18.35	32.0	19.49
32.5	33.02	35.0	28.82	35.0	29.34	33.0	29.64	35.0	17.35	36.5	18.16	34.5	19.26
35.0	32.98	36.0	28.65	36.0	29.23	33.5	29.61	35.5	15.92	37.0	18.13	35.0	19.25
36.0	32.97	37.0	28.53	36.5	29.23	35.0	29.53	36.0	16.53	37.5	18.28	35.5	19.29
37.0	32.96	37.5	28.56	37.0	29.26	35.5	29.52						
37.5	32.97	38.0	28.60			36.0	29.53						
38.0	33.00												

*Only the minimum depth was measured on the downstream side of the model.

GEOMETRY I_a

TABLE 7-1-3 CALCULATIONS FOR THE LARGE FLUME SMOOTH BOUNDARY MODEL TESTS

Measured Data

Calculated Data

1 Run No.	2 L/b	3 M	4 S_n	5 Q (cfs)	6 y_n (cm.)	7 y_1 (cm.)	8 y_3 (cm.)	9 ν x 10^5	10 y_1 Sta. (ft.)	11 y_3 Sta. (ft.)	12 Mod. Sta. (ft.)	13 R (ft.)	14 F_n	15 R_e	16 f	17 M'	18 C_d	19 y_1/y_n	20 $(F_n/M')^{2/3}$	21 h_1^* (ft.)	22 $y_1 - y_3$ (ft.)	23 L_{1-2} (ft.)	24 L_{1-3} (ft.)
1S	0.0	0.300	0.0000281	1.0	15.64	17.58	14.68	1.19	32.00	36.00	34.39	0.4244	0.0977	14,151	0.0195	0.273	0.2984	1.124	0.504	0.0637	0.0952	2.39	4.00
2S	"	"	0.000119	"	9.82	13.78	7.79	1.17	33.50	37.00	35.79	0.2848	0.1963	15,385	0.0128	0.290	0.4143	1.403	0.771	0.1299	0.1965	2.29	3.50
3S	"	"	0.000286	"	7.50	13.07	3.09	1.15	33.50	38.00	35.85	0.2237	0.2941	16,096	0.0241	0.295	0.4460	1.742	1.000	0.1827	0.3274	2.35	4.50
4S	"	"	0.000530	"	6.10	12.68	1.50	1.15	28.00	36.00	31.19	0.1850	0.4011	16,374	0.0244	0.296	0.4648	2.079	1.227	0.2159	0.3668	3.19	8.00
5S	"	"	0.000853	"	5.11	12.61	0.85	1.15	30.00	39.50	32.24	0.1570	0.5226	16,583	0.0235	0.298	0.4680	2.465	1.454	0.2458	0.3856	2.24	9.50
6S	"	"	0.001260	"	4.31	12.60	0.85	1.11	29.50	39.50	31.87	0.1337	0.6752	17,351	0.0209	0.298	0.4675	2.924	1.726	0.2720	0.3855	2.37	10.50
7S	"	"	0.001790	"	4.06	12.48	0.80	1.11	32.50	42.50	34.50	0.1263	0.7383	17,396	0.0249	0.299	0.4821	3.084	1.826	0.2776	0.3846	2.00	10.50
8S	"	"	0.002290	"	3.60	12.30	0.90	1.10	32.00	41.90	33.91	0.1277	0.8846	17,673	0.0223	0.299	0.4832	3.434	2.001	0.2874	0.3743	1.91	9.90
9S	"	"	0.003080	"	3.03	12.30	0.90	1.10	31.50	41.77	33.95	0.0955	1.1455	17,779	0.0180	0.299	0.4839	4.077	2.446	0.3058	0.3740	2.45	10.27
10S	"	"	0.003890	"	2.89	12.34	0.82	1.09	33.00	42.00	34.19	0.0913	1.2301	17,991	0.0198	0.299	0.4810	4.288	2.534	0.3117	0.3773	1.19	9.00
11S	"	0.693	0.00000712	2.0	38.65	38.72	38.51	1.10	32.00	36.50	34.43	0.8360	0.0502	24,440	0.0149	0.629	0.0776	1.001	0.185	0.0010	0.0070	2.43	4.50
12S	"	0.889	0.00000712	"	38.65	38.65	38.52	1.10	31.00	36.50	34.10	0.8360	0.0502	24,440	0.0149	0.849	0.0582	1.000	0.152	0.0000	0.0010	3.10	5.50
13S	"	0.491	0.000025	"	25.32	25.94	24.82	1.11	30.50	35.50	33.41	0.6207	0.0948	27,423	0.0166	0.458	0.1945	1.024	0.350	0.0203	0.0367	2.91	5.00
14S	"	0.693	0.000025	"	25.32	25.45	25.11	1.11	31.00	36.00	33.46	0.6207	0.0948	27,423	0.0166	0.673	0.1384	1.005	0.271	0.0043	0.0112	2.64	5.00
15S	"	0.889	0.000025	"	25.32	25.32	25.27	1.11	31.00	35.00	33.08	0.6207	0.0948	27,423	0.0166	0.879	0.1071	1.000	0.226	0.0000	0.0016	2.08	4.00
16S	"	0.491	0.000050	"	20.30	21.26	19.41	1.13	30.00	35.00	32.66	0.5239	0.1321	28,354	0.0180	0.475	0.2573	1.047	0.427	0.0315	0.0607	2.66	5.00
17S	"	0.693	0.000050	"	20.30	20.54	19.97	1.11	32.50	37.00	34.35	0.5239	0.1321	28,865	0.0180	0.583	0.1889	1.012	0.334	0.0079	0.0187	1.85	4.50
18S	"	0.889	0.000050	"	20.30	20.34	20.25	1.11	32.00	36.50	34.90	0.5239	0.1321	28,865	0.0180	0.887	0.1478	1.002	0.281	0.0013	0.0029	1.90	3.50
19S	"	0.491	0.000100	"	16.46	17.81	15.11	1.10	29.00	34.50	32.42	0.4426	0.1809	30,350	0.0200	0.489	0.3309	1.082	0.516	0.0443	0.0886	3.42	5.50
20S	"	0.693	0.000100	"	16.46	16.76	15.85	1.10	29.00	34.50	31.58	0.4426	0.1809	30,350	0.0200	0.692	0.2544	1.018	0.410	0.0099	0.0299	2.58	5.50
21S	"	0.889	0.000100	"	16.46	16.47	16.33	1.11	31.00	34.50	33.10	0.4426	0.1809	30,080	0.0200	0.891	0.2022	1.000	0.345	0.0000	0.0042	2.10	3.50
22S	"	0.300	0.000486	"	9.71	20.77	2.25	1.11	30.00	37.12	33.87	0.2825	0.3990	33,550	0.4305	0.290	0.4845	2.135	1.237	0.3615	0.6062	3.87	7.12
23S	"	0.491	0.000486	"	9.71	13.76	4.65	1.11	31.00	37.50	34.40	0.2825	0.3990	33,550	0.4305	0.494	0.4810	1.415	0.867	0.1325	0.2984	3.40	6.50
24S	"	0.693	0.000486	"	9.71	10.96	8.05	1.11	31.00	37.25	33.86	0.2825	0.3990	33,550	0.4305	0.695	0.4770	1.128	0.692	0.0405	0.0950	2.86	6.25
25S	"	0.889	0.000486	"	9.71	9.87	9.45	1.11	31.50	36.00	33.87	0.2825	0.3990	33,550	0.4305	0.897	0.4325	1.017	0.582	0.0055	0.0140	2.37	4.50
26S	"	0.491	0.000628	"	8.86	13.52	2.85	1.10	31.00	38.50	33.65	0.2605	0.4590	33,200	0.4080	0.495	0.4950	1.526	0.951	0.1535	0.3505	2.65	7.50
27S	"	0.693	0.000628	"	8.86	10.50	6.04	1.11	30.00	36.50	33.34	0.2605	0.4590	32,900	0.4080	0.696	0.5095	1.186	0.757	0.0535	0.1787	3.34	6.50
28S	"	0.889	0.000628	"	8.86	9.05	8.45	1.11	31.00	35.00	33.44	0.2605	0.4590	32,900	0.4080	0.897	0.5050	1.020	0.640	0.0062	0.0197	2.44	4.00
29S	"	0.300	0.000779	"	8.29	20.83	1.15	1.11	31.50	42.15	33.83	0.2450	0.5060	33,000	0.3915	0.293	0.4820	2.515	0.695	0.4110	0.6453	2.33	10.65
30S	"	0.491	0.000779	"	8.29	13.51	2.79	1.11	31.00	37.58	34.17	0.2450	0.5060	33,350	0.3915	0.496	0.4930	1.631	1.014	0.1775	0.3520	3.17	6.58
31S	"	0.693	0.000779	"	8.29	10.23	5.23	1.11	30.50	37.00	33.62	0.2450	0.5060	33,650	0.3915	0.697	0.5275	1.238	0.815	0.0637	0.1641	3.12	6.50
32S	"	0.889	0.000779	"	8.29	8.54	7.82	1.11	32.50	36.50	34.85	0.2450	0.5060	33,650	0.3915	0.897	0.5380	1.030	0.682	0.0080	0.0235	2.35	4.00
33S	"	0.300	0.001150	"	7.35	20.88	1.18	1.11	32.00	42.63	34.35	0.2195	0.6050	33,650	0.3635	0.294	0.4800	2.841	1.619	0.4440	0.6463	2.35	10.63
34S	"	0.491	0.001150	"	7.35	13.32	1.57	1.10	32.00	41.56	34.56	0.2195	0.6050	33,700	0.3635	0.496	0.5025	1.811	1.114	0.1960	0.3855	2.56	9.56
35S	"	0.693	0.001150	"	7.35	10.03	3.04	1.10	31.50	37.76	34.23	0.2195	0.6050	33,950	0.3635	0.698	0.5440	1.365	0.901	0.0880	0.2293	2.73	6.26
36S	"	0.889	0.001150	"	7.35	7.83	6.79	1.10	30.50	36.00	34.02	0.2195	0.6050	33,700	0.3635	0.898	0.6110	1.066	0.769	0.1555	0.0340	3.52	5.50
37S	"	0.300	0.001610	"	6.77	20.83	1.20	1.11	32.00	42.10	34.27	0.2040	0.6870	33,700	0.3465	0.295	0.3798	3.080	1.758	0.4608	0.6437	2.27	10.10
38S	"	0.491	0.001610	"	6.77	13.37	1.55	1.10	32.00	41.20	34.54	0.2040	0.6870	33,900	0.3465	0.497	0.4980	1.972	1.241	0.2163	0.3877	2.54	9.20
39S	"	0.693	0.001610	"	6.77	9.94	2.18	1.11	32.00	39.71	34.46	0.2040	0.6870	33,300	0.3465	0.698	0.5530	1.467	0.990	0.1038	0.2545	2.47	7.71
40S	"	0.889	0.001610	"	6.77	7.20	5.10	1.11	30.00	36.50	34.11	0.2040	0.6870	33,900	0.3465	0.098	0.6970	1.061	0.837	0.0140	0.0692	4.11	6.50
41S	"	0.300	0.002160	"	6.15	20.75	1.18	1.11	32.50	42.22	34.28	0.1862	0.7930	34,050	0.3362	0.296	0.4860	3.370	1.931	0.4783	0.6413	1.78	9.72
42S	"	0.491	0.002160	"	6.15	13.29	1.58	1.13	31.50	40.66	33.82	0.1862	0.7930	34,050	0.3362	0.498	0.5075	2.160	1.363	0.2338	0.3837	2.32	9.16
43S	"	0.693	0.002160	"	6.15	9.85	2.15	1.11	31.50	39.34	33.82	0.1862	0.7930	34,050	0.3362	0.698	0.5595	1.601	1.089	0.2123	0.2524	2.32	7.84
44S	"	0.889	0.002160	"	6.15	7.07	4.10	1.11	32.50	37.15	34.25	0.1862	0.7930	34,050	0.3362	0.898	0.7150	1.149	0.921	0.0303	0.0975	1.75	4.65
45S	"	0.300	0.002760	"	5.70	20.77	1.19	1.11	32.50	42.40	34.38	0.1740	0.8890	34,300	0.3115	0.296	0.4855	3.640	2.081	0.4935	0.6415	1.88	9.90
46S	"	0.491	0.002760	"	5.70	13.25	1.53	1.11	32.00	41.21	33.30	0.1740	0.8890	34,300	0.3115	0.498	0.5090	2.322	1.470	0.2475	0.3843	2.30	9.21
47S	"	0.693	0.002760	"	5.70	9.82	2.10	1.11	31.50	39.56	34.16	0.1740	0.8890	34,300	0.3115	0.698	0.5630	1.722	1.174	0.1352	0.2533	2.66	8.08
48S	"	0.889	0.002760	"	5.70	7.19	5.29	1.11	31.00	35.50	33.81	0.1740	0.8890	34,300	0.3115	0.898	0.6980	1.260	1.000	0.0488	0.0623	2.81	4.50
49S	"	0.300	0.003495	"	5.24	20.55	1.12	1.11	32.00	42.02	33.88	0.1607	1.0090	34,300	0.2960	0.297	0.4905	3.920	2.362	0.5021	0.6373	1.88	10.02
50S	"	0.491	0.003495	"	5.24	13.12	1.55	1.11	31.00	39.77	33.15	0.1607	1.0090	34,300	0.2960	0.499	0.5150	2.505	1.599	0.2586	0.3797	2.15	8.77
51S	"	0.693	0.003495	"	5.24	9.60	2.06	1.11	32.00	38.93	33.33	0.1607	1.0090	34,300	0.2960	0.699	0.5830	1.832	1.276	0.1431	0.2474	1.33	6.93
52S	"	0.889	0.003495	"	5.24	7.25	3.50	1.11	32.50	36.50	33.41	0.1607	1.0090	34,300	0.2960	0.899	0.6880	1.385	1.086	0.0659	0.1230	0.91	4.00
53S	"	0.491	0.000025	3.0	33.01	34.10	32.20	1.10	30.00	35.50	34.08	0.7515	0.0955	38,555	0.0152	0.424	0.2062	1.0331	0.380	0.0358	0.0624	4.08	5.50
54S	"	0.693	0.000025	"	33.01	33.06	32.94	1.09	32.00	37.00	34.10	0.7515	0.0955	38,908	0.0152	0.650	0.1437	1.002	0.279	0.0016	0.0032	2.10	5.00
55S	"	0.889	0.000025	"	33.01	33.06	32.96	1.10	31.00	37.00	34.20	0.7515	0.0955	38,555	0.0152	0.864	0.1092	1.002	0.230	0.0016	0.0032	3.20	6.00
56S	"	0.491	0.000050	"	29.65	30.90	28.53	1.09	30.00	37.00	34.07	0.6967	0.1123	40,111	0.0227	0.440	0.2332	1.042	0.402	0.0411	0.0778	4.07	7.00
57S	"	0.693	0.000050	"	29.65	29.91	29.23	1.09	30.00	36.00	33.82	0.6967	0.1123	40,111	0.0227	0.662	0.1648	1.011	0.306	0.0086	0.0223	3.82	6.00
58S	"	0.889	0.000050	"	29.65	29.66	29.52	1.09	32.00	35.50	33.98	0.6967	0.1123	40,111	0.0227	0.871	0.1278	1.000	0.255	0.0004	0.0046	1.98	3.50
59S	"	0.491	0.000185	3.5	19.44	22.72	15.92	1.07	31.00	35.50	34.17	0.5062	0.2467	52,878	0.0193	0.477	0.4109	1.168	0.646	0.1073	0.2227	3.17	4.50
60S	"	0.693	0.000185	"	19.44	20.27	18.13	1.13	30.00	37.00	34.56	0.5062	0.2467	50,071	0.0193	0.684	0.3370	1.043	0.508	0.0273	0.0702	4.56	7.00
61S	"	0.889	0.000185	"	19.44	19.54	19.25	1.07	31.00	35.00	33.04	0.5062	0.2467	52,878	0.0193	0.887	0.2745	1.005	0.427	0.0034	0.0095	2.04	4.00

GEOMETRY I_a AND I_b

TABLE 7-2-1 RAW DATA - LARGE FLUME - ROUGH BOUNDARIES P. 1

(Two and Three Dimensional Semicircular Model Tests)

Run No. 1-1
Q - 1 cfs
y_n - 24.32cm.
M - b/B - 0.300
L/b - 0.0
Slope - 0.0000302
Temp. - 64F
Model Sta. - 30.00

Cent. Sta. (ft.)	Depth (cm.)
Submerged	

Run No. 1-2
Q - 1 cfs
y_n -24.32cm.
M - b/B - 0.311
L/b - 0.5
Slope - 0.0000302
Temp. - 64F
Model Sta. - 30.00

Cent. Sta. (ft.)	Depth (cm.)
Submerged	

Run No. 1-3
Q - 1 cfs
y_n -24.32 cm.
M - b/B - 0.311
L/b - 1.0
Slope - 0.0000302
Temp. - 64F
Model Sta. - 30.00

Cent. Sta. (ft.)	Depth (cm.)
Submerged	

Run No. 1-4***
Q - 1 cfs
y_n -24.32 cm.
M - b/B - 0.491
L/b - 0.0
Slope - 0.0000302
Temp. - 64F
Model Sta. - 30.00

Cent. Sta. (ft.)	Depth (cm.)
20.0	24.56
24.0	24.53
25.0	24.54
26.0	24.54
27.0	24.53
28.0	24.53
28.5	24.52
29.0	24.50
29.5	24.46

Run No. 1-5**
Q - 1 cfs
y_n -24.52 cm.
M - b/B - 0.500
L/b - 0.5
Slope - 0.0000302
Temp. - 68F
Model Sta. - 30.00

Cent. Sta. (ft.)	Depth (cm.)
20.0	24.69
24.0	24.66
25.0	24.66
26.0	24.67
26.5	24.67
27.5	24.65
28.0	24.65
28.5	24.64
29.0	24.62
29.5	24.59

Run No. 1-6**
Q - 1 cfs
y_n -24.52 cm.
M - b/B - 0.500
L/b - 1.0
Slope - 0.0000302
Temp. - 68F
Model Sta. - 30.00

Cent. Sta. (ft.)	Depth (cm.)
20.0	24.67
24.0	24.63
25.0	24.65
25.5	24.65
26.0	24.68
26.5	24.70
27.5	24.66
28.0	24.64
28.5	24.63
29.0	24.61
29.5	24.59

Run No. 1-7**
Q - 1 cfs
y_n -24.52 cm.
M - b/B - 0.693
L/b - 0.0
Slope - 0.0000302
Temp. - 68F
Model Sta. - 30.00

Cent. Sta. (ft.)	Depth (cm.)
20.0	24.59
24.0	24.57
25.0	24.58
26.0	24.58
26.5	24.58
27.5	24.56
28.0	24.56
28.5	24.55
29.0	24.54
29.5	24.53

Run No. 1-8**
Q - 1 cfs
y_n - 24.52cm.
M - b/B - 0.700
L/b - 0.5
Slope - 0.0000302
Temp. - 68F
Model Sta. - 30.00

Cent. Sta. (ft.)	Depth (cm.)
20.0	24.62
24.0	24.58
25.0	24.59
25.5	24.58
26.0	24.59
26.5	24.59
27.5	24.57
28.0	24.57
28.5	24.57
29.0	24.56
29.5	24.55

Run No. 1-9**
Q - 1 cfs
y_n -24.52 cm.
M - b/B - 0.700
L/b - 1.0
Slope - 0.0000302
Temp. - 68F
Model Sta. - 30.00

Cent. Sta. (ft.)	Depth (cm.)
20.0	24.62
24.0	24.58
25.0	24.59
25.5	24.59
26.0	24.59
26.5	24.59
27.5	24.58
28.0	24.58
28.5	24.58
29.0	24.57
29.5	24.56

Run No. 1-10**
Q - 1 cfs
y_n -24.52cm.
M - b/B - 0.889
L/b - 0.0
Slope - 0.0000302
Temp. - 68F
Model Sta. - 30.00

Cent. Sta. (ft.)	Depth (cm.)
20.0	24.57
24.0	24.54
25.0	24.55
26.0	24.55
26.5	24.56
27.5	24.53
28.0	24.52
28.5	24.53
29.0	24.52
29.5	24.53

Run No. 1-11**
Q - 1 cfs
y_n - 24.52cm.
M - b/B - 0.900
L/b - 0.5
Slope - 0.0000302
Temp. - 68F
Model Sta. - 30.00

Cent. Sta. (ft.)	Depth (cm.)
20.0	24.61
24.0	24.57
25.0	24.57
25.5	24.57
26.0	24.58
26.5	24.58
27.5	24.57
28.0	24.58
28.5	24.57
29.0	24.56
29.5	24.56

Run No. 1-12**
Q - 1 cfs
y_n -24.52cm.
M - b/B - 0.900
L/b - 1.0
Slope - 0.0000302
Temp. - 68F
Model Sta. - 30.00

Cent. Sta. (ft.)	Depth (cm.)
20.0	24.62
24.0	24.57
25.0	24.60
25.5	24.58
26.0	24.60
26.5	24.60
27.5	24.59
28.0	24.59
28.5	24.58
29.0	24.57
29.5	24.56

Run No. 2-1
Q - 2 cfs
y_n -24.09 cm.
M - b/B - 0.300
L/b - 0.0
Slope - 0.000131
Temp. - 68F
Model Sta. - 30.00

Cent. Sta. (ft.)	Depth (cm.)
Submerged	

Run No. 2-2
Q - 2 cfs
y_n -24.09cm.
M - b/B - 0.311
L/b - 0.5
Slope - 0.000131
Temp. - 68F
Model Sta. - 30.00

Cent. Sta. (ft.)	Depth (cm.)
Submerged	

Run No. 2-3
Q - 2 cfs
y_n -24.09cm.
M - b/B - 0.311
L/b - 1.0
Slope - 0.000131
Temp. - 68F
Model Sta. - 30.00

Cent. Sta. (ft.)	Depth (cm.)
Submerged	

Run No. 2-4
Q - 2 cfs
y_n -24.09cm.
M - b/B - 0.491
L/b - 0.0
Slope - 0.000131
Temp. - 68F
Model Sta. - 30.00

Cent. Sta. (ft.)	Depth (cm.)
20.0	24.90
24.0	24.87
25.0	24.87
26.0	24.90
26.5	24.90
27.5	24.90
28.0	24.85
28.5	24.80
32.51	23.65*

Run No. 2-5
Q - 2 cfs
y_n -24.09cm.
M - b/B - 0.500
L/b - 0.5
Slope - 0.000131
Temp. - 68F
Model Sta. - 30.00

Cent. Sta. (ft.)	Depth (cm.)
20.0	24.58
24.0	24.56
25.0	24.57
26.0	24.58
26.5	24.58
27.5	24.57
28.0	24.53
28.5	24.49
31.5	23.80
32.0	23.81
32.5	23.77
33.0	23.81
33.5	23.82

Run No. 2-6
Q - 2 cfs
y_n -24.07cm.
M - b/B - 0.500
L/b - 1.0
Slope - 0.000131
Temp. - 68F
Model Sta. - 30.00

Cent. Sta. (ft.)	Depth (cm.)
24.0	24.49
25.0	24.49
26.0	24.50
26.5	24.49
27.5	24.47
28.0	24.45
28.5	24.42
29.0	24.39
33.0	23.76
33.5	23.74
34.0	23.77

TABLE 7-2-1 RAW DATA - LARGE FLUME - ROUGH BOUNDARIES (continued) P.2

(Two and Three Dimensional Semicircular Model Tests)

Run No. 2-7***
Q - 2 cfs
y_n - 24.09cm.
M - b/B - 0.693
L/b - 0.0
Slope - 0.000131
Temp. - 74F
Model Sta. - 30.00

Cent. Sta. (ft.)	Depth (cm.)
20.0	24.29
24.0	24.27
25.0	24.28
26.0	24.31
26.5	24.27
27.5	24.27
28.0	24.26
28.5	24.22
30.5	24.02
31.0	23.96
31.5	23.95
32.0	23.93
32.5	23.92
33.0	23.91
33.5	23.92
34.0	23.94

Run No. 2-8
Q - 2 cfs
y_n -24.07cm.
M - b/B - 0.700
L/b - 0.5
Slope - 0.000131
Temp. - 70F
Model Sta. - 30.00

Cent. Sta. (ft.)	Depth (cm.)
20.0	24.14
24.0	24.13
25.0	24.13
26.0	24.13
26.5	24.10
27.5	24.10
28.0	24.08
32.0	23.91
32.5	23.90
33.0	23.93

Run No. 2-9
Q - 2 cfs
y_n -24.07 cm.
M - b/B - 0.700
L/b - 1.0
Slope - 0.000131
Temp. - 70F
Model Sta. - 30.00

Cent. Sta. (ft.)	Depth (cm.)
24.0	24.12
25.0	24.13
26.0	24.15
26.5	24.13
27.5	24.12
28.0	24.10
28.5	24.08
29.0	24.07
32.5	23.93
33.0	23.91
33.5	23.90
34.0	23.91
34.5	23.91
35.0	23.92

Run No. 2-10
Q - 2 cfs
y_n -24.09 cm.
M - b/B - 0.889
L/b - 0.0
Slope - 0.000131
Temp. - 73F
Model Sta. - 30.00

Cent. Sta. (ft.)	Depth (cm.)
20.0	24.12
24.0	24.10
25.0	24.11
26.0	24.13
26.5	24.11
27.5	24.10
28.0	24.09
28.5	24.08
30.5	24.09
31.0	24.06
31.5	24.07
32.0	24.07
32.5	24.08

Run No. 2-11
Q - 2 cfs
y_o -24.07 cm.
M - b/B - 0.900
L/b - 0.5
Slope - 0.000131
Temp. - 70F
Model Sta. - 30.00

Cent. Sta. (ft.)	Depth (cm.)
20.0	24.09
24.0	24.05
25.0	24.06
26.0	24.08
26.5	24.08
27.5	24.08
28.0	24.07
28.5	24.06
32.5	24.06
33.0	24.05
33.5	24.06
34.0	24.07

Run No. 2-12
Q - 2 cfs
y_n -24.07 cm.
M - b/B - 0.900
L/b - 1.0
Slope - 0.000131
Temp. - 70F
Model Sta. - 30.00

Cent. Sta. (ft.)	Depth (cm.)
24.0	24.10
25.0	24.09
26.0	24.11
26.5	24.09
27.5	24.09
28.0	24.09
28.5	24.08
29.0	24.07
34.0	24.05
34.5	24.04
35.0	24.05
35.5	24.07
36.0	24.06

Run No. 3-1
Q - 3 cfs
y_n -24.05cm.
M - b/B - 0.300
L/b - 0.0
Slope - 0.000289
Temp. - 76F
Model Sta. - 30.00

Cent. Sta. (ft.)	Depth (cm.)
Submerged	

Run No. 3-2
Q - 3 cfs
y_n -24.05cm.
M - b/B - 0.311
L/b - 0.5
Slope - 0.000289
Temp. - 76F
Model Sta. - 30.00

Cent. Sta. (ft.)	Depth (cm.)
Submerged	

Run No. 3-3
Q - 3 cfs
y_n -24.05cm.
M - b/B - 0.311
L/b - 1.0
Slope - 0.000289
Temp. - 76F
Model Sta. - 30.00

Cent. Sta. (ft.)	Depth (cm.)
Submerged	

Run No. 3-4
Q - 3 cfs
y_n -24.05cm.
M - b/B - 0.491
L/b - 0.0
Slope - 0.000289
Temp. - 76F
Model Sta. - 30.00

Cent. Sta. (ft.)	Depth (cm.)
20.0	25.87
24.0	25.86
25.0	25.87
26.0	25.87
26.5	25.87
27.5	25.83
28.0	25.78
28.5	25.69
32.07	22.97*

Run No. 3-5
Q - 3 cfs
y_n -24.05cm.
M - b/B - 0.500
L/b - 0.5
Slope - 0.000289
Temp. - 72F
Model Sta. - 30.00

Cent. Sta. (ft.)	Depth (cm.)
20.0	25.33
24.0	25.33
25.0	25.36
26.0	25.35
26.5	25.35
27.5	25.32
28.0	25.26
28.5	25.18
32.33	23.23*

Run No. 3-6
Q - 3 cfs
y_n -24.05cm.
M - b/B - 0.500
L/b - 1.0
Slope - 0.000289
Temp. - 72F
Model Sta. - 30.00

Cent. Sta. (ft.)	Depth (cm.)
24.0	25.12
25.0	25.15
26.0	25.14
26.5	25.12
27.5	25.12
28.0	25.05
29.0	24.87
32.77	23.20*

Run No 3-7
Q - 3 cfs
y_n -24.05 cm.
M - b/B - 0.693
L/b - 0.0
Slope - 0.000289
Temp. - 76F
Model Sta. - 30.00

Cent. Sta. (ft.)	Depth (cm.)
20.0	24.43
24.0	24.44
25.0	24.45
26.0	24.46
26.5	24.46
27.5	24.44
28.0	24.40
30.5	23.91
31.0	23.75
31.5	23.64
32.0	23.59
32.5	23.58
33.0	23.57
33.5	23.58
34.0	23.59

Run No. 3-8
Q - 3 cfs
y_n -24.05cm.
M - b/B - 0.700
L/b - 0.5
Slope - 0.000289
Temp. - 73F
Model Sta. - 30.00

Cent. Sta. (ft.)	Depth (cm.)
20.0	24.32
24.0	24.32
25.0	24.31
26.0	24.32
26.5	24.32
27.5	24.29
28.0	24.28
28.5	24.27
32.31	23.75*

Run No. 3-9
Q - 3 cfs
y_n -24.05cm.
M - b/B - 0.700
L/b - 1.0
Slope - 0.000289
Temp. - 73F
Model Sta. - 30.00

Cent. Sta. (ft.)	Depth (cm.)
24.0	24.33
25.0	24.35
26.0	24.38
26.0	24.38
26.5	24.34
27.5	24.31
28.0	24.30
29.0	24.23
33.80	23.80*

Run No 3-10
Q - 3 cfs
y_n -24.05cm.
M - b/B - 0.889
L/b - 0.0
Slope - 0.000289
Temp. - 76F
Model Sta. - 30.00

Cent. Sta. (ft.)	Depth (cm.)
20.0	24.12
24.0	24.09
25.0	24.09
26.0	24.10
26.5	24.10
27.5	24.09
28.0	24.08
28.5	24.06
31.0	23.99
31.5	23.98
32.0	24.00

Run No. 3-11
Q - 3 cfs
y_n -24.05cm.
M - b/B - 0.900
L/b - 0.5
Slope - 0.000289
Temp. - 73F
Model Sta. - 30.00

Cent. Sta. (ft.)	Depth (cm.)
20.0	24.15
24.0	24.13
25.0	24.13
26.0	24.13
26.5	24.13
27.5	24.11
28.0	24.11
28.5	24.09
32.5	24.04
32.75	24.03
33.0	24.04
33.5	24.05

Run No. 3-12
Q - 3 cfs
y_n -24.05cm.
M - b/B - 0.900
L/b - 1.0
Slope - 0.000289
Temp. - 74F
Model Sta. - 30.00

Cent. Sta. (ft.)	Depth (cm.)
25.0	24.13
26.0	24.13
26.5	24.13
27.5	24.12
28.0	24.09
29.0	24.07
34.54	24.01*

TABLE 7-2-1 RAW DATA - LARGE FLUME - ROUGH BOUNDARIES (continued) P. 3

(Two and Three Dimensional Semicircular Model Tests)

Run No. 4-1**
Q - 1 cfs
y_n - 9.64 cm.
M - b/B - 0.300
L/b - 0.0
Slope - 0.000584
Temp. - 68F
Model Sta. - 30.00

Cent. Sta. (ft.)	Depth (cm.)
20.0	13.70
24.0	13.72
25.0	13.75
25.5	13.75
26.0	13.75
26.5	13.75
27.5	13.74
28.0	13.72
28.5	13.69
29.0	13.61
29.5	13.32

Run No. 4-2**
Q - 1 cfs
y_n - 9.64 cm.
M - b/B - 0.311
L/b - 0.5
Slope - 0.000584
Temp. - 68F
Model Sta. - 30.00

Cent. Sta. (ft.)	Depth (cm.)
20.0	12.56
24.0	12.58
25.0	12.59
25.5	12.60
26.0	12.60
26.5	12.50
27.5	12.60
28.0	12.59
28.5	12.55
29.0	12.45
29.5	12.16

Run No. 4-3**
Q - 1 cfs
y_n - 9.64 cm.
M - b/B - 0.311
L/b - 1.0
Slope - 0.000584
Temp. - 68F
Model Sta. - 30.00

Cent. Sta. (ft.)	Depth (cm.)
20.0	12.72
24.0	12.73
25.0	12.75
25.5	12.73
26.0	12.75
26.5	12.76
27.5	12.74
28.0	12.73
28.5	12.69
29.0	12.60
29.5	12.32

Run No. 4-4***
Q - 1 cfs
y_n - 9.64 cm.
M - b/B - 0.491
L/b - 0.0
Slope - 0.000584
Temp. - 68F
Model Sta. - 30.00

Cent. Sta. (ft.)	Depth (cm.)

See Table VIII

"Surface Topography"

Run No. 4-5
Q - 1 cfs
y_o - 9.64 cm.
M - b/B - 0.500
L/b - 0.5
Slope - 0.000584
Temp. - 68F
Model Sta. - 30.00

Cent. Sta. (ft.)	Depth (cm.)
20.0	10.55
24.0	10.56
25.0	10.57
26.0	10.57
26.5	10.57
27.5	10.55
28.0	10.54
29.0	10.41
32.5	9.28
33.0	9.21
33.5	9.19
34.0	9.25
34.5	9.30
35.0	9.30
36.0	9.39

Run No. 4-6
Q - 1 cfs
y_n - 9.64 cm.
M - b/B - 0.500
L/b - 1.0
Slope - 0.000584
Temp. - 68F
Model Sta. - 30.00

Cent. Sta. (ft.)	Depth (cm.)
25.0	10.59
25.5	10.59
26.0	10.60
26.5	10.59
27.5	10.57
28.0	10.53
28.5	10.51
33.0	9.36
34.0	9.33
34.5	9.31
35.0	9.29
35.5	9.36
36.0	9.37
37.0	9.54
38.0	9.55
40.0	9.59

Run No. 4-7**
Q - 1 cfs
y_n - 9.64 cm.
M - b/B - 0.693
L/b - 0.0
Slope - 0.000584
Temp. - 68F
Model Sta. - 30.00

Cent. Sta. (ft.)	Depth (cm.)
20.0	9.94
24.0	9.93
25.0	9.93
25.5	9.92
26.0	9.94
26.5	9.94
27.5	9.90
28.0	9.90
28.5	9.90
29.0	9.87
29.5	9.80

Run No. 4-8**
Q - 1 cfs
y_n - 9.64 cm.
M - b/B - 0.700
L/b - 0.5
Slope - 0.000584
Temp. - 68F
Model Sta. - 30.00

Cent. Sta. (ft.)	Depth (cm.)
20.0	9.90
24.0	9.88
25.0	9.88
25.5	9.88
26.0	9.89
26.5	9.89
27.5	9.87
28.0	9.87
28.5	9.84
29.0	9.80
29.5	9.76

Run No. 4-9**
Q - 1 cfs
y_n - 9.64 cm.
M - b/B - 0.700
L/b - 1.0
Slope - 0.000584
Temp. - 68F
Model Sta. - 30.00

Cent. Sta. (ft.)	Depth (cm.)
20.0	9.93
24.0	9.92
25.0	9.93
25.5	9.91
26.0	9.92
26.5	9.91
27.5	9.91
28.0	9.90
28.5	9.87
29.0	9.85
29.5	9.79

Run No. 4-10**
Q - 1 cfs
y_n - 9.64 cm.
M - b/B - 0.889
L/b - 0.0
Slope - 0.000584
Temp. - 68F
Model Sta. - 30.00

Cent. Sta. (ft.)	Depth (cm.)
20.0	9.69
24.0	9.66
25.0	9.66
25.5	9.66
26.0	9.66
26.5	9.67
27.5	9.66
28.0	9.66
28.5	9.65
29.0	9.64
29.5	9.63

Run No. 4-11**
Q - 1 cfs
y_n - 9.64 cm.
M - b/B - 0.900
L/b - 0.5
Slope - 0.000584
Temp. - 68F
Model Sta. - 30.00

Cent. Sta. (ft.)	Depth (cm.)
20.0	9.71
24.0	9.68
25.0	9.69
25.5	9.68
26.0	9.70
26.5	9.69
27.5	9.69
28.0	9.69
28.5	9.67
29.0	9.66
29.5	9.66

Run No. 4-12**
Q - 2 cfs
y_n - 9.64 cm.
M - b/B - 0.900
L/b - 1.0
Slope - 0.000584
Temp. - 68F
Model Sta. - 30.00

Cent. Sta. (ft.)	Depth (cm.)
20.0	9.72
24.0	9.69
25.0	9.70
25.5	9.69
26.0	9.70
26.5	9.70
27.5	9.69
28.0	9.69
28.5	9.68
29.0	9.67
29.5	9.66

Run No 5-1
Q - 2 cfs
y_n -13.28 cm.
M - b/B - 0.300
L/b - 0.0
Slope - 0.000870
Temp. - 72F
Model Sta. - 30.00

Cent. Sta. (ft.)	Depth (cm.)
20.0	21.89
24.0	21.95
25.0	21.95
26.0	21.99
26.5	22.00
27.5	22.02
28.0	22.02
28.5	22.02
29.0	21.84
31.54	8.87*

Run No. 5-2
Q - 2 cfs
y_n -13.28 cm.
M - b/B - 0.311
L/b - 0.5
Slope - 0.000870
Temp. - 73F
Model Sta. - 30.00

Cent. Sta. (ft.)	Depth (cm.)
20.0	18.86
24.0	18.90
25.0	18.91
26.0	18.95
26.5	18.95
27.5	18.95
28.0	18.92
28.5	18.85
31.25	8.55*

Run No. 5-3
Q - 2 cfs
y_n -13.28 cm.
M - b/B - 0.311
L/b -1.0
Slope - 0.000870
Temp. - 74F
Model Sta. - 30.00

Cent. Sta. (ft.)	Depth (cm.)
24.0	19.32
25.0	19.33
26.0	19.35
26.5	19.34
27.5	19.36
28.0	19.32
28.5	19.27
29.0	19.17
35.25	11.92*

Run No. 5-4
Q - 2 cfs
y_n -13.28 cm.
M - b/B - 0.491
L/b - 0.0
Slope - 0.000870
Temp. 72F
Model Sta. - 30.00

Cent. Sta. (ft.)	Depth (cm.)
20.0	15.58
24.0	15.62
25.0	15.62
26.0	15.63
26.5	15.63
27.5	15.61
28.0	15.57
31.97	11.78*

Run No. 5-5
Q - 2 cfs
y_n -13.28 cm.
M - b/B - 0.500
L/b - 0.5
Slope - 0.000870
Temp. - 74F
Model Sta. - 30.00

Cent. Sta. (ft.)	Depth (cm.)
24.0	14.89
25.0	14.90
26.0	14.90
26.5	14.90
27.5	14.90
28.0	14.85
28.5	14.78
32.95	11.87*

Run No. 5-6
Q - 2 cfs
y_n -13.28 cm.
M - b/B - 0.500
L/b - 1.0
Slope - 0.000870
Temp. - 74F
Model Sta. - 30.00

Cent. Sta. (ft.)	Depth (cm.)
26.0	15.02
26.5	15.02
27.5	15.02
28.0	14.95
28.5	14.87
29.0	14.75
33.11	11.96*

TABLE 7-2-1 RAW DATA - LARGE FLUME - ROUGH BOUNDARIES (continued) P. 4

(Two and Three Dimensional Semicircular Model Tests)

Run No. 5-7
Q - 2 cfs
y_n -13.28cm.
M - b/B - 0.693
L/b - 0.0
Slope - 0.000870
Temp. - 72F
Model Sta. - 30.00

Cent. Sta. (ft.)	Depth (cm.)
20.0	13.81
24.0	13.82
25.0	13.82
26.0	13.84
26.5	13.82
27.5	13.81
28.0	13.77
28.5	13.72
30.5	13.10
31.0	12.85
31.5	12.67
32.0	12.62
32.5	12.59
33.0	12.58
33.5	12.64
34.0	12.70

Run No. 5-8
Q - 2 cfs
y_n -13.28cm.
M - b/B - 0.700
L/b - 0.5
Slope - 0.000870
Temp. - 74F
Model Sta. - 30.00

Cent. Sta. (ft.)	Depth (cm.)
20.0	13.71
24.0	13.70
25.0	13.72
26.0	13.72
26.5	13.70
27.5	13.68
28.0	13.66
28.5	13.61
32.0	12.90
32.5	12.87
33.0	12.86
33.5	12.90

Run No. 5-9
Q - 2 cfs
y_n -13.28cm.
M - b/B - 0.700
L/b - 1.0
Slope - 0.000870
Temp. - 74F
Model Sta. - 30.00

Cent. Sta. (ft.)	Depth (cm.)
24.0	13.74
25.0	13.75
26.0	13.77
26.5	13.77
27.5	13.75
28.0	13.70
28.5	13.67
29.0	13.60
33.5	12.90
34.0	12.88
34.5	12.93
35.0	12.95

Run No. 5-10
Q - 2 cfs
y_n -13.28cm.
M - b/B - 0.889
L/b - 0.0
Slope - 0.000870
Temp. - 72F
Model Sta. - 30.00

Cent. Sta. (ft.)	Depth (cm.)
20.0	13.33
24.0	13.32
25.0	13.32
26.0	13.34
26.5	13.34
27.5	13.34
28.0	13.31
28.5	13.28
30.5	13.22
31.0	13.20
31.5	13.19
32.0	13.21
32.5	13.22
33.0	13.25
33.5	13.27

Run No. 5-11
Q - 2 cfs
y_n -13.28cm.
M - b/B - 0.900
L/b - 0.5
Slope - 0.000870
Temp. - 74F
Model Sta. - 30.00

Cent. Sta. (ft.)	Depth (cm.)
24.0	13.32
25.0	13.33
26.0	13.33
26.5	13.33
27.5	13.33
28.0	13.32
28.5	13.30
32.0	13.24
32.5	13.22
33.0	13.24
33.5	13.28

Run No. 5-12
Q - 2 cfs
y_n -13.28cm.
M - b/B - 0.900
L/b - 1.0
Slope - 0.000870
Temp. - 74F
Model Sta. - 30.00

Cent. Sta. (ft.)	Depth (cm.)
25.0	13.34
26.0	13.35
26.5	13.35
27.5	13.35
28.0	13.33
28.5	13.33
29.0	13.33
34.5	13.23
34.75	13.22
35.0	13.23
35.5	13.25

Run No. 6-1
Q - 3 cfs
y_n -15.28cm.
M - b/B - 0.300
L/b - 0.0
Slope - 0.00123
Temp. - 73F
Model Sta. - 30.00

Cent. Sta. (ft.)	Depth (cm.)
Submerged	

Run No. 6-2
Q - 3 cfs
y_n -15.28cm.
M - b/B - 0.311
L/b - 0.5
Slope - 0.00123
Temp. - 73F
Model Sta. - 30.00

Cent. Sta. (ft.)	Depth (cm.)
Submerged	

Run No. 6-3
Q - 3 cfs
y_n -15.28cm.
M - b/B - 0.311
L/b - 1.0
Slope - 0.00123
Temp. - 73F
Model Sta. - 30.00

Cent. Sta. (ft.)	Depth (cm.)
Submerged	

Run No. 6-4
Q - 3 cfs
y_n -15.28cm.
M - b/B - 0.491
L/b - 0.0
Slope - 0.00123
Temp. - 73F
Model Sta. - 30.00

Cent. Sta. (ft.)	Depth (cm.)
20.0	19.38
24.0	19.43
25.0	19.45
26.0	19.48
26.5	19.46
27.5	19.42
28.0	19.39
33.22	12.67*

Run No. 6-5
Q - 3 cfs
y_n -15.28cm.
M - b/B - 0.500
L/b - 0.5
Slope - 0.00123
Temp. - 74F
Model Sta. - 30.00

Cent. Sta. (ft.)	Depth (cm.)
20.0	18.12
24.0	18.16
25.0	18.19
26.0	18.19
26.5	18.18
27.5	18.15
28.0	18.09
32.82	12.34*

Run No. 6-6
Q - 3 cfs
y_n -15.28 cm.
M - b/B - 0.500
L/b - 1.0
Slope - 0.00123
Temp. - 74F
Model Sta. - 30.00

Cent. Sta. (ft.)	Depth (cm.)
24.0	18.35
25.0	18.37
26.0	18.38
26.5	18.38
27.5	18.34
28.0	18.29
29.0	17.98
32.74	12.15*

Run No 6-7
Q - 3 cfs
y_n -15.28 cm.
M - b/B - 0.693
L/b - 0.0
Slope - 0.00123
Temp. - 73F
Model Sta. - 30.00

Cent. Sta. (ft.)	Depth (cm.)
20.0	16.33
24.0	16.34
25.0	16.35
26.0	16.36
26.5	16.37
27.5	16.33
28.0	16.28
33.03	14.01*

Run No. 6-8
Q - 3 cfs
y_n -15.28cm.
M - b/B - 0.700
L/b - 0.5
Slope - 0.00123
Temp. - 75F
Model Sta. - 30.00

Cent. Sta. (ft.)	Depth (cm.)
20.0	16.05
24.0	16.05
25.0	16.06
26.0	16.06
26.5	16.05
27.5	16.03
28.0	15.98
29.0	15.83
33.05	14.50*

Run No. 6-9
Q - 3 cfs
y_n -15.28cm.
M - b/B - 0.700
L/b - 1.0
Slope - 0.00123
Temp. - 75F
Model Sta. - 30.00

Cent. Sta. (ft.)	Depth (cm.)
20.0	16.15
24.0	16.15
25.0	16.17
26.0	16.17
26.5	16.17
27.5	16.15
28.0	16.08
33.87	14.21*

Run No. 6-10
Q - 3 cfs
y_n -15.28cm.
M - b/B - 0.889
L/b - 0.0
Slope - 0.00123
Temp. - 73F
Model Sta. - 30.00

Cent. Sta. (ft.)	Depth (cm.)
20.0	15.41
24.0	15.38
25.0	15.40
26.0	15.39
26.5	15.39
27.5	15.37
28.0	15.36
31.0	15.19
31.5	15.16
32.0	15.17

Run No. 6-11
Q - 3 cfs
y_n -15.28cm.
M - b/B - 0.900
L/b - 0.5
Slope - 0.00123
Temp. - 76F
Model Sta. - 30.00

Cent. Sta. (ft.)	Depth (cm.)
20.0	15.36
24.0	15.38
25.0	15.38
26.0	15.39
26.5	15.39
27.5	15.39
28.0	15.38
28.5	15.35
32.5	15.22
33.0	15.20
33.5	15.24

Run No. 6-12
Q - 3 cfs
y_n -15.28cm.
M - b/B - 0.900
L/b - 1.0
Slope - 0.00123
Temp. - 76F
Model Sta. - 30.00

Cent. Sta. (ft.)	Depth (cm.)
25.0	15.42
26.0	15.43
26.5	15.43
27.5	15.42
28.0	15.39
29.0	15.36
33.5	15.22
34.0	15.21
34.5	15.22
35.0	15.22
35.5	15.24

TABLE 7-2-1 RAW DATA - LARGE FLUME - ROUGH BOUNDARIES (continued) P. 5

(Two and Three Dimensional Semicircular Model Tests)

Run No. 7-1
Q - 1 cfs
y_n - 6.79cm.
M - b/B - 0.300
L/b - 0.0
Slope - 0.00191
Temp. - 70F
Model Sta. - 30.00

Cent. Sta. (ft.)	Depth (cm.)
20.0	12.25
24.0	12.42
25.0	12.48
26.0	12.55
26.5	12.55
27.5	12.59
28.0	12.60
28.5	12.57
29.0	12.50
31.57	5.46*

Run No. 7-2
Q - 1 cfs
y_n - 6.69 cm.
M - b/B - 0.311
L/b - 0.5
Slope - 0.00191
Temp. - 70F
Model Sta. - 30.00

Cent. Sta. (ft.)	Depth (cm.)
20.0	10.25
24.0	10.43
25.0	10.46
26.0	10.58
26.5	10.54
27.5	10.57
28.0	10.57
28.5	10.55
29.0	10.48
32.10	5.16*

Run No. 7-3
Q - 1 cfs
y_n - 6.69 cm.
M - b/B - 0.311
L/b - 1.0
Slope - 0.00191
Temp. - 70F
Model Sta. - 30.00

Cent. Sta. (ft.)	Depth (cm.)
25.0	11.17
26.0	11.91
26.5	11.21
27.5	11.26
28.0	11.24
28.5	11.22
29.0	11.17
29.5	10.91
32.15	5.37*

Run No. 7-4
Q - 1 cfs
y_n - 6.79 cm.
M - b/B - 0.491
L/b - 0.0
Slope - 0.00191
Temp. - 69F
Model Sta. - 30.00

Cent. Sta. (ft.)	Depth (cm.)
20.0	8.79
24.0	8.91
25.0	8.94
26.0	8.99
26.5	9.00
27.5	9.01
28.0	9.00
28.5	8.95
29.0	8.90
31.0	6.47
31.5	5.82
32.0	5.57
32.5	5.74

Run No. 7-5
Q - 1 cfs
y_n - 6.79 cm.
M - b/B - 0.500
L/b - 0.5
Slope - 0.00191
Temp. - 70F
Model Sta. - 30.00

Cent. Sta. (ft.)	Depth (cm.)
20.0	8.47
24.0	8.59
25.0	8.62
26.0	8.65
26.5	8.66
27.5	8.68
28.0	8.65
28.5	8.62
29.0	8.54
31.5	6.06
32.0	5.92
32.5	6.05

Run No. 7-6
Q - 1 cfs
y_n - 6.69 cm.
M - b/B - 0.500
L/b - 1.0
Slope - 0.00191
Temp. - 70F
Model Sta. - 30.00

Cent. Sta. (ft.)	Depth (cm.)
24.0	8.63
25.0	8.64
26.0	8.69
26.5	8.71
27.5	8.72
28.0	8.70
28.5	8.68
29.0	8.58
32.70	5.94*

Run No. 7-7
Q - 1 cfs
y_n - 6.79 cm.
M - b/B - 0.693
L/b - 0.0
Slope - 0.00191
Temp. - 70F
Model Sta. - 30.00

Cent. Sta. (ft.)	Depth (cm.)
20.0	7.41
24.0	7.45
25.0	7.48
26.0	7.49
26.5	7.50
27.5	7.50
28.0	7.48
28.5	7.45
29.0	7.39
31.52	5.18*

Run No. 7-8
Q - 1 cfs
y_n - 6.69 cm.
M - b/B - 0.700
L/b - 0.5
Slope - 0.00191
Temp. - 70F
Model Sta. - 30.00

Cent. Sta. (ft.)	Depth (cm.)
20.0	7.25
24.0	7.28
25.0	7.29
26.0	7.31
26.5	7.32
27.5	7.31
28.0	7.29
28.5	7.25
29.0	7.09
32.11	6.10*

Run No. 7-9
Q - 1 cfs
y_n - 6.69 cm.
M - b/B - 0.700
L/b - 1.0
Slope - 0.00191
Temp. - 70F
Model Sta. - 30.00

Cent. Sta. (ft.)	Depth (cm.)
24.0	7.40
25.0	7.40
26.0	7.42
26.5	7.43
27.5	7.43
28.0	7.40
29.0	7.37
34.42	6.11*

Run No. 7-10
Q - 1 cfs
y_n - 6.79 cm.
M - b/B - 0.889
L/b - 0.0
Slope - 0.00191
Temp. - 70F
Model Sta. - 30.00

Cent. Sta. (ft.)	Depth (cm.)
20.0	6.92
24.0	6.93
25.0	6.92
26.0	6.92
26.5	6.92
27.5	6.92
28.0	6.90
28.5	6.87
31.0	6.75
32.0	6.74
33.0	6.76

Run No. 7-11
Q - 1 cfs
y_n - 6.69 cm.
M - b/B - 0.900
L/b - 0.5
Slope - 0.00191
Temp. - 70F
Model Sta. - 30.00

Cent. Sta. (ft.)	Depth (cm.)
24.0	6.80
25.0	6.81
26.0	6.82
26.5	6.82
27.5	6.80
28.0	6.77
28.5	6.75
29.0	6.75
32.0	6.66
33.0	6.65
34.0	6.66

Run No. 7-12
Q - 1 cfs
y_n - 6.69 cm.
M - b/B - 0.900
L/b - 1.0
Slope - 0.00191
Temp. - 70F
Model Sta. - 30.00

Cent. Sta. (ft.)	Depth (cm.)
20.0	6.85
24.0	6.85
25.0	6.85
26.0	6.85
26.5	6.86
27.5	6.86
28.0	6.84
29.0	6.80
34.5	6.59
35.0	6.53
35.5	6.60

Run No. 8-1
Q - 2 cfs
y_n - 9.66 cm.
M - b/B - 0.300
L/b - 0.0
Slope - 0.00231
Temp. - 76F
Model Sta. - 30.00

Cent. Sta. (ft.)	Depth (cm.)
20.0	20.31
24.0	20.54
25.0	20.59
26.0	20.67
26.5	20.70
27.5	20.72
28.0	20.71
28.5	20.67
29.0	20.56
33.15	4.29*

Run No. 8-2
Q - 2 cfs
y_n - 9.66 cm.
M - b/B - 0.311
L/b - 0.5
Slope - 0.00231
Temp. - 77F
Model Sta. - 30.00

Cent. Sta. (ft.)	Depth (cm.)
20.0	17.89
24.0	18.19
25.0	18.28
26.0	18.36
26.5	18.37
27.5	18.40
28.0	18.42
28.5	18.38
29.0	18.22
31.90	5.66*

Run No. 8-3
Q - 2 cfs
y_n - 9.66 cm.
M - b/B - 0.311
L/b - 1.0
Slope - 0.00231
Temp. - 77F
Model Sta. - 30.00

Cent. Sta. (ft.)	Depth (cm.)
25.0	18.95
26.0	18.99
26.5	19.00
27.5	19.00
28.0	19.01
28.5	18.96
29.0	18.82
33.51	5.77*

Run No. 8-4
Q - 2 cfs
y_n - 9.66 cm.
M - b/B - 0.491
L/b - 0.0
Slope - 0.00231
Temp. - 75F
Model Sta. - 30.00

Cent. Sta. (ft.)	Depth (cm.)
20.0	13.49
24.0	13.69
25.0	13.74
26.0	13.78
26.5	13.80
27.5	13.81
28.0	13.77
28.5	13.71
32.63	6.94*

Run No. 8-5
Q - 2 cfs
y_n - 9.66 cm.
M - b/B - 0.500
L/b - 0.5
Slope - 0.00231
Temp. - 76F
Model Sta. - 30.00

Cent. Sta. (ft.)	Depth (cm.)
24.0	13.01
25.0	13.06
26.0	13.10
26.5	13.12
27.5	13.15
28.0	13.10
28.5	13.04
33.00	7.17*

Run No. 8-6
Q - 2 cfs
y_n - 9.66 cm.
M - b/B - 0.500
L/b - 1.0
Slope - 0.00231
Temp. - 76F
Model Sta. - 30.00

Cent. Sta. (ft.)	Depth (cm.)
24.0	13.26
25.0	13.30
26.0	13.35
26.5	13.37
27.5	13.38
28.0	13.35
28.5	13.30
29.0	13.24
35.42	7.95*

TABLE 7-2-1 RAW DATA - LARGE FLUME - ROUGH BOUNDARIES (continued) P. 6

(Two and Three Dimensional Semicircular Model Tests)

Run No. 8-7
Q - 2 cfs
y_n - 9.66 cm.
M - b/B - 0.693
L/b - 0.0
Slope - 0.00231
Temp. - 76F
Model Sta. - 30.00

Cent. Sta. (ft.)	Depth (cm.)
20.0	10.86
24.0	10.93
25.0	10.93
26.0	10.93
26.5	10.95
27.5	10.96
28.0	10.95
28.5	10.91
31.0	9.06
31.5	8.55
32.0	8.48
32.5	8.27
33.0	8.45

Run No. 8-8
Q - 2 cfs
y_n - 9.66 cm.
M - b/B - 0.700
L/b - 0.5
Slope - 0.00231
Temp. - 77F
Model Sta. - 30.00

Cent. Sta. (ft.)	Depth (cm.)
24.0	10.72
25.0	10.75
25.5	10.76
26.0	10.77
26.5	10.78
27.5	10.78
28.0	10.75
28.5	10.69
32.0	8.82
32.5	8.74
33.0	8.75
33.5	8.80

Run No. 8-9
Q - 2 cfs
y_n - 9.66 cm.
M - b/B - 0.700
L/b - 1.0
Slope - 0.00231
Temp. - 77F
Model Sta. - 30.00

Cent. Sta. (ft.)	Depth (cm.)
25.0	11.00
26.0	11.04
26.5	11.04
27.5	11.02
28.0	10.98
28.5	10.92
29.0	10.85
35.1	8.45*

Run No. 8-10
Q - 2 cfs
y_n - 9.66 cm.
M - b/B - 0.889
L/b - 0.0
Slope - 0.00231
Temp. - 77F
Model Sta. - 30.00

Cent. Sta. (ft.)	Depth (cm.)
20.0	9.79
24.0	9.80
25.0	9.80
26.0	9.77
26.5	9.75
27.5	9.72
28.0	9.70
30.5	9.60
31.0	9.56
31.5	9.42
32.0	9.50

Run No. 8-11
Q - 2 cfs
y_o - 9.66 cm.
M - b/B - 0.900
L/b - 0.5
Slope - 0.00231
Temp. - 77F
Model Sta. - 30.00

Cent. Sta. (ft.)	Depth (cm.)
24.0	9.81
25.0	9.76
26.0	9.77
26.5	9.78
27.5	9.67
28.0	9.65
28.5	9.66
32.50	9.45*

Run No. 8-12
Q - 2 cfs
y_n - 9.66 cm.
M - b/B - 0.900
L/b - 1.0
Slope - 0.00231
Temp. - 77F
Model Sta. - 30.00

Cent. Sta. (ft.)	Depth (cm.)
24.0	9.72
25.0	9.74
26.0	9.75
26.5	9.76
27.5	9.79
28.0	9.78
28.5	9.75
29.0	9.74
34.50	9.35*

Run No. 9-1
Q - 3 cfs
y_n - 11.59 cm.
M - b/B - 0.300
L/b - 0.0
Slope - 0.00294
Temp. - 72F
Model Sta. - 30.00

Cent. Sta. (ft.)	Depth (cm.)
Submerged	

Run No. 9-2
Q - 3 cfs
y_n - 11.59 cm.
M - b/B - 0.311
L/b - 0.5
Slope - 0.00294
Temp. - 72F
Model Sta. - 30.00

Cent. Sta. (ft.)	Depth (cm.)
Submerged	

Run No. 9-3
Q - 3 cfs
y_n - 11.59 cm.
M - b/B - 0.311
L/b - 1.0
Slope - 0.00294
Temp. - 72F
Model Sta. - 30.00

Cent. Sta. (ft.)	Depth (cm.)
Submerged	

Run No. 9-4
Q - 3 cfs
y_n - 11.59 cm.
M - b/B - 0.491
L/b - 0.0
Slope - 0.00294
Temp. - 72F
Model Sta. - 30.00

Cent. Sta. (ft.)	Depth (cm.)
20.0	16.86
24.0	17.13
25.0	17.17
26.0	17.26
26.5	17.28
27.5	17.32
28.0	17.26
28.5	17.14
32.57	7.05*

Run No. 9-5
Q - 3 cfs
y_n - 11.59 cm.
M - b/B - 0.500
L/b - 0.5
Slope - 0.00294
Temp. - 73F
Model Sta. - 30.00

Cent. Sta. (ft.)	Depth (cm.)
20.0	17.03
24.0	17.28
25.0	17.34
26.0	17.41
26.5	17.46
27.5	17.47
28.0	17.43
28.5	17.35
34.11	6.67*

Run No. 9-6
Q - 3 cfs
y_n - 11.59 cm.
M - b/B - 0.500
L/b - 1.0
Slope - 0.00294
Temp. - 73F
Model Sta. - 30.00

Cent. Sta. (ft.)	Depth (cm.)
25.0	17.59
26.0	17.68
26.5	17.70
27.5	17.73
28.0	17.68
28.5	17.60
29.0	17.39
33.68	7.47*

Run No. 9-7
Q - 3 cfs
y_n - 11.59 cm.
M - b/B - 0.693
L/b - 0.0
Slope - 0.00294
Temp. - 73F
Model Sta. - 30.00

Cent. Sta. (ft.)	Depth (cm.)
20.0	13.37
24.0	13.59
25.0	13.63
26.0	13.65
26.5	13.68
27.5	13.68
28.0	13.63
28.5	13.55
32.50	9.18*

Run No. 9-8
Q - 3 cfs
y_n - 11.59 cm.
M - b/B - 0.700
L/b - 0.5
Slope - 0.00294
Temp. - 73F
Model Sta. - 30.00

Cent. Sta. (ft.)	Depth (cm.)
25.0	13.43
26.0	13.47
26.5	13.52
27.5	13.52
28.0	13.47
28.5	13.36
29.0	13.23
33.12	9.45*

Run No. 9-9
Q - 3 cfs
y_n - 11.59 cm.
M - b/B - 0.700
L/b - 1.0
Slope - 0.00294
Temp. - 73F
Model Sta. - 30.00

Cent. Sta. (ft.)	Depth (cm.)
20.0	13.42
24.0	13.64
25.0	13.64
26.0	13.66
26.5	13.72
27.5	13.74
28.0	13.69
28.5	13.62
29.0	13.62
34.57	9.33*

Run No. 9-10
Q - 3 cfs
y_n - 11.59 cm.
M - b/B - 0.889
L/b - 0.0
Slope - 0.00294
Temp. - 72F
Model Sta. - 30.00

Cent. Sta. (ft.)	Depth (cm.)
20.0	11.71
24.0	11.76
25.0	11.79
26.0	11.81
26.5	11.81
27.5	11.79
28.0	11.74
31.30	11.16*

Run No. 9-11
Q - 3 cfs
y_n - 11.59 cm.
M - b/B - 0.900
L/b - 0.5
Slope - 0.00294
Temp. - 73F
Model Sta. - 30.00

Cent. Sta. (ft.)	Depth (cm.)
20.0	11.73
24.0	11.79
25.0	11.78
26.0	11.79
26.5	11.79
27.5	11.76
28.0	11.71
28.5	11.70
32.53	11.15*

Run No. 9-12
Q - 3 cfs
y_n - 11.59 cm.
M - b/B - 0.900
L/b - 1.0
Slope - 0.00294
Temp. - 74F
Model Sta. - 30.00

Cent. Sta. (ft.)	Depth (cm.)
25.0	11.78
26.0	11.80
26.5	11.80
27.5	11.80
28.0	11.78
28.5	11.75
29.0	11.72
33.73	11.13*

TABLE 7-2-1 RAW DATA - LARGE FLUME - ROUGH BOUNDARIES (continued) P. 7

(Two and Three Dimensional Semicircular Model Tests)

Run No. 10-1
Q - 1 cfs
y_n - 5.35cm.
M - b/B - 0.300
L/b - 0.0
Slope - 0.00408
Temp. - 70F
Model Sta. - 30.00

Cent. Sta. (ft.)	Depth (cm)
20.0	11.22
24.0	11.67
25.0	11.78
26.0	11.91
26.5	11.95
27.5	12.05
28.0	12.11
28.5	12.11
29.0	12.09
29.5	11.83
31.0	5.33
31.5	3.61
32.0	3.37
32.5	3.41
33.0	3.43
33.5	4.95

Run No. 10-2
Q - 1 cfs
y_n - 5.35 cm.
M - b/B - 0.311
L/b - 0.5
Slope - 0.00408
Temp. - 70F
Model Sta. - 30.00

Cent. Sta. (ft.)	Depth (cm.)
20.0	9.63
24.0	10.07
25.0	10.10
26.0	10.31
26.5	10.36
27.5	10.44
28.0	10.51
28.5	10.51
29.0	10.48
29.5	10.25
32.70	3.12*

Run No. 10-3
Q - 1 cfs
y_n - 5.35 cm.
M - b/B - 0.311
L/b - 1.0
Slope - 0.00408
Temp. - 70F
Model Sta. - 30.00

Cent. Sta. (ft.)	Depth (cm.)
26.5	11.51
27.5	11.61
28.0	11.64
28.5	11.64
29.0	11.60
29.5	11.38
33.78	3.35*

Run No. 10-4
Q - 1 cfs
y_n - 5.35 cm.
M - b/B - 0.491
L/b - 0.0
Slope - 0.00408
Temp. - 70F
Model Sta. - 30.00

Cent. Sta. (ft.)	Depth (cm.)
20.0	7.71
24.0	8.08
25.0	8.16
26.0	8.30
26.5	8.33
27.5	8.41
28.0	8.42
28.5	8.42
29.0	8.35
29.5	8.14
32.70	3.79*

Run No. 10-5
Q - 1 cfs
y_n - 5.35 cm.
M - b/B - 0.500
L/b - 0.5
Slope - 0.00408
Temp. - 71F
Model Sta. - 30.00

Cent. Sta. (ft.)	Depth (cm.)
20.0	7.02
24.0	7.36
25.0	7.50
26.0	7.58
26.5	7.63
27.5	7.69
28.0	7.72
28.5	7.74
29.0	7.66
32.18	4.45*

Run No. 10-6
Q - 1 cfs
y_n - 5.35 cm.
M - b/B - 0.500
L/b - 1.0
Slope - 0.00408
Temp. - 70F
Model Sta. - 30.00

Cent. Sta. (ft.)	Depth (cm.)
20.0	7.47
24.0	7.87
25.0	7.98
26.0	8.07
26.5	8.13
27.5	8.20
28.0	8.23
28.5	8.22
29.0	8.16
34.07	4.19*

Run No. 10-7
Q - 1 cfs
y_n - 5.35 cm.
M - b/B - 0.693
L/b - 0.0
Slope - 0.00408
Temp. - 70F
Model Sta. - 30.00

Cent. Sta. (ft.)	Depth (cm.)
20.0	6.20
24.0	6.44
25.0	6.47
26.0	6.47
26.5	6.56
27.5	6.63
28.0	6.61
28.5	6.60
29.0	6.57
33.00	4.70*

Run No. 10-8
Q - 1 cfs
y_n - 5.35 cm.
M - b/B - 0.700
L/b - 0.5
Slope - 0.00408
Temp. - 70F
Model Sta. - 30.00

Cent. Sta. (ft.)	Depth (cm.)
20.0	6.19
24.0	6.43
25.0	6.47
26.0	6.53
26.5	6.55
27.5	6.62
28.0	6.63
28.5	6.60
29.0	6.59
32.16	4.79*

Run No. 10-9
Q - 1 cfs
y_n - 5.35 cm.
M - b/B - 0.700
L/b - 1.0
Slope - 0.00408
Temp. - 70F
Model Sta. - 30.00

Cent. Sta. (ft.)	Depth (cm.)
20.0	6.70
26.5	6.78
27.5	6.84
28.0	6.85
28.5	6.85
29.0	6.82
34.39	4.70*

Run No. 10-10
Q - 1 cfs
y_n - 5.35 cm.
M - b/B - 0.889
L/b - 0.0
Slope - 0.00408
Temp - 69F
Model Sta. - 30.00

Cent. Sta. (ft.)	Depth (cm.)
20.0	5.59
24.0	5.69
25.0	5.69
26.0	5.71
26.5	5.71
27.0	5.71
27.5	5.68
28.0	5.65
30.5	5.25
31.0	5.21
31.5	5.17
32.0	5.07
32.5	5.05
33.0	5.03
34.0	5.05
35.0	5.05
37.0	5.35

Run No. 10-11
Q - 1 cfs
y_n - 5.35 cm.
M - b/B - 0.900
L/b - 0.5
Slope - 0.00408
Temp. - 70F
Model Sta. - 30.00

Cent. Sta. (ft.)	Depth (cm.)
20.0	5.67
24.0	5.79
25.0	5.68
26.0	5.79
26.5	5.75
27.5	5.71
28.0	5.70
28.5	5.73
29.0	5.70
29.5	5.65
34.0	4.87*

Run No. 10-12
Q - 1 cfs
y_n - 5.35 cm.
M - b/B - 0.900
L/b - 1.0
Slope - 0.00408
Temp. - 70F
Model Sta. - 30.00

Cent. Sta. (ft.)	Depth (cm.)
25.0	5.71
26.0	5.78
26.5	5.79
27.5	5.76
28.0	5.78
28.5	5.80
29.0	5.80
29.5	5.68
35.0	4.97*

Run No 11-1
Q - 2 cfs
y_n - 7.49 cm.
M - b/B - 0.300
L/b - 0.0
Slope - 0.00534
Temp. - 78F
Model Sta. - 30.00

Cent. Sta. (ft.)	Depth (cm.)
20.0	18.97
24.0	19.61
25.0	19.79
26.0	19.95
26.5	20.00
27.5	20.12
28.0	20.18
28.5	20.19
29.0	20.10
33.25	3.43*

Run No. 11-2
Q - 2 cfs
y_n - 7.49 cm.
M - b/B - 0.311
L/b - 0.5
Slope - 0.00534
Temp. - 80F
Model Sta. - 30.00

Cent. Sta. (ft.)	Depth (cm.)
24.0	18.48
25.0	18.65
26.0	18.83
26.5	18.92
27.5	19.04
28.0	19.10
28.5	19.09
29.0	19.03
34.6	3.71*

Run No. 11-3
Q - 2 cfs
y_n - 7.49 cm.
M - b/B - 0.311
L/b - 1.0
Slope - 0.00534
Temp - 80F
Model Sta. - 30.00

Cent. Sta. (ft.)	Depth (cm.)
27.0	19.38
27.5	19.51
28.0	19.55
28.5	19.58
29.0	19.50
34.67	3.48*

Run No. 11-4
Q - 2 cfs
y_n - 7.49 cm.
M - b/B - 0.491
L/b - 0.0
Slope - 0.00534
Temp. 78F
Model Sta. - 30.00

Cent. Sta. (ft.)	Depth (cm.)
20.0	11.89
24.0	12.58
25.0	12.82
26.0	12.83
26.5	12.88
27.5	13.01
28.0	13.02
28.5	12.98
29.0	12.90
33.20	4.33*

Run No. 11-5
Q - 2 cfs
y_n - 7.49 cm.
M - b/B - 0.500
L/b - 0.5
Slope - 0.00534
Temp. - 80F
Model Sta. - 30.00

Cent. Sta. (ft.)	Depth (cm.)
24.0	12.03
25.0	12.14
26.0	12.34
26.5	12.39
27.5	12.50
28.0	12.48
28.5	12.39
33.60	4.11*

Run No. 11-6
Q - 2 cfs
y_n - 7.49 cm.
M - b/b - 0.500
L/b - 1.0
Slope - 0.00534
Temp. - 80F
Model Sta. - 30.00

Cent. Sta. (ft.)	Depth (cm.)
26.5	12.66
27.5	12.85
28.0	12.87
28.5	12.83
29.0	12.73
34.91	4.47*

TABLE 7-2-1 RAW DATA - LARGE FLUME - ROUGH BOUNDARIES (continued) P. 8

(Two and Three Dimensional Semicircular Model Tests)

Run No. 11-7
Q - 2 cfs
y_n - 7.49 cm.
M - b/B - 0.693
L/b - 0.0
Slope 0.00534
Temp. - 78F
Model Sta. - 30.00

Cent. Sta. (ft.)	Depth (cm.)
20.0	9.01
24.0	9.43
25.0	9.56
26.0	9.65
26.5	9.69
27.5	9.76
28.0	9.78
28.5	9.74
29.0	9.71
32.62	5.60*

Run No. 11-8
Q - 2 cfs
y_n -7.49 cm.
M - b/B - 0.700
L/b - 0.5
Slope - 0.00534
Temp. - 80F
Model Sta. - 30.00

Cent. Sta. (ft.)	Depth (cm.)
20.0	9.48
24.0	9.55
25.0	9.65
26.0	9.71
26.5	9.79
27.5	9.88
28.0	9.88
28.5	9.86
33.21	5.96*

Run No. 11-9
Q - 2 cfs
y_n -7.49 cm.
M - b/B - 0.700
L/b - 1.0
Slope - 0.00534
Temp. - 78F
Model Sta. - 30.00

Cent. Sta. (ft.)	Depth (cm.)
26.0	10.01
26.5	10.12
27.5	10.20
28.0	10.20
28.5	10.20
29.0	10.14
35.26	5.45*

Run No. 11-10
Q - 2 cfs
y_n -7.49 cm.
M - b/B - 0.889
L/b - 0.0
Slope - 0.00534
Temp. - 78F
Model Sta. - 30.00

Cent. Sta. (ft.)	Depth (cm.)
20.0	7.80
24.0	7.90
25.0	7.91
26.0	7.91
26.5	7.93
27.5	7.95
28.0	8.02
28.5	7.85
31.5	6.38
32.0	6.33
32.5	6.37

Run No. 11-11
Q - 2 cfs
y_n -7.49 cm.
M - b/B - 0.900
L/b - 0.5
Slope - 0.00534
Temp. - 78F
Model Sta. - 30.00

Cent. Sta. (ft.)	Depth (cm.)
24.0	7.93
25.0	8.00
26.0	8.02
26.5	7.99
27.5	8.03
28.0	7.96
28.5	7.95
29.0	7.89
32.5	7.05*

Run No. 11-12
Q - 2 cfs
y_n -7.49 cm.
M - b/B - 0.900
L/b - 1.0
Slope - 0.00534
Temp. - 78F
Model Sta. - 30.00

Cent. Sta. (ft.)	Depth (cm.)
24.0	8.05
25.0	8.08
25.5	7.97
26.0	8.20
26.5	8.20
27.5	8.19
28.0	8.17
28.5	8.15
29.0	8.10
34.61	7.25*

Run No. 12-1
Q - 3 cfs
y_n -8.70 cm.
M - b/B - 0.300
L/b - 0.0
Slope - 0.00748
Temp. - 72F
Model Sta. - 30.00

Cent. Sta. (ft.)	Depth (cm.)
Submerged	

Run No. 12-2
Q - 3 cfs
y_n -8.70 cm.
M - b/B - 0.311
L/b - 0.5
Slope - 0.00748
Temp. - 72F
Model Sta. - 30.00

Cent. Sta. (ft.)	Depth (cm.)
Submerged	

Run No. 12-3
Q - 3 cfs
y_n -8.70 cm.
M - b/B - 0.311
L/b - 1.0
Slope - 0.00748
Temp. - 72F
Model Sta. - 30.00

Cent. Sta. (ft.)	Depth (cm.)
Submerged	

Run No. 12-4
Q - 3 cfs
y_n - 8.70 cm.
M - b/B - 0.491
L/b - 0.0
Slope - 0.00748
Temp. - 72F
Model Sta. - 30.00

Cent. Sta. (ft.)	Depth (cm.)
20.0	14.75
24.0	15.66
25.0	15.88
26.0	16.03
26.5	16.20
27.5	16.35
28.0	16.39
28.5	16.33
29.0	16.19
33.59	4.79*

Run No. 12-5
Q - 3 cfs
y_n - 8.70 cm.
M - b/B - 0.500
L/b - 0.5
Slope - 0.00748
Temp. - 70F
Model Sta. - 30.00

Cent. Sta. (ft.)	Depth (cm.)
20.0	15.34
24.0	16.33
25.0	16.52
26.0	16.75
26.5	16.84
27.5	17.01
28.0	17.05
28.5	17.05
29.0	16.96
29.5	16.49
35.05	4.13*

Run No. 12-6
Q - 3 cfs
y_n -8.70 cm.
M - b/B - 0.500
L/b - 1.0
Slope - 0.00748
Temp. - 71F
Model Sta. - 30.00

Cent. Sta. (ft.)	Depth (cm.)
26.5	17.06
27.5	17.26
28.0	17.27
28.5	17.25
29.0	17.14
36.48	4.55*

Run No. 12-7
Q - 3 cfs
y_n -8.70 cm.
M - b/B -0.693
L/b - 0.0
Slope - 0.00748
Temp. - 70F
Model Sta. - 30.00

Cent. Sta. (ft.)	Depth (cm.)
20.0	11.13
24.0	11.91
25.0	12.10
26.0	12.29
26.5	12.35
27.5	12.54
28.0	12.58
28.5	12.60
29.0	12.40
33.33	5.56*

Run No. 12-8
Q - 3 cfs
y_n -8.70 cm.
M - b/B -0.700
L/b - 0.5
Slope - 0.00748
Temp. - 71F
Model Sta. - 30.00

Cent. Sta. (ft.)	Depth (cm.)
20.0	11.14
24.0	12.03
25.0	12.17
26.0	12.32
26.5	12.39
27.5	12.54
28.0	12.59
28.5	12.65
29.0	12.45
34.36	5.44*

Run No. 12-9
Q - 3 cfs
y_n - 8.70 cm.
M - b/B -0.700
L/b - 1.0
Slope - 0.00748
Temp. - 71F
Model Sta. - 30.00

Cent. Sta. (ft.)	Depth (cm.)
26.5	12.77
27.5	12.85
28.0	12.37
28.5	12.83
29.0	12.72
35.48	6.00*

Run No. 12-10
Q - 3 cfs
y_n - 8.70 cm.
M - b/B - 0.889
L/b - 0.0
Slope - 0.00748
Temp. - 72F
Model Sta. - 30.00

Cent. Sta. (ft.)	Depth (cm.)
20.0	9.02
24.0	9.27
25.0	9.38
26.0	9.40
26.5	9.44
27.5	9.54
28.0	9.46
28.5	9.41
31.93	8.03*

Run No. 12-11
Q - 3 cfs
y_n - 8.70 cm.
M - b/B - 0.900
L/b - 0.5
Slope - 0.00748
Temp. - 72F
Model Sta. - 30.00

Cent. Sta. (ft.)	Depth (cm.)
20.0	9.20
24.0	9.31
25.0	9.42
26.0	9.51
26.5	9.55
27.5	9.72
28.0	9.02
28.5	9.65
29.0	9.60
33.19	7.71*

Run No. 12-12
Q - 3 cfs
y_n - 8.70 cm.
M - b/B - 0.900
L/b - 1.0
Slope - 0.00748
Temp. - 72F
Model Sta. - 30.00

Cent. Sta. (ft.)	Depth (cm.)
26.0	9.61
26.5	9.63
27.5	9.82
28.0	9.77
28.5	9.60
29.0	9.72
36.0	7.75*

TABLE 7-2-1 RAW DATA - LARGE FLUME - ROUGH BOUNDARIES (continued) P. 9

(Two and Three Dimensional Semicircular Model Tests)

Run No. 13-1
Q - 1 cfs
y_n - 4.12 cm.
M - b/B - 0.300
L/b - 0.0
Slope - 0.0112
Temp. - 78F
Model Sta. - 30.00

Cent. Sta. (ft.)	Depth (cm.)
20.0	8.89
24.0	10.25
25.0	10.80
26.0	11.07
26.5	11.20
27.5	11.60
28.0	11.69
28.5	11.77
29.0	11.86
29.5	11.72
33.08	2.52*

Run No. 13-2
Q - 1 cfs
y_n - 4.12 cm.
M - b/B - 0.311
L/b - 0.5
Slope - 0.0112
Temp. - 80F
Model Sta. - 30.00

Cent. Sta. (ft.)	Depth (cm.)
28.62	10.77****
33.28	2.52*

Run No. 13-3
Q - 1 cfs
y_n - 4.12 cm.
M - b/B - 0.311
L/b - 1.0
Slope - 0.0112
Temp. - 80F
Model Sta. - 30.00

Cent. Sta. (ft.)	Depth (cm.)
28.80	11.08****
34.64	2.66*

Run No. 13-4
Q - 1 cfs
y_n - 4.12 cm.
M - b/B - 0.491
L/b - 0.0
Slope - 0.0112
Temp. - 80F
Model Sta. - 30.00

Cent. Sta. (ft.)	Depth (cm.)
28.81	7.90****
33.50	2.83*

Run No. 13-5
Q - 1 cfs
y_o - 4.12 cm.
M - b/B - 0.500
L/b - 0.5
Slope - 0.0112
Temp. - 80F
Model Sta. - 30.00

Cent. Sta. (ft.)	Depth (cm.)
28.50	7.28****
33.65	3.15*

Run No. 13-6
Q - 1 cfs
y_n - 4.12 cm.
M - b/B - 0.500
L/b - 1.0
Slope - 0.0112
Temp. - 80F
Model Sta. - 30.00

Cent. Sta. (ft.)	Depth (cm.)
29.00	7.50****
34.63	3.09*

Run No. 13-7
Q - 1 cfs
y_n - 4.12 cm.
M - b/B - 0.693
L/b - 0.0
Slope - 0.0112
Temp. - 78F
Model Sta. - 30.00

Cent. Sta. (ft.)	Depth (cm.)
20.0	4.22
24.0	4.63
25.0	4.75
26.0	4.81
26.5	4.88
27.5	5.80
28.0	5.42
33.02	3.29*

Run No. 13-8
Q - 1 cfs
y_n - 4.12 cm.
M - b/B - 0.700
L/b - 0.5
Slope - 0.0112
Temp. - 80F
Model Sta. - 30.00

Cent. Sta. (ft.)	Depth (cm.)
27.50	5.95****
33.51	3.38*

Run No. 13-9
Q - 1 cfs
y_o - 4.12 cm.
M - b/B - 0.700
L/b - 1.0
Slope - 0.0112
Temp. - 80F
Model Sta. - 30.00

Cent. Sta. (ft.)	Depth (cm.)
28.00	6.05****
35.08	3.55*

Run No. 13-10
Q - 1 cfs
y_n - 4.12 cm.
M - b/B - 0.889
L/b - 0.0
Slope - 0.0212
Temp. - 80F
Model Sta. - 30.00

Cent. Sta. (ft.)	Depth (cm.)
27.83	4.55****
32.86	3.84*

Run No. 13-11
Q - 1 cfs
y_n - 4.12 cm.
M - b/B - 0.900
L/b - 0.5
Slope - 0.0112
Temp. - 80F
Model Sta. - 30.00

Cent. Sta. (ft.)	Depth (cm.)
27.90	4.58****
32.77	3.32*

Run No. 13-12
Q - 1 cfs
y_n - 4.12 cm.
M - b/B - 0.900
L/b - 1.0
Slope - 0.0112
Temp. - 80F
Model Sta. - 30.00

Cent. Sta. (ft.)	Depth (cm.)
28.10	4.55****
34.60	3.97*

Run No. 14-1
Q - 2 cfs
y_n - 6.02 cm.
M - b/B - 0.300
L/b - 0.0
Slope - 0.0123
Temp. - 80F
Model Sta. - 30.00

Cent. Sta. (ft.)	Depth (cm.)
20.0	16.65
24.0	18.17
25.0	18.57
26.0	18.96
26.5	19.18
27.5	19.55
28.0	19.71
28.5	19.83
29.0	19.85
28.5	19.57
34.05	3.48*

Run No. 14-2
Q - 2 cfs
y_n - 6.02 cm.
M - b/B - 0.311
L/b - 0.5
Slope - 0.0123
Temp. - 74F
Model Sta. - 30.00

Cent. Sta. (ft.)	Depth (cm.)
28.90	16.81****
34.55	3.31*

Run No. 14-3
Q - 2 cfs
y_n - 6.02 cm.
M - b/B - 0.311
L/b - 1.0
Slope - 0.0123
Temp. - 74F
Model Sta. - 30.00

Cent. Sta. (ft.)	Depth (cm.)
28.92	17.60****
35.16	3.25*

Run No. 14-4
Q - 2 cfs
y_n - 6.02 cm.
M - b/B - 0.491
L/b - 0.0
Slope - 0.0123
Temp. - 74F
Model Sta. - 30.00

Cent. Sta. (ft.)	Depth (cm.)
24.0	10.98
25.0	11.33
26.0	11.69
26.5	11.99
27.5	12.25
28.0	12.45
28.5	12.49
29.0	12.48
29.5	12.18
34.00	3.69*

Run No. 14-5
Q - 2 cfs
y_n - 6.02 cm.
M - b/B - 0.500
L/b - 0.5
Slope - 0.0123
Temp. - 74F
Model Sta. - 30.00

Cent. Sta. (ft.)	Depth (cm.)
28.88	11.75****
34.04	3.55*

Run No. 14-6
Q - 2 cfs
y_n - 6.02 cm.
M - b/B - 0.500
L/b - 1.0
Slope - 0.0123
Temp. - 76F
Model Sta. - 30.00

Cent. Sta. (ft.)	Depth (cm.)
29.00	12.07****
35.30	3.90*

TABLE 7-2-1 RAW DATA - LARGE FLUME - ROUGH BOUNDARIES (continued) P.10

(Two and Three Dimensional Semicircular Model Tests)

Run No. 14-7		Run No. 14-8		Run No. 14-9		Run No. 14-10		Run No. 14-11		Run No. 14-12	
Q - 2 cfs		Q - 2 cfs		Q - 2 cfs		Q - 2 cfs		Q - 2 cfs		Q - 2 cfs	
y_n - 6.02 cm.		y_n - 6.02 cm.		y_n - 6.02 cm.		y_n - 6.02 cm.		y_n - 6.02 cm.		y_n - 6.02 cm.	
M - b/B - 0.693		M - b/B - 0.700		M - b/B - 0.700		M - b/B - 0.889		M - b/B - 0.900		M - b/B - 0.900	
L/b - 0.0		L/b - 0.5		L/b - 1.0		L/b - 0.0		L/b - 0.5		L/b - 1.0	
Slope - 0.0123		Slope - 0.0123		Slope - 0.0123		Slope - 0.0123		Slope - 0.0123		Slope - 0.0123	
Temp. - 74F		Temp. - 76F		Temp. - 76F		Temp. - 74F		Temp. - 74F		Temp. - 74F	
Model Sta. - 30.00		Model Sta. - 30.00		Model Sta. - 30.00		Model Sta. - 30.00		Model Sta. - 30.00		Model Sta. - 30.00	
Cent. Sta. (ft.)	Depth (cm.)	Cent. Sta. (ft.)	Depth (cm.)	Cent. Sta. (ft.)	Depth (cm.)	Cent. Sta. (ft.)	Depth (cm.)	Cent. Sta. (ft.)	Depth (cm.)	Cent. Sta. (ft.)	Depth (cm.)
28.82	9.01****	28.20	9.13****	28.73	9.40****	27.31	6.69****	29.34	6.95****	29.38	7.03****
33.10	4.56*	34.59	4.23*	36.10	4.42*	32.57	5.53*	32.86	5.13*	36.50	5.40*

Notes:

* Only the minimum depth was measured on the downstream side of the bridge model.

** Runs for which no measurements were taken on the downstream side of the bridge model.

*** Runs for which a detail of the regain curve is given in Table VIII.

**** Runs for which only the maximum and minimum depths were read and recorded. No other measurements were taken.

GEOMETRY I_a AND I_b

TABLE 7-2-2 CALCULATIONS FOR THE LARGE FLUME ROUGH BOUNDARY MODEL TESTS P. I

Measured Data | Calculated Data

1 Run No.	2 L/b	3 M	4 S_n	5 Q (cfs)	6 y_n (cm.)	7 y_1 (cm.)	8 y_3 (cm.)	9 ν x 10^5	10 y_1 Sta. (ft.)	11 y_3 Sta. (ft.)	12 Mod. Sta. (ft.)	13 R (ft.)	14 F_n	15 R_e	16 f	17 M'	18 C_d	19 y_1/y_n	20 $(F_n/M')^{2/3}$	21 h_1^* (ft.)	22 $y_1 - y_3$ (ft.)	23 L_{1-2} (ft.)	24 L_{1-3} (ft.)
*1-1	0.0	0.300	0.000030	1.0	24.52	-	-	-	-	-	-	-	-	-	-	-	-	-	-	-	-	-	-
*1-2	0.5	0.311	"	"	"	-	-	-	-	-	-	-	-	-	-	-	-	-	-	-	-	-	-
*1-3	1.0	0.311	"	"	"	-	-	-	-	-	-	-	-	-	-	-	-	-	-	-	-	-	-
1-4	0.0	0.491	"	"	"	24.54	-	1.164	26.00	-	30.00	0.6085	0.0489	13,005	0.0764	0.4546	0.1052	1.0058	0.236	0.0040	-	4.00	-
1-5	0.5	0.500	"	"	"	24.67	-	1.091	26.50	-	"	"	"	13,879	"	0.4620	0.1027	1.0061	-	0.0049	-	3.50	-
1-6	1.0	0.500	"	"	"	24.70	-	"	"	-	"	"	"	"	"	0.4620	0.1026	1.0073	-	0.0059	-	"	-
1-7	0.0	0.693	"	"	"	24.58	-	"	"	-	"	"	"	"	"	0.6677	0.0722	1.0024	0.175	0.0020	-	"	-
1-8	0.5	0.700	"	"	"	24.59	-	"	"	-	"	"	"	"	"	0.6739	0.0715	1.0028	-	0.0023	-	"	-
1-9	1.0	0.700	"	"	"	24.59	-	"	"	-	"	"	"	"	"	0.6739	0.0715	1.0028	-	0.0023	-	"	-
1-10	0.0	0.889	"	"	"	24.56	-	"	"	-	"	"	"	"	"	0.8696	0.0557	1.0016	0.146	0.0013	-	"	-
1-11	0.5	0.900	"	"	"	24.58	-	"	"	-	"	"	"	"	"	0.8798	0.0550	1.0024	-	0.0020	-	"	-
1-12	1.0	0.900	"	"	"	24.60	-	"	"	-	"	"	"	"	"	0.8798	0.0549	1.0033	-	0.0026	-	"	-
*2-1	0.0	0.300	0.000131	2.0	24.09	-	-	-	-	-	-	-	-	-	-	-	-	-	-	-	-	-	-
*2-2	0.5	0.311	"	"	"	-	-	-	-	-	-	-	-	-	-	-	-	-	-	-	-	-	-
*2-3	1.0	0.311	"	"	"	-	-	-	-	-	-	-	-	-	-	-	-	-	-	-	-	-	-
2-4	0.0	0.491	"	"	"	24.90	23.65	1.007	27.50	32.51	30.00	0.6004	0.1005	30,204	0.0789	0.4545	0.2070	1.034	0.365	0.0266	0.0410	2.50	5.01
2-5	0.5	0.500	"	"	24.09	24.58	23.77	1.007	26.50	32.50	"	0.6004	0.1005	30,204	0.0789	0.4643	0.2064	1.020	-	0.0161	0.0266	3.50	6.00
2-6	1.0	0.500	"	"	24.07	24.50	23.74	1.059	26.00	33.50	"	0.6000	0.1006	28,726	0.0787	0.4643	0.2084	1.014	-	0.0108	0.0217	4.00	7.50
2-7	0.0	0.693	"	"	24.09	24.31	23.91	1.007	26.00	33.00	"	0,6004	0.1005	30,204	0.0789	0.6681	0.1469	1.009	0.283	0.0072	0.0131	4.00	7.00
2-8	0.5	0.700	"	"	24.07	24.13	23.90	1.059	26.00	32.50	"	0.6000	0.1006	28,726	0.0787	0.6754	0.1469	1.002	-	0.0020	0.0076	4.00	6.50
2-9	1.0	0.700	"	"	24.07	24.15	23.90	1.059	26.00	33.50	"	0.6000	0.1006	28,726	0.0787	0.6754	0.1467	1.003	-	0.0026	0.0082	4.00	7.50
2-10	0.0	0.889	"	"	24.09	24.13	24.06	1.020	26.00	31.00	"	0.6004	0.1005	30,204	0.0789	0.8699	0.1144	1.002	0.236	0.0013	0.0023	4.00	5.00
2-11	0.5	0.900	"	"	24.07	24.08	24.05	1.059	27.50	33.00	"	0.6000	0.1006	28,726	0.0787	0.8811	0.1133	1.000	-	0.0003	0.0098	2.50	5.50
2-12	1.0	0.900	"	"	24.07	24.09	24.04	1.059	28.00	34.50	"	0.6000	0.1006	28,726	0.0787	0.8811	0.1205	1.001	-	0.0007	0.0016	2.00	6.50
*3-1	0.0	0.300	0.000289	3.0	24.05	-	-	-	-	-	-	-	-	-	-	-	-	-	-	-	-	-	-
*3-2	0.5	0.311	"	"	"	-	-	-	-	-	-	-	-	-	-	-	-	-	-	-	-	-	-
*3-3	1.0	0.311	"	"	"	-	-	-	-	-	-	-	-	-	-	-	-	-	-	-	-	-	-
3-4	0.0	0.491	"	"	"	25.87	22.97	0.970	26.50	32.07	30.00	0.5996	0.1511	47,052	0.0770	0.4560	0.2939	1.076	0.479	0.0597	0.0951	3.50	5.57
3-5	0.5	0.500	"	"	"	25.36	23.23	1.033	25.00	32.33	"	"	"	44,183	"	0.4636	0.2970	1.054	-	0.0430	0.0699	5.00	7.33
3-6	1.0	0.500	"	"	"	25.15	23.20	1.033	25.00	32.77	"	"	"	44,183	"	0.4636	0.3003	1.046	-	0.0361	0.0640	5.00	7.77
3-7	0.0	0.693	"	"	"	24.46	23.57	0.970	26.50	33.00	"	"	"	47,052	"	0.6686	0.2182	1.017	0.370	0.0135	0.0292	3.50	6.50
3-8	0.5	0.700	"	"	"	24.32	23.75	1.020	26.50	32.31	"	"	"	44,746	"	0.6749	0.2179	1.011	-	0.0089	0.0187	3.50	5.81
3-9	1.0	0.700	"	"	"	24.38	23.80	1.020	26.00	33.80	"	"	"	44,746	"	0.6749	0.2172	1.014	-	0.0108	0.0190	4.00	7.80
3-10	0.0	0.889	"	"	"	24.10	23.98	0.970	26.50	31.50	"	"	"	47,052	"	0.8704	0.1719	1.002	0.311	0.0016	0.0039	3.50	5.00
3-11	0.5	0.900	"	"	"	24.13	24.03	1.020	26.50	32.75	"	"	"	44,746	"	0.8807	0.1696	1.003	-	0.0026	0.0033	3.50	6.25
3-12	1.0	0.900	"	"	"	24.13	24.01	1.009	26.50	34.54	"	"	"	45,323	"	0.8807	0.1696	1.003	-	0.0026	0.0039	3.50	8.04
4-1	0.0	0.300	0.000584	1.0	9.64	13.75	-	1.091	26.50	-	30.00	0.2807	0.1984	16,288	0.1053	0.2908	0.4077	1.426	0.775	0.1348	-	3.50	-
4-2	0.5	0.311	"	"	"	12.60	-	"	27.50	-	"	"	"	"	"	0.3012	0.4448	1.307	-	0.0971	-	2.50	-
4-3	1.0	0.311	"	"	"	12.76	-	"	26.50	-	"	"	"	"	"	0.3012	0.4370	1.323	-	0.1024	-	3.50	-
4-4	0.0	0.491	"	"	"	10.66	-	"	26.50	-	"	"	"	"	"	0.4857	0.3505	1.106	0.550	0.0335	-	3.50	-
4-5	0.5	0.500	"	"	"	10.58	9.19	"	26.50	33.50	"	"	"	"	"	0.4944	0.3481	1.098	-	0.0308	0.0456	3.50	7.00
4-6	1.0	0.500	"	"	"	10.60	9.31	"	26.00	34.50	"	"	"	"	"	0.4944	0.3471	1.099	-	0.0315	0.0423	4.00	8.00
4-7	0.0	0.693	"	"	"	9.94	-	"	26.50	-	"	"	"	"	"	0.6892	0.2742	1.031	0.436	0.0098	-	3.50	-
4-8	0.5	0.700	"	"	"	9.89	-	"	26.50	-	"	"	"	"	"	0.6960	0.2735	1.026	-	0.0082	-	3.50	-
4-9	1.0	0.700	"	"	"	9.92	-	"	26.00	-	"	"	"	"	"	0.6960	0.2723	1.029	-	0.0092	-	4.00	-
4-10	0.0	0.889	"	"	"	9.66	-	"	28.00	-	"	"	"	"	"	0.8860	0.2227	1.002	0.369	0.0007	-	2.00	-
4-11	0.5	0.900	"	"	"	9.69	-	"	28.00	-	"	"	"	"	"	0.8969	0.2189	1.005	-	0.0016	-	2.00	-
4-12	1.0	0.900	"	"	"	9.70	-	"	26.50	-	"	"	"	"	"	0.8969	0.2185	1.006	-	0.0020	-	3.50	-
5-1	0.0	0.300	0.000870	2.0	13.28	22.02	8.87	1.033	28.50	31.54	30.00	0.3710	0.2455	33,003	0.0984	0.2821	0.4425	1.658	0.912	0.2867	0.4314	1.50	3.04
5-2	0.5	0.311	"	"	"	18.95	8.55	1.020	27.50	31.25	"	"	"	33,424	"	0.2938	0.5080	1.427	-	0.1860	0.3412	2.50	3.75
5-3	1.0	0.311	"	"	"	19.36	11.92	1.007	27.50	35.25	"	"	"	33,856	"	0.2838	0.4943	1.458	-	0.1995	0.2441	2.50	7.75
5-4	0.0	0.491	"	"	"	15.63	11.78	1.033	26.50	31.97	"	"	"	33,003	"	0.4805	0.4001	1.177	0.638	0.0771	0.1263	3.50	5.47
5-5	0.5	0.500	"	"	"	14.90	11.87	1.007	27.50	32.95	"	"	"	33,856	"	0.4897	0.4208	1.122	-	0.0532	0.0994	2.50	5.45
5-6	1.0	0.500	"	"	"	15.02	11.96	1.007	27.50	33.11	"	"	"	33,856	"	0.4897	0.4160	1.131	-	0.0571	0.1004	2.50	5.61
5-7	0.0	0.693	"	"	"	13.84	12.58	1.033	26.00	33.00	"	"	"	33,003	"	0.6856	0.3353	1.042	0.504	0.0184	0.0413	4.00	7.00
5-8	0.5	0.700	"	"	"	13.72	12.86	1.007	26.00	33.00	"	"	"	33,856	"	0.6927	0.3362	1.033	-	0.0144	0.0282	4.00	7.00
5-9	1.0	0.700	"	"	"	13.77	12.98	1.007	26.50	34.00	"	"	"	33,856	"	0.6927	0.3343	1.037	-	0.0161	0.0276	3.50	7.50
5-10	0.0	0.889	"	"	"	13.34	13.19	1.033	26.50	31.50	"	"	"	33,003	"	0.8833	0.2751	1.005	0.426	0.0020	0.0049	2.50	4.00
5-11	0.5	0.900	"	"	"	13.33	13.22	1.007	27.50	32.50	"	"	"	33,856	"	0.8943	0.2763	1.004	-	0.0016	0.0036	2.50	5.00
5-12	1.0	0.900	"	"	"	13.35	13.22	1.007	27.50	34.75	"	"	"	33,856	"	0.8943	0.2714	1.005	-	0.0023	0.0043	2.50	7.25

TABLE 7-2-2 CALCULATIONS FOR THE LARGE FLUME ROUGH BOUNDARY MODEL TESTS (continued) P. 2

Measured Data (columns 1–12) · Calculated Data (columns 13–24)

1 Run No.	2 L/b	3 M	4 S_n	5 Q (cfs)	6 y_n (cm.)	7 y_1 (cm.)	8 y_3 (cm.)	9 $\nu \times 10^5$	10 y_1 Sta. (ft.)	11 y_3 Sta. (ft.)	12 Mod. Sta. (ft.)	13 R (ft.)	14 F_n	15 R_e	16 f	17 M'	18 C_d	19 y_1/y_n	20 $(F_n/M')^{2/3}$	21 h_1^* (ft.)	22 $y_1 - y_3$ (ft.)	23 L_{1-2} (ft.)	24 L_{1-3} (ft.)
*6-1	0.0	0.300	0.00123	3.0	15.28	-	-	-	-	-	-	-	-	-	-	-	-	-	-	-	-	-	-
*6-2	0.5	0.311	"	"	"	-	-	-	-	-	-	-	-	-	-	-	-	-	-	-	-	-	-
*6-3	1.0	0.311	"	"	"	-	-	-	-	-	-	-	-	-	-	-	-	-	-	-	-	-	-
6-4	0.0	0.491	"	"	"	19.48	12.67	1.020	26.00	33.22	30.00	0.4175	0.2983	49,040	0.0921	0.4774	0.4366	1.275	0.731	0.1278	0.2234	4.00	7.22
6-5	0.5	0.500	"	"	"	18.19	12.34	1.007	26.00	32.82	"	"	"	49,672	"	0.4859	0.4732	1.190	-	0.0955	0.1919	4.00	6.82
6-6	1.0	0.500	"	"	"	18.38	12.15	1.007	26.50	32.74	"	"	"	49,672	"	0.4859	0.4662	1.203	-	0.1017	0.2044	[illegible]	[illegible]
6-7	0.0	0.693	"	"	"	16.37	14.01	1.020	26.50	33.03	"	"	"	49,040	"	0.6833	0.3923	1.071	0.576	0.0358	0.0774	[illegible]	6.53
6-8	0.5	0.700	"	"	"	16.07	14.50	0.984	25.00	33.05	"	"	"	50,833	"	0.6900	0.3992	1.052	-	0.0259	0.0515	5.00	8.05
6-9	1.0	0.700	"	"	"	16.17	14.21	0.984	26.50	33.87	"	"	"	50,833	"	0.6900	0.3956	1.058	-	0.0292	0.0643	3.50	[illegible]
6-10	0.0	0.889	"	"	"	15.39	15.16	1.020	26.50	31.50	"	"	"	49,040	"	0.8815	0.3335	1.007	0.486	0.0036	0.0075	[illegible]	5.00
6-11	0.5	0.900	"	"	"	15.39	15.20	0.970	27.50	33.00	"	"	"	51,567	"	0.8923	0.3295	1.007	-	0.0036	0.0062	[illegible]	5.50
6-12	1.0	0.900	"	"	"	15.43	15.21	0.970	26.50	34.00	"	"	"	51,567	"	0.8923	0.3282	1.009	-	0.0049	0.0072	[illegible]	7.50
7-1	0.0	0.300	0.00191	1.0	6.79	12.60	5.46	1.059	28.00	31.57	30.00	0.2045	0.3357	17,357	0.1245	0.2955	0.4608	1.856	1.089	[illegible]	0.2343	[illegible]	[illegible]
7-2	0.5	0.311	"	"	6.69	10.57	5.16	"	28.00	32.10	"	0.2018	0.3432	17,377	0.1192	0.3102	0.5713	1.580	-	0.1273	0.1775	[illegible]	4.10
7-3	1.0	0.311	"	"	6.69	11.26	5.37	"	27.50	32.15	"	0.2018	0.3432	17,377	0.1192	0.3102	0.5218	1.683	-	0.1499	0.1932	[illegible]	4.65
7-4	0.0	0.491	"	"	6.79	9.01	5.57	"	27.50	32.00	"	0.2045	0.3357	17,357	0.1245	0.4883	0.4497	1.327	0.778	0.0728	0.1128	[illegible]	4.50
7-5	0.5	0.500	"	"	6.79	8.68	5.92	"	27.50	32.00	"	0.2045	0.3357	17,357	0.1245	0.4972	0.4668	1.278	-	0.0620	0.0906	[illegible]	4.50
7-6	1.0	0.500	"	"	6.69	8.72	5.94	"	27.50	32.70	"	0.2018	0.3432	17,377	0.1192	0.4972	0.4637	1.303	-	[illegible]	0.0912	[illegible]	5.20
7-7	0.0	0.693	"	"	6.79	7.50	5.18	"	27.50	31.50	"	0.2045	0.3357	17,357	0.1245	0.6911	0.4175	1.105	0.618	0.0233	0.0761	[illegible]	4.00
7-8	0.5	0.700	"	"	6.69	7.32	6.10	"	26.50	32.11	"	0.2018	0.3432	17,377	0.1192	0.6981	0.4287	1.094	-	0.0207	0.0400	[illegible]	5.16
7-9	1.0	0.700	"	"	6.69	7.43	6.11	"	27.50	34.42	"	0.2018	0.3432	17,377	0.1192	0.6981	0.4192	1.111	-	0.0243	0.0433	[illegible]	[illegible]
7-10	0.0	0.889	"	"	6.79	6.92	6.74	"	27.50	32.00	"	0.2045	0.3357	17,357	0.1245	0.8875	0.3668	1.019	0.523	0.0043	0.0059	[illegible]	[illegible]
7-11	0.5	0.900	"	"	6.69	6.82	6.65	"	26.50	33.50	"	0.2018	0.3432	17,377	0.1192	0.8885	0.3703	1.019	-	0.0043	0.0056	[illegible]	7.00
7-12	1.0	0.900	"	"	6.69	6.86	6.53	"	27.50	35.00	"	0.2018	0.3432	17,377	0.1192	0.8885	0.3671	1.025	-	0.0056	0.0108	2.00	[illegible]
8-1	0.0	0.300	0.00231	2.0	9.66	20.72	4.29	0.970	27.50	33.15	30.00	0.2012	0.3956	36,630	0.1048	0.2908	0.4754	2.145	1.228	0.3629	0.5390	[illegible]	[illegible]
8-2	0.5	0.311	"	"	"	18.42	5.66	0.957	28.00	31.90	"	"	"	37,128	"	0.3021	0.5270	1.907	-	0.2874	0.4186	[illegible]	3.90
8-3	1.0	0.311	"	"	"	19.01	5.77	0.984	28.00	33.51	"	"	"	36,109	"	0.3021	0.5059	1.968	-	0.3068	0.4344	[illegible]	[illegible]
8-4	0.0	0.491	"	"	"	13.81	6.94	0.984	27.50	32.63	"	"	"	36,109	"	0.4855	0.4792	1.430	0.872	0.1362	0.2254	[illegible]	5.13
8-5	0.5	0.500	"	"	"	13.15	7.17	0.970	27.50	33.00	"	"	"	36,630	"	0.4946	0.5052	1.361	-	0.1145	0.1962	2.50	5.50
8-6	1.0	0.500	"	"	"	13.38	7.95	0.970	27.50	35.42	"	"	"	36,630	"	0.4946	0.4925	1.385	-	0.1220	0.1781	2.50	7.92
8-7	0.0	0.693	"	"	"	10.96	8.27	0.970	27.50	32.50	"	"	"	36,630	"	0.6891	0.4742	1.135	0.691	0.0426	0.0883	2.50	5.00
8-8	0.5	0.700	"	"	"	10.78	8.74	0.957	27.50	32.50	"	"	"	37,128	"	0.6961	0.4812	1.116	-	0.0368	0.0669	2.50	5.00
8-9	1.0	0.700	"	"	"	11.04	8.45	0.957	26.50	35.10	"	"	"	37,128	"	0.6961	0.4644	1.143	-	0.0453	0.0850	3.50	8.60
8-10	0.0	0.889	"	"	"	9.80	9.42	0.957	25.50	31.50	"	"	"	37,128	"	0.8860	0.4359	1.014	0.584	0.0046	0.0125	5.00	6.50
8-11	0.5	0.900	"	"	"	9.78	9.45	0.957	26.50	32.50	"	"	"	37,128	"	0.8970	0.4319	1.012	-	0.0039	0.0108	3.50	6.00
8-12	1.0	0.900	"	"	"	9.79	9.35	0.957	27.50	34.50	"	"	"	37,128	"	0.8970	0.4312	1.013	-	0.0043	0.0144	2.50	7.00
*9-1	0.0	0.300	0.00294	3.0	11.59	-	-	-	-	-	-	-	-	-	-	-	-	-	-	-	-	-	-
*9-2	0.5	0.311	"	"	"	-	-	-	-	-	-	-	-	-	-	-	-	-	-	-	-	-	-
*9-3	1.0	0.311	"	"	"	-	-	-	-	-	-	-	-	-	-	-	-	-	-	-	-	-	-
9-4	0.0	0.491	"	"	"	17.32	7.05	1.033	27.50	32.57	30.00	0.3300	0.4516	50,459	0.1001	0.4871	0.5168	1.494	0.951	0.1880	0.3369	2.50	5.07
9-5	0.5	0.500	"	"	"	17.47	6.67	1.020	27.50	34.11	"	"	"	51,102	"	0.4922	0.5015	1.507	-	0.1929	0.3543	2.50	6.61
9-6	1.0	0.500	"	"	"	17.73	7.47	1.020	27.50	33.68	"	"	"	51,102	"	0.4922	0.4909	1.530	-	0.2014	0.3366	2.50	6.18
9-7	0.0	0.693	"	"	"	13.68	9.18	1.020	27.50	32.50	"	"	"	51,102	"	0.6874	0.5116	1.180	0.756	0.0687	0.1476	2.50	5.00
9-8	0.5	0.700	"	"	"	13.52	9.45	1.020	27.50	33.12	"	"	"	51,102	"	0.6944	-	-	-	-	-	2.50	5.62
9-9	1.0	0.700	"	"	"	13.74	9.33	1.020	27.50	34.57	"	"	"	51,102	"	0.6944	0.5033	1.185	-	0.0705	0.1447	2.50	7.07
9-10	0.0	0.889	"	"	"	11.81	11.16	1.033	26.50	31.30	"	"	"	50,459	"	0.8846	0.4948	1.019	0.638	0.0072	0.0213	3.50	4.80
9-11	0.5	0.900	"	"	"	11.79	11.15	1.020	26.50	32.53	"	"	"	51,102	"	0.8957	0.4900	1.017	-	0.0066	0.0210	3.50	6.03
9-12	1.0	0.900	"	"	"	11.80	11.13	1.007	27.50	33.73	"	"	"	51,762	"	0.8957	0.4894	1.018	-	0.0069	0.0220	2.50	6.23
10-1	0.0	0.300	0.00408	1.0	5.35	12.11	3.37	1.059	28.50	32.00	30.00	0.1640	0.4800	17,663	0.1324	0.2972	0.4874	2.264	1.376	0.2218	0.2867	1.50	3.50
10-2	0.5	0.311	"	"	"	10.51	3.12	"	28.50	32.70	"	"	"	"	"	0.3079	0.5760	1.964	-	0.1693	0.2424	1.50	4.20
10-3	1.0	0.311	"	"	"	11.64	3.35	"	28.50	33.78	"	"	"	"	"	0.3079	0.4977	2.176	-	0.2063	0.2720	1.50	5.28
10-4	0.0	0.491	"	"	"	8.42	3.79	"	28.50	32.70	"	"	"	"	"	0.4890	0.4973	1.574	0.987	0.1007	0.1519	1.50	4.20
10-5	0.5	0.500	"	"	"	7.74	4.45	"	28.50	32.18	"	"	"	"	"	0.4983	0.5537	1.447	-	0.0784	0.1079	1.50	3.68
10-6	1.0	0.500	"	"	"	8.23	4.19	"	28.00	34.07	"	"	"	"	"	0.4983	0.5647	1.538	-	0.0945	0.1325	2.00	6.07
10-7	0.0	0.693	"	"	"	6.63	4.70	"	27.50	33.00	"	"	"	"	"	0.6918	0.5021	1.239	0.784	0.0420	0.0633	2.50	5.50
10-8	0.5	0.700	"	"	"	6.63	4.79	"	28.00	32.61	"	"	"	"	"	0.6988	0.4971	1.239	-	0.0420	0.0604	2.00	4.61
10-9	1.0	0.700	"	"	"	6.85	4.70	"	28.50	34.39	"	"	"	"	"	0.6988	0.4734	1.280	-	0.0492	0.0705	1.50	5.79
10-10	0.0	0.889	"	"	"	5.71	5.03	"	27.00	33.00	"	"	"	"	"	0.8981	0.4891	1.067	0.659	0.0118	0.0223	3.00	6.00
10-11	0.5	0.900	"	"	"	5.79	4.87	"	26.00	34.00	"	"	"	"	"	0.8891	0.4732	1.082	-	0.0144	0.0303	4.00	8.00
10-12	1.0	0.900	"	"	"	5.80	4.97	"	29.00	35.00	"	"	"	"	"	0.8891	0.4720	1.084	-	0.0148	0.0272	1.00	6.00

TABLE 7-2-2 CALCULATIONS FOR THE LARGE FLUME ROUGH BOUNDARY MODEL TESTS (continued) P. 3

Measured Data (columns 1–11) — Calculated Data (columns 12–24)

1 Run No.	2 L/b	3 M	4 S_n	5 Q (cfs)	6 y_n (cm.)	7 y_1 (cm.)	8 y_3 (cm.)	9 ν x 10^5	10 y_1 Sta. (ft.)	11 y_3 Sta. (ft.)	12 Mod. Sta. (ft.)	13 R (ft.)	14 F_n	15 R_e	16 f	17 M'	18 C_d	19 y_1/y_n	20 $(F_n/M')^{2/3}$	21 h_1^* (ft.)	22 $y_1 - y_3$ (ft.)	23 L_{1-2} (ft.)	24 L_{1-3} (ft.)
11-1	0.0	0.300	0.00534	2.0	7.49	20.19	3.43	0.944	28.50	33.25	30.00	0.2237	0.5795	38,616	0.1158	0.2945	0.4906	2.696	1.570	0.4167	0.5499	1.50	4.75
11-2	0.5	0.311	"	"	"	19.10	3.71	0.917	28.00	34.60	"	"	"	39,753	"	0.3057	0.5029	2.550	-	0.3809	0.5049	2.00	5.60
11-3	1.0	0.311	"	"	"	19.58	3.48	0.917	28.50	34.67	"	"	"	39,753	"	0.3057	0.4872	2.614	-	0.3967	0.5282	1.50	6.17
11-4	0.0	0.491	"	"	"	13.02	4.33	0.944	28.00	33.20	"	"	"	38,616	"	0.4877	0.5224	1.738	1.122	0.1814	0.2851	2.00	5.20
11-5	0.5	0.500	"	"	"	12.50	4.11	0.917	27.50	33.60	"	"	"	38,753	"	0.4968	0.5443	1.669	-	0.1644	0.2753	2.50	6.10
11-6	1.0	0.500	"	"	"	12.87	4.77	0.917	28.00	34.91	"	"	"	39,753	"	0.4968	0.5215	1.718	-	0.1765	0.2756	2.00	6.91
11-7	0.0	0.693	"	"	"	9.78	5.60	0.944	28.00	32.62	"	"	"	38,616	"	0.6907	0.5619	1.306	0.889	0.0751	0.1371	2.00	4.62
11-8	0.5	0.700	"	"	"	9.88	5.96	0.917	28.00	33.21	"	"	"	39,753	"	0.6977	0.5479	1.319	-	0.0784	0.1286	2.00	5.21
11-9	1.0	0.700	"	"	"	10.20	5.45	0.944	28.50	35.26	"	"	"	38,616	"	0.6977	0.5225	1.362	-	0.0889	0.1558	1.50	6.76
11-10	0.0	0.889	"	"	"	8.02	6.33	0.944	28.00	32.00	"	"	"	38,616	"	0.8872	0.5883	1.071	0.752	0.0174	0.0554	2.00	4.00
11-11	0.5	0.900	"	"	"	8.03	7.05	0.944	27.50	32.50	"	"	"	38,616	"	0.8982	0.5800	1.072	-	0.0177	0.0322	2.50	5.00
11-12	1.0	0.900	"	"	"	8.20	7.25	0.944	26.50	34.61	"	"	"	38,616	"	0.8982	0.5621	1.095	-	0.0233	0.0312	3.50	8.11
*12-1	0.0	0.300	0.00748	3.0	8.70	-	-	-	-	-	-	-	-	-	-	-	-	-	-	-	-	-	-
*12-2	0.5	0.311	"	"	"	-	-	-	-	-	-	-	-	-	-	-	-	-	-	-	-	-	-
*12-3	1.0	0.311	"	"	"						-	-	-		-				-				
12-4	0.0	0.491	"	"	"	16.39	4.79	1.033	28.00	33.59	30.00	0.2562	0.6943	52,178	0.1114	0.4906	0.5596	1.884	1.261	0.2523	0.3806	2.00	5.59
12-5	0.5	0.500	"	"	"	17.05	4.13	1.059	28.50	35.05	"	"	"	50,897	"	0.4956	0.5197	1.960	-	0.2740	0.4239	1.50	6.55
12-6	1.0	0.500	"	"	"	17.27	4.55	1.046	28.50	36.48	"	"	"	51,530	"	0.4956	0.5098	1.985	-	0.2812	0.4173	2.00	8.48
12-7	0.0	0.693	"	"	"	12.60	5.56	1.059	28.50	33.33	"	"	"	50,897	"	0.6898	0.5780	1.448	1.004	0.1280	0.2310	1.50	4.83
12-8	0.5	0.700	"	"	"	12.65	5.44	1.046	28.50	34.36	"	"	"	51,530	"	0.6969	0.5690	1.454	-	0.1296	0.2365	1.50	5.86
12-9	1.0	0.700	"	"	"	12.87	6.00	1.046	28.00	35.48	"	"	"	51,530	"	0.6969	0.5545	1.479	-	0.1368	0.2251	2.00	7.48
12-10	0.0	0.889	"	"	"	9.54	8.03	1.033	27.50	31.93	"	"	"	52,178	"	0.8865	0.6807	1.097	0.842	0.0276	0.0495	2.50	4.43
12-11	0.5	0.900	"	"	"	9.72	7.71	1.033	27.50	33.19	"	"	"	52,178	"	0.8976	0.6539	1.117	-	0.0335	0.0659	2.50	5.69
12-12	1.0	0.900	"	"	"	9.82	7.75	1.033	27.50	36.00	"	"	"	52,178	"	0.8976	0.6440	1.129	-	0.0367	0.0679	2.50	8.50
13-1	0.0	0.300	0.01120	1.0	4.12	11.86	2.52	0.944	29.00	33.08	30.00	0.1282	0.7202	20,119	0.1685	0.2984	0.5020	2.878	1.784	0.2539	0.3064	1.00	4.08
13-2	0.5	0.311	"	"	"	10.77	2.52	0.917	28.62	33.28	"	"	"	20,711	"	0.3094	0.5546	2.614	-	0.2182	0.2707	1.38	4.66
13-3	1.0	0.311	"	"	"	11.08	2.66	0.917	28.80	34.64	"	"	"	20,711	"	0.3094	0.5324	2.689	-	0.2283	0.2762	1.20	5.84
13-4	0.0	0.491	"	"	"	7.90	2.83	0.917	28.81	33.50	"	"	"	20,711	"	0.4900	0.5470	1.917	1.280	0.1240	0.1663	1.19	4.70
13-5	0.5	0.500	"	"	"	7.28	3.15	0.917	28.50	33.65	"	"	"	20,711	"	0.4990	0.6065	1.767	-	0.1037	0.1335	1.50	5.15
13-6	1.0	0.500	"	"	"	7.50	3.09	0.917	29.00	34.63	"	"	"	20,711	"	0.4990	0.5802	1.820	-	0.1109	0.1447	1.00	5.63
13-7	0.0	0.693	"	"	"	5.90	3.29	0.944	27.50	33.02	"	"	"	20,119	"	0.6293	0.6134	1.408	1.017	0.0551	0.0824	2.50	5.52
13-8	0.5	0.700	"	"	"	5.96	3.34	0.917	27.50	33.51	"	"	"	20,711	"	0.6993	0.5845	1.444	-	0.0600	0.0843	2.50	6.01
13-9	1.0	0.700	"	"	"	6.05	3.55	0.917	28.00	35.08	"	"	"	20,711	"	0.6993	0.5701	1.468	-	0.0633	0.0820	2.00	7.08
13-10	0.0	0.889	"	"	"	4.55	3.84	0.917	27.83	32.86	"	"	"	20,711	"	0.8885	0.6875	1.104	0.861	0.0141	0.0233	2.17	5.03
13-11	0.5	0.900	"	"	"	4.58	3.32	0.917	27.90	32.77	"	"	"	20,711	"	0.8995	0.6725	1.112	-	0.0151	0.0413	2.10	4.87
13-12	1.0	0.900	"	"	"	4.55	3.97	0.917	28.10	34.60	"	"	"	20,711	"	0.8995	0.6791	1.104	-	0.0141	0.0190	1.90	6.50
14-1	0.0	0.300	0.01230	2.0	6.02	19.85	3.48	1.020	29.00	34.05	30.00	0.1830	0.8042	36,378	0.1410	0.2965	0.5009	3.297	1.946	0.4537	0.5371	1.00	5.05
14-2	0.5	0.311	"	"	"	16.81	3.31	1.007	28.90	34.55	"	"	"	36,848	"	0.3076	0.5947	2.792	-	0.3540	0.4429	1.10	5.65
14-3	1.0	0.311	"	"	"	17.60	3.25	1.007	28.92	35.16	"	"	"	36,848	"	0.3076	0.5594	2.924	-	0.3799	0.4708	1.08	6.24
14-4	0.0	0.491	"	"	"	12.49	3.69	1.007	28.50	34.00	"	"	"	36,848	"	0.4889	0.5552	2.075	1.394	0.2123	0.2887	1.50	5.50
14-5	0.5	0.500	"	"	"	11.75	3.55	1.007	28.88	34.04	"	"	"	36,848	"	0.4979	0.5962	1.952	-	0.1880	0.2690	1.12	5.16
14-6	1.0	0.500	"	"	"	12.07	3.90	0.970	29.00	35.30	"	"	"	38,253	"	0.4979	0.5731	2.005	-	0.1985	0.2680	1.00	6.30
14-7	0.0	0.693	"	"	"	9.01	4.56	1.007	28.82	33.10	"	"	"	36,848	"	0.6915	0.6351	1.497	1.106	0.0981	0.1460	1.18	4.28
14-8	0.5	0.700	"	"	"	9.13	4.73	0.970	28.20	34.50	"	"	"	38,253	"	0.6985	0.6164	1.517	-	0.1020	0.1444	1.80	6.30
14-9	1.0	0.700	"	"	"	9.40	4.42	0.970	28.73	36.10	"	"	"	38,253	"	0.6985	0.5901	1.561	-	0.1109	0.1634	1.27	7.37
14-10	0.0	0.889	"	"	"	6.69	5.53	1.007	27.30	32.57	"	"	"	36,848	"	0.8878	0.7718	1.111	0.936	0.0220	0.0381	2.70	5.27
14-11	0.5	0.900	"	"	"	6.95	5.13	1.007	29.34	32.86	"	"	"	36,848	"	0.8988	0.7200	1.154	-	0.0305	0.0597	0.66	3.52
14-12	1.0	0.900	"	"	"	7.03	5.40	0.970	29.38	36.50	"	"	"	38,253	"	0.8988	0.7078	1.168	-	0.0331	0.0535	0.62	7.12

* Test runs where the crown of the arch was submerged.

Geometry Ia

TABLE 7-2-3 - SURFACE TOPOGRAPHY & REGAIN CURVE DATA

A) Surface Topography

Run No. 4-4; Q = 1 cfs; S = 0.000584; y_n = 9.72 cm.; M = 0.491;

1/b = 0; Model Station = 29.90 ft.:

Centerline Station	Station Left	Depths (cm.) Centerline	Depths (cm.) Left
15.00		10.58	
	1.00		10.57
	2.00		10.54
16.00		10.56	
17.00		10.58	
18.00		10.61	
	1.00		10.61
	2.00		10.62
19.00		10.63	
20.00		10.63	
	1.00		10.61
	2.00		10.59
21.00		10.62	
22.00		10.63	
	1.00		10.61
	2.00		10.58
23.00		10.63	
24.00		10.63	
	1.00		10.63
	2.00		10.61
25.00		10.64	
26.00		10.65	
	1.00		10.66
	2.00		10.63
26.50		10.65	
27.50		10.64	
	1.00		10.64
	2.00		10.65
28.00		10.61	
	1.00		10.65
	2.00		10.66
28.50		10.56	
	1.00		10.60
	2.00		10.66
29.00		10.47	
	0.50		10.51
	1.00		10.56
	1.50		10.64
	2.00		10.72

7-2-3 (CONTD.)

Centerline Station	Station Left	Depths (cm.) Centerline	Left
29.25		10.39	
	0.50		10.43
	1.00		10.50
	1.50		10.65
	2.00		10.71
29.50		10.21	
	0.50		10.25
	1.00		10.34
	1.50		10.75
	2.00		10.72
	2.32		10.70
29.79	-	10.09	
	0.50		10.09
	0.75		10.07
	1.00		10.17
	1.25		10.53
	1.50		10.72
	1.75		10.76
	2.00		10.76
	2.32		10.73
30.20		9.95	
	0.50		9.86
	0.75		9.74
	1.00		9.55
	1.25		9.09
	1.50		9.07
	2.00		9.05
30.50		9.57	
	0.50		9.45
	1.00		9.17
	1.50		9.07
	2.00		9.06
31.00		9.27	
	1.00		9.13
	1.50		9.08
	2.00		9.07
31.50		9.06	
	1.00		9.07
	2.00		9.08
32.0		9.02	
	1.00		9.10
	2.00		9.07
32.50		9.05	
33.00		9.04	
	1.00		9.07
	2.00		9.13
34.00		9.15	
	2.00		9.14
35.00		9.12	

Centerline Station	Station Left	Depths (cm.) Centerline	Left
36.00		9.22	
	2.00		9.18
37.00		9.35	
38.00		9.38	
39.00		9.40	
40.00		9.43	
41.00		9.45	
42.00		9.50	
43.00		9.53	
44.00		9.55	
45.00		9.57	
46.00		9.58	

B) Regain Curves

Run No. 1-4; Q = 1 cfs; y_n = 24.50 cm.; S = 0.0000302; M = 0.491; L/b = 0; Model Station = 30.00 ft.:

Centerline	Depth (cm.)
31.00	24.24
31.50	24.15
32.00	24.13
32.50	24.11
33.00	24.10
33.50	24.07
34.00	24.14
34.50	24.17
35.00	24.20
36.00	24.22
37.00	24.26
38.00	24.30
39.00	24.34
42.00	24.35
44.00	24.40
46.00	24.44
48.00	24.46
50.00	24.50
52.00	24.51
54.00	24.50

Run No. 2-7; Q = 2 cfs; y_n = 24.30 cm.; S = 0.000131; M = 0.693; L/b = 0; Model Station = 30.00 ft.:

Centerline	Depth (cm.)
31.00	24.20
31.50	24.15
32.00	24.12
32.50	24.13
33.00	24.14
33.50	24.14
34.00	24.15
35.00	24.19
36.00	24.21
37.00	24.24
38.00	24.27
39.00	24.30
40.00	24.29
41.00	24.30

Geometry I

TABLE 7-2-4 VELOCITY MEASUREMENTS

A) Velocity Profiles for Run No. 4-4

Q = 1 cfs; S = 0.000584; y_n = 9.72 cm.; M = 0.491; L/b = 0;
Model Station = 30.00 ft.:

a. Normal Depth

Centerline		1 ft. Left		2 ft. Left	
Depth ft.	Velocity fps	Depth ft.	Velocity fps	Depth ft.	Velocity fps
0.010	0.447	0.010	0.447	0.010	0.347
0.015	0.490	0.020	0.425	0.020	0.347
0.020	0.490	0.030	0.490	0.030	0.347
0.025	0.490	0.040	0.470	0.040	0.347
0.030	0.565	0.050	0.470	0.060	0.490
0.035	0.565	0.060	0.528	0.080	0.528
0.040	0.565	0.070	0.585	0.100	0.565
0.045	0.618	0.080	0.600	0.120	0.600
0.050	0.635	0.090	0.650	0.140	0.635
0.060	0.650	0.100	0.650	0.160	0.650
0.070	0.695	0.120	0.665	0.200	0.695
0.080	0.695	0.140	0.722	0.240	0.748
0.090	0.695	0.160	0.708	0.280	0.762
0.100	0.748	0.200	0.735		
0.120	0.762	0.240	0.748		
0.140	0.788	0.280	0.775		
0.160	0.788				
0.200	0.837				
0.240	0.837				
0.280	0.850				

b. Maximum Depth

Centerline		1 ft. Left		2 ft. Left	
Depth ft.	Velocity fps	Depth ft.	Velocity fps	Depth ft.	Velocity fps
0.040	0.528	0.040	0.566	0.050	0.447
0.045	0.547	0.050	0.602	0.060	0.447
0.050	0.547	0.060	0.618	0.070	0.468
0.055	0.547	0.070	0.634	0.080	0.468
0.060	0.547	0.080	0.650	0.090	0.509
0.070	0.547	0.090	0.695	0.100	0.489
0.080	0.566	0.100	0.695	0.120	0.566
0.090	0.634	0.120	0.708	0.140	0.566
0.100	0.618	0.140	0.722	0.160	0.566
0.110	0.650	0.160	0.749	0.180	0.634
0.120	0.695	0.180	0.749	0.200	0.650

7-2-4 (CONTD.)

0.130	0.695	0.200	0.775	0.220	0.650
0.140	0.695	0.220	0.788	0.240	0.680
0.160	0.695	0.240	0.813	0.260	0.695
0.180	0.749	0.260	0.837	0.280	0.695
0.200	0.749	0.280	0.837	0.300	0.695
0.220	0.749	0.300	0.813		
0.240	0.749				
0.260	0.788				
0.280	0.800				
0.300	0.837				

c. Vena Contracta

Centerline		0.5 ft. Left		1.0 ft. Left	
Depth ft.	Velocity fps	Depth ft.	Velocity fps	Depth ft.	Velocity fps
0.010	1.145	0.010	1.206	0.010	1.090
0.015	1.154	0.020	1.215	0.020	1.180
0.020	1.163	0.030	1.230	0.030	1.300
0.025	1.170	0.040	1.240	0.040	1.390
0.030	1.180	0.050	1.280	0.050	1.490
0.035	1.206	0.060	1.313	0.060	1.581
0.040	1.230	0.070	1.367	0.070	1.594
0.045	1.265	0.080	1.432	0.080	1.642
0.050	1.300	0.090	1.470	0.090	1.654
0.060	1.350	0.100	1.490	0.100	1.690
0.070	1.367	0.120	1.524	0.120	1.690
0.080	1.410	0.140	1.534	0.140	1.724
0.090	1.420	0.160	1.543	0.160	1.770
0.100	1.455	0.180	1.555	0.200	1.758
0.120	1.490	0.200	1.570	0.240	1.834
0.140	1.510	0.220	1.588		
0.160	1.517	0.240	1.618		
0.180	1.517	0.260	1.623		
0.200	1.524	0.280	1.642		
0.220	1.555				
0.240	1.550				
0.260	1.555				
0.280	1.570				

d. Minimum Depth

Centerline		1.0 ft. Left		1.5 ft. left		2.21 ft. Left	
Depth ft.	Velocity fps	Depth ft.	Velocity fps	Depth ft.	Velocity fps	Depth ft.	Velocity fps
0.010	0.695	0.010	0.915	0.010	0.447	0.010	0.200
0.015	0.708	0.020	1.036	0.020	0.425	0.020	0.200
0.020	0.722	0.030	1.162	0.030	0.425	0.030	0.200
0.025	0.749	0.040	1.265	0.040	0.400	0.040	0.200
0.030	0.775	0.050	1.280	0.050	0.400	0.060	0.200

7-2-4 (CONTD.)

0.035	0.850	0.060	1.360	0.060	0.347	0.080	0.200
0.040	0.936	0.070	1.542	0.070	0.347	0.100	0.200
0.045	0.980	0.080	1.618	0.080	0.347	0.120	0.200
0.050	0.980	0.090	1.735	0.090	0.347	0.160	0.200
0.060	1.170	0.100	1.770	0.100	0.347	0.200	0.200
0.070	1.265	0.120	1.835	0.120	0.347	0.240	0.200
0.080	1.420	0.140	1.813	0.140	0.347		
0.090	1.505	0.160	1.758	0.160	0.347		
0.100	1.570	0.180	1.758	0.200	0.347		
0.120	1.700	0.200	1.770	0.240	0.347		
0.140	1.780	0.220	1.687				
0.160	1.824	0.240	1.735				
0.200	1.940						
0.240	2.030						

B) Velocity Profile for Normal Depth Run No. 2

$Q = 2$ cfs; $S = 0.000131$; $y_n = 24.30$ cm.:

Centerline		1 ft. Left		2 ft. Left	
Depth ft.	Velocity fps	Depth ft.	Velocity fps	Depth ft.	Velocity fps
0.010	0.200	0.010	0.347	0.010	0.401
0.020	0.200	0.050	0.401	0.100	0.547
0.030	0.245	0.100	0.401	0.200	0.650
0.040	0.315	0.150	0.491	0.300	0.665
0.050	0.347	0.200	0.547	0.400	0.665
0.060	0.315	0.250	0.566	0.500	0.665
0.070	0.315	0.300	0.602	0.600	0.665
0.080	0.375	0.350	0.650	0.700	0.665
0.090	0.375	0.400	0.665		
0.100	0.401	0.500	0.665		
0.120	0.425	0.600	0.694		
0.140	0.447	0.700	0.722		
0.160	0.401				
0.180	0.491				
0.200	0.491				
0.240	0.510				
0.280	0.510				
0.320	0.566				
0.360	0.547				
0.400	0.566				
0.500	0.633				
0.600	0.633				
0.700	0.650				

7-2-4 (CONTD.)

C) Velocity Profile for Normal Depth Run No. 10

Q = 1 cfs; S = 0.00408; y_n = 5.35 cm.:

Centerline		1 ft. Left		2 ft. Left		2.23 ft. Left	
Depth ft.	Velocity fps	Depth ft.	Velocity fps	Depth ft.	Velocity fps	Depth ft.	Velocity fps
0.010	0.665	0.010	0.750	0.010	0.775	0.010	0.775
0.015	0.695	0.020	0.775	0.020	0.775	0.020	0.775
0.020	0.750	0.030	0.825	0.030	0.775	0.030	0.775
0.025	0.775	0.040	0.875	0.040	0.875	0.040	0.825
0.030	0.825	0.050	1.015	0.050	0.915	0.060	0.980
0.035	0.875	0.060	1.075	0.060	1.035	0.080	1.145
0.040	0.915	0.070	1.145	0.070	1.095	0.100	1.230
0.050	1.180	0.080	1.250	0.080	1.180	0.120	1.340
0.060	1.215	0.090	1.330	0.100	1.340	0.140	1.475
0.070	1.265	0.100	1.390	0.120	1.505		
0.080	1.340	0.120	1.505	0.140	1.550		
0.090	1.410	0.140	1.580				
0.100	1.475						
0.120	1.540						
0.140	1.630						

TABLE 7-3 GEOMETRY II RAW and CALCULATED DATA.

1	2	3	4	5	6	7	8	9	10	11	12	13
Run NO	M	$\vec{F}_n$	Q cfs	y_n cm	S_n	M'	$\frac{L_d b}{A_{n2}}$	y_1 cm	$\frac{h_1^*}{y_n}$	$(\frac{F_n^2}{M'})$	K	D
1	0.5	0.050	1.0	24.09	0.00003	0.464	0.	24.32	0.00955	0.01161	1.85832	0.50180
2	0.5	0.050	1.0	24.09	0.00003	0.464	4.1	24.29	0.00830	0.01161	1.64962	0.36721
3	0.5	0.050	1.0	24.09	0.00003	0.464	8.2	24.34	0.01038	0.01161	1.99746	0.56668
4	0.5	0.050	1.0	24.05	0.00003	0.464	8.2	24.24	0.00790	0.01161	1.57565	0.56668
5	0.5	0.050	1.0	24.05	0.00003	0.464	13.7	24.28	0.00956	0.01161	1.85299	0.56668
6	0.7	0.065	1.0	24.05	0.00003	0.675	0.	24.11	0.00249	0.00927	1.42707	0.50452
7	0.7	0.065	1.0	24.05	0.00003	0.675	3.9	24.13	0.00333	0.00927	1.72052	0.35816
8	0.7	0.065	1.0	24.05	0.00003	0.675	7.9	24.25	0.00832	0.00927	3.48124	0.56350
9	0.7	0.065	1.0	24.05	0.00003	0.675	10.5	24.23	0.00748	0.00927	3.18778	0.56350
10	0.7	0.065	1.0	24.05	0.00003	0.675	13.1	24.24	0.00790	0.00927	3.33451	0.56350
11	0.9	0.065	1.0	24.05	0.00003	0.882	0.	24.23	0.00748	0.00543	5.44274	0.55560
12	0.9	0.065	1.0	24.05	0.00003	0.882	3.9	24.25	0.00832	0.00543	5.94379	0.33751
13	0.9	0.065	1.0	24.05	0.00003	0.882	7.8	24.26	0.00873	0.00543	6.19431	0.55601
14	0.9	0.065	1.0	24.05	0.00003	0.882	10.3	24.27	0.00915	0.00543	6.44484	0.55601
15	0.9	0.065	1.0	24.05	0.00003	0.882	12.9	24.28	0.00956	0.00543	6.69536	0.55601
16	0.9	0.396	2.0	9.80	0.00230	0.896	0.	9.88	0.00816	0.19533	1.03396	0.46894
17	0.9	0.396	2.0	9.80	0.00230	0.896	9.4	9.98	0.01837	0.19533	1.12271	0.60811
18	0.9	0.396	2.0	9.80	0.00230	0.896	18.7	9.96	0.01633	0.19533	1.10491	0.60655
19	0.9	0.396	2.0	9.80	0.00230	0.896	25.0	9.98	0.01837	0.19533	1.12271	0.60655
20	0.9	0.396	2.0	9.80	0.00233	0.896	31.2	9.90	0.01020	0.19533	1.05166	0.
21	0.7	0.396	2.0	9.80	0.00233	0.695	31.3	11.36	0.15918	0.32465	1.44173	0.
22	0.7	0.396	2.0	9.80	0.00233	0.695	25.1	11.35	0.15816	0.32465	1.43601	0.81028
23	0.7	0.396	2.0	9.80	0.00233	0.695	18.8	11.26	0.14898	0.32465	1.38466	0.81028
24	0.7	0.396	2.0	9.80	0.00233	0.695	9.4	11.05	0.12755	0.32465	1.26550	0.61588
25	0.7	0.396	2.0	9.80	0.00233	0.695	0.	10.77	0.09898	0.32465	1.10816	0.46325
26	0.5	0.396	2.0	9.80	0.00233	0.495	0.	13.30	0.35714	0.64000	1.30955	0.45577
27	0.5	0.396	2.0	9.80	0.00233	0.495	31.4	14.55	0.48469	0.64000	1.69398	0.
28	0.5	0.396	2.0	9.80	0.00233	0.495	25.1	14.55	0.48469	0.64000	1.69398	1.19302
29	0.5	0.396	2.0	9.80	0.00233	0.495	18.8	14.34	0.46327	0.64000	1.62892	1.19302
30	0.3	0.393	2.0	9.80	0.00233	0.291	0.	19.53	0.99286	1.82389	1.13038	0.44446
31	0.3	0.393	2.0	9.80	0.00233	0.291	9.6	23.12	1.35918	1.82389	1.53068	0.64304
32	0.3	0.393	2.0	9.80	0.00233	0.291	19.2	23.09	1.35612	1.82389	1.52732	2.16718
33	0.3	0.393	2.0	9.80	0.00233	0.291	25.6	22.65	1.31122	1.82389	1.47808	0.
34	0.3	0.393	2.0	9.80	0.00233	0.291	32.1	22.65	1.31122	1.82389	1.47808	0.
35	0.5	0.393	2.0	9.80	0.00233	0.463	0.	25.80	1.63265	0.72048	4.63614	0.45447
36	0.5	0.393	2.0	9.80	0.00013	0.463	0.	25.80	1.63265	0.72048	4.63614	0.45447
37	0.5	0.393	2.0	9.80	0.00013	0.463	10.1	25.75	1.62755	0.72048	4.62191	0.62828
38	0.5	0.393	2.0	9.80	0.00013	0.463	20.2	25.88	1.64082	0.72048	4.65891	1.27635
39	0.5	0.393	2.0	9.80	0.00013	0.463	26.9	25.91	1.64388	0.72048	4.66745	0.
40	0.5	0.393	2.0	9.80	0.00013	0.463	33.6	25.96	1.64898	0.72048	4.68168	0.
41	0.3	0.155	1.0	9.88	0.00071	0.291	0.	13.33	0.34919	0.44904	1.64844	0.45966
42	0.3	0.155	1.0	9.88	0.00071	0.291	9.5	14.47	0.46457	0.44904	2.16624	0.62090
43	0.3	0.155	1.0	9.88	0.00071	0.291	19.1	14.15	0.43219	0.44904	2.02069	0.97483
44	0.3	0.155	1.0	9.88	0.00071	0.291	25.4	14.62	0.47976	0.44904	2.23452	0.97483
45	0.3	0.155	1.0	9.88	0.00071	0.291	31.8	14.38	0.45547	0.44904	2.12529	0.
46	0.5	0.155	1.0	9.88	0.00071	0.495	0.	10.97	0.11032	0.15519	1.69444	0.47153
47	0.5	0.155	1.0	9.88	0.00071	0.495	18.7	11.13	0.12652	0.15519	1.90135	0.53200
48	0.5	0.155	1.0	9.88	0.00071	0.495	24.9	11.24	0.13765	0.15519	2.04376	0.53200
49	0.5	0.155	1.0	9.88	0.00071	0.495	31.2	11.28	0.14170	0.15519	2.09558	0.
50	0.3	0.250	2.0	13.40	0.00085	0.282	0.	20.64	0.54030	0.78593	1.48359	0.45353
51	0.3	0.250	2.0	13.40	0.00085	0.282	7.3	23.60	0.76119	0.78593	2.06425	0.58627
52	0.3	0.250	2.0	13.40	0.00085	0.282	14.5	23.33	0.74104	0.78593	2.01113	0.62965

Contd.

1 Run No	2 M^{*}	3 F_n	4 Q cfs	5 y_n cms	6 S_n	7 M'	8 $\frac{L_{db}}{A_{n2}}$	9 y_1 cms	10* $\frac{h_1}{y_n}$	11 $(\frac{F_n}{M'})^2$	12 K	13 D
53	0.3	0.250	2.0	13.40	0.00085	0.282	19.4	15.73	0.17388	0.78593	0.53376	1.34120
54	0.5	0.250	2.0	13.40	0.00085	0.489	7.0	15.70	0.17164	0.26137	1.58778	0.51884
55	0.5	0.250	2.0	13.40	0.00085	0.489	14.0	15.91	0.18731	0.26137	1.70819	0.61255
56	0.5	0.250	2.0	13.40	0.00085	0.489	18.6	15.98	0.19254	0.26137	1.74837	0.71609
57	0.5	0.250	2.0	13.40	0.00085	0.489	23.3	16.02	0.19552	0.26137	1.77134	0.71609
58	0.7	0.250	2.0	13.40	0.00085	0.694	22.9	14.11	0.05299	0.12977	1.37853	0.48043
59	0.7	0.250	2.0	13.40	0.00085	0.694	18.4	14.11	0.05299	0.12977	1.37853	0.48043
60	0.7	0.250	2.0	13.40	0.00085	0.694	13.8	14.10	0.05224	0.12977	1.36720	0.60192
61	0.7	0.250	2.0	13.40	0.00085	0.694	6.9	13.98	0.04328	0.12977	1.23131	0.48004
62	0.7	0.250	2.0	13.40	0.00085	0.694	0.	13.98	0.04328	0.12977	1.23131	0.47356
63	0.5	0.141	3.0	25.38	0.00029	0.461	0.	26.97	0.06265	0.09355	1.57646	0.47730
64	0.5	0.141	3.0	25.38	0.00029	0.461	3.9	26.72	0.05280	0.09355	1.36834	0.46291
65	0.5	0.141	3.0	25.38	0.00029	0.461	7.8	27.09	0.06738	0.09355	1.67639	0.59702
66	0.5	0.141	3.0	25.38	0.00029	0.461	10.4	27.23	0.07289	0.09355	1.79302	0.59702
67	0.5	0.141	3.0	25.38	0.00029	0.461	13.0	27.35	0.07762	0.09355	1.89301	0.59702
68	0.7	0.141	3.0	25.38	0.00029	0.674	12.5	25.94	0.02206	0.04376	1.53866	0.58579
69	0.7	0.141	3.0	25.38	0.00029	0.674	10.0	25.89	0.02009	0.04376	1.44989	0.58579
70	0.7	0.141	3.0	25.38	0.00029	0.674	7.5	25.90	0.02049	0.04376	1.46764	0.58579
71	0.7	0.141	3.0	25.38	0.00029	0.674	3.7	25.88	0.01970	0.04376	1.43214	0.42548
72	0.7	0.141	3.0	25.38	0.00029	0.674	0.	25.76	0.01497	0.04376	1.21915	0.48608
73	0.5	0.300	3.0	15.45	0.00123	0.487	0.	19.10	0.23625	0.37948	1.46843	0.46152
74	0.5	0.300	3.0	15.45	0.00123	0.487	6.1	19.36	0.25307	0.37948	1.55479	0.54076
75	0.5	0.300	3.0	15.45	0.00123	0.487	12.2	19.80	0.28155	0.37948	1.70139	0.61829
76	0.5	0.300	3.0	15.45	0.00123	0.487	16.2	19.89	0.28738	0.37948	1.73144	0.88565
77	0.5	0.300	3.0	15.45	0.00123	0.487	20.3	19.99	0.29385	0.37948	1.76486	0.88565
78	0.7	0.300	3.0	15.45	0.00123	0.690	20.0	16.76	0.08479	0.18904	1.40929	0.59533
79	0.7	0.300	3.0	15.45	0.00123	0.690	16.0	16.71	0.08155	0.18904	1.37694	0.59533
80	0.7	0.300	3.0	15.45	0.00123	0.690	12.0	16.60	0.07443	0.18904	1.30587	0.60761
81	0.7	0.300	3.0	15.45	0.00123	0.690	6.0	16.39	0.06084	0.18904	1.17054	0.50051
82	0.7	0.300	3.0	15.45	0.00123	0.690	0.	16.34	0.05761	0.18904	1.13839	0.46930
83	0.7	0.300	3.0	15.45	0.00294	0.690	0.	16.34	0.05761	0.18904	1.13839	0.46930
84	0.5	0.450	3.0	11.61	0.00294	0.493	0.	17.40	0.49871	0.83317	1.30688	0.45289
85	0.5	0.450	3.0	11.61	0.00294	0.493	8.0	18.46	0.59001	0.83317	1.50788	0.63057
86	0.5	0.450	3.0	11.61	0.00294	0.493	16.0	18.39	0.58398	0.83317	1.49452	1.38657
87	0.5	0.450	3.0	11.61	0.00294	0.493	21.3	18.83	0.62188	0.83317	1.57860	1.38657
88	0.5	0.450	3.0	11.61	0.00294	0.493	26.6	18.80	0.61929	0.83317	1.57286	0.
89	0.7	0.450	3.0	11.61	0.00294	0.693	26.5	14.06	0.21102	0.42166	1.37707	0.
90	0.7	0.450	3.0	11.61	0.00294	0.693	21.2	14.01	0.20672	0.42166	1.35980	0.94049
91	0.7	0.450	3.0	11.61	0.00294	0.693	15.9	13.99	0.20500	0.42166	1.35289	0.94049
92	0.7	0.450	3.0	11.61	0.00294	0.693	8.0	13.86	0.19380	0.42166	1.30816	0.61992
93	0.3	0.200	1.0	10.00	0.00013	0.292	9.4	14.46	0.44600	0.46913	2.17263	0.62158
94	0.3	0.250	2.0	13.42	0.00018	0.282	4.8	21.03	0.56706	0.78593	1.56053	0.58627
95	0.3	0.100	1.0	14.83	0.00014	0.278	13.3	17.00	0.14633	0.12939	2.13037	0.60188
96	0.5	0.100	1.0	14.83	0.00014	0.487	12.7	15.37	0.03641	0.04216	1.83795	0.58524
97	0.3	0.300	2.0	11.48	0.00130	0.288	8.3	23.42	1.04007	1.08507	1.84615	0.63474
98	0.3	0.300	2.0	11.48	0.00130	0.492	9.7	14.87	0.29530	0.37180	1.68302	0.61797
99	0.3	0.400	2.0	9.80	0.00230	0.290	1.6	20.12	1.05306	1.90250	1.18769	0.64672
100	0.3	0.400	2.0	9.77	0.00014	0.290	9.7	22.90	1.34391	1.90250	1.48994	0.64372
101	0.5	0.400	3.0	12.65	0.00230	0.490	7.4	18.48	0.46087	0.66639	1.52493	0.57563
102	0.7	0.400	3.0	12.65	0.00230	0.694	24.3	14.64	0.15731	0.33220	1.38322	0.82096
103	0.9	0.400	3.0	12.65	0.00230	0.895	7.3	12.89	0.01897	0.19974	1.11666	0.50358
104	0.5	0.300	3.0	15.39	0.00021	0.468	21.2	20.04	0.30214	0.41091	1.65183	0.92675
105	0.5	0.300	3.0	15.39	0.00021	0.486	20.4	20.04	0.30214	0.38104	1.78134	0.88773
106	0.7	0.300	3.0	15.39	0.00021	0.691	20.1	16.65	0.08187	0.18849	1.37374	0.59435
107	0.9	0.300	3.0	15.39	0.00021	0.892	20.0	15.52	0.00845	0.11311	1.09089	0.44425
108	0.5	0.150	3.0	25.48	0.00028	0.460	13.0	27.50	0.07928	0.10633	1.93592	0.59893
109	0.7	0.150	3.0	25.48	0.00028	0.674	12.4	25.95	0.01845	0.04953	1.38570	0.58760
110	0.9	0.150	3.0	25.48	0.00028	0.879	3.7	25.58	0.00392	0.02912	1.23120	0.40667
111	0.5	0.100	3.0	32.87	0.00012	0.428	10.8	34.28	0.04290	0.05459	1.93374	0.58903
112	0.7	0.100	3.0	32.87	0.00012	0.654	6.0	33.12	0.00761	0.02338	1.22242	0.39688
113	0.5	0.200	3.0	20.12	0.00050	0.476	15.9	23.02	0.14414	0.17654	1.85821	0.57257
114	0.7	0.200	3.0	20.12	0.00050	0.684	15.5	20.95	0.04125	0.08550	1.49325	0.37874
115	0.5	0.250	3.0	17.63	0.00085	0.482	17.9	21.14	0.19909	0.26902	1.76663	0.72795
116	0.7	0.250	3.0	17.63	0.00085	0.688	17.6	18.58	0.05389	0.13204	1.37868	0.48521
117	0.9	0.250	3.0	17.63	0.00085	0.890	17.5	17.66	0.00170	0.07890	0.99312	0.36180

TABLE 7-4 GEOMETRY III RAW and CALCULATED DATA.

1	2	3	4	5	6	7	8	9	10	11	12	13	14
Run No	M	F_n	Q cfs	y_n cm	S_n	M'	Φ_1	y_1 cm	$\frac{h_1^*}{y_n}$	$(\frac{F_n}{M'})^2$	K	D	$(\frac{h_1^*}{y_n})(\frac{M'}{F_n})^2$
W-1-1	0.5	0.096	3.0	32.70	0.00012	0.427	30.00	33.56	0.02630	0.05049	1.03070	0.23441	0.521
	0.5	0.096	3.0	32.70	0.00012	0.427	45.00	33.63	0.02844	0.05049	1.11463	0.27311	0.563
	0.5	0.096	3.0	32.70	0.00012	0.427	60.00	33.71	0.03089	0.05049	1.21055	0.35825	0.612
	0.5	0.096	3.0	32.70	0.00012	0.427	90.00	33.76	0.03242	0.05049	1.27051	0.37485	0.642
W-1-2	0.7	0.096	3.0	32.70	0.00012	0.652	30.00	33.90	0.03670	0.02166	3.35284	0.22092	1.694
	0.7	0.096	3.0	32.70	0.00012	0.652	45.00	32.94	0.00734	0.02166	0.67026	0.26626	0.339
	0.7	0.096	3.0	32.70	0.00012	0.652	90.00	32.95	0.00765	0.02166	0.69819	0.35389	0.353
W-1-3	0.7	0.147	3.0	24.65	0.00028	0.674	30.00	24.88	0.00933	0.04741	0.38360	0.23338	0.197
	0.7	0.147	3.0	24.65	0.00028	0.674	45.00	24.98	0.01339	0.04741	0.55047	0.27259	0.282
	0.7	0.147	3.0	24.65	0.00028	0.674	90.00	24.98	0.01339	0.04741	0.55047	0.37325	0.282
W-1-4	0.5	0.147	3.0	24.65	0.00028	0.462	30.00	25.87	0.04949	0.10092	0.95725	0.24605	0.490
	0.5	0.147	3.0	24.65	0.00028	0.462	45.00	26.12	0.05963	0.10092	1.15381	0.27884	0.591
	0.5	0.147	3.0	24.65	0.00028	0.462	60.00	26.21	0.06329	0.10092	1.22460	0.38129	0.627
	0.5	0.147	3.0	24.65	0.00028	0.462	90.00	26.27	0.06572	0.10092	1.27180	0.39293	0.651
W-1-5	0.5	0.201	3.0	20.00	0.00048	0.476	30.00	22.23	0.11150	0.17818	1.19983	0.25604	0.626
	0.5	0.201	3.0	20.00	0.00048	0.476	45.00	21.00	0.05000	0.17818	0.53600	0.28364	0.281
	0.5	0.201	3.0	20.00	0.00048	0.476	60.00	20.12	0.00600	0.17818	0.06412	0.40130	0.034
	0.5	0.201	3.0	20.00	0.00048	0.476	90.00	20.24	0.01200	0.17818	0.12830	0.40841	0.067
W-1-6	0.7	0.201	3.0	20.00	0.00048	0.683	30.00	20.35	0.01750	0.08639	0.38606	0.24339	0.203
	0.7	0.201	3.0	20.00	0.00048	0.683	45.00	20.42	0.02100	0.08639	0.46339	0.27754	0.243
	0.7	0.201	3.0	20.00	0.00048	0.683	60.00	20.48	0.02400	0.08639	0.52971	0.37599	0.278
	0.7	0.201	3.0	20.00	0.00048	0.683	90.00	20.48	0.02400	0.08639	0.52971	0.38879	0.278
	0.9	0.201	3.0	20.00	0.00048	0.887	30.00	20.12	0.00600	0.05123	0.22302	0.23465	0.117
	0.9	0.201	3.0	20.00	0.00048	0.887	90.00	20.11	0.00550	0.05123	0.20443	0.37522	0.107
W-1-7	0.3	0.194	1.0	9.82	0.00050	0.290	30.00	12.28	0.25051	0.44869	1.08015	0.27314	0.558
	0.3	0.194	1.0	9.82	0.00050	0.290	45.00	12.69	0.29226	0.44869	1.26214	0.29160	0.651
	0.3	0.194	1.0	9.82	0.00050	0.290	60.00	12.89	0.31263	0.44869	1.35106	0.43608	0.697
	0.3	0.194	1.0	9.82	0.00050	0.290	90.00	13.15	0.33910	0.44869	1.46677	0.43488	0.756
W-2-1	0.5	0.250	3.0	17.27	0.00084	0.482	30.00	19.01	0.10075	0.26938	0.69935	0.26356	0.374
	0.5	0.250	3.0	17.27	0.00084	0.482	45.00	19.49	0.12855	0.26938	0.89451	0.28717	0.477
	0.5	0.250	3.0	17.27	0.00084	0.482	60.00	19.92	0.15345	0.26938	1.07002	0.41651	0.570
	0.5	0.250	3.0	17.27	0.00084	0.482	90.00	20.28	0.17429	0.26938	1.21742	0.42005	0.647
W-2-2	0.7	0.250	3.0	17.27	0.00084	0.687	30.00	17.37	0.00579	0.13245	0.08092	0.25078	0.044
	0.7	0.250	3.0	17.27	0.00084	0.687	45.00	17.85	0.03358	0.13245	0.47087	0.28112	0.254
	0.7	0.250	3.0	17.27	0.00084	0.687	60.00	17.88	0.03532	0.13245	0.49532	0.39073	0.267
	0.7	0.250	3.0	17.27	0.00084	0.687	90.00	17.94	0.03880	0.13245	0.54425	0.40026	0.293
	0.9	0.250	3.0	17.27	0.00084	0.890	30.00	17.37	0.00579	0.07896	0.13575	0.24186	0.073
	0.9	0.250	3.0	17.27	0.00084	0.890	90.00	17.40	0.00753	0.07896	0.17651	0.38642	0.095
W-2-3	0.7	0.299	3.0	15.32	0.00123	0.690	30.00	15.81	0.03198	0.18824	0.30495	0.25703	0.170
	0.7	0.299	3.0	15.32	0.00123	0.690	45.00	15.92	0.03916	0.18824	0.37385	0.28410	0.208
	0.7	0.299	3.0	15.32	0.00123	0.690	60.00	16.09	0.05026	0.18824	0.48062	0.40329	0.267
	0.7	0.299	3.0	15.32	0.00123	0.690	90.00	16.16	0.05483	0.18824	0.52469	0.40994	0.291
W-2-5	0.5	0.299	3.0	15.32	0.00123	0.486	30.00	17.66	0.15274	0.37964	0.73454	0.	0.402
	0.5	0.299	3.0	15.32	0.00123	0.486	45.00	17.93	0.17037	0.37964	0.82101	0.29015	0.449
	0.5	0.299	3.0	15.32	0.00123	0.486	60.00	18.48	0.20627	0.37964	0.99801	0.42957	0.543
	0.5	0.299	3.0	15.32	0.00123	0.486	90.00	18.85	0.23042	0.37964	1.11768	0.42997	0.607
W-2-7	0.9	0.299	3.0	15.32	0.00123	0.892	30.00	15.38	0.00392	0.11258	0.06214	0.24794	0.035
	0.9	0.299	3.0	15.32	0.00123	0.892	90.00	15.39	0.00457	0.11258	0.07250	0.39586	0.041

7- 4 COntd.

1 Run No.	2 M	3 Fn	4 Q cfs	5 y_n cm	6 S_n	7 M'	8 ϕ_1	9 y_1 cm	10 $\frac{h_1^*}{y_n}$	11 $(\frac{F_n}{M'})^2$	12 K	13 D	14 $(\frac{h_1^*}{y_n})(\frac{M'}{F_n})^2$
W-2-8	0.5	0.394	3.0	12.76	0.00220	0.490	30.00	16.82	0.31818	0.64533	0.86364	0.28018	0.493
	0.5	0.394	3.0	12.76	0.00220	0.490	45.00	17.07	0.33777	0.64533	0.91953	0.29480	0.523
	0.5	0.394	3.0	12.76	0.00220	0.490	60.00	17.12	0.34169	0.64533	0.93074	0.45058	0.529
	0.5	0.394	3.0	12.76	0.00220	0.490	90.00	17.43	0.36599	0.64533	1.00038	0.44576	0.567
	0.7	0.394	3.0	12.76	0.00220	0.693	30.00	13.74	0.07680	0.32291	0.39638	0.26692	0.238
	0.7	0.394	3.0	12.76	0.00220	0.693	45.00	13.82	0.08307	0.32291	0.42947	0.28874	0.257
	0.7	0.394	3.0	12.76	0.00220	0.693	60.00	13.89	0.08856	0.32291	0.45850	0.42336	0.274
	0.7	0.394	3.0	12.76	0.00220	0.693	90.00	14.01	0.09796	0.32291	0.50845	0.42526	0.303
	0.9	0.394	3.0	12.76	0.00220	0.895	30.00	12.81	0.00392	0.19382	0.03295	0.25755	0.020
	0.9	0.394	3.0	12.76	0.00220	0.895	90.00	12.84	0.00627	0.19382	0.05276	0.41075	0.032
W-3-1	0.5	0.507	3.0	10.78	0.00360	0.493	30.00	12.76	0.18367	1.05808	0.26365	0.29004	0.174
	0.5	0.507	3.0	10.78	0.00360	0.493	45.00	12.89	0.19573	1.05808	0.28227	0.29921	0.185
	0.5	0.507	3.0	10.78	0.00360	0.493	60.00	13.00	0.20594	1.05808	0.29811	0.47109	0.195
	0.5	0.507	3.0	10.78	0.00360	0.493	90.00	17.18	0.59369	1.05808	0.94530	0.46101	0.561
	0.7	0.507	3.0	10.78	0.00360	0.695	30.00	12.76	0.18367	0.53249	0.52389	0.27643	0.345
	0.7	0.507	3.0	10.78	0.00360	0.695	45.00	12.89	0.19573	0.53249	0.56088	0.29311	0.368
	0.7	0.507	3.0	10.78	0.00360	0.695	60.00	13.00	0.20594	0.53249	0.59237	0.44286	0.387
	0.7	0.507	3.0	10.78	0.00360	0.695	90.00	13.09	0.21429	0.53249	0.61826	0.43998	0.402
	0.9	0.507	3.0	10.78	0.00360	0.896	30.00	10.96	0.01670	0.32033	0.07285	0.26677	0.052
	0.9	0.507	3.0	10.78	0.00360	0.896	90.00	11.06	0.02597	0.32033	0.11398	0.42503	0.081
W-3-3	0.3	0.406	2.0	9.54	0.00360	0.291	30.00	18.26	0.91405	1.94996	0.86368	0.30273	0.469
	0.3	0.406	2.0	9.54	0.00360	0.291	45.00	18.81	0.97170	1.94996	0.92122	0.30474	0.498
	0.3	0.406	2.0	9.54	0.00360	0.291	60.00	18.97	0.98847	1.94996	0.93798	0.49773	0.507
	0.3	0.406	2.0	9.54	0.00360	0.291	90.00	19.24	1.01677	1.94996	0.96629	0.48058	0.521
W-3-4	0.3	0.394	2.0	9.74	0.00220	0.290	30.00	18.55	0.90452	1.83732	0.91127	0.30147	0.492
	0.3	0.394	2.0	9.74	0.00220	0.290	45.00	18.90	0.94045	1.83732	0.94936	0.30420	0.512
	0.3	0.394	2.0	9.74	0.00220	0.290	60.00	19.14	0.96509	1.83732	0.97551	0.49508	0.525
	0.3	0.394	2.0	9.74	0.00220	0.290	90.00	19.30	0.98152	1.83732	0.99296	0.47863	0.534
W-3-5	0.3	0.301	2.0	11.66	0.00135	0.289	30.00	17.85	0.53087	1.07956	0.92591	0.29045	0.492
	0.3	0.301	2.0	11.66	0.00135	0.289	45.00	18.29	0.56861	1.07956	0.99378	0.29939	0.527
	0.3	0.301	2.0	11.66	0.00135	0.289	60.00	18.90	0.62093	1.07956	1.08811	0.47194	0.575
	0.3	0.301	2.0	11.66	0.00135	0.289	90.00	19.65	0.68525	1.07956	1.20441	0.46164	0.635
W-4-1	0.3	0.232	1.0	8.73	0.00088	0.292	30.00	11.85	0.35739	0.62957	1.08843	0.27969	0.568
	0.3	0.232	1.0	8.73	0.00088	0.292	45.00	12.09	0.38488	0.62957	1.17358	0.29458	0.611
	0:3	0.232	1.0	8.73	0.00088	0.292	60.00	12.25	0.40321	0.62957	1.23041	0.44958	0.640
	0.3	0.232	1.0	8.73	0.00088	0.292	90.00	12.58	0.44101	0.62957	1.34780	0.44501	0.700
W-4-2	0.3	0.131	1.0	12.80	0.00031	0.283	30.00	13.68	0.06875	0.21297	0.63365	0.25926	0.323
	0.3	0.131	1.0	12.80	0.00031	0.283	45.00	13.97	0.09141	0.21297	0.84295	0.28516	0.429
	0.3	0.131	1.0	12.80	0.00031	0.283	60.00	14.13	0.10391	0.21297	0.95852	0.40780	0.488
	0.3	0.131	1.0	12.80	0.00031	0.283	90.00	14.40	0.12500	0.21297	1.15368	0.41340	0.587
W-4-3	0.3	0.103	1.0	14.96	0.00014	0.276	30.00	16.23	0.08489	0.13993	1.19957	0.25175	0.607
	0.3	0.103	1.0	14.96	0.00014	0.276	45.00	16.52	0.10428	0.13993	1.47393	0.28159	0.745
	0.3	0.103	1.0	14.96	0.00014	0.276	60.00	16.63	0.11163	0.13993	1.57803	0.39267	0.798
	0.3	0.103	1.0	14.96	0.00014	0.276	90.00	16.73	0.11832	0.13993	1.67269	0.40176	0.846

TABLE 7-5 - GEOMETRY IV RAW and CALCULATED DATA.

1	2	3	4	5	6	7	8	9	10	11	12	13	14
Run No	M	F_n	Q	y_n	S_n	M'	e	y_1	$\frac{h_1^*}{y_n}$	$(\frac{F_n}{M'})^2$	K	D	$(\frac{h_1^*}{y_n})(\frac{M'}{F_n})^2$
			cfs	cm				cm					
E-2-1	0.3	0.108	1.0	14.57	0.00014	0.278	0.	16.70	0.14619	0.15004	1.92652	0.55879	0.974
	0.3	0.108	1.0	14.57	0.00014	0.278	0.80	16.66	0.14345	0.15004	1.89027	0.62400	0.956
	0.3	0.108	1.0	14.57	0.00014	0.278	0.85	16.68	0.14482	0.15004	1.90840	0.56346	0.965
	0.3	0.108	1.0	14.57	0.00014	0.278	0.90	16.69	0.14550	0.15004	1.91746	0.57252	0.970
	0.3	0.108	1.0	14.57	0.00014	0.278	0.95	16.69	0.14550	0.15004	1.91746	0.58354	0.970
	0.3	0.108	1.0	14.57	0.00014	0.278	1.00	16.85	0.15649	0.15004	2.06250	0.62834	1.043
E-2-3	0.3	0.151	1.0	11.63	0.00038	0.286	0.	14.52	0.24850	0.27786	1.75339	0.55687	0.894
	0.3	0.151	1.0	11.63	0.00038	0.286	0.80	14.51	0.24764	0.27786	1.74729	0.62124	0.891
	0.3	0.151	1.0	11.63	0.00038	0.286	0.85	14.59	0.25451	0.27786	1.79611	0.56107	0.916
	0.3	0.151	1.0	11.63	0.00038	0.286	0.90	14.48	0.24506	0.27786	1.72898	0.56376	0.882
	0.3	0.151	1.0	11.63	0.00038	0.286	0.95	14.53	0.24936	0.27786	1.75949	0.57760	0.897
	0.3	0.151	1.0	11.63	0.00038	0.286	1.00	14.70	0.26397	0.27786	1.86326	0.61759	0.950
E-3-1	0.3	0.196	1.0	9.78	0.00060	0.290	0.	13.51	0.38139	0.45397	1.63208	0.55534	0.840
	0.3	0.196	1.0	9.78	0.00060	0.290	0.80	13.41	0.37117	0.45397	1.58783	0.61905	0.818
	0.3	0.196	1.0	9.78	0.00060	0.290	0.85	13.52	0.38241	0.45397	1.63651	0.55917	0.842
	0.3	0.196	1.0	9.78	0.00060	0.290	0.90	13.42	0.37219	0.45397	1.59226	0.55689	0.820
	0.3	0.196	1.0	9.78	0.00060	0.290	0.95	13.47	0.37730	0.45397	1.61438	0.57292	0.831
	0.3	0.196	1.0	9.78	0.00060	0.290	1.00	13.94	0.42536	0.45397	1.82257	0.60916	0.937
E-3-3	0.3	0.243	1.0	8.46	0.00110	0.293	0.	12.89	0.52364	0.68956	1.46019	0.55404	0.759
	0.3	0.243	1.0	8.46	0.00110	0.293	0.80	12.89	0.52364	0.68956	1.46019	0.61719	0.759
	0.3	0.243	1.0	8.46	0.00110	0.293	0.85	12.91	0.52600	0.68956	1.46691	0.55756	0.763
	0.3	0.243	1.0	8.46	0.00110	0.293	0.90	12.94	0.52955	0.68956	1.47699	0.55110	0.768
	0.3	0.243	1.0	8.46	0.00110	0.293	0.95	12.91	0.52600	0.68956	1.46691	0.56895	0.763
	0.3	0.243	1.0	8.46	0.00110	0.293	1.00	13.25	0.56619	0.68956	1.58123	0.60207	0.821
E-3-5	0.3	0.316	2.0	11.27	0.00120	0.287	0.	20.34	0.80479	1.21396	1.25734	0.55229	0.663
	0.3	0.316	2.0	11.27	0.00120	0.287	0.80	20.27	0.79858	1.21396	1.24732	0.61468	0.658
	0.3	0.316	2.0	11.27	0.00120	0.287	0.85	20.38	0.80834	1.21396	1.26307	0.55539	0.666
	0.3	0.316	2.0	11.27	0.00120	0.287	0.90	20.38	0.80834	1.21396	1.26307	0.54336	0.666
	0.3	0.316	2.0	11.27	0.00120	0.287	0.95	20.38	0.80834	1.21396	1.26307	0.56364	0.666
	0.3	0.316	2.0	11.27	0.00120	0.287	1.00	20.94	0.85803	1.21396	1.34334	0.59261	0.707
E-4-1	0.3	0.407	2.0	9.52	0.00210	0.291	0.	19.88	1.08824	1.96174	1.03119	0.55080	0.555
	0.3	0.407	2.0	9.52	0.00210	0.291	0.80	19.99	1.09979	1.96174	1.04271	0.61256	0.561
	0.3	0.407	2.0	9.52	0.00210	0.291	0.85	20.02	1.10294	1.96174	1.04585	0.55356	0.562
	0.3	0.407	2.0	9.52	0.00210	0.291	0.90	20.06	1.10714	1.96174	1.05005	0.53688	0.564
	0.3	0.407	2.0	9.52	0.00210	0.291	0.95	20.21	1.12290	1.96174	1.06577	0.55917	0.572
	0.3	0.407	2.0	9.52	0.00210	0.291	1.00	20.74	1.17857	1.96174	1.12139	0.58470	0.601
E-4-3	0.3	0.497	2.0	8.34	0.00360	0.293	0.	19.56	1.34532	2.87497	0.85155	0.54963	0.468
	0.3	0.497	2.0	8.34	0.00360	0.293	0.80	19.56	1.34532	2.87497	0.85155	0.61087	0.468
	0.3	0.497	2.0	8.34	0.00360	0.293	0.85	19.91	1.38729	2.87497	0.88009	0.55210	0.483
	0.3	0.497	2.0	8.34	0.00360	0.293	0.90	19.72	1.36451	2.87497	0.86459	0.53177	0.475
	0.3	0.497	2.0	8.34	0.00360	0.293	0.95	19.77	1.37050	2.87497	0.86867	0.55563	0.477
	0.3	0.497	2.0	8.34	0.00360	0.293	1.00	20.53	1.46163	2.87497	0.93073	0.57848	0.508
E-5-1	0.7	0.094	3.0	33.09	0.00012	0.651	0.	33.38	0.00876	0.02098	0.82654	0.56498	0.418
	0.7	0.094	3.0	33.09	0.00012	0.651	0.80	33.36	0.00816	0.02098	0.76953	0.63290	0.389
	0.7	0.094	3.0	33.09	0.00012	0.651	0.85	33.37	0.00846	0.02098	0.79803	0.57116	0.403
	0.7	0.094	3.0	33.09	0.00012	0.651	0.90	33.43	0.01027	0.02098	0.96907	0.60138	0.490
	0.7	0.094	3.0	33.09	0.00012	0.651	0.95	33.40	0.00937	0.02098	0.88355	0.60291	0.446
	0.7	0.094	3.0	33.09	0.00012	0.651	1.00	33.46	0.01118	0.02098	1.05459	0.66392	0.533

7-5 Contd.

1 Run No.	2 M	3 F_n	4 Q cfs	5 y_n cm	6 S_n	7 M'	8 e	9 y_1 cm	10 $\frac{h_1^*}{y_n}$	11 $(\frac{F_n}{M'})^2$	12 K	13 D	14 $(\frac{h_1^*}{y_n})(\frac{M'}{F_n})^2$
E-5-3	0.5	0.094	3.0	33.09	0.00012	0.425	0.	34.30	0.03657	0.04922	1.47087	0.56229	0.743
	0.5	0.094	3.0	33.09	0.00012	0.425	0.80	34.27	0.03566	0.04922	1.43439	0.62903	0.725
	0.5	0.094	3.0	33.09	0.00012	0.425	0.85	34.28	0.03596	0.04922	1.44655	0.56781	0.731
	0.5	0.094	3.0	33.09	0.00012	0.425	0.90	34.29	0.03626	0.04922	1.45871	0.58869	0.737
	0.5	0.094	3.0	33.09	0.00012	0.425	0.95	34.33	0.03747	0.04922	1.50736	0.59444	0.761
	0.5	0.094	3.0	33.09	0.00012	0.425	1.00	34.39	0.03929	0.04922	1.58034	0.64826	0.798
E-6-1	0.5	0.142	3.0	25.19	0.00027	0.460	0.	26.85	0.06590	0.09533	1.35211	0.56021	0.691
	0.5	0.142	3.0	25.19	0.00027	0.460	0.80	26.90	0.06788	0.09533	1.39293	0.62604	0.712
	0.5	0.142	3.0	25.19	0.00027	0.460	0.85	26.94	0.06947	0.09533	1.42558	0.56523	0.729
	0.5	0.142	3.0	25.19	0.00027	0.460	0.90	26.94	0.06947	0.09533	1.42558	0.57904	0.729
	0.5	0.142	3.0	25.19	0.00027	0.460	0.95	27.01	0.07225	0.09533	1.48273	0.58795	0.758
	0.5	0.142	3.0	25.19	0.00027	0.460	1.00	27.06	0.07424	0.09533	1.52356	0.63637	0.779
E-6-3	0.5	0.142	3.0	25.19	0.00027	0.460	0.	25.71	0.02064	0.09533	0.42292	0.56021	0.217
	0.5	0.142	3.0	25.19	0.00027	0.460	0.80	25.71	0.02064	0.09533	0.42292	0.62604	0.217
	0.5	0.142	3.0	25.19	0.00027	0.460	0.85	25.71	0.02064	0.09533	0.42292	0.56523	0.217
	0.5	0.142	3.0	25.19	0.00027	0.460	0.90	25.71	0.02064	0.09533	0.42292	0.57904	0.217
	0.5	0.142	3.0	25.19	0.00027	0.460	0.95	25.68	0.01945	0.09533	0.39850	0.58795	0.204
	0.5	0.142	3.0	25.19	0.00027	0.460	1.00	25.71	0.02064	0.09533	0.42292	0.63637	0.217
E-6-5	0.7	0.199	3.0	20.11	.00046	0.683	0.	20.76	0.03232	0.08503	0.72581	0.56057	0.380
	0.7	0.199	3.0	20.11	0.00046	0.683	0.80	20.84	0.03630	0.08503	0.81536	0.62656	0.427
	0.7	0.199	3.0	20.11	0.00046	0.683	0.85	20.82	0.03531	0.08503	0.79297	0.56568	0.415
	0.7	0.199	3.0	20.11	0.00046	0.683	0.90	20.89	0.03879	0.08503	0.87136	0.58070	0.456
	0.7	0.199	3.0	20.11	0.00045	0.683	0.95	20.91	0.03978	0.08503	0.89376	0.58907	0.468
	0.7	0.199	3.0	20.11	0.00046	0.683	1.00	20.97	0.04276	0.08503	0.96098	0.63841	0.503
E-6-7	0.5	0.199	3.0	20.11	0.00046	0.475	0.	22.62	0.12481	0.17548	1.36572	0.55830	0.711
	0.5	0.200	3.0	20.04	0.00046	0.475	0.80	22.62	0.12874	0.17719	1.39480	0.62325	0.727
	0.5	0.199	3.0	20.11	0.00046	0.475	0.85	22.64	0.12581	0.17548	1.37667	0.56285	0.717
	0.5	0.199	3.0	20.11	0.00046	0.475	0.90	22.63	0.12531	0.17548	1.37120	0.57028	0.714
	0.5	0.199	3.0	20.11	0.00046	0.475	0.95	22.72	0.12979	0.17548	1.42051	0.58203	0.740
	0.5	0.199	3.0	20.11	0.00046	0.475	1.00	22.88	0.13774	0.17548	1.50823	0.62559	0.785
E-7-1	0.5	0.249	3.0	17.31	0.00085	0.482	0.	20.58	0.18891	0.26761	1.33030	0.55698	0.706
	0.5	0.249	3.0	17.31	0.00085	0.482	0.80	20.53	0.18602	0.26761	1.30967	0.62141	0.695
	0.5	0.249	3.0	17.31	0.00085	0.482	0.85	20.48	0.18313	0.26761	1.28905	0.56122	0.684
	0.5	0.249	3.0	17.31	0.00085	0.482	0.90	20.55	0.18718	0.26761	1.31792	0.56429	0.699
	0.5	0.249	3.0	17.31	0.00085	0.482	0.95	20.59	0.18949	0.26761	1.33442	0.57796	0.708
	0.5	0.249	3.0	17.31	0.00085	0.482	1.00	20.82	0.20277	0.26761	1.42940	0.61824	0.758
E-7-3	0.7	0.249	3.0	17.31	0.00085	0.687	0.	18.08	0.04448	0.13156	0.62899	0.55920	0.338
	0.7	0.249	3.0	17.31	0.00085	0.687	0.80	18.19	0.05084	0.13156	0.71933	0.62459	0.386
	0.7	0.249	3.0	17.31	0.00085	0.687	0.85	18.23	0.05315	0.13156	0.75221	0.56397	0.404
	0.7	0.249	3.0	17.31	0.00085	0.687	0.90	18.23	0.05315	0.13156	0.75221	0.57440	0.404
	0.7	0.249	3.0	17.31	0.00085	0.687	0.95	18.20	0.05142	0.13156	0.72754	0.58482	0.391
	0.7	0.249	3.0	17.31	0.00085	0.687	1.00	18.34	0.05950	0.13156	0.84270	0.63065	0.452
E-7-6	0.5	0.304	3.0	15.15	0.00011	0.486	0.	19.21	0.26799	0.39205	1.25984	0.55579	0.684
	0.5	0.304	3.0	15.15	0.00011	0.486	0.80	19.17	0.26535	0.39205	1.24711	0.61970	0.677
	0.5	0.304	3.0	15.15	0.00011	0.486	0.85	19.22	0.26865	0.39205	1.26302	0.55974	0.685
	0.5	0.304	3.0	15.15	0.00011	0.486	0.90	19.28	0.27261	0.39205	1.28213	0.55893	0.695
	0.5	0.304	3.0	15.15	0.00011	0.486	0.95	19.12	0.26205	0.39205	1.23120	0.57431	0.668
	0.5	0.304	3.0	15.15	0.00011	0.486	1.00	19.52	0.28845	0.39205	1.35866	0.61166	0.736

7-5 Contd.

1	2	3	4	5	6	7	8	9	10	11	12	13	14
Run No	M	F_n	Q cfs	y_n cm	S_n	M'	e	y_1 cm	$\frac{h_1^*}{y_n}$	$(\frac{F_n}{M'})^2$	K	D	$(\frac{h_1^*}{y_n})(\frac{M'}{F_n})^2$
E-7-8	0.7	0.304	3.0	15.15	0.00011	0.690	0.	16.24	0.07195	0.19452	0.66554	0.55798	0.370
	0.7	0.304	3.0	15.15	0.00011	0.690	0.80	16.27	0.07393	0.19452	0.68407	0.62283	0.380
	0.7	0.304	3.0	15.15	0.00011	0.690	0.85	16.35	0.07921	0.19452	0.73352	0.56245	0.407
	0.7	0.304	3.0	15.15	0.00011	0.690	0.90	16.34	0.07855	0.19452	0.72733	0.56881	0.404
	0.7	0.304	3.0	15.15	0.00011	0.690	0.95	16.41	0.08317	0.19452	0.77065	0.58103	0.428
	0.7	0.304	3.0	15.15	0.00011	0.690	1.00	16.54	0.09175	0.19452	0.85125	0.62379	0.472
E-8-1	0.7	0.406	3.0	12.50	0.00220	0.693	0.	14.18	0.13440	0.34321	0.65457	0.55621	0.392
	0.7	0.406	3.0	12.50	0.00220	0.693	0.80	14.30	0.14400	0.34321	0.70302	0.62029	0.420
	0.7	0.406	3.0	12.50	0.00220	0.693	0.85	14.31	0.14480	0.34321	0.70707	0.56025	0.422
	0.7	0.406	3.0	12.50	0.00220	0.693	0.90	14.31	0.14480	0.34321	0.70707	0.56079	0.422
	0.7	0.406	3.0	12.50	0.00220	0.693	0.95	14.42	0.15360	0.34321	0.75166	0.57558	0.448
	0.7	0.406	3.0	12.50	0.00220	0.693	1.00	14.60	0.16800	0.34321	0.82495	0.61395	0.489
E-8-3	0.5	0.406	3.0	12.50	0.00220	0.491	0.	17.97	0.43760	0.68533	1.12790	0.55406	0.639
	0.5	0.406	3.0	12.50	0.00220	0.491	0.80	18.00	0.44000	0.68533	1.13444	0.61721	0.642
	0.5	0.406	3.0	12.50	0.00220	0.491	0.85	17.89	0.43120	0.68533	1.11048	0.55759	0.629
	0.5	0.406	3.0	12.50	0.00220	0.491	0.90	18.07	0.44560	0.68533	1.14970	0.55118	0.650
	0.5	0.406	3.0	12.50	0.00220	0.491	0.95	18.18	0.45440	0.68533	1.17372	0.56901	0.663
	0.5	0.406	3.0	12.50	0.00220	0.491	1.00	18.56	0.48480	0.68533	1.25690	0.60217	0.707
E-8-5	0.5	0.526	3.0	10.52	0.00360	0.493	0.	17.58	0.67110	1.13695	0.99297	0.55249	0.590
	0.5	0.526	3.0	10.52	0.00360	0.493	0.80	17.66	0.67871	1.13695	1.00540	0.61497	0.597
	0.5	0.526	3.0	10.52	0.00360	0.493	0.85	17.64	0.67681	1.13695	1.00229	0.55564	0.595
	0.5	0.526	3.0	10.52	0.00360	0.493	0.90	17.63	0.67586	1.13695	1.00073	0.54425	0.594
	0.5	0.526	3.0	10.52	0.00360	0.493	0.95	17.79	0.69106	1.13695	1.02563	0.56425	0.608
	0.5	0.583	3.0	9.82	0.00360	0.494	1.00	18.10	0.84318	1.39302	1.00367	0.59033	0.605
E-8-7	0.7	0.526	3.0	10.52	0.00360	0.695	0.	13.36	0.26996	0.57257	0.72253	0.55462	0.471
	0.7	0.526	3.0	10.52	0.00360	0.695	0.80	13.32	0.26616	0.57257	0.71141	0.61801	0.465
	0.7	0.526	3.0	10.52	0.00360	0.695	0.85	13.49	0.28232	0.57257	0.75880	0.55828	0.493
	0.7	0.526	3.0	10.52	0.00360	0.695	0.90	13.56	0.28897	0.57257	0.77840	0.55366	0.505
	0.7	0.526	3.0	10.52	0.00360	0.695	0.95	13.72	0.30418	0.57257	0.82343	0.57071	0.531
	0.7	0.526	3.0	10.52	0.00360	0.695	1.00	13.94	0.32510	0.57257	0.88580	0.60521	0.568

TABLE 7-6 . GEOMETRY V_a RAW and CALCULATED DATA.

1	2	3	4	5	6	7	8	9	10	11	12	13	14
Run No.	M	F_n	Q cfs	y_n cms	S_n	M'	ϕ_2	y_1 cms	$\frac{h_1^*}{y_n}$	$(\frac{F_n^2}{M'})$	K	D	$(\frac{h_1^*}{y_n})(\frac{M'}{F_n})^2$
S-1-1	0.5	0.502	3.0	10.85	0.00360	0.493	0.	17.95	0.65438	1.03811	1.26071	0.58523	0.630
	0.5	0.502	3.0	10.85	0.00360	0.493	15.0	17.38	0.60184	1.03811	1.15949	0.63151	0.580
	0.5	0.502	3.0	10.85	0.00360	0.493	30.0	16.54	0.52442	1.03811	1.01034	0.53265	0.505
	0.5	0.502	3.0	10.85	0.00360	0.493	45.0	15.32	0.41198	1.03811	0.79371	0.43046	0.397
S-1-2	0.5	0.502	3.0	10.85	0.00360	0.493	0.	13.60	0.25346	1.03811	0.48830	0.58523	0.244
	0.5	0.502	3.0	10.85	0.00360	0.493	15.0	13.28	0.22396	1.03811	0.43148	0.63151	0.216
	0.5	0.502	3.0	10.85	0.00360	0.493	30.0	13.13	0.21014	1.03811	0.40485	0.53265	0.202
	0.5	0.502	3.0	10.85	0.00360	0.493	45.0	12.68	0.16866	1.03811	0.32494	0.43046	0.162
S-1-3	0.9	0.504	3.0	10.83	0.00210	0.896	0.	11.17	0.03139	0.31594	0.19873	0.55936	0.099
	0.9	0.504	3.0	10.83	0.00210	0.896	15.0	11.13	0.02770	0.31594	0.17535	0.55208	0.088
S-1-4	0.5	0.393	3.0	12.78	0.00210	0.490	0.	18.28	0.43036	0.64239	1.33987	0.57465	0.670
	0.5	0.393	3.0	12.78	0.00210	0.490	15.0	17.89	0.39984	0.64239	1.24486	0.59817	0.622
	0.5	0.393	3.0	12.78	0.00210	0.490	30.0	17.21	0.34664	0.64239	1.07921	0.51683	0.540
	0.5	0.393	3.0	12.78	0.00210	0.490	45.0	16.10	0.25978	0.64239	0.80879	0.41247	0.404
	0.7	0.393	3.0	12.78	0.00210	0.693	0.	14.45	0.13067	0.32142	0.81310	0.55972	0.407
	0.7	0.393	3.0	12.78	0.00210	0.693	15.0	14.36	0.12363	0.32142	0.76928	0.55315	0.385
	0.7	0.393	3.0	12.78	0.00210	0.693	30.0	14.19	0.11033	0.32142	0.68651	0.49484	0.343
	0.7	0.393	3.0	12.78	0.00210	0.693	45.0	13.81	0.08059	0.32142	0.50149	0.38785	0.251
S-1-5	0.7	0.289	3.0	15.70	0.00120	0.690	0.	16.72	0.06497	0.17516	0.74182	0.54696	0.371
	0.7	0.289	3.0	15.70	0.00120	0.690	15.0	16.58	0.05605	0.17516	0.64001	0.51648	0.320
	0.7	0.289	3.0	15.70	0.00120	0.690	30.0	16.55	0.05414	0.17516	0.61819	0.47633	0.309
	0.7	0.289	3.0	15.70	0.00120	0.690	45.0	16.36	0.04204	0.17516	0.48000	0.36747	0.240
	0.5	0.289	3.0	15.70	0.00120	0.485	0.	19.69	0.25414	0.35380	1.43664	0.56177	0.718
	0.5	0.289	3.0	15.70	0.00120	0.485	15.0	19.41	0.23631	0.35380	1.33582	0.55918	0.668
	0.5	0.289	3.0	15.70	0.00120	0.485	30.0	18.87	0.20191	0.35380	1.14139	0.49783	0.571
	0.5	0.289	3.0	15.70	0.00120	0.485	45.0	18.05	0.14968	0.35380	0.84614	0.39117	0.423
S-1-6	0.5	0.193	3.0	20.55	0.00048	0.474	0.	22.98	0.11825	0.16525	1.43113	0.54575	0.716
	0.5	0.193	3.0	20.55	0.00048	0.474	15.0	22.79	0.10900	0.16525	1.31923	0.51309	0.660
	0.5	0.193	3.0	20.55	0.00048	0.474	30.0	22.39	0.08954	0.16525	1.08366	0.47459	0.542
	0.5	0.193	3.0	20.55	0.00048	0.474	45.0	22.90	0.11436	0.16525	1.38402	0.36558	0.692
	0.7	0.193	3.0	20.55	0.00048	0.682	0.	21.15	0.02920	0.07986	0.73117	0.53088	0.366
	0.7	0.193	3.0	20.55	0.00048	0.682	15.0	21.10	0.02676	0.07986	0.67024	0.47262	0.335
	0.7	0.193	3.0	20.55	0.00048	0.682	30.0	21.00	0.02190	0.07986	0.54838	0.45341	0.274
	0.7	0.193	3.0	20.55	0.00048	0.682	45.0	20.91	0.01752	0.07986	0.43870	0.34269	0.219
S-2-1	0.7	0.094	3.0	33.11	0.00012	0.651	0.	33.38	0.00815	0.02095	0.77852	0.50456	0.389
	0.7	0.094	3.0	33.11	0.00012	0.651	15.0	33.38	0.00815	0.02095	0.77852	0.35955	0.389
	0.7	0.094	3.0	33.11	0.00012	0.651	30.0	33.33	0.00664	0.02095	0.63435	0.41686	0.317
	0.7	0.094	3.0	33.11	0.00012	0.651	45.0	33.27	0.00483	0.02095	0.46135	0.30425	0.231
S-2-3	0.5	0.094	3.0	33.11	0.00012	0.425	0.	34.33	0.03685	0.04915	1.49921	0.52118	0.750
	0.5	0.094	3.0	33.11	0.00012	0.425	30.0	33.97	0.02597	0.04915	1.05682	0.43980	0.528
	0.5	0.094	3.0	33.11	0.00012	0.425	45.0	33.68	0.01722	0.04915	0.70045	0.32822	0.350
S-2-2	0.3	0.105	1.0	14.78	0.00014	0.277	0.	17.07	0.15494	0.14447	2.14500	0.54297	1.072
	0.3	0.105	1.0	14.78	0.00014	0.277	15.0	17.03	0.15223	0.14447	2.10753	0.50536	1.054
	0.3	0.105	1.0	14.78	0.00014	0.277	30.0	16.52	0.11773	0.14447	1.62982	0.47060	0.815
	0.3	0.105	1.0	14.78	0.00014	0.277	45.0	16.21	0.09675	0.14447	1.33945	0.36123	0.670
S-2-3	0.3	0.189	1.0	10.00	0.00013	0.290	0.	13.95	0.39500	0.42598	1.85453	0.56575	0.927
	0.3	0.189	1.0	10.00	0.00013	0.290	15.0	13.84	0.38400	0.42598	1.80289	0.57104	0.901

7-6 Contd.

1 Run No.	2 M	3 F_n	4 Q cfs	5 y_n cms	6 S_n	7 M'	8	9 y_1 cms	10 $\frac{h_1^*}{y_n}$	11 $(\frac{F_n}{M'})^2$	12 K	13 D	14 $(\frac{h_1^*}{y_n})(\frac{M'}{F_n})^2$
	0.3	0.189	1.0	10.00	0.00013	0.290	30.00	13.04	0.30400	0.42598	1.42729	0.50367	0.714
S-3-1	0.3	0.303	2.0	11.60	0.00013	0.286	0.	20.90	0.80172	1.11951	1.43228	0.58691	0.716
	0.3	0.303	2.0	11.60	0.00013	0.286	15.00	20.40	0.75862	1.11951	1.35528	0.63692	0.678
	0.3	0.303	2.0	11.60	0.00013	0.286	30.00	19.28	0.66207	1.11951	1.18279	0.53518	0.591
	0.3	0.303	2.0	11.60	0.00013	0.286	45.00	18.08	0.55862	1.11951	0.99798	0.43335	0.499
S-3-2	0.3	0.385	2.0	9.88	0.00220	0.290	0.	20.89	1.11437	1.76376	1.26363	0.59713	0.632
	0.3	0.385	2.0	9.88	0.00220	0.290	15.00	20.29	1.05364	1.76376	1.19477	0.67049	0.597
	0.3	0.385	2.0	9.88	0.00220	0.290	30.00	18.59	0.88158	1.76376	0.99966	0.55068	0.500
	0.3	0.385	2.0	9.88	0.00220	0.290	45.00	17.51	0.77227	1.76376	0.87570	0.45122	0.438
S-3-3	0.3	0.480	2.0	8.53	0.00370	0.293	0.	20.22	1.36962	2.69036	1.01817	0.60679	0.509
	0.3	0.480	2.0	8.53	0.00370	0.293	15.00	19.89	1.33095	2.69036	0.98942	0.70325	0.495
	0.3	0.480	2.0	8.53	0.00370	0.293	30.00	18.13	1.12469	2.69036	0.83609	0.56548	0.418
	0.3	0.480	2.0	8.53	0.00370	0.293	45.00	16.95	0.98641	2.69036	0.73329	0.46848	0.367
S-4-1	0.5	0.139	3.0	25.53	0.00380	0.459	0.	27.22	0.06620	0.09205	1.43828	0.53375	0.719
	0.5	0.139	3.0	25.53	0.00380	0.459	15.00	27.01	0.05797	0.09205	1.25956	0.48026	0.630
	0.5	0.139	3.0	25.53	0.00380	0.459	30.00	26.73	0.04700	0.09205	1.02127	0.45747	0.511
	0.5	0.139	3.0	25.53	0.00380	0.459	45.00	26.41	0.03447	0.09205	0.74893	0.34704	0.374
	0.7	0.139	3.0	25.53	0.00380	0.672	0.	25.88	0.01371	0.04293	0.63874	0.51850	0.319
	0.7	0.139	3.0	25.53	0.00380	0.672	15.00	25.88	0.01371	0.04293	0.63874	0.44060	0.319
	0.7	0.139	3.0	25.53	0.00380	0.672	30.00	25.81	0.01097	0.04293	0.51099	0.43607	0.255
	0.7	0.139	3.0	25.53	0.00380	0.672	45.00	25.74	0.00823	0.04293	0.38324	0.32429	0.192
S-4-2	0.3	0.142	1.0	12.12	0.00040	0.285	0.	15.18	0.25248	0.24765	2.03895	0.55421	1.019
	0.3	0.142	1.0	12.12	0.00040	0.285	15.00	15.00	0.23762	0.24765	1.91901	0.53709	0.960
	0.3	0.142	1.0	12.12	0.00040	0.285	30.00	14.36	0.18482	0.24765	1.49257	0.48680	0.746
	0.3	0.142	1.0	12.12	0.00040	0.285	45.00	14.07	0.16089	0.24765	1.29933	0.37896	0.650
S-5-1	0.3	0.231	1.0	8.76	0.00110	0.292	0.	13.48	0.53881	0.62335	1.72876	0.57399	0.864
	0.3	0.231	1.0	8.76	0.00110	0.292	15.00	13.33	0.52169	0.62335	1.67382	0.59614	0.837
	0.3	0.231	1.0	8.76	0.00110	0.292	30.00	12.46	0.42237	0.62335	1.35517	0.51586	0.678
	0.3	0.231	1.0	8.76	0.00110	0.292	45.00	11.98	0.36758	0.62335	1.17937	0.41137	0.590
S-5-2	0.5	0.220	3.0	18.80	0.00089	0.478	0.	20.97	0.11543	0.21186	1.08962	0.55093	0.545
	0.5	0.220	3.0	18.80	0.00089	0.478	15.00	20.76	0.10426	0.21186	0.98417	0.52770	0.492
	0.5	0.220	3.0	18.80	0.00089	0.478	30.00	20.30	0.07979	0.21186	0.75319	0.48206	0.377
	0.5	0.220	3.0	18.80	0.00089	0.478	45.00	19.65	0.04521	0.21186	0.42681	0.37374	0.213

TABLE 7-7 GEOMETRY V_b RAW and CALCULATED DATA.

1	2	3	4	5	6	7	8	9	10	11	12
Run No	M	F_n	Q cfs	y_n cm	S_n	M'	ϕ_2	y_1 cm	$\frac{h_1}{y_n}$	$(\frac{F_n}{M'})^2$	K
1	0.2	0.462	2.0	8.76	0.00364	0.241	15.00	23.90	1.72831	3.67779	0.87967
2	0.2	0.388	1.0	6.20	0.00254	0.245	15.00	13.44	1.16774	2.49464	0.87930
3	0.2	0.310	1.0	7.20	0.00138	0.244	15.00	14.22	0.97500	1.61427	1.15494
4	0.2	0.194	1.0	9.84	0.00058	0.238	15.00	14.92	0.51626	0.66266	1.51967
5	0.2	0.096	1.0	15.70	0.00013	0.217	15.00	18.40	0.17197	0.19649	1.73509
6	0.2	0.462	2.0	8.76	0.00364	0.241	30.00	22.54	1.57306	3.67779	0.79641
7	0.2	0.750	2.0	6.34	0.00254	0.245	30.00	13.67	1.15615	9.34820	0.19072
8	0.2	0.310	1.0	7.19	0.00138	0.244	30.00	13.80	0.91933	1.62078	1.08246
9	0.2	0.194	1.0	9.84	0.00058	0.238	30.00	15.79	0.60467	0.66266	1.78335
10	0.2	0.096	1.0	15.70	0.00013	0.217	30.00	18.33	0.16752	0.19649	1.69002
11	0.5	0.467	2.0	8.69	0.00364	0.496	15.00	13.27	0.52704	0.88892	1.01749
12	0.5	0.387	2.0	9.85	0.00234	0.494	15.00	13.59	0.37970	0.61357	1.09851
13	0.5	0.292	2.0	11.89	0.00128	0.492	15.00	14.63	0.23045	0.35263	1.20857

TABLE 7-8 GEOMETRY VI RAW and CALCULATED DATA.

1	2	3	4	5	6	7	8	9	10	11	12	13
Run No.	M	F_n	Q cfs	y_n cm	S_n	M'	y_1 cm	$\frac{h_1^*}{y_n}$	$(\frac{F_n^2}{M})$	K	D	$(\frac{h_1^*}{y_n})(\frac{M'^2}{F_n})$
1	0.5	0.466	2.0	8.46	0.003750	0.546	12.42	0.46809	0.79310	0.98852	0.71329	0.590
2	0.5	0.389	2.0	9.82	0.002310	0.545	12.98	0.32179	0.50961	1.11056	0.73540	0.631
3	0.5	0.303	2.0	11.59	0.001350	0.543	14.04	0.21139	0.31233	1.24103	0.76066	0.677
4	0.5	0.197	2.0	15.44	0.000610	0.537	17.09	0.10687	0.13493	1.52036	0.80601	0.792
5	0.5	0.099	1.0	15.40	0.000175	0.537	15.87	0.03052	0.03399	1.77568	0.88646	0.898
6	0.3	0.452	1.0	5.60	0.004080	0.347	11.37	1.03036	1.69008	1.10963	0.67701	0.610
7	0.3	0.364	1.0	6.47	0.002650	0.346	11.58	0.78980	1.10151	1.33494	0.69731	0.717
8	0.3	0.280	1.0	7.71	0.001380	0.345	11.99	0.55512	0.65662	1.60710	0.72265	0.845
9	0.3	0.188	1.0	10.06	0.000584	0.341	13.24	0.31610	0.30188	2.03513	0.76245	1.047
10	0.3	0.096	1.0	15.68	0.000132	0.328	18.60	0.18622	0.08623	4.28165	0.83130	2.160
11	0.7	0.498	3.0	10.92	0.003680	0.745	13.17	0.20604	0.44557	0.71653	0.74224	0.462
12	0.7	0.392	3.0	12.80	0.002230	0.744	14.40	0.12500	0.27798	0.76010	0.76680	0.450
13	0.7	0.291	3.0	15.60	0.001220	0.740	16.65	0.06731	0.15487	0.78886	0.79839	0.435
14	0.7	0.190	3.0	20.73	0.000523	0.733	21.36	0.03039	0.06736	0.86489	0.84559	0.451
15	0.7	0.097	2.0	24.82	0.000131	0.725	25.10	0.01128	0.01781	1.25267	0.92688	0.633
10	0.3	0.100	0.7	12.10	0.000133	0.337	13.01	0.07521	0.08778	1.69501	0.83028	0.857
10'	0.3	0.095	0.5	9.41	0.000140	0.342	10.19	0.08289	0.07621	2.15473	0.83842	1.088
4a	0.5	0.190	3.0	20.78	0.005230	0.526	23.84	0.14726	0.12978	2.18955	0.80818	1.135
5a	0.5	0.098	2.0	24.66	0.000131	0.516	26.14	0.06002	0.03592	3.30676	0.88309	1.671
6a	0.3	0.475	2.0	8.60	0.003640	0.344	22.85	1.65698	1.90630	1.61674	0.67141	0.869
7a	0.3	0.394	2.0	9.74	0.002340	0.342	22.54	1.31417	1.32619	1.86779	0.68843	0.991
8a	0.3	0.296	2.0	11.78	0.001280	0.338	23.12	0.96265	0.76689	2.40901	0.71495	1.255
9a	0.3	0.192	2.0	15.70	0.000560	0.328	26.41	0.68217	0.34374	3.88548	0.75565	1.985
10a	0.3	0.096	1.0	15.68	0.000535	0.328	18.60	0.18622	0.08623	4.28165	0.83130	2.160
10b	0.3	0.096	0.7	12.94	0.000147	0.335	14.54	0.12365	0.08262	2.96521	0.83376	1.497
16a	0.7	0.045	3.0	33.03	0.000125	0.705	33.77	0.02240	0.01800	2.46396	0.92622	1.245
17a	0.7	0.147	3.8	28.67	0.000287	0.717	29.68	0.03523	0.04206	1.63389	0.87352	0.838
18a	0.7	0.080	2.1	28.77	0.000081	0.716	29.06	0.01008	0.01251	1.59942	0.94976	0.806
4b	0.5	0.201	3.0	19.89	0.005110	0.528	22.84	0.14832	0.14517	1.96248	0.80196	1.022

TABLE 7-9 GEOMETRY VII RAW and CALVULATED DATA.

1	2	3	4	5	6	7	8	9	10	11	12	13	14
Run No.	M	F_n	Q cfs	y_n cm	S_n	M'	β	y_1 cm	$\frac{h_1^*}{y_n}$	$(\frac{F_n}{M'})^2$	K	D	$(\frac{h_1^*}{y_n})(\frac{M'}{F_n})^2$
1	0.35	0.447	1.0	5.64	0.004100	0.329	0.50	12.22	1.16667	1.84420	6.41940	0.39976	0.633
2	0.35	0.355	1.0	6.58	0.002540	0.318	0.50	12.39	0.88298	1.23920	5.36265	0.40714	0.713
3	0.35	0.278	1.0	7.74	0.001380	0.310	0.50	12.67	0.63695	0.80499	4.43386	0.41530	0.791
4	0.35	0.187	1.0	10.08	0.000584	0.294	0.50	13.83	0.37202	0.40454	3.55381	0.42865	0.920
5	0.35	0.092	0.7	12.73	0.000124	0.271	0.50	14.26	0.12019	0.11561	2.63145	0.45407	1.040
6	0.35	0.475	2.0	8.59	0.003640	0.325	0.30	19.49	1.26892	2.13313	6.65206	0.42191	0.595
7	0.35	0.391	2.0	9.79	0.002340	0.318	0.30	19.70	1.01226	1.50498	5.81817	0.42427	0.673
8	0.35	0.278	1.0	7.73	0.001380	0.328	0.30	12.24	0.58344	0.72092	4.25285	0.42930	0.809
9	0.35	0.191	1.0	9.94	0.000560	0.320	0.30	13.28	0.33602	0.35711	3.45520	0.43415	0.941
10	0.35	0.096	1.0	15.71	0.000132	0.286	0.30	17.50	0.11394	0.11296	2.52687	0.44222	1.009
11	0.35	0.478	2.0	8.56	0.003640	0.326	0.	17.68	1.06542	2.15100	4.64210	0.65525	0.495
12	0.35	0.397	2.0	9.68	0.002340	0.325	0.	17.97	0.85640	1.49063	4.27092	0.63444	0.575
13	0.35	0.294	3.0	15.49	0.001400	0.294	0.	25.26	0.63073	1.00092	3.52401	0.61259	0.630
14	0.35	0.193	2.0	15.67	0.000560	0.316	0.	20.49	0.30759	0.37354	2.90076	0.56170	0.823
15	0.35	0.096	1.0	15.71	0.000132	0.327	0.	17.04	0.08466	0.08643	2.32732	0.49382	0.979
16	0.50	0.478	2.7	10.59	0.003410	0.445	0.50	18.59	0.75543	1.15158	4.53756	0.40851	0.656
17	0.50	0.388	2.0	9.83	0.002340	0.452	0.50	15.02	0.52798	0.73655	3.67511	0.41700	0.717
18	0.50	0.291	2.0	11.91	0.001280	0.436	0.50	15.92	0.33669	0.44504	2.88341	0.42678	0.757
19	0.50	0.191	1.0	9.94	0.000584	0.428	0.50	11.46	0.15292	0.19860	2.11948	0.44291	0.770
20	0.50	0.101	1.0	15.22	0.000132	0.412	0.50	16.03	0.05322	0.05970	2.00016	0.46809	0.892
21	0.50	0.490	3.8	13.02	0.003280	0.460	0.30	21.16	0.62519	1.13661	3.32239	0.42618	0.550
22	0.50	0.392	3.8	15.12	0.002090	0.449	0.30	23.22	0.53571	0.76175	3.64584	0.42892	0.703
23	0.50	0.295	3.8	18.26	0.001150	0.435	0.30	24.83	0.35980	0.46076	3.08060	0.43238	0.781
24	0.50	0.199	2.0	15.33	0.000560	0.450	0.30	17.67	0.15264	0.19636	2.14544	0.43832	0.777
25	0.50	0.100	1.0	15.27	0.000132	0.449	0.30	15.93	0.04322	0.04978	1.91126	0.44895	0.868
26	0.50	0.490	3.8	13.02	0.003280	0.470	0.	22.56	0.73272	1.08644	4.58154	0.61703	0.674
27	0.50	0.392	3.8	15.12	0.002090	0.472	0.	21.96	0.45238	0.68786	3.07178	0.59270	0.658
28	0.50	0.295	3.8	18.26	0.001500	0.468	0.	23.33	0.27766	0.39723	2.44863	0.56475	0.699
29	0.50	0.195	3.8	24.08	0.000501	0.453	0.	27.24	0.13123	0.18486	1.88590	0.52798	0.710
30	0.50	0.097	3.0	32.50	0.000125	0.422	0.	33.31	0.02492	0.05260	1.00630	0.47270	0.474
31	0.75	0.496	3.0	10.94	0.003680	0.697	0.50	13.51	0.23492	0.50599	1.72257	0.42426	0.464
32	0.75	0.400	3.0	12.62	0.002230	0.690	0.50	14.39	0.14025	0.33683	1.25428	0.43228	0.416
33	0.75	0.295	2.0	11.80	0.001280	0.694	0.50	12.64	0.07119	0.18115	0.98696	0.44479	0.393
34	0.75	0.195	2.0	15.56	0.000131	0.670	0.50	16.06	0.03213	0.08477	0.84279	0.46060	0.379
35	0.75	0.101	2.0	24.13	0.000131	0.615	0.50	24.44	0.01285	0.02696	0.98953	0.48553	0.477
36	0.75	0.496	3.0	10.94	0.003680	0.721	0.30	12.88	0.17733	0.47289	1.28077	0.43220	0.375
37	0.75	0.403	3.0	12.57	0.002230	0.718	0.30	14.14	0.12490	0.31501	1.16752	0.43502	0.396
38	0.75	0.295	2.0	11.80	0.001280	0.715	0.30	12.51	0.06017	0.17066	0.86852	0.43931	0.353
39	0.75	0.195	2.0	15.56	0.000560	0.706	0.30	15.96	0.02571	0.07618	0.74123	0.44502	0.337
40	0.75	0.101	2.0	24.06	0.000131	0.668	0.30	24.32	0.01081	0.02303	0.97040	0.45362	0.469
41	0.75	0.496	3.0	10.94	0.003680	0.729	0.	12.88	0.17733	0.46321	1.30753	0.57243	0.383
42	0.75	0.402	3.0	12.58	0.002300	0.742	0.	13.92	0.10652	0.29366	1.03667	0.54993	0.363
43	0.75	0.443	3.0	11.80	0.001280	0.744	0.	12.41	0.05169	0.35440	0.39313	0.55910	0.146
44	0.75	0.195	2.0	15.54	0.000560	0.744	0.	15.87	0.02124	0.06896	0.67082	0.48410	0.308
45	0.75	0.101	2.0	24.15	0.000131	0.726	0.	24.29	0.00580	0.01930	0.61519	0.43277	0.300

TABLE VIII - RAW DATA - AREA OF VENA CONTRACTA - BACKWATER AND PROFILE

Run No. = 2
Q = 4.74 cfs.
y_1 = 50.52 cm.
y_2 = 0.0 cm.
M b/B = 0.30
Model Sta. = 30.00 ft.
A_o = 0.884 sq. ft.
L/b = 0.0

Profile of Jet Sta. ft.	Profile of Jet Depth ft.	Crossection Sta. Traverse 30.235 ft.	Crossection Depth ft.
		0.81	0.0
		0.85	0.133
		0.90	0.258
		0.95	0.334
		1.00	0.398
		1.10	0.483
		1.20	0.542
		1.30	0.582
		1.40	0.602
		1.50	0.613
		1.60	0.592
		1.70	0.578
		1.80	0.540
		1.90	0.473
		2.00	0.369
		2.05	0.304
		2.10	0.205
		2.178	0.000

Run No. = 3
Q = 4.04 cfs.
y_1 = 41.00 cm.
y_2 = 0.0 cm.
M b/B = 0.30
Model Sta. = 30.00 ft.
A_o = 0.884 sq. ft.
L/b = 0.0

Profile of Jet Sta. ft.	Profile of Jet Depth ft.	Crossection Sta. Traverse 30.215 ft.	Crossection Depth ft.
30.18	0.621	0.815	0.00
30.30	0.592	0.85	0.167
30.40	0.568	0.90	0.270
30.50	0.542	1.00	0.402
30.60	0.518	1.10	0.488
31.00	0.426	1.20	0.543
31.50	0.321	1.30	0.579
32.00	0.245	1.40	0.602
		1.50	0.612
		1.60	0.598
		1.70	0.575
		1.80	0.535
		1.90	0.466
		2.00	0.366
		2.05	0.292
		2.10	0.201
		2.15	0.00

Run No. = 4
Q = 3.735 cfs.
y_1 = 30.53 cm.
y_2 = 0.0 cm.
M = b/B = 0.30
Model Sta. = 30.00 ft.
A_o = 0.884 sq. ft.
L/b = 0.0

Profile of Jet Sta. ft.	Profile of Jet Depth ft.	Crossection Sta. Traverse 30.21 ft.	Crossection Depth ft.
30.18	0.619	0.8175	0.00
30.30	0.58	0.85	0.151
30.40	0.554	0.90	0.270
30.50	0.523	1.00	0.402
30.60	0.504	1.10	0.483
31.00	0.387	1.20	0.542
31.50	0.293	1.30	0.578
32.00	0.227	1.40	0.598
		1.50	0.612
		1.60	0.594
		1.70	0.572
		1.80	0.533
		1.90	0.464
		2.00	0.363
		2.05	0.292
		2.10	0.203
		2.15	0.000

Run No. = 5
Q = 3.58 cfs.
y_1 = 35.37 cm.
y_2 = 14.05 cm.
M = b/B = 0.30
Model Sta. = 30.00 ft.
A_o = 0.884 sq. ft.
L/b = 0.0

Profile of Jet Sta. ft.	Profile of Jet Depth ft.	Crossection Sta. Traverse 30.23 ft.	Crossection Depth ft.
		0.814	0.081
		0.9	0.277
		1.0	0.404
		1.1	0.491
		1.2	0.549
		1.3	0.587
		1.4	0.607
		1.5	0.616
		1.6	0.604
		1.7	0.578
		1.8	0.538
		1.9	0.476
		2.0	0.379
		2.1	0.228
		2.162	0.0073

Run No. = 6
Q = 3.40 cfs.
y_1 = 32.75 cm.
y_2 = 1.07 cm.
M = b/B = 0.30
Model Sta. = 30.00 ft.
A_o = 0.884 sq. ft.
L/b = 0.0

Profile of Jet Sta. ft.	Profile of Jet Depth ft.	Crossection Sta. Traverse 30.208 ft.	Crossection Depth ft.
30.18	0.612	0.80	0.00
30.30	0.576	0.85	0.165
30.40	0.543	0.90	0.264
30.50	0.507	1.00	0.393
30.60	0.478	1.10	0.476
31.00	0.365	1.20	0.532
31.50	0.265	1.30	0.565
32.00	0.203	1.40	0.590
		1.50	0.607
		1.60	0.588
		1.70	0.562
		1.80	0.523
		1.90	0.459
		2.00	0.361
		2.05	0.293
		2.10	0.202
		2.16	0.000

Run No. = 7
Q = 3.18 cfs.
y_1 = 30.45 cm.
y_2 = 14.60 cm.
M = b/B = 0.30
Model Sta. = 30.00 ft.
A_o = 0.884 sq. ft.
L/b = 0.0

Profile of Jet Sta. ft.	Profile of Jet Depth ft.	Crossection Sta. Traverse 30.215 ft.	Crossection Depth ft.
		0.83	0.000
		0.85	0.162
		0.90	0.258
		1.00	0.387
		1.10	0.468
		1.20	0.527
		1.30	0.565
		1.40	0.586
		1.50	0.603
		1.60	0.587
		1.70	0.559
		1.80	0.523
		1.90	0.463
		2.00	0.363
		2.05	0.307
		2.10	0.224
		2.16	0.000

Run No. = 8
Q = 2.89 cfs.
y_1 = 27.83 cm.
y_2 = 0.0 cm.
M = b/B = 0.30
Model Sta. = 30.00 ft.
A_o = 0.884 sq. ft.
L/b = 0.0

Profile of Jet Sta. ft.	Profile of Jet Depth ft.	Crossection Sta. Traverse 30.19 ft.	Crossection Depth ft.
30.18	0.612	0.81	0.00
30.30	0.564	0.85	0.175
30.40	0.521	0.90	0.268
30.50	0.487	1.00	0.402
30.60	0.443	1.10	0.476
31.00	0.326	1.20	0.533
31.50	0.230	1.30	0.564
32.00	0.177	1.40	0.597
		1.50	0.613
		1.60	0.592
		1.70	0.567
		1.80	0.534
		1.90	0.463
		2.00	0.360
		2.05	0.301
		2.10	0.215
		2.16	0.000

Run No. = 10
Q = 2.535 cfs.
y_1 = 24.43 cm.
y_2 = 2.11 cm.
M = b/B = 0.30
Model Sta. = 30.00 ft.
A_o = 0.884 sq. ft.
L/b = 0.0

Profile of Jet Sta. ft.	Profile of Jet Depth ft.	Crossection Sta. Traverse 30.175 ft.	Crossection Depth ft.
30.18	0.629	0.805	0.000
30.30	0.572	0.850	0.186
30.40	0.520	0.900	0.316
30.50	0.469	1.000	0.402
30.60	0.419	1.100	0.478
31.00	0.295	1.200	0.533
31.50	0.206	1.300	0.579
32.00	0.159	1.400	0.621
		1.500	0.631
		1.600	0.608
		1.700	0.569
		1.800	0.528
		1.900	0.473
		2.000	0.366
		2.050	0.303
		2.100	0.216
		2.155	0.000

TABLE 8-1- RAW DATA - AREA OF VENA CONTRACTA - BACKWATER AND PROFILE

Run No. = 11
Q = 4.71 cfs.
y_1 = 49.75 cm.
y_2 = 0.0 cm.
M = b/B = 0.30
Model Sta. = 30.00 ft.
A_o = 0.884 sq. ft.
L/b = 0.0

Profile of Jet Sta. ft.	Profile of Jet Depth ft.	Crossection Sta. Traverse 30.325 ft.	Crossection Depth ft.
30.18	0.624	0.83	0.00
30.30	0.588	0.90	0.231
30.40	0.571	1.00	0.372
30.50	0.550	1.10	0.457
30.60	0.534	1.20	0.515
31.00	0.463	1.30	0.552
31.50	0.360	1.40	0.572
32.00	0.281	1.50	0.586
		1.60	0.572
		1.70	0.551
		1.80	0.509
		1.90	0.444
		2.00	0.341
		2.10	0.177
		2.156	0.00

Run No. = 12
Q = 4.02 cfs.
y_1 = 41.20 cm.
y_2 = 0.78 cm.
M = b/B = 0.30
Model Sta. = 30.00 ft.
A_o = 0.884 sq. ft.
L/b = 0.0

Profile of Jet Sta. ft.	Profile of Jet Depth ft.	Crossection Sta. Traverse 30.265 ft.	Crossection Depth ft.
30.18	0.617	0.827	0.00
30.30	0.580	0.85	0.127
30.40	0.551	0.90	0.245
30.50	0.536	1.00	0.382
30.60	0.513	1.10	0.466
31.00	0.426	1.20	0.521
31.50	0.319	1.30	0.556
32.00	0.243	1.40	0.577
		1.50	0.592
		1.60	0.576
		1.70	0.557
		1.80	0.523
		1.90	0.449
		2.00	0.348
		2.10	0.190
		2.141	0.00

Run No. = 13
Q = 3.735 cfs.
y_1 = 36.14 cm.
y_2 = 1.23 cm.
M = b/B = 0.30
Model Sta. = 30.00 ft.
A_o = 0.884 sq. ft.
L/b = 0.0

Profile of Jet Sta. ft.	Profile of Jet Depth ft.	Crossection Sta. Traverse 30.23 ft.	Crossection Depth ft.
30.18	0.612	0.831	0.00
30.30	0.576	0.850	0.142
30.40	0.543	0.90	0.251
30.50	0.518	1.00	0.382
30.60	0.490	1.10	0.471
31.00	0.392	1.20	0.524
31.50	0.288	1.30	0.561
32.00	0.218	1.40	0.581
		1.50	0.594
		1.60	0.581
		1.70	0.559
		1.80	0.519
		1.90	0.453
		2.00	1.354
		2.10	0.200
		2.138	0.00

Run No. = 14
Q = 3.33 cfs.
y_1 = 32.28 cm.
y_2 = 0.98 cm.
M = b/B = 0.30
Model Sta. = 30.00 ft.
A_o = 0.884 sq. ft.
L/b = 0.0

Profile of Jet Sta. ft.	Profile of Jet Depth ft.	Crossection Sta. Traverse 30.20 ft.	Crossection Depth ft.
30.18	0.609	0.821	0.00
30.30	0.565	0.85	0.155
30.40	0.534	0.90	0.262
30.50	0.503	1.00	0.392
30.60	0.474	1.10	0.476
31.00	0.364	1.20	0.529
31.50	0.228	1.30	0.565
32.00	0.198	1.40	0.586
		1.50	0.598
		1.60	0.588
		1.70	0.565
		1.80	0.525
		1.90	0.460
		2.00	0.361
		2.10	0.210
		2.158	0.00

Run No. = 15
Q = 2.88 cfs.
y_1 = 27.56 cm.
y_2 = 1.57 cm.
M = b/B = 0.30
Model Sta. = 30.00 ft.
A_o = 0.884 sq. ft.
L/b = 0.0

Profile of Jet Sta. ft.	Profile of Jet Depth ft.	Crossection Sta. Traverse 30.18 ft.	Crossection Depth ft.
30.18	0.604	0.81	0.00
30.30	0.556	0.85	0.165
30.40	0.518	0.90	0.201
30.50	0.475	1.00	0.389
30.60	0.435	1.10	0.477
31.00	0.315	1.20	0.532
31.50	0.222	1.30	0.561
32.00	0.139	1.40	0.588
		1.50	0.603
		1.60	0.588
		1.70	0.559
		1.80	0.519
		1.90	0.461
		2.00	0.364
		2.10	0.215
		2.16	0.00

Run No. = 16
Q = 4.180 cfs.
y_1 = 52.24 cm.
y_2 = 0.00 cm.
M = b/B = 0.275
Model Sta. = 30.00 ft.
A_o = 0.741 sq. ft.
L/b =

Profile of Jet Sta. ft.	Profile of Jet Depth ft.	Crossection Sta. Traverse 30.23 ft.	Crossection Depth ft.
30.18	0.573	0.87	0.00
30.30	0.550	0.90	0.103
30.40	0.521	0.95	0.244
30.50	0.514	1.00	0.322
30.60	0.502	1.05	0.379
31.00	0.429	1.10	0.421
31.50	0.336	1.20	0.487
32.00	0.265	1.30	0.529
		1.40	0.552
		1.50	0.565
		1.60	0.546
		1.70	0.516
		1.80	0.467
		1.90	0.354
		1.95	0.334
		2.00	0.263
		2.05	0.190
		2.095	0.00

Run No. = 17
Q = 3.705 cfs.
y_1 = 43.73 cm.
y_2 = 0.0 cm.
M = b/B = 0.275
Model Sta. = 30.00 ft.
A_o = 0.741 sq. ft.
L/b = 0.0

Profile of Jet Sta. ft.	Profile of Jet Depth ft.	Crossection Sta. Traverse 30.20 ft.	Crossection Depth ft.
30.18	0.566	0.87	0.00
30.30	0.536	0.90	0.136
30.40	0.511	0.95	0.255
30.50	0.491	1.00	0.330
30.60	0.472	1.10	0.424
31.00	0.395	1.20	0.490
31.50	0.299	1.30	0.533
32.00	0.231	1.40	0.552
		1.50	0.559
		1.60	0.549
		1.70	0.517
		1.80	0.468
		1.90	0.389
		2.00	0.271
		2.05	0.169
		2.09	0.00

Run No. = 18
Q = 3.635 cfs.
y_1 = 42.64 cm.
y_2 = 1.53 cm.
M = b/B = 0.275
Model Sta. = 30.00 ft.
A_o = 0.741 sq. ft.
L/b = 0.0

Profile of Jet Sta. ft.	Profile of Jet Depth ft.	Crossection Sta. Traverse 30.18 ft.	Crossection Depth ft.
30.18	0.563	0.88	0.00
30.30	0.524	0.90	0.138
30.40	0.505	0.95	0.248
30.50	0.487	1.00	0.334
30.60	0.470	1.05	0.388
31.00	0.390	1.10	0.431
31.50	0.292	1.20	0.496
32.00	0.226	1.30	0.536
		1.40	0.556
		1.50	0.562
		1.60	0.554
		1.70	0.523
		1.80	0.472
		1.90	0.395
		1.95	0.345
		2.00	0.281
		2.05	0.181
		2.09	0.00

TABLE 8-1 RAW DATA - AREA OF VENA CONTRACTA - BACKWATER AND PROFILE

Run No. = 19
Q = 3.480 cfs.
y_1 = 40.36 cm.
y_2 = 1.51 cm.
M = b/B = 0.275
Model Sta. = 30.00 ft.
A_o = 0.741 sq. ft.
L/b = 0.0

Profile of Jet Sta. ft.	Profile of Jet Depth ft.	Crossection Sta. Traverse 30.18 ft.	Crossection Depth ft.
30.18	0.558	0.88	0.00
30.30	0.530	0.90	0.144
30.40	0.512	0.95	0.260
30.50	0.482	1.00	0.329
30.60	0.468	1.10	0.426
31.00	0.380	1.20	0.492
32.00	0.218	1.40	0.554
		1.50	0.558
		1.60	0.551
		1.70	0.519
		1.80	0.471
		1.90	0.392
		2.00	0.277
		2.05	0.175
		2.09	0.00

Run No. = 20
Q = 3.100 cfs.
y_1 = 34.76 cm.
y_2 = 2.13 cm.
M = b/B = 0.275
Model Sta. = 30.00 ft.
A_o = 0.741 sq. ft.
L/b = 0.0

Profile of Jet Sta. ft.	Profile of Jet Depth ft.	Crossection Sta. Traverse 30.17 ft.	Crossection Depth ft.
		0.89	0.00
		0.90	0.143
		0.95	0.262
		1.00	0.332
		1.05	0.384
		1.10	0.426
		1.20	0.489
		1.30	0.532
		1.40	0.552
		1.50	0.561
		1.60	0.549
		1.70	0.517
		1.80	0.470
		1.90	0.342
		1.95	0.344
		2.00	0.280
		2.05	0.185
		2.09	0.00

Run No. = 21
Q = 2.930 cfs.
y_1 = 32.36 cm.
y_2 = 1.58 cm.
M = b/B = 0.275
Model Sta. = 30.00 ft.
A_o = 0.741 sq. ft.
L/b = 0.0

Profile of Jet Sta. ft.	Profile of Jet Depth ft.	Crossection Sta. Traverse 30.158 ft.	Crossection Depth ft.
30.18	0.560	0.87	0.00
30.30	0.516	0.90	0.149
30.40	0.492	0.95	0.261
30.50	0.460	1.00	0.331
30.60	0.435	1.10	0.426
31.00	0.329	1.20	0.488
31.50	0.237	1.30	0.529
32.00	0.181	1.40	0.555
		1.50	0.567
		1.60	0.549
		1.70	0.516
		1.80	0.469
		1.90	0.391
		2.00	0.276
		2.05	0.184
		2.10	0.00

Run No. = 22
Q = 2.732 cfs.
y_1 = 29.93 cm.
y_2 = 1.66 cm.
M = b/B = 0.275
Model Sta. = 30.00 ft.
A_o = 0.741 sq. ft.
L/b = 0.0

Profile of Jet Sta. ft.	Profile of Jet Depth ft.	Crossection Sta. Traverse 30.157 ft.	Crossection Depth ft.
30.18	0.562	0.86	0.00
30.30	0.516	0.90	0.152
30.40	0.482	0.95	0.259
30.50	0.447	1.00	0.329
30.60	0.418	1.10	0.424
31.00	0.310	1.20	0.487
31.50	0.218	1.30	0.526
32.00	0.165	1.40	0.552
		1.50	0.561
		1.60	0.546
		1.70	0.513
		1.80	0.468
		1.90	0.392
		2.00	0.279
		2.05	0.184
		2.11	0.00

Run No. = 23
Q = 2.720 cfs.
y_1 = 29.53 cm.
y_2 = 2.13 cm.
M = b/B = 0.275
Model Sta. = 30.00 ft.
A_o = 0.741 sq. ft.
L/b = 0.0

Profile of Jet Sta. ft.	Profile of Jet Depth ft.	Crossection Sta. Traverse 30.15 ft.	Crossection Depth ft.
		0.88	0.00
		0.90	0.154
		0.95	0.266
		1.00	0.333
		1.05	0.388
		1.10	0.427
		1.20	0.491
		1.30	0.532
		1.40	0.556
		1.50	0.568
		1.60	0.550
		1.70	0.518
		1.80	0.475
		1.90	0.396
		1.95	0.314
		2.00	0.286
		2.05	0.190
		2.10	0.00

Run No. = 24
Q = 2.518 cfs.
y_1 = 27.33 cm.
y_2 = 1.87 cm.
M = b/B = 0.275
Model Sta. = 30.00 ft.
A_o = 0.741 sq. ft.
L/b = 0.0

Profile of Jet Sta. ft.	Profile of Jet Depth ft.	Crossection Sta. Traverse 30.155 ft.	Crossection Depth ft.
30.18	0.553	0.87	0.00
30.30	0.507	0.90	0.159
30.40	0.470	0.95	0.264
30.50	0.430	1.00	0.335
30.60	0.404	1.10	0.429
31.00	0.293	1.20	0.490
31.50	0.206	1.30	0.512
32.00	0.156	1.40	0.558
		1.50	0.570
		1.60	0.549
		1.70	0.518
		1.80	0.474
		1.90	0.397
		2.00	0.282
		2.05	0.192
		2.10	0.0695
		2.105	0.00

Run No. = 25
Q = 2.394 cfs.
y_1 = 26.00 cm.
y_2 = 0.0 cm.
M = b/B = 0.275
Model Sta. = 30.00 ft.
A_o = 0.741 sq. ft.
L/b = 0.0

Profile of Jet Sta. ft.	Profile of Jet Depth ft.	Crossection Sta. Traverse 30.145 ft.	Crossection Depth ft.
30.18	0.556	0.88	0.00
30.30	0.523	0.90	0.168
30.40	0.465	0.95	0.272
30.50	0.426	1.00	0.339
30.60	0.389	1.05	0.388
31.00	0.280	1.10	0.428
31.50	0.197	1.20	0.490
32.00	0.152	1.30	0.529
		1.40	0.562
		1.50	0.567
		1.60	0.549
		1.70	0.512
		1.80	0.474
		1.90	0.396
		1.95	0.352
		2.00	0.286
		2.05	0.194
		2.10	0.00

Run No. = 26
Q = 2.190 cfs.
y_1 = 23.54 cm.
y_2 = 0.43 cm.
M = b/B = 0.275
Model Sta. = 30.00 ft.
A_o = 0.741 sq. ft.
L/b = 0.0

Profile of Jet Sta. ft.	Profile of Jet Depth ft.	Crossection Sta. Traverse 30.14 ft.	Crossection Depth ft.
		0.87	0.00
		0.90	0.169
		0.95	0.270
		1.00	0.375
		1.05	0.388
		1.10	0.431
		1.20	0.480
		1.30	0.529
		1.40	0.565
		1.50	0.608
		1.60	0.552
		1.70	0.510
		1.80	0.467
		1.85	0.442
		1.90	0.396
		1.95	0.346
		2.00	0.288
		2.05	0.200
		2.09	0.00

TABLE 8-1 RAW DATA - AREA OF VENA CONTRACTA - BACKWATER AND PROFILE

Run No. = 27
Q = 2.535 cfs.
y_1 = 27.02 cm.
y_2 = 1.08 cm.
M = b/B = 0.275
Model Sta. = 30.00 ft.
A_o = 0.741 sq. ft.
L/b = 0.0

Profile of Jet Sta. ft.	Profile of Jet Depth ft.	Crossection Sta. Traverse 30.16 ft.	Crossection Depth ft.
30.18	0.550	0.869	0.00
30.30	0.500	0.90	0.148
30.40	0.466	1.00	0.320
30.50	0.428	1.10	0.417
30.60	0.392	1.20	0.477
31.00	0.281	1.30	0.519
31.50	0.198	1.40	0.543
32.00	0.152	1.50	0.559
		1.60	0.535
		1.70	0.505
		1.80	0.464
		1.90	0.388
		2.00	0.277
		2.05	0.189
		2.10	0.062
		2.109	0.00

Run No. = 28
Q = 2.762 cfs.
y_1 = 29.28 cm.
y_2 = 0.88 cm.
M = b/B = 0.275
Model Sta. = 30.00 ft.
A_o = 0.741 sq. ft.
L/b = 0.0

Profile of Jet Sta. ft.	Profile of Jet Depth ft.	Crossection Sta. Traverse 30.165 ft.	Crossection Depth ft.
30.18	0.552	0.869	0.00
30.30	0.510	0.90	0.141
30.40	0.477	1.00	0.318
30.50	0.444	1.10	0.413
30.60	0.415	1.20	0.475
31.00	0.304	1.30	0.517
31.50	0.215	1.40	0.543
32.00	0.165	1.50	0.552
		1.60	0.539
		1.70	0.506
		1.80	0.461
		1.90	0.387
		2.00	0.243
		2.05	0.188
		2.091	0.00

Run No. = 29
Q = 2.963 cfs.
y_1 = 32.03 cm.
y_2 = 0.88 cm.
M = b/B = 0.275
Model Sta. = 30.00 ft.
A_o = 0.741 sq. ft.
L/b = 0.0

Profile of Jet Sta. ft.	Profile of Jet Depth ft.	Crossection Sta. Traverse 30.185 ft.	Crossection Depth ft.
30.18	0.555	0.87	0.00
30.30	0.514	0.90	0.139
30.40	0.486	1.00	0.319
30.50	0.457	1.10	0.413
30.60	0.430	1.20	0.475
31.00	0.329	1.30	0.517
31.50	0.284	1.40	0.542
32.00	0.177	1.50	0.549
		1.60	0.536
		1.70	0.506
		1.80	0.457
		1.90	0.384
		2.00	0.270
		2.05	0.179
		2.078	0.00

Run No. = 30
Q = 3.225 cfs.
y_1 = 36.03 cm.
y_2 = 0.0 cm.
M = b/B = 0.275
Model Sta. = 30.00 ft.
A_o = 0.741 sq. ft.
L/b = 0.0

Profile of Jet Sta. ft.	Profile of Jet Depth ft.	Crossection Sta. Traverse 30.21 ft.	Crossection Depth ft.
30.18	0.552	0.872	0.00
30.30	0.522	0.90	0.127
30.40	0.498	1.00	0.316
30.50	0.473	1.10	0.412
30.60	0.450	1.20	0.475
31.00	0.354	1.30	0.515
31.50	0.255	1.40	0.534
32.00	0.193	1.50	0.543
		1.60	0.532
		1.70	0.501
		1.80	0.454
		1.90	0.379
		2.00	0.263
		2.05	0.171
		2.08	0.00

Run No. = 31
Q = 3.56 cfs.
y_1 = 41.73 cm.
y_2 = 1.35 cm.
M = b/B = 0.275
Model Sta. = 30.00 ft.
A_o = 0.741 sq. ft.
L/b = 0.0

Profile of Jet Sta. ft.	Profile of Jet Depth ft.	Crossection Sta. Traverse 30.27 ft.	Crossection Depth ft.
30.18	0.562	0.883	0.00
30.30	0.528	0.95	0.227
30.40	0.516	1.00	0.302
30.50	0.493	1.10	0.398
30.60	0.469	1.20	0.464
31.00	0.382	1.30	0.503
31.50	0.281	1.40	0.524
32.00	0.214	1.50	0.535
		1.60	0.520
		1.70	0.4915
		1.80	0.442
		1.90	0.369
		2.00	0.250
		2.05	0.154
		2.078	0.00

Run No. = 32
Q = 3.690 cfs.
y_1 = 55.26 cm.
y_2 = 0.0 cm.
M = b/B = 0.25
Model Sta. = 30.00 ft.
A_o = 0.614 sq. ft.
L/b = 0.0

Profile of Jet Sta. ft.	Profile of Jet Depth ft.	Crossection Sta. Traverse 30.32 ft.	Crossection Depth ft.
30.18	0.526	0.951	0.00
30.30	0.500	0.975	0.152
30.40	0.481	1.00	0.211
30.50	0.468	1.10	0.342
30.60	0.455	1.20	0.420
31.00	0.407	1.30	0.464
31.50	0.320	1.40	0.488
32.00	0.251	1.50	0.499
		1.60	0.480
		1.70	0.447
		1.80	0.392
		1.90	0.292
		1.95	0.218
		2.00	0.104
		2.021	0.00

Run No. = 33
Q = 3.485 cfs.
y_1 = 50.84 cm.
y_2 = 0.00 cm.
M = b/B = 0.25
Model Sta. = 30.00 ft.
A_o = 0.614 sq. ft.
L/b = 0.0

Profile of Jet Sta. ft.	Profile of Jet Depth ft.	Crossection Sta. Traverse 30.323 ft.	Crossection Depth ft.
30.18	0.524	0.952	0.00
30.30	0.498	0.975	0.160
30.40	0.483	1.00	0.212
30.50	0.472	1.10	0.342
30.60	0.444	1.20	0.419
31.00	0.398	1.30	0.463
31.50	0.307	1.40	0.484
32.00	0.235	1.50	0.493
		1.60	0.475
		1.70	0.444
		1.80	0.386
		1.90	0.289
		1.95	0.216
		2.00	0.108
		2.031	0.0

Run No. = 34
Q = 3.410 cfs.
y_1 = 47.90 cm.
y_2 = 0.00 cm.
M = b/B = 0.25
Model Sta. = 30.00 ft.
A_o = 0.614 sq. ft.
L/b = 0.0

Profile of Jet Sta. ft.	Profile of Jet Depth ft.	Crossection Sta. Traverse 30.285 ft.	Crossection Depth ft.
30.18	0.520	0.942	0.00
30.30	0.491	0.975	0.162
30.40	0.479	1.00	0.218
30.50	0.461	1.10	0.346
30.60	0.447	1.20	0.422
31.00	0.382	1.30	0.465
31.50	0.296	1.40	0.487
32.00	0.223	1.50	0.494
		1.60	0.478
		1.70	0.455
		1.80	0.391
		1.90	0.296
		1.95	0.224
		2.00	0.115
		2.03	0.00

TABLE 8-1 - RAW DATA - AREA OF VENA CONTRACTA - BACKWATER AND PROFILE

Run No. = 35
Q = 3.098 cfs.
y_1 = 42.32 cm.
y_2 = 0.00 cm.
M = b/B = 0.25
Model Sta. = 30.00 ft.
A_o = 0.614 sq. ft.
L/b = 0.0

Profile of Jet Sta. ft.	Profile of Jet Depth ft.	Crossection Sta. Traverse 30.24 ft.	Crossection Depth ft.
30.18	0.513	0.935	0.00
30.30	0.490	0.95	0.111
30.40	0.469	1.00	0.223
30.50	0.451	1.10	0.351
30.60	0.437	1.20	0.422
31.00	0.359	1.30	0.470
31.50	0.264	1.40	0.490
32.00	0.203	1.50	0.496
		1.60	0.484
		1.70	0.454
		1.80	0.396
		1.90	0.306
		1.95	0.232
		2.00	0.135
		2.036	0.00

Run No. = 36
Q = 3.020 cfs.
y_1 = 40.28 cm.
y_2 = 0.0 cm.
M = b/B = 0.25
Model Sta. = 30.00 ft.
A_o = 0.614 sq. ft.
L/b = 0.0

Profile of Jet Sta. ft.	Profile of Jet Depth ft.	Crossection Sta. Traverse 30.275 ft.	Crossection Depth ft.
30.18	0.512	0.938	0.00
30.30	0.485	0.95	0.100
30.40	0.463	1.00	0.218
30.50	0.448	1.10	0.342
30.60	0.432	1.20	0.415
31.00	0.352	1.30	0.457
31.50	0.258	1.40	0.482
32.00	0.194	1.50	0.490
		1.60	0.474
		1.70	0.443
		1.80	0.388
		1.90	0.294
		1.95	0.226
		2.00	0.1[illegible]
		2.03	0.00

Run No. = 37
Q = 2.920 cfs.
y_1 = 38.14 cm.
y_2 = 0.00 cm.
M = b/B = 0.25
Model Sta. = 30.00 ft.
A_o = 0.614 sq. ft.
L/b = 0.0

Profile of Jet Sta. ft.	Profile of Jet Depth ft.	Crossection Sta. Traverse 30.23 ft.	Crossection Depth ft.
30.18	0.510	0.935	0.00
30.30	0.484	0.95	0.106
30.40	0.461	1.00	0.226
30.50	0.445	1.10	0.346
30.60	0.425	1.20	0.421
31.00	0.33[illegible]	1.30	0.466
31.50	0.238	1.40	0.490
32.00	0.182	1.50	0.500
		1.60	0.481
		1.70	0.450
		1.80	0.398
		1.90	0.304
		1.95	0.234
		2.00	0.136
		2.03	0.00

Run No. = 38
Q = 2.7826 cfs.
y_1 = 35.22 cm.
y_2 = 0.93 cm.
M = b/B = 0.25
Model Sta. = 30.00 ft.
A_o = 0.614 sq. ft.
L/b = 0.0

Profile of Jet Sta. ft.	Profile of Jet Depth ft.	Crossection Sta. Traverse 30.22 ft.	Crossection Depth ft.
30.18	0.506	0.925	0.00
30.30	0.477	0.95	0.116
30.40	0.454	1.00	0.228
30.50	0.436	1.10	0.350
30.60	0.416	1.20	0.425
31.00	0.290	1.30	0.465
31.50	0.229	1.40	0.487
32.00	0.172	1.50	0.496
		1.60	0.480
		1.70	0.450
		1.80	0.394
		1.90	0.304
		1.95	0.238
		2.00	0.141
		2.032	0.00

Run No. = 39
Q = 2.52 cfs.
y_1 = 32.25 cm.
y_2 = 1.59 cm.
M = b/B = 0.25
Model Sta. = 30.00 ft.
A_o = 0.614 sq. ft.
L/b = 0.0

Profile of Jet Sta. ft.	Profile of Jet Depth ft.	Crossection Sta. Traverse 30.21 ft.	Crossection Depth ft.
30.18	0.505	0.935	0.00
30.30	0.472	0.950	0.123
30.40	0.441	1.00	0.228
30.50	0.421	1.10	0.352
30.60	0.404	1.20	0.422
31.00	0.303	1.30	0.469
31.50	0.211	1.40	0.496
32.00	0.161	1.50	0.499
		1.60	0.485
		1.70	0.454
		1.80	0.399
		1.90	0.310
		1.95	0.242
		2.00	0.151
		2.03	0.00

Run No. = 40
Q = 2.385 cfs.
y_1 = 29.94 cm.
y_2 = 1.95 cm.
M = b/B = 0.25
Model Sta. = 30.00 ft.
A_o = 0.614 sq. ft.
L/b = 0.00

Profile of Jet Sta. ft.	Profile of Jet Depth ft.	Crossection Sta. Traverse 30.20 ft.	Crossection Depth ft.
30.18	0.604	0.926	0.00
30.30	0.469	0.95	0.130
30.40	0.442	1.00	0.237
30.50	0.419	1.10	0.353
30.60	0.388	1.20	0.424
31.00	0.291	1.30	0.468
31.50	0.202	1.40	0.493
32.00	0.151	1.50	0.504
		1.60	0.484
		1.70	0.455
		1.80	0.398
		1.90	0.307
		1.95	0.241
		2.00	0.149
		2.028	0.00

Run No. = 41
Q = 2.100 cfs.
y_1 = 26.83 cm.
y_2 = 2.29 cm.
M = b/B = 0.25
Model Sta. = 30.00 ft.
A_o = 0.614 sq. ft.
L/b = 0.0

Profile of Jet Sta. ft.	Profile of Jet Depth ft.	Crossection Sta. Traverse 30.181 ft.	Crossection Depth ft.
30.18	0.506	0.922	0.00
30.30	0.462	0.95	0.141
30.40	0.430	1.00	0.238
30.50	0.401	1.10	0.353
30.60	0.368	1.20	0.424
31.00	0.265	1.30	0.467
31.50	0.216	1.40	0.496
32.00	0.136	1.50	0.506
		1.60	0.483
		1.70	0.448
		1.80	0.402
		1.90	0.310
		1.95	0.213
		2.00	0.157
		2.03	0.00

Run No. = 42
Q = 2.03 cfs.
y_1 = 24.63 cm.
y_2 = 2.33 cm.
M = b/B = 0.25
Model Sta. = 30.00 ft.
A_o = 0.614 sq. ft.
L/b = 0.0

Profile of Jet Sta. ft.	Profile of Jet Depth ft.	Crosssection Sta. Traverse 30.188 ft.	Crosssection Depth ft.
30.18	0.504	0.922	0.00
30.30	0.458	0.950	0.145
30.40	0.423	1.00	0.288
30.50	0.386	1.10	0.349
30.60	0.352	1.20	0.417
31.00	0.247	1.30	0.460
31.50	0.168	1.40	0.490
32.00	0.128	1.50	0.503
		1.60	0.477
		1.70	0.447
		1.80	0.400
		1.90	0.307
		2.00	0.245
		2.027	0.159
			0.00

TABLE 8-1 - RAW DATA - AREA OF VENA CONTRACTA - BACKWATER AND PROFILE

Run No. = 43
Q = 1.873 cfs.
y_1 = 23.43 cm.
y_2 = 0.0 cm.
M = b/B = 0.25
Model Sta. = 30.00 ft.
A_o = 0.614 sq. ft.
L/b = 0.0

Profile of Jet Sta. ft.	Profile of Jet Depth ft.	Crossection Sta. Traverse 30.185 ft.	Crossection Depth ft.
30.18	0.507	0.92	0.00
30.30	0.454	0.95	0.144
30.40	0.414	1.00	0.240
30.50	0.378	1.10	0.358
30.60	0.341	1.20	0.418
31.00	0.236	1.30	0.463
31.50	0.162	1.40	0.497
32.00	0.122	1.50	0.507
		1.60	0.482
		1.70	0.449
		1.80	0.399
		1.90	0.311
		2.00	0.163
		2.04	0.00

Run No. = 44
Q = 1.742 cfs.
y_1 = 20.88 cm.
y_2 = 0.0 cm.
M = b/B = 0.25
Model Sta. = 30.00 ft.
A_o = 0.614 sq. ft.
L/b = 0.0

Profile of Jet Sta. ft.	Profile of Jet Depth ft.	Crossection Sta. Traverse 30.175 ft.	Crossection Depth ft.
30.18	0.510	0.92	0.00
30.30	0.451	0.95	0.151
30.40	0.398	1.00	0.243
30.50	0.356	1.10	0.358
30.60	0.314	1.20	0.416
31.00	0.213	1.30	0.451
31.50	0.144	1.40	0.504
32.00	0.110	1.50	0.514
		1.60	0.486
		1.70	0.443
		1.80	0.391
		1.90	0.308
		2.00	0.169
		2.04	0.00

Run No. = 45
Q = 3.70 cfs.
y_1 = 55.50 cm.
y_2 = 0.00 cm.
M = b/B = 0.25
Model Sta. = 30.00 ft.
A_o = 0.614 sq. ft.
L/b = 0.0

Profile of Jet Sta. ft.	Profile of Jet Depth ft.	Crossection Sta. Traverse 30.23 ft.	Crossection Depth ft.
		0.95	0.00
		1.00	0.220
		1.05	0.303
		1.10	0.361
		1.20	0.439
		1.30	0.486
		1.40	0.510
		1.50	0.522
		1.60	0.503
		1.70	0.474
		1.80	0.418
		1.85	0.377
		1.90	0.326
		1.95	0.256
		2.00	0.133
		2.04	0.00

Run No. = 46
Q = 2.835 cfs.
y_1 = 36.66 cm.
y_2 = 0.00 cm.
M = b/B = 0.25
Model Sta. = 30.00 ft.
A_o = 0.614 sq. ft.
L/b = 0.0

Profile of Jet Sta. ft.	Profile of Jet Depth ft.	Crossection Sta. Traverse 30.19 ft.	Crossection Depth ft.
		0.915	0.00
		0.950	0.087
		1.00	0.226
		1.05	0.302
		1.10	0.356
		1.20	0.433
		1.30	0.479
		1.40	0.503
		1.50	0.510
		1.60	0.498
		1.70	0.468
		1.80	0.413
		1.90	0.328
		1.95	0.262
		2.00	0.172
		2.06	0.00

Run No. = 47
Q = 2.515 cfs.
y_1 = 31.50 cm.
y_2 = 2.08 cm.
M = b/B = 0.25
Model Sta. = 30.00 ft.
A_o = 0.614 sq. ft.
L/b = 0.0

Profile of Jet Sta. ft.	Profile of Jet Depth ft.	Crossection Sta. Traverse 30.205 ft.	Crossection Depth ft.
		0.93	0.00
		0.95	0.113
		1.00	0.223
		1.05	0.294
		1.10	0.349
		1.20	0.422
		1.30	0.467
		1.40	0.492
		1.50	0.503
		1.60	0.487
		1.70	0.457
		1.80	0.408
		1.85	0.366
		1.90	0.320
		1.95	0.253
		2.00	0.170
		2.045	0.00

Run No. = 48
Q = 2.112 cfs.
y_1 = 25.40 cm.
y_2 = 2.33 cm.
M = b/B = 0.250
Model Sta. = 30.00 ft.
A_o = 0.614 sq. ft.
L/b = 0.0

Profile of Jet Sta. ft.	Profile of Jet Depth ft.	Crossection Sta. Traverse 30.185 ft.	Crossection Depth ft.
		0.93	0.00
		0.95	0.127
		1.00	0.236
		1.10	0.344
		1.20	0.417
		1.30	0.458
		1.40	0.491
		1.50	0.502
		1.60	0.485
		1.70	0.453
		1.80	0.404
		1.90	0.316
		1.95	0.258
		2.00	0.173
		2.045	0.00

Run No. = 49
Q = 1.820 cfs.
y_1 = 21.53 cm.
y_2 = 2.55 cm.
M = b/B = 0.25
Model Sta. = 30.00 ft.
A_o = 0.614 sq. ft.
L/b = 0.0

Profile of Jet Sta. ft.	Profile of Jet Depth ft.	Crossection Sta. Traverse 30.18 ft.	Crossection Depth ft.
		0.903	0.00
		0.95	0.139
		1.00	0.231
		1.05	0.293
		1.10	0.349
		1.20	0.409
		1.30	0.458
		1.40	0.507
		1.50	0.525
		1.60	0.493
		1.70	0.447
		1.80	0.393
		1.90	0.316
		1.95	0.257
		2.00	0.183
		2.045	0.00

Run No. = 51
Q = 2.552 cfs.
y_1 = 59.95 cm.
y_2 = 0.0 cm.
M^2 = b/B = 0.20
Model Sta. = 30.00 ft.
A_o = 0.393 sq. ft.
L/b = 0.0

Profile of Jet Sta. ft.	Profile of Jet Depth ft.	Crossection Sta. Traverse 30.33 ft.	Crossection Depth ft.
30.18	0.421	1.067	0.00
30.30	0.407	1.10	0.147
30.40	0.388	1.20	0.284
30.50	0.377	1.30	0.351
30.60	0.369	1.40	0.388
31.00	0.326	1.50	0.397
31.50	0.258	1.60	0.387
32.00	0.198	1.70	0.338
		1.80	0.259
		1.90	0.080
		1.904	0.00

TABLE 8-1- RAW DATA - AREA OF VENA CONTRACTA - BACKWATER AND PROFILE

Run No. = 52
Q = 2.442 cfs.
y_1 = 56.03 cm.
y_2 = 0.0 cm.
M = b/B = 0.20
Model Sta. = 30.00 ft.
A_9 = 0.393 sq. ft.
L/b = 0.0

Profile of Jet Sta. ft.	Profile of Jet Depth ft.	Crossection Sta. (Traverse 30.32) ft.	Crossection Depth ft.
30.18	0.420	1.066	0.00
30.30	0.401	1.10	0.152
30.40	0.387	1.20	0.286
30.50	0.376	1.30	0.353
30.60	0.365	1.40	0.386
31.00	0.320	1.50	0.397
31.50	0.245	1.60	0.387
32.00	0.185	1.70	0.338
		1.80	0.258
		1.90	0.0772
		1.911	0.00

Run No. = 53
Q = 2.290 cfs.
y_1 = 50.68 cm.
y_2 = 0.0 cm.
M = b/B = 0.20
Model Sta. = 30.00 ft.
A_9 = 0.393 sq. ft.
L/b = 0.0

Profile of Jet Sta. ft.	Profile of Jet Depth ft.	Crossection Sta. (Traverse 30.282) ft.	Crossection Depth ft.
30.18	0.417	1.067	0.00
30.30	0.397	1.10	0.156
30.40	0.380	1.20	0.287
30.50	0.373	1.30	0.354
30.60	0.360	1.40	0.388
31.00	0.306	1.50	0.404
31.50	0.223	1.60	0.382
32.00	0.173	1.70	0.339
		1.80	0.260
		1.90	0.084
		1.921	0.00

Run No. = 54
Q = 2.170 cfs.
y_1 = 46.94
y_2 = 0.93 cm.
M = b/B = 0.20
Model Sta. = 30.00 ft.
A_9 = 0.393 sq. ft.
L/b = 0.0

Profile of Jet Sta. ft.	Profile of Jet Depth ft.	Crossection Sta. (Traverse 30.26) ft.	Crossection Depth ft.
30.18	0.414	1.065	0.00
30.30	0.396	1.10	0.157
30.40	0.378	1.20	0.288
30.50	0.366	1.30	0.352
30.60	0.360	1.40	0.387
31.00	0.293	1.50	0.398
31.50	0.221	1.60	0.382
32.00	0.160	1.70	0.339
		1.80	0.262
		1.90	0.089
		1.920	0.00

Run No. = 55
Q = 2.12 cfs.
y_1 = 43.96 cm.
y_2 = 1.23 cm.
M = b/B = 0.20
Model Sta. = 30.00 ft.
A_9 = 0.393 sq. ft.
L/b = 0.0

Profile of Jet Sta. ft.	Profile of Jet Depth ft.	Crossection Sta. (Traverse 30.25) ft.	Crossection Depth ft.
30.18	0.411	1.062	0.00
30.30	0.390	1.10	0.159
30.40	0.382	1.20	0.290
30.50	0.369	1.30	0.353
30.60	0.351	1.40	0.386
31.00	0.290	1.50	0.398
31.50	0.207	1.60	0.383
32.00	0.159	1.70	0.341
		1.80	0.263
		1.90	0.937
		1.921	0.00

Run No. = 56
Q = 1.975 cfs.
y_1 = 40.44 cm.
y_2 = 1.31 cm.
M = b/B = 0.20
Model Sta. = 30.00 ft.
A_9 = 0.393 sq. ft.
L/b = 0.0

Profile of Jet Sta. ft.	Profile of Jet Depth ft.	Crossection Sta. (Traverse 30.24) ft.	Crossection Depth ft.
30.18	0.407	1.061	0.00
30.30	0.384	1.10	0.164
30.40	0.366	1.20	0.286
30.50	0.358	1.30	0.352
30.60	0.347	1.40	0.383
31.00	0.271	1.50	0.396
31.50	0.188	1.60	0.381
32.00	0.140	1.70	0.339
		1.80	0.261
		1.90	0.101
		1.927	0.00

Run No. = 57
Q = 1.937 cfs.
y_1 = 38.45 cm.
y = 1.33 cm.
M = b/B = 0.20
Model Sta. = 30.00 ft.
A_9 = 0.393 sq. ft.
L/b = 0.0

Profile of Jet Sta. ft.	Profile of Jet Depth ft	Crossection Sta. (Traverse 30.235) ft.	Crossection Depth ft.
30.18	0.401	1.062	0.00
30.30	0.383	1.10	0.161
30.40	0.368	1.20	0.286
30.50	0.350	1.30	0.352
30.60	0.337	1.40	0.381
31.00	0.261	1.50	0.398
31.50	0.179	1.60	0.378
32.00	0.135	1.70	0.336
		1.80	0.256
		1.90	0.103
		1.922	0.00

Run No. = 58
Q = 1.800 cfs.
y_1 = 34.75 cm.
y_2 = 1.33 cm.
M = b/B = 0.20
Model Sta. = 30.00 ft.
A_9 = 0.393 sq. ft.
L/b = 0.0

Profile of Jet Sta. ft.	Profile of Jet Depth ft.	Crossection Sta. (Traverse 30.228) ft.	Crossection Depth ft.
30.18	0.402	1.063	0.00
30.30	0.379	1.10	0.164
30.40	0.364	1.20	0.286
30.50	0.340	1.30	0.348
30.60	0.326	1.40	0.378
31.00	0.246	1.50	0.392
31.50	0.167	1.60	0.376
32.00	0.127	1.70	0.336
		1.80	0.261
		1.90	0.108
		1.927	0.00

Run No. = 59
Q = 1.75 cfs.
y_1 = 32.55 cm.
y_2 = 1.33 cm.
M = b/B = 0.20
Model Sta. = 30.00 ft.
A_9 = 0.393 sq. ft.
L/b = 0.0

Profile of Jet Sta. ft.	Profile of Jet Depth ft.	Crossection Sta. (Traverse 30.215) ft.	Crossection Depth ft.
30.18	0.398	1.059	0.00
30.30	0.375	1.10	0.164
30.40	0.354	1.20	0.286
30.50	0.336	1.30	0.349
30.60	0.319	1.40	0.379
31.00	0.234	1.50	0.391
31.50	0.158	1.60	0.376
32.00	0.120	1.70	0.339
		1.80	0.263
		1.90	0.112
		1.926	0.00

TABLE 8-1- RAW DATA - AREA OF VENA CONTRACTA - BACKWATER AND PROFILE

Run No. = 60
Q = 1.62 cfs.
y_1 = 29.65 cm.
y_2 = 1.35 cm.
M = b/B = 0.20
Model Sta. = 30.00 ft.
A_o = 0.393 sq. ft.
L/b = 0.0

Profile of Jet Sta. ft.	Profile of Jet Depth ft.	Crossection Sta. Traverse 30.190 ft.	Crossection Depth ft.
30.18	0.394	1.057	0.00
30.30	0.369	1.10	0.177
30.40	0.348	1.20	0.292
30.50	0.326	1.30	0.352
30.60	0.302	1.40	0.384
31.00	0.217	1.50	0.391
31.50	0.145	1.60	0.379
32.00	0.112	1.70	0.341
		1.80	0.266
		1.90	0.119
		1.930	0.00

Run No. = 61
Q = 1.570 cfs.
y_1 = 28.28 cm.
y_2 = 1.38 cm.
M = b/B = 0.20
Model Sta. = 30.00 ft.
A_o = 0.393 sq. ft.
L/b = 0.0

Profile of Jet Sta. ft.	Profile of Jet Depth ft.	Crossection Sta. Traverse 30.185 ft.	Crossection Depth ft.
30.18	0.389	1.055	0.00
30.30	0.362	1.10	0.173
30.40	0.340	1.20	0.287
30.50	0.322	1.30	0.351
30.60	0.300	1.40	0.381
31.00	0.210	1.50	0.389
31.50	0.141	1.60	0.378
32.00	0.102	1.70	0.339
		1.80	0.264
		1.90	0.124
		1.936	0.00

Run No. = 62
Q = 1.530 cfs.
y_1 = 27.46 cm.
y_2 = 1.43 cm.
M = b/B = 0.20
Model Sta. = 30.00 ft.
A_o = 0.393 sq. ft.
L/b = 0.0

Profile of Jet Sta. ft.	Profile of Jet Depth ft.	Crossection Sta. Traverse 30.173 ft.	Crossection Depth ft.
30.18	0.390	1.05	0.00
30.30	0.362	1.10	0.176
30.40	0.339	1.20	0.288
30.50	0.317	1.30	0.355
30.60	0.295	1.40	0.385
31.00	0.205	1.50	0.390
31.50	0.135	1.60	0.382
32.00	0.103	1.70	0.342
		1.80	0.268
		1.90	0.125
		1.935	0.00

Run No. = 63
Q = 1.45 cfs.
y_1 = 15.18 cm.
y_2 = 1.55 cm.
M = b/B = 0.20
Model Sta. = 30.00 ft.
A_o = 0.393 sq. ft.
L/b = 0.0

Profile of Jet Sta. ft.	Profile of Jet Depth ft.	Crossection Sta. Traverse 30.165 ft.	Crossection Depth ft.
30.18	0.391	1.053	0.00
30.30	0.356	1.10	0.178
30.40	0.299	1.20	0.292
30.50	0.275	1.30	0.353
30.60	0.248	1.40	0.385
31.00	0.192	1.50	0.396
31.50	0.125	1.60	0.381
32.00	0.092	1.70	0.344
		1.80	0.270
		1.90	0.136
		1.932	0.00

Run No. = 64
Q = 1.311 cfs.
y_1 = 22.12 cm.
y_2 = 1.64 cm.
M = b/B = 0.20
Model Sta. = 30.00 ft.
A_o = 0.393 sq. ft.
L/b = 0.0

Profile of Jet Sta. ft.	Profile of Jet Depth ft.	Crossection Sta. Traverse 30.165 ft.	Crossection Depth ft.
30.18	0.388	1.04	0.00
30.30	0.352	1.10	0.185
30.40	0.320	1.20	0.291
30.50	0.290	1.30	0.349
30.60	0.264	1.40	0.382
31.00	0.178	1.50	0.394
31.50	0.117	1.60	0.378
32.00	0.087	1.70	0.336
		1.80	0.264
		1.90	0.133
		1.937	0.00

Run No. = 65
Q = 1.27 cfs.
y_1 = 21.11 cm.
y_2 = 1.77 cm.
M = b/B = 0.20
Model Sta. = 30.00 ft.
A_o = 0.393 sq. ft.
L/b = 0.0

Profile of Jet Sta. ft.	Profile of Jet Depth ft.	Crossection Sta. Traverse 30.16 ft.	Crossection Depth ft.
30.18	0.390	1.042	0.00
30.30	0.345	1.10	0.181
30.40	0.314	1.20	0.288
30.50	0.285	1.30	0.349
30.60	0.255	1.40	0.384
31.00	0.171	1.50	0.398
31.50	0.112	1.60	0.380
32.00	0.083	1.70	0.339
		1.80	0.267
		1.90	0.144
		1.940	0.00

Run No. = 66
Q = 1.20 cfs.
y_1 = 19.73 cm.
y_2 = 1.75 cm.
M = b/B = 0.20
Model Sta. = 30.00 ft.
A_o = 0.393 sq. ft.
L/b = 0.0

Profile of Jet Sta. ft.	Profile of Jet Depth ft.	Crossection Sta. Traverse 30.155 ft.	Crossection Depth ft.
30.18	0.392	1.046	0.00
30.30	0.343	1.10	0.185
30.40	0.307	1.20	0.294
30.50	0.274	1.30	0.350
30.60	0.243	1.40	0.384
31.00	0.160	1.50	0.402
31.50	0.106	1.60	0.378
32.00	0.076	1.70	0.336
		1.80	0.267
		1.90	0.141
		1.940	0.00

Run No. = 67
Q = 1.08 cfs.
y_1 = 17.83 cm.
y_2 = 1.98 cm.
M = b/B = 0.20
Model Sta. = 30.00 ft.
A_o = 0.393 sq. ft.
L/b = 0.0

Profile of Jet Sta. ft.	Profile of Jet Depth ft.	Crossection Sta. Traverse 30.15 ft.	Crossection Depth ft.
30.18	0.392	1.051	0.00
30.30	0.302	1.10	0.184
30.40	0.294	1.20	0.292
30.50	0.258	1.30	0.348
30.60	0.226	1.40	0.338
31.00	0.146	1.50	0.408
31.50	0.097	1.60	0.378
32.00	0.040	1.70	0.336
		1.80	0.270
		1.90	0.145
		1.938	0.00

TABLE 8-2 RAW DATA - SUBMERGED TESTS

Run No.	101	102	103	104	105	106	107	108
Geometry	Ia	Ia	Ia	Ia	Ia	Ia	Ia	Ia
n	0.0110	0.0110	0.0110	0.0110	0.0110	0.0110	0.0110	0.110
Q (cfs.)	2.5	2.5	2.5	2.5	2.0	2.0	2.0	2.0
Y_n (ft.)	0.92	0.92	0.92	0.92	0.80	0.80	0.80	0.80
F_n	0.10	0.10	0.10	0.10	0.10	0.10	0.10	0.10
S	0.000026	0.000026	0.000026	0.000026	0.0000255	0.0000255	0.0000255	0.0000255
M=b/B	0.20	0.25	0.275	0.30	0.20	0.25	0.275	0.30
L/b	0.0	0.0	0.0	0.0	0.0	0.0	0.0	0.0
Temp. (F)	68°	68°	68°	48°	68°	68°	68°	68°
Model Sta.	30.00	30.00	30.00	30.00	30.00	30.00	30.00	30.00
Y_1 (cm.)		43.57	36.86	34.12	50.82	34.45	30.95	28.01
Y_2 (cm.)		22.20	23.20	24.05	18.15	19.89	20.82	21.30
N	1.0	1.0	1.0	1.0	1.0	1.0	1.0	1.0
Φ 2	0.0	0.0	0.0	0.0	0.0	0.0	0.0	0.0

Run 101: OVERTOPPED MODEL

Run	Sta. ft.	L cm.	Depth Cent. cm.	R cm.
102	10		43.57	
	15		43.56	
	20		43.58	
	25		43.57	
	29.9		43.57	
	30.3	22.20		
103	10		36.86	
	15		"	
	20		"	
	25		"	
	29.9		"	
	30.3	23.20		
104	10		34.12	
	15		"	
	20		"	
	25		"	
	29.9		"	
	30.3	24.05		
105	10		50.82	
	15		"	
	20		"	
	25		"	
	24.9		"	
	30.30	18.15		20.37
106	10		34.45	
	15		"	
	20		"	
	25		"	
	29.9		"	
	30.3	19.89		21.21
107	10		30.95	
	15		"	
	20		"	
	25		"	
	29.9		"	
	30.0	20.82		
108	10		28.01	
	15		"	
	20		"	
	25		"	
	29.9		"	
	30.3	21.30		

Run No.	109	110	111	112	113	114	115	116
Geometry	Ia	Ia	Ia	Ia	Ia	Ia	Ia	Ia
n	0.0110	0.0110	0.0110	0.0110	0.0110	0.0110	0.0110	0.0110
Q (cfs.)	2.5	2.5	2.5	2.46	2.46	2.46	2.46	3.0
Y_n (ft.)	0.92	0.92	0.92	0.70	0.70	0.70	0.70	0.80
F_n	0.10	0.10	0.10	0.15	0.15	0.15	0.15	0.15
S	.000026	0.000026	0.000026	0.000062	0.000062	0.000062	0.000062	0.000052
M=b/B	0.25	0.275	0.30	0.20	0.25	0.275	0.30	0.25
L/b	0.0	0.0	0.0	0.0	0.0	0.0	0.0	0.0
Temp. (F)	68°	68°	68°	68°	68°	68°	68°	68°
Model Sta.	30.00	30.00	30.00	30.00	30.00	30.00	30.00	30.00
Y_1 (cm.)	44.12	42.92	34.86	59.20	36.80	30.24	27.43	48.82
Y_2 (cm.)	23.90	22.88	23.78	14.82	14.0	15.76	16.46	16.27
N	1.0	1.0	1.0	1.0	1.0	1.0	1.0	1.0
Φ 2	0.0	0.0	0.0	0.0	0.0	0.0	0.0	0.0

Run	Sta. ft.	L cm.	Depth Cent. cm.	R cm.
109	10		44.12	
	15		"	
	20		"	
	25		"	
	29.9		"	
	30.3	23.90		
110	10		42.92	
	15		"	
	20		"	
	25		"	
	29.9		"	
	30.3	22.88		
111	10		34.86	
	15		"	
	20		"	
	25		"	
	29.9		"	
	30.3	23.78		
112	10		59.20	
	15		"	
	20		"	
	25		"	
	29.9		"	
	30.3	14.82		
113	10		36.80	
	15		"	
	20		"	
	25		"	
	29.9		"	
	30.3	14.0		
114	10		30.20	
	15		"	
	20		"	
	25		"	
	29.9		"	
	30.3	15.76		
115	10		27.43	
	15		"	
	20		"	
	25		"	
	29.9		"	
	30.3	16.46		
116	10		48.82	
	15		"	
	20		"	
	25		"	
	29.9		"	
	30.3	16.27		

TABLE 8-2- RAW DATA - SUBMERGED TESTS

Run No.	117	118	119	120	121	122	123	124	125
Geometry	Ia	Ia	Ia	Ia	Ia	Ia	Ia	Ia	Ia
n	0.0110	0.0110	0.0110	0.0110	0.0110	0.0110	0.0110	0.0110	0.0110
Q	3.0 cfs.	3.0 cfs.	3.5 cfs.	3.5 cfs.	2.5 cfs.	2.5 cfs.	2.5 cfs.	2.5 cfs.	2.5 cfs.
Y_n	0.80 ft.	0.80 ft.	0.88 ft.	0.88 ft.	0.70 ft.	0.70 ft.	0.70 ft.	0.70 ft.	0.585 ft
F_n	0.15	0.15	0.15	0.15	0.15	0.15	0.15	0.15	0.20
S	0.000052	0.00005	0.000062	0.000062	0.000026	0.000062	0.000062	0.000062	0.00011
M=b/B	0.275	0.30	0.275	0.30	0.20	0.25	0.275	0.30	0.20
L/b	0.0	0.0	0.0	0.0	0.0	0.0	0.0	0.0	0.0
Temp.	68° F	68° F	68° F	68° F	68° F	68° F	68° F	68° F	68° F
Model Sta.	30.00	30.00	30.00	30.00	30.00	30.00	30.00	30.00	30.00
Y_1	41.62 cm.	35.86 cm.	48.27 cm.	41.72 cm.	59.69 cm.	37.41 cm.	32.29 cm.	27.94 cm.	58.90 cm
Y_2	19.76 cm.	18.88 cm.	21.62 cm.	22.62 cm.	8.92 cm.	14.12 cm.	15.15 cm.	16.82 cm.	5.12 cm
N	1.0	1.0	1.0	1.0	1.0	1.0	1.0	1.0	1.0
Φ_2	0.0	0.0	0.0	0.0	0.0	0.0	0.0	0.0	0.0

Sta. ft.	117 L cm.	117 Depth Cent. cm.	117 R cm.	118 L cm.	118 Depth Cent. cm.	118 R cm.	119 L cm.	119 Depth Cent. cm.	119 R cm.
10		41.62			35.86			48.27	
15		"			"			"	
20		"			"			"	
25		"			"			"	
29.9		"			"			"	
30.3	19.76			18.88			21.62		18.42

Sta. ft.	120 L cm.	120 Depth Cent. cm.	120 R cm.	121 L cm.	121 Depth Cent. cm.	121 R cm.	122 L cm.	122 Depth Cent. cm.	122 R cm.
10		41.72			59.69			37.41	
15		"			"			"	
20		"			"			"	
25		"			"			"	
29.9		"			"			"	
30.3	22.62		20.00	8.92		14.89	14.12		

Sta. ft.	123 L cm.	123 Depth Cent. cm.	123 R cm.	124 L cm.	124 Depth Cent. cm.	124 R cm.	125 L cm.	125 Depth Cent. cm.	125 R cm.
10		32.29			27.94			58.90	
15		"			"			"	
20		"			"			"	
25		"			"			"	
29.9		"			"			"	
30.3	15.15			16.82			5.12		

Run No.	126	127	128	129	130	131	132	133	134
Geometry	Ia	Is	Ia	Ia	Ia	Is	Ia	Ia	Ia
n	0.0110	0.0110	0.0110	0.0110	0.0110	0.0110	0.0110	0.0110	0.0110
Q	2.5 cfs.	2.5 cfs.	2.5 cfs.	3.0 cfs.	3.0 cfs.	3.0 cfs.	3.5 cfs.	3.5 cfs.	3.5 cfs.
Y_n	0.585 ft.	0.585 ft.	0.585 ft.	0.66 ft.	0.66 ft.	0.66 ft.	0.725 ft.	0.725 ft.	0.725 ft.
F_n	0.20	0.20	0.20	0.20	0.20	0.20	0.20	0.20	0.20
S	0.00011	0.00011	0.00011	0.000098	0.000098	0.000098	0.000115	0.000115	0.000115
M=b/B	0.25	0.275	0.30	0.25	0.275	0.30	0.20	0.275	0.30
L/b	0.0	0.0	0.0	0.0	0.0	0.0	0.0	0.0	0.0
Temp.	68° F	68° F	68°F	68° F	68° F	68° F	68° F	68° F	68° F
Model Sta.	30.00	30.00	30.00	30.00	30.00	30.00	30.00	30.00	30.00
Y_1	36.64 cm.	30.80 cm.	26.20 cm.	43.96 cm.	36.49 cm.	31.22 cm.	53.72 cm.	44.70 cm.	37.43 cm.
Y_2	8.22 cm.	10.12 cm.	11.31 cm.	14.54 cm.	14.82 cm.	16.00 cm.	15.00 cm.	15.88 cm.	16.83 cm.
N	1.0	1.0	1.0	1.0	1.0	1.0	1.0	1.0	1.0
Φ_2	0.0	0.0	0.0	0.0	0.0	0.0	0.0	0.0	0.0

Sta. ft.	126 L cm.	126 Depth Cent. cm.	126 R cm.	127 L cm.	127 Depth Cent. cm.	127 R cm.	128 L cm.	128 Depth Cent. cm.	128 R cm.
10		36.60			30.80			26.30	
15		"			"			"	
20		"			"			"	
25		"			"			"	
29.9		"			"				
30.3	8.22			10.12			11.31		

Sta. ft.	129 L cm.	129 Depth Cent. cm.	129 R cm.	130 L cm.	130 Depth Cent. cm.	130 R cm.	131 L cm.	131 Depth Cent. cm.	131 R cm.
10		43.96			36.69			31.22	
15		"			"			"	
20		"			"			"	
25		"			"			"	
29.9									
30.3	14.54			14.82			16.00		

Sta. ft.	132 L cm.	132 Depth Cent. cm.	132 R cm.	133 L cm.	133 Depth Cent. cm.	133 R cm.	134 L cm.	134 Depth Cent. cm.	134 R cm.
10		53.72			44.70			37.43	
15		"			"			"	
20		"			"			"	
25		"			"			"	
29.9									
30.3	15.00		8.62	15.88			16.83		

TABLE 8-2 RAW DATA - SUBMERGED TESTS

Run No.	135	136	137	138	139	140	141	142	143
Geometry	Ib	Ib	1b	Ib	Ib	Ib	Ib	Ib	Ib
n	0.0110	0.0110	0.0110	0.0110	0.0110	0.0110	0.0110	0.0110	0.0110
Q	2.0 cfs.	2.0 cfs.	2.0 cfs.	2.0 cfs.	2.0 cfs.	2.0 cfs.	2.0 cfs.	2.0 cfs.	2.0 cfs.
Y_n	0.80 ft.	0.80 ft.	0.80 ft.	0.80 ft.	0.80 ft.	0.80 ft.	0.80 ft.	0.80 ft.	0.80 ft.
F_n	0.10	0.10	0.10	0.10	0.10	0.10	0.10	0.10	0.10
S	0.0000255	0.0000255	0.0000255	0.0000255	0.0000255	0.0000255	0.0000255	0.0000255	0.00002
M=b/B	0.20	0.20	0.20	0.20	0.25	0.25	0.25	0.25	0.30
L/b	0.25	0.50	0.75	1.0	0.25	0.50	0.75	1.0	0.25
Temp.	72° F	72° F	72° F	72° F	72° F	72° F	72° F	72° F	72° F
Model Sta.	30.00	30.00	30.00	30.00	30.00	30.00	30.00	30.00	30.00
Y_1	47.62 cm.	44.40 cm.	43.64 cm.	41.07 cm.	37.64 cm.	33.88 cm.	32.16 cm.	31.85 cm.	27.90 cm
Y_2	19.55 cm.	21.00 cm.	21.0 cm.	20.77 cm.	21.0 cm.	21.80 cm.	22.34 cm.	21.94 cm.	22.8 cm
N	1.0	1.0	1.0	1.0	1.0	1.0	1.0	1.0	1.0
Φ 2	0.0	0.0	0.0	0.0	0.0	0.0	0.0	0.0	0.0

Run 135

Sta. ft.	L cm.	Depth Cent. cm.	R cm.
10		47.62	
15		"	
20		"	
25		"	
27		"	
29.7	47.69	"	
30.3	19.55		20.98
44.0		20.5	

Run 136

Sta. ft.	L cm.	Depth Cent. cm.	R cm.
10		44.40	
15		"	
20		"	
25		"	
27		"	
29.4	44.40	"	
30.3	21.0		21.21
44.0		21.1	

Run 137

Sta. ft.	L cm.	Depth Cent. cm.	R cm.
10		43.64	
15		"	
20		"	
25		"	
27		"	
29.15	43.64	"	
30.3	21.0		22.03
44.0		21.55	

Run 138

Sta. ft.	L cm.	Depth Cent. cm.	R cm.
10		41.09	
15		41.08	
20		"	
25		"	
27		"	
28.9	41.08	41.07	
30.3	20.77		22.43
44		21.75	

Run 139

Sta. ft.	L cm.	Depth Cent. cm.	R cm.
10		37.82	
15		37.78	
20		37.72	
25		37.69	
27		37.68	
29.6	37.65	37.64	
30.3	21.0		22.31
44.0		22.0	

Run 140

Sta. ft.	L cm.	Depth Cent. cm.	R cm.
10		33.92	
15		33.91	
20		33.89	
25		33.88	
27		33.88	
29.3	33.90	33.88	
30.3	21.80		22.50
44.0		22.30	

Run 141

Sta. ft.	L cm.	Depth Cent. cm.	R cm.
10		32.28	
15		32.27	
20		32.26	
25		32.24	
27		32.22	
29.0	32.19	32.16	
30.3	22.34		22.25
44.0		22.80	

Run 142

Sta. ft.	L cm.	Depth Cent. cm.	R cm.
10		32.11	
15		32.08	
20		32.06	
25		31.96	
27		31.87	
28.6	31.90	31.85	
30.3	21.94		22.86
44.0		22.60	

Run 143

Sta. ft.	L cm.	Depth Cent. cm.	R cm.
10		28.26	
15		28.25	
20		28.24	
25		28.23	
27		28.22	
29.5	28.28	27.90	
30.3	22.80		22.50
44.0		22.60	

Run No.	144	145	146	147	148	149	150	151	152
Geometry	Ib	Ib	Ib	Ib	Ib	Ib	Ib	Ib	Ib
n	0.0110	0.0110	0.0110	0.0110	0.0110	0.0110	0.0110	0.0110	0.0110
Q	2.0 cfs.	2.0 cfs.	2.0 cfs.	2.5 cfs.	2.5 cfs.	2.5 cfs.	2.5 cfs.	2.5 cfs.	2.5 cfs.
Y_n	0.80 ft.	0.80ft.	0.80 ft.	0.92 ft.	0.92 ft.	0.92 ft.	0.92 ft.	0.70 ft.	0.70 ft.
F_n	0.10	0.10	0.10	0.10	0.10	0.10	0.10	0.15	0.15
S	0.0000255	0.0000255	0.0000255	0.000026	0.000026	0.000026	0.000026	0.000062	0.000062
M=b/B	0.30	0.30	0.30	0.25	0.25	0.25	0.25	0.20	0.20
L/b	0.50	0.75	1.0	0.25	0.50	0.75	1.0	0.25	0.50
Temp.	72° F	72° F	72° F	72° F	72° F	72° F	72° F	72° F	72° F
Model Sta.	30.00	30.00	30.00	30.00	30.00	30.00	30.00	30.00	30.00
Y_1	27.66 cm.	27.40 cm.	26.58 cm.	47.34 cm.	40.58 cm.	40.00 cm.	39.20 cm.	58.00 cm.	56.00 cm.
Y_2	22.01 cm.	22.50 cm.	23.00 cm.	23.20 cm.	24.0 cm.	25.80 cm.	26.00 cm.	9.0 cm.	11.00 cm.
N	1.0	1.0	1.0	1.0	1.0	1.0	1.0	1.0	1.0
Φ 2	0.0	0.0	0.0	0.0	0.0	0.0	0.0	0.0	0.0

Run 144

Sta. ft.	L cm.	Depth Cent. cm.	R cm.
10		28.14	
15		28.10	
20		28.08	
25		28.00	
27		27.94	
29.2	28.14	27.66	
30.3	22.01		23.04
44.0		22.4	

Run 145

Sta. ft.	L cm.	Depth Cent. cm.	R cm.
10		27.81	
15		27.81	
20		27.80	
25		27.78	
27		27.76	
28.8	27.70	27.40	
30.3	22.50		22.50
44.0		22.50	

Run 146

Sta. ft.	L cm.	Depth Cent. cm.	R cm.
10		37.4	
15		37.3	
20		37.2	
25		37.1	
27		37.0	
28.4	26.90	26.58	
30.3	23.0		22.62
44.0		23.28	

Run 147

Sta. ft.	L cm.	Depth Cent. cm.	R cm.
10		47.34	
15		"	
20		"	
25		"	
27		"	
29.6	47.34	"	
30.3	23.20		25.14
44.0		23.9	

Run 148

Sta. ft.	L cm.	Depth Cent. cm.	R cm.
10		40.58	
15		"	
20		"	
25		"	
27		"	
29.3	40.58	"	
30.3	24.0		25.33
44.0		24.60	

Run 149

Sta. ft.	L cm.	Depth Cent. cm.	R cm.
10		40.00	
15		"	
20		"	
25		"	
27		"	
28.9	40.00	"	
30.3	25.80		24.02
44.0		24.6	

Run 150

Sta. ft.	L cm.	Depth Cent. cm.	R cm.
10		39.28	
15		39.27	
20		39.27	
25		39.25	
27		39.24	
28.6	39.23	39.22	
30.3	26.0		24.42
25.8		25.8	

Run 151

Sta. ft.	L cm.	Depth Cent. cm.	R cm.
10		58.00	
15		"	
20		"	
25		"	
27		"	
29.7	58.00		
30.3	9.0		14.90
44		14.90	

Run 152

Sta. ft.	L cm.	Depth Cent. cm.	R cm.
10		56.00	
15		"	
20		"	
25		"	
27		"	
29.5	56.00	"	
30.3	11.00		15.10
44.0		15.20	

TABLE 8-2 RAW DATA - SUBMERGED TESTS

Run No.	153	154	155	156	157	158	159	160	161
Geometry	Ib	Ib	Ib	Ib	Ib	Ib	Ib	Ib	Ib
n	0.0110	0.0110	0.0110	0.0110	0.0110	0.0110	0.0110	0.0110	0.0110
Q	2.5 cfs.	2.5 cfs.	2.5 cfs.	2.5 cfs.	2.5 cfs.	2.5 cfs.	2.5 cfs.	2.5 cfs.	2.5cfs.
Y_n	0.70 ft.	0.70 ft.	0.70 ft.	0.70 ft.	0.70 ft.	0.70 ft.	0.70 ft.	0.70 ft.	0.70 ft
F_n	0.15	0.15	0.15	0.15	0.15	0.15	0.15	0.15	0.15
S	0.000062	0.000062	0.000062	0.000062	0.000062	0.000062	0.000062	0.000062	0.000062
M=b/B	0.20	0.20	0.25	0.25	0.25	0.25	0.30	0.30	0.30
L/b	0.75	1.0	0.25	0.50	0.75	1.0	0.25	0.50	0.75
Temp.	72° F	70° F	72° F	72° F	72° F	72° F	72° F	72° F	70° F
Model Sta.	30.00	30.00	30.00	30.00	30.00	30.00	30.00	30.00	30.00
Y_1	54.0 cm.	52.44 cm.	36.86 cm.	34.72 cm.	33.54 cm.	31.63 cm.	26.92 cm.	25.22 cm.	24.92 cm
Y_2	11.26 cm.	12.12 cm.	14.27 cm.	17.40 cm.	16.60 cm.	30.30 cm.	---	17.54 cm.	18.00 cm
N	1.0	1.0	1.0	1.0	1.0	1.0	1.0	1.0	1.0
ϕ_2	0.0	0.0	0.0	0.0	0.0	0.0	0.0	0.0	0.0

Run 153

Sta. ft.	L cm.	Depth Cent. cm.	R cm.
10		54.00	
15		"	
20		"	
25		"	
27		"	
29.2	54.00	"	
30.3	11.26		15.30
44		14.85	

Run 154

Sta. ft.	L cm.	Depth Cent. cm.	R cm.
10		52.42	
15		"	
20		"	
25		"	
27		"	
28.9		"	
30.3	12.12		15.62
44.0		15.08	

Run 155

Sta. ft.	L cm.	Depth Cent. cm.	R cm.
10		36.92	
15		36.90	
20		36.88	
25		36.88	
27		36.96	
29.6	36.86	36.86	
30.3	14.27		16.47
44.0		16.00	

Run 156

Sta. ft.	L cm.	Depth Cent. cm.	R cm.
10		34.85	
15		34.83	
20		34.80	
25		34.77	
27		34.74	
29.3	34.72	34.72	
30.3	17.40		15.84
44.0		17.20	

Run 157

Sta. ft.	L cm.	Depth Cent. cm.	R cm.
10		33.70	
15		33.68	
20		33.67	
25		33.66	
27		33.61	
29.0	33.64	33.54	
30.3	16.60		17.66
44.0		17.00	

Run 158

Sta. ft.	L cm.	Depth Cent. cm.	R cm.
10		31.78	
15		31.76	
20		31.75	
25		31.70	
27		31.63	
28.7	31.74	31.63	
30.3	16.56		17.58
44.0		17.15	

Run 159

Sta. ft.	L cm.	Depth Cent. cm.	R cm.
10		27.35	
15		27.30	
20		27.28	
25		27.27	
27		27.22	
29.6	27.28	26.92	
44.0		18.00	

Run 160

Sta. ft.	L cm.	Depth Cent. cm.	R cm.
10		25.40	
15		"	
20		"	
25		"	
28		25.65	
28.5		25.42	
29.2		25.22	
30.3	17.54		18.50

Run 161

Sta. ft.	L cm.	Depth Cent. cm.	R cm.
10		25.62	
15		25.60	
20		25.57	
25		25.50	
27		25.44	
28.8	25.52	24.92	
30.3	18.00		18.52
44		18.35	

Run No.	162	163	164	165	166	167	168	169	170
Geometry	Ib	Ib	Ib	Ib	Ib	Ib	Ib	Ib	Ib
n	0.0110	0.0110	0.0110	0.0110	0.0110	0.0110	0.0110	0.0110	0.0110
Q	2.5 cfs.	3.0 cfs.	3.0 cfs.	3.0 cfs.	3.0 cfs.	3.0 cfs.	3.0 cfs.	3.0 cfs.	3.0 cfs
Y_n	0.70 ft.	0.80 ft.	0.80 ft.	0.80 ft.	0.80 ft.	0.80 ft.	0.80 ft.	0.80 ft.	0.80
F_n	0.15	0.15	0.15	0.15	0.15	0.15	0.15	0.15	0.15
S	0.000062	0.000062	0.000052	0.000052	0.000052	0.000052	0.000052	0.000052	0.000
M=b/B	0.30	0.25	0.25	0.25	0.25	0.30	0.30	0.30	0.30
L/b	1.0	0.25	0.50	0.75	1.0	0.25	0.50	0.75	1.0
Temp.	72° F	72° F	72° F	72° F	72° F	72° F	72° F	72° F	72° F
Model Sta.	30.00	30.3	30.00	30.00	30.00	30.00	30.00	30.00	30.00
Y_1	24.24 cm.	45.16 cm.	41.52 cm.	41.36 cm	37.18 cm.	32.67 cm.	32.05 cm.	30.88 cm.	29.74
Y_2	18.00 cm.	16.42 cm.	19.70 cm.	19.40 cm.	20.00 cm.	19.52 cm.	20.30 cm.	20.64 cm.	21.50
N	1.0	1.0	1.0	1.0	1.0	1.0	1.0	1.0	1.0
ϕ_2	0.0	0.0	0.0	0.0	0.0	0.0	0.0	0.0	0.0

Run 162

Sta. ft.	L cm.	Depth Cent. cm.	R cm.
10		25.32	
15		25.28	
20		25.24	
25		25.22	
27		25.14	
28.4	25.30	24.24	
30.3	18.00		18.65
44		18.08	

Run 163

Sta. ft.	L cm.	Depth Cent. cm.	R cm.
10		45.16	
15		"	
20		"	
25		"	
27		"	
29.5	45.16	"	
30.3	16.42		19.0
44		19.02	

Run 164

Sta. ft.	L cm.	Depth Cent. cm.	R cm.
10		41.63	
15		41.63	
20		41.60	
25		41.56	
27		41.56	
29.3	41.52	41.52	
30.3	19.70		20.26
44		19.5	

Run 165

Sta. ft.	L cm.	Depth Cent. cm.	R cm.
10		41.43	
15		"	
20		41.42	
25		41.40	
27		"	
29.0	41.36	41.36	
30.3	19.40		20.55
44		20.62	

Run 166

Sta. ft.	L cm.	Depth Cent. cm.	R cm.
10		37.29	
15		37.29	
20		37.28	
25		37.27	
27		37.24	
28.6	37.18	37.18	
30.3	20.00		21.05
44		21.00	

Run 167

Sta. ft.	L cm.	Depth Cent. cm.	R cm.
10		32.64	
15		"	
20		"	
25		"	
27		"	
29.5	32.67	32.48	
30.3	19.50		20.76
44		20.75	

Run 168

Sta. ft.	L cm.	Depth Cent. cm.	R cm.
10		32.31	
15		32.28	
20		32.30	
25		32.29	
27		32.29	
29.2	32.95	32.05	
30.3	20.30		21.30
44		21.00	

Run 169

Sta. ft.	L cm.	Depth Cent. cm.	R cm.
10		31.09	
15		31.08	
20		31.05	
25		31.00	
27		31.00	
29.8	31.11	30.88	
30.3	20.64		21.67
44		21.50	

Run 170

Sta. ft.	L cm.	Depth Cent. cm.	R cm.
10		30.02	
15		30.00	
20		30.00	
25		29.95	
27		29.85	
28.4	30.00	29.74	
30.3	21.50		20.66
44		21.17	

TABLE 8-2 RAW DATA - SUBMERGED TESTS

Run No.	171	172	173	174	175	176	177	178	179
Geometry	Ia	Ib	Ib	Ib	Ib	Ib	Ib	Ib	Ib
n	0.0110	0.0110	0.0110	0.0110	0.0110	0.0110	0.0110	0.0110	0.0110
Q	3.5 cfs.	3.5 cfs.	3.5 cfs.	3.5 cfs.	3.5 cfs.	3.5 cfs.	3.5 cfs.	3.5 cfs.	3.5 cfs.
Y_n	0.88 ft.	0.88 ft.	0.88 ft.	0.88 ft.	0.88 ft.	0.88 ft.	0.88 ft.	0.88 ft.	0.88 ft.
F_n	0.15	0.15	0.15	0.15	0.15	0.15	0.15	0.15	0.15
S	0.000062	0.000062	0.000062	0.000062	0.000062	0.000062	0.000062	0.000062	0.000062
M=b/B	0.25	0.25	0.25	0.25	0.25	0.30	0.30	0.30	0.30
L/b	0.0	0.25	0.50	0.75	1.0	0.25	0.50	0.75	1.00
Temp.	72° F	72° F	72° F	72° F	72° F	72° F	72° F	72° F	72° F
Model Sta.	30.00	30.00	30.00	30.00	30.00	30.00	30.00	30.00	30.00
Y_1	56.30 cm.	53.5 cm.	50.30 cm.	49.40 cm.	44.14 cm.	38.18 cm.	37.85 cm.	36.35 cm.	35.00 cm.
Y_2	17.90 cm.	18.10 cm.	20.50 cm.	21.0 cm.	22.20 cm.	22.10 cm.	22.20 cm.	22.90 cm.	23.00 cm.
N	1.0	1.0	1.0	1.0	1.0	1.0	1.0	1.0	1.0
Φ 2	0.0	0.0	0.0	0.0	0.0	0.0	0.0	0.0	0.0

Run No.	Sta. ft.	L cm.	Depth Cent. cm.	R cm.
171	10		56.30	
	15		"	
	20		"	
	25		"	
	27		"	
	29.9	56.30	"	
	30.3	17.90		21.10
	44		20.0	
172	10		53.5	
	15		"	
	20		"	
	25		"	
	27		"	
	29.65	53.50	"	
	30.3	18.10		21.40
	44		20.2	
173	10		50.30	
	15		"	
	20		"	
	25		"	
	27		"	
	28.5	50.30	"	
	30.3	20.50		22.34
	44		21.00	
174	10		45.40	
	15		"	
	20		"	
	25		"	
	27		"	
	28.9	49.40	49.40	
	30.3	21.00		23.20
	44		23.0	
175	10		44.14	
	15		"	
	20		"	
	25		"	
	27		"	
	28.6	44.14	"	
	30.3	22.20		22.80
	44		23.5	
176	10		38.18	
	15		"	
	20		"	
	25		"	
	27		"	
	29.5	38.18	"	
	30.3	22.10		23.60
	44		22.5	
177	10		37.85	
	15		"	
	20		"	
	25		"	
	27		"	
	29.2	37.85	"	
	30.3	22.20		23.27
	44		23.0	
178	10		36.35	
	15		"	
	20		"	
	25		"	
	27		"	
	28.8	36.35	"	
	30.3	22.90		23.90
	44		22.0	
179	10		35.02	
	15		35.00	
	20		34.96	
	25		34.93	
	27		34.90	
	28.4	35.02	35.00	
	30.3	23.00		24.35
	44		24.00	

Run No.	180	181	182	183	184	185	186	187	188
Geometry	Ia	Ib	Ib	Ib	Ib	Ib	Ib	Ib	Ib
n	0.0110	0.0110	0.0110	0.0110	0.0110	0.0110	0.0110	0.0110	0.0110
Q	4.0 cfs.	4.0 cfs.	4.0 cfs.	2.5 cfs.	2.5 cfs.	2.5 cfs.	2.5 cfs.	2.5 cfs.	2.5 cfs.
Y_n	0.50 ft.	0.965 ft.	0.965 ft.	0.585 ft.	0.585 ft.	0.585 ft.	0.585 ft.	0.585 ft.	0.585 ft.
F_n	0.40	0.15	0.15	0.20	0.20	0.20	0.20	0.20	0.20
S	0.00046	0.000058	0.000058	0.00011	0.00011	0.00011	0.00011	0.00011	0.00011
M=b/B	0.30	0.30	0.30	0.20	0.25	0.25	0.30	0.30	0.30
L/b	0.0	0.75	1.00	1.0	0.25	1.0	0.25	0.50	0.75
Temp.	72° F	72° F	72° F	72° F	72° F	72° F	72° F	72° F	72° F
Model Sta.	30.00	30.00	30.00	30.00	30.00	30.00	30.00	30.00	30.00
Y_1	38.00	41.75 cm.	38.52 cm.	56.58 cm.	35.50 cm.	34.0 cm.	24.42 cm.	25.50 cm.	26.27 cm.
Y_2	4.00 cm.	25.50 cm.	25.0 cm.	5.33 cm.	8.30 cm.	10.0 cm.	12.0 cm.	12.0 cm.	12.0 cm.
N	1.0	1.0	1.0	1.0	1.0	1.0	1.0	1.0	1.0
Φ 2	0.0	0.0	0.0	0.0	0.0	0.0	0.0	0.0	0.0

Run No.	Sta. ft.	L cm.	Depth Cent. cm.	R cm.
180	10		38.00	
	15		"	
	20		"	
	25		"	
	27		"	
	29.9	38.00	"	
	30.3	4.0		4.0
	45		14.7	
181	10		41.75	
	15		"	
	20		"	
	25		"	
	27		"	
	28.8	41.75	"	
	30.3	25.50		26.50
	44		26.0	
182	10		38.52	
	15		"	
	20		"	
	25		"	
	27		"	
	28.4	38.52	"	
	30.3	25.0		26.0
	44		25.8	
183	10		56.58	
	15		"	
	20		"	
	25		"	
	27		"	
	28.9	56.58	"	
	30.3	5.33		10.07
	44		8.0	
184	10		35.50	
	15		"	
	20		"	
	25		"	
	27		"	
	29.6	35.50	"	
	30.3	8.30		11.50
	44		10.0	
185	10		28.6	
	15		"	
	20		"	
	25		"	
	27		"	
	28.6	28.6	34.0	
	30.3	10.0		11.94
	44		11.5	
186	10		24.49	
	15		25.48	
	20		25.48	
	25		25.46	
	27		25.44	
	29.55	25.46	24.42	
	30.3	12.0		12.22
	44		12.1	
187	10		26.24	
	15		26.23	
	20		26.21	
	25		26.20	
	27		26.15	
	29.2	26.12	25.50	
	30.3	12.0		13.58
	44		12.8	
188	10		26.72	
	15		26.70	
	20		26.68	
	25		26.62	
	27		26.60	
	28.75	26.67	26.27	
	30.3	12.0		13.36
	44		12.65	

TABLE 6-2 RAW DATA - SUBMERGED TESTS

Run No.	189	190	191	192	193	194	195	196	197
Geometry	Ib	Ib	Ia	Ib	Ia	Ia	Ia	Ia	Ia
n	0.0110	0.0110	0.0110	0.0110	0.0238	0.0238	0.0238	0.0238	0.0238
Q	2.5 cfs.	3.0 cfs.	3.5 cfs.	3.5 cfs.	2.0 cfs.	2.0 cfs.	2.0	2.0 cfs.	2.5 cfs.
Y_n	0.585 ft.	0.66 ft.	0.725 ft.	0.725 ft.	0.80 ft.	0.80 ft.	0.80 ft.	0.80 ft.	0.706 ft.
F_n	0.20	0.20	0.20	0.20	0.10	0.10	0.10	0.10	0.15
S	0.00011	0.000098	0.000115	0.000115	0.000128	0.000128	0.000128	0.000128	0.000295
M=b/B	0.30	0.25	0.25	0.25	0.20	0.25	0.275	0.30	0.20
L/b	1.0	1.0	0.0	1.0	0.0	0.0	0.0	0.0	0.0
Temp.	72° F	72° F	72° F	72° F	70° F	70° F	70° F	70° F	70o F
Model Sta.	30.00	30.00	30.00	30.00	30.00	30.00	30.0	30.00	30.00
Y_1	24.60 cm.	42.08 cm.	56.67 cm.	50.47 cm.	51.62 cm.	37.70 cm.	33.93 cm.	30.52 cm.	50.62 cm.
Y_2	12.50 cm.	12.1 cm.	9.0 cm.	13.6 cm.	19.30 cm.	21.40 cm.	21.80 cm.	22.20 cm.	18.0 cm.
N	1.0	1.0	1.0	1.0	1.0	1.0	1.0	1.0	1.0
Φ 2	0.0	0.0	0.0	0.0	0.0	0.0	0.0	0.0	0.0

Run 189

Sta. ft.	L cm.	Depth Cent. cm.	R cm.
10		25.56	
15		25.50	
20		25.48	
25		25.45	
27		25.35	
28.4	25.35	24.60	
30.3	12.50		13.82
44		13.6	

Run 190

Sta. ft.	L cm.	Depth Cent. cm.	R cm.
10		42.10	
15		"	
20		"	
25		"	
27		"	
28.6	42.10	42.08	
30.3	12.1		15.6
44		16.3	

Run 191

Sta. ft.	L cm.	Depth Cent. cm.	R cm.
10		56.57	
15		"	
20		"	
25		"	
27		"	
	56.57	56.67	
30.3	9.0		15.33
44		13.0	

Run 192

Sta. ft.	L cm.	Depth Cent. cm.	R cm.
10		50.47	
15		"	
20		"	
25		"	
27		"	
29.65		"	
30.3	13.6		15.9
44			

Run 193

Sta. ft.	L cm.	Depth Cent. cm.	R cm.
10		51.62	
15		"	
20		"	
25		"	
27		"	
29.9	51.62	"	
30.3	19.30		20.96
44		21.3	

Run 194

Sta. ft.	L cm.	Depth Cent. cm.	R cm.
10		37.70	
15		"	
20		"	
25		"	
27		"	
29.9	37.70	"	
30.3	21.40		22.40
44		22.50	

Run 195

Sta. ft.	L cm.	Depth Cent. cm.	R cm.
10		33.95	
15		"	
20		"	
25		"	
27		"	
29.9	33.94	33.93	
30.3	21.80		22.53
44		22.90	

Run 196

Sta. ft.	L cm.	Depth Cent. cm.	R cm.
10		30.67	
15		30.65	
20		30.64	
25		30.62	
27		30.60	
29.9	30.58	30.52	
30.3	22.20		22.96
44		23.10	

Run 197

Sta. ft.	L cm.	Depth Cent. cm.	R cm.
10		50.62	
15		"	
20		"	
25		"	
27		"	
29.9	50.62	"	
30.3	18.0		15.75
44		18.10	

Run No.	198	199	200	201	202	203	204	205	206
Geometry	Ia	Ia	Ia	Ia	Ia	Ia	Ia	Ia	Ib
n	0.0238	0.0238	0.0238	0.0238	0.0238	0.0238	0.0238	0.0235	0.0238
Q	2.5 cfs.	2.5 cfs.	2.5 cfs.	2.0 cfs.	2.5 cfs.	2.5 cfs.	2.5 cfs.	2.5 cfs.	2.0 cfs.
Y_n	0.706 ft.	0.706 ft.	0.706 ft.	0.50 ft.	0.585 ft.	0.585 ft.	0.585 ft.	0.585 ft.	0.80 ft.
F_n	0.15	0.15	0.15	0.20	0.20	0.20	0.20	0.20	0.10
S	0.000295	0.000295	0.000295	0.000565	0.00053	0.00053	0.00053	0.00053	0.000128
M=b/B	0.25	0.275	0.30	0.20	0.20	0.25	0.275	0.30	0.20
L/b	0.0	0.0	0.0	0.0	0.0	0.0	0.0	0.0	0.25
Temp.	70° F	70° F	70° F	70° F	70° F	70° F	70° F	70° F	70° F
Model Sta.	30.00	30.00	30.00	30.00	30.00	30.00	30.00	30.00	30.00
Y_1	37.10 cm.	32.90 cm.	27.91 cm.	35.24 cm.	44.56 cm.	30.07 cm.	26.70 cm.	23.80 cm.	44.76 cm.
Y_2	17.86 cm.	18.00 cm.	18.70 cm.	12.3 cm.	12.88 cm.	14.0 cm.	14.50 cm.	14.80 cm.	20.30 cm.
N	1.0	1.0	1.0	1.0	1.0	1.0	1.0	1.0	1.0
Φ 2	0.0	0.0	0.0	0.0	0.0	0.0	0.0	0.0	0.0

Run 198

Sta. ft.	L cm.	Depth Cent. cm.	R cm.
10		37.10	
15		"	
20		"	
25		"	
27		"	
29.9	37.10	"	
30.3	17.86		18.87
44		19.0	

Run 199

Sta. ft.	L cm.	Depth Cent. cm.	R cm.
10		32.90	
15		"	
20		"	
25		"	
27		"	
29.9	32.90	"	
30.3	18.00		19.0
44		19.50	

Run 200

Sta. ft.	L cm.	Depth Cent. cm.	R cm.
10		28.19	
15		28.17	
20		28.16	
25		28.14	
27		28.16	
29.9	28.20	27.91	
30.3	18.70		19.30
44		19.55	

Run 201

Sta. ft.	L cm.	Depth Cent. cm.	R cm.
10		35.24	
15		"	
20		"	
25		"	
27		"	
29.9	35.24	"	
30.3	12.3		11.13
44		12.7	

Run 202

Sta. ft.		Depth Cent. cm.	
10		44.56	
15		"	
20		"	
25		"	
27		"	
29.9	44.56	"	
30.3	12.88		14.16
44		14.15	

Run 203

Sta. ft.	L cm.	Depth Cent. cm.	R cm.
10		30.10	
15		30.08	
20		30.07	
25		30.05	
27		30.03	
29.9	30.07	30.07	
30.3	14.00		15.00
44		15.00	

Run 204

Sta. ft.	L cm.	Depth Cent. cm.	R cm.
10		26.70	
15		26.69	
20		26.68	
25		26.62	
27		26.58	
29.9	26.70	26.70	
30.3	14.50		15.38
44		15.40	

Run 205

Sta. ft.	L cm.	Depth Cent. cm.	R cm.
10		23.84	
15		23.83	
20		23.82	
25		23.80	
27		23.78	
29.9	23.80	23.80	
30.3	14.80		16.54
44		16.70	

Run 206

Sta. f ft.	L cm.	Depth Cent. cm.	R cm.
10		44.76	
15		"	
20		"	
25		"	
27		"	
29.6	44.76	"	
30.3	20.30		21.18
44		22.4	

TABLE 8-2 RAW DATA - SUBMERGED TESTS

Run No.	- 207
Geometry	- Ib
n	- 0.0238
Q	- 2.0
Y_n	- 0.80 ft.
F_n	- 0.10
S	- 0.000128
M=b/B	- 0.20
L/b	- 1.0
Temp.	- 70° F
Model Sta.	- 30.00
Y_1	- 41.70 cm.
Y_2	- 21.50 cm.
N	- 1.0
℄ 2	- 0.0

Sta. ft.	L cm.	Depth Cent. cm.	R cm.
10		41.70	
15		"	
20		"	
25		"	
27		"	
28.9	41.70	"	
30.3	21.50		22.10
44		23.60	

Run No.	- 208
Geometry	- Ib
n	- 0.0238
Q	- 2.0 cfs.
Y_n	- 0.80 ft.
F_n	- 0.10
S	- 0.000128
M=b/B	- 0.25
L/b	- 0.25
Temp.	- 70° F
Model Sta.	- 30.00
Y_1	- 37.55 cm.
Y_2	- 22.30 cm.
N	- 1.0
℄ 2	- 0.0

Sta. ft.	L cm.	Depth Cent. cm.	R cm.
10		37.55	
		"	
20		"	
25		"	
27		"	
29.55	37.55	"	
30.3	22.30		21.03
44		23.8	

Run No.	- 209
Geometry	- Ib
n	- 0.0238
Q	- 2.0 cfe.
Y_n	- 0.80 ft.
F_n	- 0.10
S	- 0.000128
M=b/B	- 0.25
L/b	- 1.0
Temp.	- 70° F
Model Sta.	- 30.00
Y_1	- 31.88 cm.
Y_2	- 22.2 cm.
N	- 1.0
℄ 2	- 0.0

Sta. ft.	L cm.	Depth Cent. cm.	R cm.
10		31.88	
15		"	
20		"	
25		"	
27		"	
28.65	31.88	"	
30.3	22.2		22.76
44		23.10	

Run No.	- 210
Geometry	- Ib
n	- 0.0238
Q	- 2.0 cfs.
Y_n	- 0.80 ft.
F_n	- 0.10
S	- 0.000128
M=b/B	- 0.30
L/b	- 0.75
Temp.	- 70° F
Model Sta.	- 30.00
Y_1	- 27.33 cm.
Y_2	- 23.96 cm.
N	- 1.0
℄ 2	- 0.0

Sta. ft.	L cm.	Depth Cent. cm.	R cm.
10		27.75	
15		27.72	
20		27.70	
25		27.65	
27		27.60	
28.8	27.73	27.33	
30.3	23.96		23.96
44		23.96	

Run No.	- 211
Geometry	- Ib
n	- 0.0238
Q	- 2.5 cfs.
Y_n	- 0.92 ft.
F_n	- 0.10
S	- 0.000295
M=b/B	- 0.20
L/b	- 0.25
Temp.	- 70° F
Model Sta.	- 30.00
Y_1	- 44.70 cm.
Y_2	- 17.00 cm.
N	- 1.0
℄ 2	- 0.0

Sta. ft.	L cm.	Depth Cent. cm.	R cm.
10		44.70	
15		"	
20		"	
25		"	
27		"	
29.7	44.70	"	
30.3	17.00		17.66
44		18.0	

Run No.	- 212
Geometry	- Ib
n	- 0.0238
Q	- 2.5 cfs.
Y_n	- 0.706 ft.
F_n	- 0.15
S	- 0.000295
M=b/B	- 0.20
L/b	- 0.75
Temp.	- 70° F
Model Sta.	- 30.00
Y_1	- 40.60 cm.
Y_2	- 18.50 cm.
N	- 1.0
℄ 2	- 0.0

Sta. ft.	L cm.	Depth Cent. cm.	R cm.
10		40.60	
15		"	
20		"	
25		"	
27		"	
29.15	40.60	"	
30.3	18.50		17.04
44		18.7	

Run No.	- 213
Geometry	- Ib
n	- 0.0238
Q	- 2.5 cfs.
Y_n	- 0.706 ft.
F_n	- 0.15
S	- 0.000295
M=b/B	- 0.20
L/b	- 1.0
Temp.	- 70° F
Model Sta.	- 30.00
Y_1	- 40.20 cm.
Y_2	- 17.60 cm.
N	- 1.0
℄ 2	- 0.0

Sta. ft.	L cm.	Depth Cent. cm.	R cm.
10		40.20	
15		"	
20		"	
25		"	
27		"	
28.9	40.20	"	
30.3	17.60		18.40
44		19.10	

Run No.	- 214
Geometry	- Ib
n	- 0.0238
Q	- 2.5 cfs.
Y_n	- 0.706 ft.
F_n	- 0.15
S	- 0.000295
M=b/B	- 0.25
L/b	- 0.25
Temp.	- 70° F
Model Sta.	- 30.00
Y_1	- 37.02 cm.
Y_2	- 17.60 cm.
N	- 1.0
℄ 2	- 0.0

Sta. ft.	L cm.	Depth Cent. cm.	R cm.
10		37.02	
15		"	
20		"	
25		"	
27		"	
29.65	37.02	"	
30.3	17.60		18.97
44		19.30	

Run No.	- 215
Geometry	- Ib
n	- 0.0238
Q	- 2.5 cfs.
Y_n	- 0.706 ft.
F_n	- 0.15
S	- 0.000295
M=b/B	- 0.25
L/b	- 0.75
Temp.	- 70° F
Model Sta.	- 30.00
Y_1	- 32.23 cm
Y_2	- 18.40 cm
N	- 1.0
℄ 2	- 0.0

Sta. ft.	L cm.	Depth Cent. cm.	R cm.
10		32.23	
15		"	
20		"	
25		"	
27		"	
29.0	32.23	"	
30.3	18.40		19.2
44		19.0	

Run No.	- 216
Geometry	- Ib
n	- 0.0238
Q	- 2.5 cfs.
Y_n	- 0.706 ft.
F_n	- 0.15
S	- 0.000295
M=b/B	- 0.25
L/b	- 1.0
Temp.	- 70° F
Model Sta.	- 30.00
Y_1	- 30.50 cm.
Y_2	- 19.00 cm.
N	- 1.0
℄ 2	- 0.0

Sta. ft.	L cm.	Depth Cent. cm.	R cm.
10		30.52	
15		30.52	
20		30.51	
25		30.50	
27		30.50	
28.7	30.50	30.50	
30.3	19.00		19.66
44		19.70	

Run No.	- 217
Geometry	- Ia
n	- 0.0238
Q	- 3.5 cfs.
Y_n	- 0.88 ft.
F_n	- 0.15
S	- 0.000295
M=b/B	- 0.25
L/b	- 0.0
Temp.	- 70° F
Model Sta.	- 30.00
Y_1	- 49.50 cm.
Y_2	- 21.16 cm.
N	- 1.0
℄ 2	- 0.0

Sta. ft.	L cm.	Depth Cent. cm.	R cm.
10		49.50	
15		"	
20		"	
25		"	
27		"	
29.9	49.50	"	
30.3	21.16		23.10
44		23.10	

Run No.	- 218
Geometry	- Ib
n	- 0.0238
Q	- 3.5 cfs.
Y_n	- 0.88 ft.
F_n	- 0.15
S	- 0.000295
M=b/B	- 0.25
L/b	- 0.25
Temp.	- 70° F
Model Sta.	- 30.00
Y_1	- 41.70 cm.
Y_2	- 21.40 cm.
N	- 1.0
℄ 2	- 0.0

Sta. ft.	L cm.	Depth Cent. cm.	R cm.
10		47.70	
15		"	
20		"	
25		"	
27		"	
29.6	47.70	"	
30.3	21.40		23.30
44		23.30	

Run No.	- 219
Geometry	- Ib
n	- 0.0238
Q	- 3.5 cfs.
Y_n	- 0.88 ft.
F_n	- 0.15
S	- 0.000295
M=b/B	- 0.25
L/b	- 0.50
Temp.	- 70° F
Model Sta.	- 30.00
Y_1	- 41.60 cm.
Y_2	- 22.00 cm.
N	- 1.0
℄ 2	- 0.0

Sta. ft.	L cm.	Depth Cent. cm.	R cm.
10		41.60	
15		"	
20		"	
25		"	
27		"	
29.25	41.60	"	
30.3	22.0		23.54
44		23.60	

Run No.	- 220
Geometry	- Ib
n	- 0.0238
Q	- 3.5 cfs.
Y_n	- 0.88 ft.
F_n	- 0.15
S	- 0.000295
M=b/B	- 0.25
L/b	- 1.0
Temp.	- 70° F
Model Sta.	- 30.00
Y_1	- 38.20 cm.
Y_2	- 23.0 cm.
N	- 1.0
℄ 2	- 0.0

Sta. ft.	L cm.	Depth Cent. cm.	R cm.
10		38.20	
15		"	
20		"	
25		"	
27		"	
28.35	38.20	"	
30.3	23.0		24.0
44		24.0	

Run No.	- 221
Geometry	- Ib
n	- 0.0238
Q	- 2.5 cfs.
Y_n	- 0.706 cfs.
F_n	- 0.15
S	- 0.000295
M=b/B	- 0.30
L/b	- 0.25
Temp.	- 70° F
Model Sta.	- 30.00
Y_1	- 28.00 cm.
Y_2	- 19.60 cm.
N	- 1.0
℄ 2	- 0.0

Sta. ft.	L cm.	Depth Cent. cm.	R cm.
10		28.28	
15		28.27	
20		28.26	
25		28.20	
27		28.16	
29.5	28.20	28.00	
30.3	19.60		18.77
44		19.80	

Run No.	- 222
Geometry	- Ib
n	- 0.0238
Q	- 2.5 cfs.
Y_n	- 0.706 ft.
F_n	- 0.15
S	- 0.000295
M=b/B	- 0.30
L/b	- 0.50
Temp.	- 70° F
Model Sta.	- 30.00
Y_1	- 27.64 cm.
Y_2	- 20.00 cm.
N	- 1.0
℄ 2	- 0.0

Sta. ft.	L cm.	Depth Cent. cm.	R cm.
10		27.85	
15		27.84	
20		27.83	
25		27.82	
27		27.74	
29.15	27.90	27.64	
30.3	20.00		19.24
44		19.24	

Run No.	- 223
Geometry	- Ib
n	- 0.0238
Q	- 2.5 cfs.
Y_n	- 0.706 ft.
F_n	- 0.15
S	- 0.000295
M=b/B	- 0.30
L/b	- 0.75
Temp.	- 70° F
Model Sta.	- 30.00
Y_1	- 25.73 cm.
Y_2	- 18.58 cm.
N	- 1.0
℄ 2	- 0.0

Sta. ft.	L cm	Depth Cent. cm.	R cm.
10		26.18	
15		26.17	
20		26.16	
25		26.15	
27		26.11	
28.75	26.16	25.73	
30.3	18.58		19.96
44		20.20	

Run No.	- 224
Geometry	- Ib
n	- 0.0238
Q	- 2.0 cfs.
Y_n	- 0.50 ft.
F_n	- 0.20
S	- 0.000565
M=b/B	- 0.20
L/b	- 0.25
Temp.	- 70° F
Model Sta.	- 30.00
Y_1	- 32.75 cm.
Y_2	- 11.0 cm.
N	- 1.0
℄ 2	- 0.0

Sta. ft.	L cm.	Depth Cent. cm.	R cm.
10		32.75	
15		"	
20		"	
25		"	
27		"	
29.7	32.75	"	
30.3	11.0		12.26
44		12.3	

TABLE 8-2- RAW DATA - SUBMERGED TESTS

Run No.	225	226	227	228	229	230	231	232	233
Geometry	Ib	Ib	Ib	Ib	Ib	Ib	Ib	Vb	Vb
n	0.0238	0.0238	0.0235	0.0238	0.0238	0.0238	0.0238	0.0238	0.0238
Q	2.0 cfs.	2.0 cfs.	2.5 cfs.	2.5 cfs.	2.5 cfs.	2.5 cfs.	2.5 cfs.	2.0 cfs.	2.0 cfs.
Y_n	0.50 ft.	0.50 ft.	0.585 ft.	0.585 ft.	0.585 ft.	0.585 ft.	0.585 ft.	0.80 ft.	0.80 ft.
F_n	0.20	0.20	0.20	0.20	0.20	0.20	0.20	0.10	0.10
S	0.000565	0.000565	0.00053	0.00053	0.00053	0.00053	0.00053	0.000128	0.000128
M=b/B	0.20	0.20	0.20	0.20	0.25	0.25	0.30	0.20	0.30
L/b	0.50	1.0	0.25	1.0	0.25	1.0	0.75	0.50	0.30
Temp.	70° F	70° F	70° F	70° F	70° F	70° F	72° F	68° F	68° F
Model Sta.	30.00	30.00	30.00	30.00	30.00	30.00	30.00	30.00	30.00
Y_1	30.80 cm.	28.80 cm.	38.82 cm.	38.10 cm.	29.30 cm.	26.04 cm.	22.00 cm.	32.50 cm.	23.00 cm.
Y_2	22.0 cm.	12.4 cm.	13.60 cm.	13.0 cm.	14.0 cm.	14.50 cm.	15.60 cm.	21.0 cm.	21.5 cm.
N	1.0	1.0	1.0	1.0	1.0	1.0	1.0	1.0	1.0
ϕ_2	0.0	0.0	0.0	0.0	0.0	0.0	0.0	15°	15°

Run No.	234	235	236	237	238	239	240	241	242
Geometry	Vb	Vb	Vb	Vb	Vb	Vb	Vb	Vb	Vb
n	0.0238	0.0238	0.0238	0.0238	0.0238	0.0238	0.0238	0.0238	0.0238
Q	2.0 cfs	2.0 cfs.	2.0 cfs.	2.0 cfs.	3.0 cfs.	3.0 cfs.	3.0 cfs.	3.0 cfs.	2.0 cfs.
Y_n	0.80 ft.	0.80 ft.	0.80 ft.	0.80 ft.	1.04 ft.	1.04 ft.	1.04 ft.	1.04 ft.	0.61 ft.
F_n	0.10	0.10	0.10	0.10	0.10	0.10	0.10	0.10	0.15
S	0.000128	0.000128	0.000128	0.000128	0.000125	0.000125	0.000125	0.000125	0.0003
M=b/B	0.20	0.30	0.20	0.30	0.20	0.30	0.20	0.30	0.20
L/b	0.50	0.50	0.50	0.50	0.50	0.50	0.50	0.50	0.50
Temp.	68° F	68° F	68° F	68° F	66° F	66° F	66° F	66° F	66° F
Model Sta.	30.00	30.00	30.00	30.00	30.00	30.0	30.0	30.0	30.00
Y_1	33.0 cm.	23.40 cm.	34.14 cm.	23.93 cm.	44.50 cm.	32.95 cm.	46.70 cm.	33.40 cm.	23.50 cm.
Y_2	20.10 cm.	21.30 cm.	21.0 cm.	21.3 cm.	27.6 cm.	28.3 cm.	26.96 cm.	28.1 cm.	15.1 cm.
N	1.0	1.0	1.0	1.0	1.0	1.0	1.0	1.0	1.0
ϕ_2	22½°	22½°	30°	30°	15°	15°	30°	30°	15°

Run 225

Sta. ft.	L cm.	Depth Cent. cm.	R cm.
10		30.80	
15		"	
20		"	
25		"	
27		"	
29.4	30.80	"	
30.3	22.0		23.54
44		23.00	

Run 226

Sta. ft.	L cm.	Depth Cent. cm.	R cm.
10		28.80	
15		"	
20		"	
25		"	
27		"	
28.65	28.80	"	
30.3	12.40		11.2
44		13.0	

Run 227

Sta. ft.	L cm.	Depth Cent. cm.	R cm.
10		38.82	
15		"	
20		"	
25		"	
27		"	
29.65	38.82	"	
30.3	13.60		14.46
44		15.0	

Run 228

Sta. ft.	L cm.	Depth Cent. cm.	R cm.
10		38.10	
15		"	
20		"	
25		"	
27		"	
28.9	38.10	"	
30.3	13.0		14.4
44		14.8	

Run 229

Sta. ft.	L cm.	Depth Cent. cm.	R cm.
10		29.30	
15		"	
20		"	
25		"	
27		"	
29.6	29.30	"	
30.3	14.0		15.16
44		15.3	

Run 230

Sta. ft.	L cm.	Depth Cent. cm.	R cm.
10		26.04	
15		"	
20		"	
25		"	
27		"	
28.5	26.04	"	
30.3	14.50		15.30
44		15.62	

Run 231

Sta. ft.	L cm.	Depth Cent. cm.	R cm.
10		22.14	
15		22.12	
20		22.10	
25		21.90	
27		21.80	
28.7	22.00	22.00	
30.3	15.60		15.16
44		15.8	

Run 232

Sta. ft.	L cm.	Depth Cent. cm.	R cm.
10		32.50	
15		"	
20		"	
25		"	
27		"	
28.4		"	20.45
28.75		"	
29.2	32.50		
30.3	21.00		
44		21.20	

Run 233

Sta. ft.	L cm.	Depth Cent. cm.	R cm.
10		23.73	
15		23.73	
20		23.72	
25		23.70	
27		23.70	
28.2		23.65	21.0
28.55		23.00	
29.0	23.60		
30.0	21.50		
44		21.20	

Run 234

Sta. ft.	L cm.	Depth Cent. cm.	R cm.
10		33.0	
15		"	
20		"	
25		"	
27		"	
27.4	33.0	"	
28.35		"	
29.0	20.10		33.10
30.3			20.80
44		21.0	

Run 235

Sta. ft.	L cm.	Depth Cent. cm.	R cm.
10		24.17	
15		24.15	
20		24.12	
25		24.11	
27	24.02	24.1	
28		23.40	
28.6			24.17
29	21.30		
30			21.50
44		21.7	

Run 236

Sta. ft.	L cm.	Depth Cent. cm.	R cm.
10		34.14	
15		"	
20		"	
25		"	
27		"	31.54
27.9		"	
28.0			21.0
29.0	31.54		
30.00	20.03		
44		21.3	

Run 237

Sta. ft.	L cm.	Depth Cent. cm.	R cm.
10		24.5	
15		24.45	
20		24.43	
25		24.4	
26.7		24.4	24.6
27			
27.65		23.93	
28.0			21.3
28.7	24.5		
30.0	21.3		
44		21.62	

Run 238

Sta. ft.	L cm.	Depth Cent. cm.	R cm.
10		44.5	
15		"	
20		"	
25		"	
27		"	
28.40			44.54
28.75		44.50	
29.20	44.50		27.2
30.0	27.6		
44		27.5	

Run 239

Sta. ft.	L cm.	Depth Cent. cm.	R cm.
10		33.0	
15		"	
20		"	
25		"	
27		"	
28.2			33.02
28.55		32.95	
29.0	32.95		
29.2			28.14
30.00	28.3		
44		28.45	

Run 240

Sta. ft.	L cm.	Depth Cent. cm.	R cm.
10		46.79	
15		"	
20		"	
25		"	
27		"	
27.1		46.75	46.75
27.9		46.70	
28.0			27.0
29.0	46.70		
30.1	26.96		
44		27.40	

Run 241

Sta. ft.	L cm.	Depth Cent. cm.	R cm.
10		33.40	
15		"	
20		"	
25		"	
26.8		"	33.6
27		"	
27.65		"	
28			28.4
28.8	33.40		
30	28.1		
44		28.5	

Run 242

Sta. ft.	L cm.	Depth Cent. cm.	R cm.
10		23.68	
15		23.65	
20		23.62	
25		23.60	
27		23.60	
28.40			23.65
28.75		23.50	
29.20	23.60		15.22
30.00	15.1		
44		15.35	

TABLE 8-2- RAW DATA - SUBMERGED TESTS

Run No.	243	244	245	246	247	248	249	250
Geometry	Vb	Vb	Vb	Vb	Vb	Vb	Vb	Vb
n	0.0238	0.0238	0.0238	0.0238	0.0238	0.0238	0.0238	0.0238
Q	2.0 cfs.	2.0 cfs.	3.0 cfs.	3.0 cfs.	3.0 cfs.	3.0 cfs.	2.0 cfs.	2.0 cfs.
Y_n	0.61 ft.	0.61 ft.	0.80 ft.	0.80 ft.	0.80 ft.	0.80 ft.	0.50 ft.	0.50 ft.
F_n	0.15	0.15	0.15	0.15	0.15	0.15	0.20	0.20
S	0.0003	0.0003	0.000285	0.000285	0.000285	0.000285	0.000 565	0.000565
M=b/B	0.20	0.20	0.20	0.30	0.20	0.30	0.20	0.20
L/b	0.50	0.50	0.50	0.50	0.50	0.50	0.50	0.50
Temp.	66° F	66° F	66° F	66° F	66° F	66° F	66° F	66° F
Model Sta.	30.0	30.00	30.0	30.00	30.00	30.00	30.00	30.00
Y_1	24.14 cm.	24.40 cm.	41.00 cm.	29.10 cm.	41.35 cm.	30.40 cm.	22.30 cm.	22.10 cm.
Y_2	14.3 cm.	14.95 cm.	21.0 cm.	21.10 cm.	21.60 cm.	21.0 cm.	11.4 cm.	11.3 cm.
N	1.0	1.0	1.0	1.0	1.0	1.0	1.0	1.0
$\phi 2$	22½°	30°	15°	15°	30°	30°	15°	22½°

Run 243

Sta. ft.	L cm.	Depth Cent. cm.	R cm.
10		24.30	
15		24.27	
20		24.25	
25		24.18	
27		24.20	
27.30	24.14		
28.30	14.30	24.14	
28.90			24.30
29.8			14.95
44		15.50	

Run 244

Sta. ft.	L cm.	Depth Cent. cm.	R cm.
10		24.46	
15		24.45	
20		24.44	
25		24.42	
27		24.43	
27.3			24.45
27.9		24.40	
28.0			14.50
29.0	24.45		
30.1	14.95		
44		15.50	

Run 245

Sta. ft.	L cm.	Depth Cent. cm.	R cm.
10		41.00	
15		"	
20		"	
25		"	
27		"	
28.4			41.05
28.75		41.00	
29.20	41.00		21.08
30.0	21.00		
44		21.6	

Run 246

Sta. ft.	L cm.	Depth Cent. cm.	R cm.
10		29.18	
15		29.16	
20		29.15	
25		29.10	
26.8			29.18
27.		29.12	
27.65		29.10	
28.0			20.88
28.8	29.15		
30.00			21.10
44		21.40	

Run 247

Sta. ft.	L cm.	Depth Cent. cm.	R cm.
10		31.35	
15		"	
20		"	
25		"	
27		"	
27.1			41.44
27.9		41.35	
28.0			19.70
29.0	41.35		
30.1	21.60		
44		20.8	

Run 248

Sta. ft.	L cm.	Depth Cent. cm.	R cm.
10		30.60	
15		30.55	
20		30.50	
25		30.38	
26.8			30.62
27		30.40	
27.65		30.40	
28			20.78
28.8	30.44		
30	21.0		
44		21.5	

Run 249

Sta. ft.	L cm.	Depth Cent. cm.	R cm.
10		22.48	
15		22.46	
20		22.43	
25		22.40	
27		22.38	
28.40			22.50
28.75		22.30	
29.20	22.40		11.85
30.0	11.4		
44		12.2	

Run 250

Sta. ft.	L cm.	Depth Cent. cm.	R cm
10		22.4	
15		22.36	
20		22.31	
25		22.28	
27		22.30	
27.4	22.3		
28.3		22.10	
28.5	11.3		
29.0			22.45
29.8			11.80
44		12.10	

Run No.	251	252	253	254	255	256	257	258
Geometry	Vb	Vb	Vb	Vb	Vb	VI	VI	VI
n	0.0238	0.0238	0.0238	0.0238	0.0238	0.0238	0.0238	0.0238
Q	2.0 cfs.	3.0 cfs.	3.0 cfs.	3.0 cfs.	3.0 cfs.	2.0 cfs.	2.0 cfs.	2.0 cfs.
Y_n	0.50 ft.	0.66 ft.	0.66 ft.	0.66 ft.	0.65 ft.	0.80 ft.	0.80 ft.	0.80 ft.
F_n	0.20	0.20	0.20	0.20	0.20	0.10	0.10	0.10
S	0.000565	0.000525	0.000525	0.000525	0.000525	0.000128	0.000128	0.000128
M=b/B	0.20	0.20	0.30	0.20	0.30	0.15	0.20	0.25
L/b	0.50	0.50	0.50	0.50	0.50	0.50	0.50	0.50
Temp.	66° F	66° F	66° F	66° F	66° F	68° F	68° F	68° F
Model Sta.	30.00	30.0	30.00	30.00	30.00	30.0	30.00	30.0
Y_1	22.50 cm.	37.85 cm.	26.80 cm.	39.50 cm.	27.81 cm.	32.61 cm.	24.20 cm.	22.80 cm.
Y_2	11.9 cm.	16.40 cm.	21.11 cm.	15.2 cm.	17.0 cm.	20.8 cm.	21.50	21.6 cm.
N	1.0	1.0	1.0	1.0	1.0	2.0	2.0	2.0
$\phi 2$	30°	15°	15°	30°	30°	0.0	0.0	0.0

Run 251

Sta. ft.	L cm.	Depth Cent. cm.	R cm.
10		22.69	
15		22.65	
20		22.61	
25		22.56	
27		22.60	
27.1			22.80
27.9		22.50	
28.0			11.45
29.0	22.70		
30.1	11.9		
44		12.40	

Run 252

Sta. ft.	L cm.	Depth Cent. cm.	R cm.
10		37.90	
15		"	
20		"	
25		"	
27		"	
28.4			38.0
28.75		37.85	
29.20	37.85		15.20
30.0	16.40		-
44		16.2	

Run 253

Sta. ft.	L cm.	Depth Cent. cm.	R cm.
10		26.90	
15		26.88	
20		26.85	
25		26.80	
26.8			26.91
27.0		26.83	
27.65		26.80	
28.0			20.90
28.8	26.84		
30.0	21.11		
44		21.3	

Run 254

Sta. ft.	L cm.	Depth Cent. cm.	R cm.
10		39.50	
15		"	
20		"	
25		"	
27		"	
27.1			39.61
27.9		39.50	
28.0			14.7
29.0	39.50		
30.1	15.2		
44		15.5	

Run 255

Sta. ft.		Depth Cent. cm.	
10		27.84	
15		"	
20		"	
25		"	
26.8			27.92
27.0		27.82	
27.65		27.81	
28.0			16.8
28.8	27.86		
30.0	17.00		
44		17.30	

Run 256

Sta. ft.	L cm.	Depth Cent. cm.	R cm.
10		32.61	
15		"	
20		"	
25		"	
27		"	
29.55	32.61	"	
30.3	20.8		20.8
44		21.7	

Run 257

Sta. ft.	L cm.	Depth Cent. cm.	R cm.
10		24.20	
15		"	
20		"	
25		"	
27		"	
29.4	24.20	"	
30.3	21.50		21.36
44		19.9	

Run 258

Sta. ft.	L cm.	Depth Cent. cm.	R cm.
10		22.80	
15		22.80	
20		22.80	
25		22.80	
27		22.80	
29.3	22.80	22.80	
30.3	21.60		21.8
44		22.0	

TABLE 8-2 RAW DATA - SUBMERGED TESTS

Run No.	259	260	261	262	263	264	265	266	267
Geometry	VI	VI	VI	VI	VI	VI	VI	VI	VI
n	0.0238	0.0238	0.0238	0.0238	0.0238	0.0238	0.0238	0.0238	0.0238
Q	2.5 cfs.	2.5 cfs.	2.5 cfs.	3.0 cfs.	3.0 cfs.	3.0 cfs.	2.0 cfs.	2.0 cfs.	2.0 cfs
Y_n	0.92 ft.	0.92 ft.	0.92 ft.	1.04 ft.	1.04 ft.	1.04 ft.	0.61 ft.	0.61 ft.	0.61 ft
F_n	0.10	0.10	0.10	0.10	0.10	0.10	0.15	0.15	0.15
S	0.000026	0.000026	0.000026	0.000125	0.000125	0.000125	0.0003	0.0003	0.0003
M=b/B	0.15	0.20	0.25	0.15	0.20	0.25	0.15	0.20	0.25
L/b	0.50	0.50	0.50	0.50	0.50	0.50	0.50	0.50	0.50
Temp.	70° F	70° F	70° F	68° F	68° F	70° F	68° F	68° F	68° F
Model Sta.	30.0	30.00	30.00	30.0	30.00	30.0	30.0	30.0	30.0
Y_1	39.40 cm.	30.75 cm.	27.60 cm.	48.46 cm.	36.72 cm.	32.40 cm.	27.83 cm.	19.22 cm.	-
Y_2	24.0 cm.	25.0 cm.	25.83 cm.	28.7 cm.	28.48 cm.	29.40 cm.	15.9 cm.	16.0 cm.	-
N	2.0	2.0	2.0	2.0	2.0	2.0	2.0	2.0	2.0
Ø2	0.0	0.0	0.0	0.0	0.0	0.0	0.0	0.0	0.0

Run 259

Sta. ft.	L cm.	Depth Cent. cm.	R cm.
10		39.40	
15		"	
20		"	
25		"	
27		"	
29.55	39.40	"	
30.3	24.00		23.96
44		26.6	

Run 260

Sta. ft.	L cm.	Depth Cent. cm.	R cm.
10		30.75	
15		"	
20		"	
25		"	
27		"	
29.4	30.75	"	
30.3	25.00		25.34
44		25.75	

Run 261

Sta. ft.	L cm.	Depth Cent. cm.	R cm.
10		27.60	
15		"	
20		"	
25		"	
27		"	
29.3	27.60	"	
30.3	25.83		25.73
44		26.30	

Run 262

Sta. ft.	L cm.	Depth Cent. cm.	R cm.
10		48.46	
15		"	
20		"	
25		"	
27		"	
29.55	48.46	"	
30.3	28.70		28.8
44		29.0	

Run 263

Sta. ft.	L cm.	Depth Cent. cm.	R cm.
10		36.72	
15		"	
20		"	
25		"	
27		"	
29.4	36.72	"	
30.3	28.48		28.58
44		29.7	

Run 264

Sta. ft.	L cm.	Depth Cent. cm.	R cm.
10		32.40	
15		"	
20		"	
25		"	
27		"	
29.3	32.40	"	
30.3	29.40		29.40
44		29.80	

Run 265

Sta. ft.	L cm.	Depth Cent. cm.	R cm.
10		27.83	
15		"	
20		"	
25		"	
27		"	
29.55	27.81	"	
30.3	15.90		15.40
44		16.4	

Run 266

Sta. ft.	L cm.	Depth Cent. cm.	R cm.
10		19.23	
15		19.24	
20		19.25	
25		19.24	
27		19.23	
29.4	19.23	19.22	
30.3	16.0		16.3
44		16.54	

Run 267

Sta. ft.	L cm.	Depth Cent cm	R cm

NOT SUBMERGED INLET

Run No.	268	269	270	271	272	273	274	275	276
Geometry	VI	VI	VI	VI	VI	VI	VI	VI	VI
n	0.0238	0.0238	0.0238	0.0238	0.0238	0.0238	0.0238	0.0238	0.0238
Q	2.5 cfs.	2.5 cfs.	2.5 cfs.	3.0 cfs.	3.0 cfs.	3.0 cfs.	2.0 cfs.	2.0 cfs.	2.0 cfs
Y_n	0.706 ft.	0.706 ft.	0.706 ft.	.80 ft.	0.80 ft.	0.80 ft.	0.50 ft.	0.50 ft.	0.50
F_n	0.15	0.15	0.15	0.15	0.15	0.15	0.20	0.20	0.20
S	0.000295	0.000295	0.000295	0.000285	0.000285	0.000285	0.000565	0.000565	0.000565
M=b/B	0.15	0.20	0.25	0.15	0.20	0.25	0.15	0.20	0.25
L/b	0.50	0.50	0.50	0.50	0.50	0.50	0.50	0.50	0.50
Temp.	70° F	70° F	70° F	70° F	70° F	70° F	68° F	68° F	68° F
Model Sta.	30.0	30.0	30.0	30.0	30.0	30.0	30.0	30.0	30.0
Y_1	34.50	23.75 cm.	21.50 cm.	42.27 cm.	29.50 cm.	25.14 cm.	24.40 cm.	16.60 cm.	-
Y_2	18.0	18.95 cm.	19.2 cm.	20.0 cm.	21.0 cm.	22.0 cm.	12.0 cm.	12.60 cm.	-
N	2.0	2.0	2.0	2.0	2.0	2.0	2.0	2.0	2.0
Ø2	0.0	0.0	0.0	0.0	0.0	0.0	0.0	0.0	0.0

Run 268

Sta. ft.	L cm.	Depth Cent. cm.	R cm.
10		34.50	
15		"	
20		"	
25		"	
27		"	
29.55	34.50	"	
30.3	18.0		17.5
44	19.2		

Run 269

Sta. ft	L cm.	Depth Cent. cm.	R cm.
10		23.75	
15		"	
20		"	
25		"	
27		"	
29.5	23.75	"	
30.3	18.95		18.7
44		20.0	

Run 270

Sta. ft.	L cm.	Depth Cent. cm.	R cm.
10		21.8	
15		21.7	
20		21.6	
25		21.5	
27		"	
29.3	21.50	"	
30.3	19.2	"	20.6
44		20.6	

Run 271

Sta. ft.	L. cm.	Depth Cent. cm.	R. cm.
10		42.27	
15		"	
20		"	
25		"	
27		"	
29.55	42.27	"	
30.3	20.0		20.0
44		22.6	

Run 272

Sta. ft.	L. cm.	Depth Cent. cm.	R. cm.
10		29.50	
15		"	
20		"	
25		"	
27		"	
29.4	29.50	"	
30.3	21.0		21.8
44		22.7	

Run 273

Sta. ft.	L cm.	Depth Cent. cm.	R cm.
10		25.14	
15		"	
20		"	
25		"	
27		"	
29.3	25.14	"	
30.3	22.0		22.30
44		22.9	

Run 274

Sta. ft.	L cm.	Depth Cent. cm.	R cm.
10		24.40	
15		"	
20		"	
25		24.39	
27		24.40	
29.55	24.40	"	
30.3	12.0		12.5
44		13.10	

Run 275

Sta. ft.	L cm.	Depth Cent. cm.	R cm.
10		16.39	
15		16.40	
20		16.44	
25		16.45	
27		16.50	
29.4	16.40	16.60	
30.3	12.60		13.20
44		13.52	

Run 276

Sta. ft.	L cm.	Depth Cent. cm.	R cm.

NOT SUBMERGED INLET

TABLE 8-2- RAW DATA - SUBMERGED TESTS

Run No.	277	278	279	280	281	282	285	286	287
Geometry	VI	VI	VI	VI	VI	VI	VII	VII	VII
n	0.0238	0.0238	0.0238	0.0238	0.0238	0.0238	0.0238	0.0238	0.0238
Q	2.5 cfs.	2.5 cfs.	2.5 cfs.	3.0 cfs.	3.0 cfs.	3.0 cfs.	2.0 cfs.	2.0 cfs.	2.0 cfs.
Y_n	0.585 ft.	0.585 ft.	0.585 ft.	0.66 ft.	0.66 ft.	0.66 ft.	0.33 ft.	0.37 ft.	0.46 ft
F_n	0.20	0.20	0.20	0.20	0.20	0.20	0.5	0.4	0.30
S	0.00053	0.00053	0.00053	0.000525	0.000525	0.000525	0.0006	0.0005	0.0003
M=b/B	0.15	0.20	0.25	0.15	0.20	0.25	0.35	0.35	0.35
L/b	0.50	0.50	0.50	0.50	0.50	0.50	0.0	0.0	0.0
Temp.	70° F	70° F	70° F	70° F	70° F	70° F	66° F	66° F	66° F
Model Sta.	30.0	30.0	30.0	30.0	30.0	30.0	30.0	30.0	30.0
Y_1	30.56 cm.	20.60 cm.	-	38.10 cm.	25.74 cm.	21.50 cm.	26.62 cm.	27.08 cm.	27.73 cm.
Y_2	15.6 cm.	15.30 cm.	-	16.70 cm.	17.4 cm.	18.0	7.52 cm.	8.17 cm.	10.80 cm.
N	2.0	2.0	2.0	2.0	2.0 cm.	2.0	1.0	1.0	1.0
ϕ_2	0.0	0.0	0.0	0.0	0.0 cm.	0.0	0.0	0.0	0.0
β							0.5	0.5	0.5

Run 277

Sta. ft.	L cm.	Depth Cent. cm.	R cm.
10		30.56	
15		"	
20		"	
25		"	
27		"	
29.55	30.56	"	
30.3	15.6		14.8
44		16.0	

Run 278

Sta. ft.	L cm.	Depth Cent. cm.	R cm.
10		20.60	
15		"	
20		"	
25		"	
27		"	
29.4	20.60	"	
30.3	15.30		15.83
44			

Run 279

Sta. ft.	L cm.	Depth Cent. cm.	R cm.
NOT SUBMERGED INLET			

Run 280

Sta. ft.	L cm.	Depth Cent. cm.	R cm.
10		38.10	
15		"	
20		"	
25		"	
27		"	
29.55	38.10	"	
30.3	16.70		15.08
44		18.10	

Run 281

Sta. ft.	L cm.	Depth Cent. cm.	R cm.
10		25.74	
15		"	
20		"	
25		"	
27		"	
29.6	25.74	"	
30.3	17.4		17.8
44		18.3	

Run 282

Sta. ft.	L cm.	Depth Cent. cm.	R cm.
10		21.0	
15		21.1	
20		21.3	
25		21.4	
27		21.5	
29.3	21.50	21.5	
30.3	18.0		18.41
44		19.0	

Run 285

Sta. ft.	L cm.	Depth Cent. cm.	R cm.
10		25.10	
15		25.16	
20		25.80	
25		26.35	
27.5		26.56	
29.9		26.62	
30.3	7.52		7.73

Run 286

Sta. ft.	L cm.	Depth Cent. cm.	R cm.
10		26.06	
15		26.16	
20		26.57	
25		26.89	
27.5		27.00	
29.9		27.08	
30.3	8.17		10.10

Run 287

Sta. ft.	L cm.	Depth Cent. cm.	R cm.
10		27.22	
15		27.34	
20		27.60	
25		27.72	
27.5		27.81	
29.9		27.73	
30.3	10.80		12.25

Run No.	288	289	290	291	292	293	294	295	296
Geometry	VII	VII	VII	VII	VII	VII	VII	VII	VII
n	0.0238	0.0238	0.0238	0.0238	0.0238	0.0238	0.0238	0.0238	0.0238
Q	2.0 cfs.	1.0 cfs.	2.75 cfs.	2.5 cfs.	2.0 cfs.	2.0 cfs.	2.0 cfs.	3.85 cfs.	3.85 cfs.
Y_n	0.59 ft.	0.50 ft.	0.34 ft.	0.37 ft.	0.39 ft.	0.50 ft.	0.80 ft.	0.41 ft.	0.49 ft.
F_n	0.20	0.10	0.5	0.4	0.3	0.20	0.1	0.50	0.4
S	0.000175	0.00025	0.0007	0.0005	0.00031	0.00019	0.00006	0.0007	0.00049
M=b/B	0.35	0.35	0.35	0.35	0.35	0.35	0.35	0.35	0.35
L/b	0.0	0.0	0.0	0.0	0.0	0.0	0.0	0.0	0.0
Temp.	66° F	66° F	64° F	66° F	66° F	66° F	66° F	66° F	66° F
Model Sta.	30.0	30.0	30.0	30.0	30.0	30.0	30.0	30.0	30.0
Y_1	29.81 cm.	21.56 cm.	30.67 cm.	28.03 cm.	22.70 cm.	25.67 cm.	34.84 cm.	32.71 cm.	33.43 cm.
Y_2	15.27 cm.	18.25 cm.	9.70 cm.	9.97 cm.	12.10 cm.	16.72 cm.	27.10 cm.	9.84 cm.	14.76 cm.
N	1.0	1.0	1.0	1.0	1.0	1.0	1.0	1.0	1.0
ϕ_2	0.0	0.0	0.0	0.0	0.0	0.0	0.0	0.0	0.0
β	0.5	0.5	0.3	0.3	0.3	0.3	0.3	0.0	0.0

Run 288

Sta. ft.	L cm.	Depth Cent. cm.	R cm.
10		27.78	
15		29.76	
20		29.91	
25		29.92	
27.5		29.98	
29.9		29.81	
30.3	15.27		16.27

Run 289

Sta. ft.	L cm.	Depth Cent. cm.	R cm.
10		21.77	
15		21.78	
20		21.78	
25		21.79	
27.5		21.80	
29.9		21.56	
30.3	18.25		18.54

Run 290

Sta. ft.	L cm.	Depth Cent. cm.	R cm.
10		29.10	
15		29.29	
20		29.83	
25		30.34	
27.5		30.60	
29.9		30.67	
30.3	9.70		

Run 291

Sta. ft.	L cm.	Depth Cent. cm.	R cm.
10		27.28	
15		27.34	
20		27.70	
25		28.01	
27.5		28.13	
29.9		28.03	
30.3	9.97		9.60

Run 292

Sta. ft.	L cm.	Depth Cent. cm.	R cm.
10		23.30	
15		23.42	
20		23.53	
25		23.67	
27.5		23.75	
29.9		22.70	
30.3	12.10		

Run 293

Sta. ft.	L cm	Depth Cent. cm.	R cm.
10		25.70	
15		25.92	
20		26.03	
25		26.03	
27.5		26.05	
29.9		25.67	
30.3	16.60		17.29

Run 294

Sta. ft.	L cm.	Depth Cent. cm.	R cm.
10		34.60	
15		34.86	
20		34.87	
25		34.90	
27.5		34.85	
29.9		34.84	
30.3	27.10		26.34

Run 295

Sta. ft.	L cm.	Depth Cent. cm.	R cm.
10		31.24	
15		31.69	
20		32.13	
25		32.60	
27.5		32.76	
29.9		32.71	
30.3	9.84		9.65

Run 296

Sta. ft.	L cm.	Depth Cent. cm.	R cm.
10		32.20	
15		32.81	
20		33.09	
25		33.41	
27.5		33.49	
29.9		33.43	
30.3	14.76		10.48

TABLE 8 - 2 - RAW DATA - SUBMERGED TESTS

Run No.	297	298	299	300	301	302	303	304	305	306	307
Geometry	VII	VII	VII	VII	VII	VII	VII	VII	VII	VII	VII
n	0.0238	0.0238	0.0238	0.0238	0.0238	0.0 238	0.0238	0.0238	0.0238	0.0238	0.0238
Q	3.85 cfs.	3.0 cfs.	2.5 cfs.	3.85 cfs.	3.85 cfs.	3.85 cfs.	3.0 cfs.	2.0 cfs.	3.85 cfs.	3.0 cfs.	3.85 cfs.
Y_n	0.60 ft.	0.67 ft.	0.92 ft.	0.42 ft.	0.49 ft.	0.60 ft.	0.67	0.80 ft.	0.78 ft.	1.04 ft.	1.45 ft.
F_n	0.3	0.2	0.10	0.5	0.40	0.30	0.20	0.1	0.2	0.1	0.10
S	0.00031	0.00018	0.000058	0.0007	0.00048	0.0003	0.00019	0.000062	0.00019	0.000052	0.000057
M=b/B	0.35	0.35	0.35	0.5	0.5	0.50	0.50	0.50	0.5	0.5	0.50
L/b	0.0	0.0	0.0	0.0	0.0	0.0	0.0	0.0	0.0	0.0	0.0
Temp.	68° F	66° F	66° F	66° F	66° F	66° F	66° F	66° F	68° F	68° F	68° F
Model Sta.	30.0	30.0	30.0	30.0	30.00	30.0	30.0	30.0	30.0	30.0	30.0
Y_1	34.70	30.33 cm.	35.79 cm.	28.97 cm.	29.81 cm.	31.48 cm.	29.02 cm.	29.95 cm.	31.43 cm.	38.85 cm.	43.19 cm.
Y_2	18.10	21.22 cm.	30.04 cm.	9.49 cm.	13.70 cm.	16.43 cm.	21.12 cm.	26.95 cm.	24.67 cm.	34.84 cm.	40.57 cm.
N	1.0	1.0	1.0	1.0	1.0	1.0	1.0	1.0	1.0	1.0	1.0
$\varnothing_2$	0.0	0.0	0.0	0.0	0.0	0.0	0.0	0.0	0.0	0.0	0.0
β	0.0	0.0	0.0	0.5	0.5	0.5	0.5	0.5	0.3	0.3	0.0

Run 297

Sta. ft.	L cm.	Depth Cent. cm.	R cm.
10		34.18	
15		34.60	
20		34.72	
25		34.75	
27.5		34.92	
29.9		34.70	
30.3	18.10		16.62

Run 298

Sta. ft.	L cm.	Depth Cent. cm.	R cm.
10		30.95	
15		31.15	
20		31.28	
25		31.26	
27.5		31.25	
29.9		30.33	
30.3	21.22		22.20

Run 299

Sta. ft.	L cm.	Depth Cent. cm.	R cm.
10		35.86	
15		35.97	
20		35.99	
25		35.98	
27.5		35.97	
29.9		35.79	
30.3	30.04		30.71

Run 300

Sta. ft.	L cm.	Depth Cent. cm.	R cm.
10		27.76	
15		27.82	
20		28.27	
25		28.59	
27.5		28.84	
29.9		28.97	
30.3	9.49		9.26

Run 301

Sta. ft.	L cm.	Depth Cent. cm.	R cm.
10		28.73	
15		28.95	
20		29.30	
25		29.54	
27.5		29.56	
29.9		29.81	
30.3	13.70		10.60

Run 302

Sta. ft.	L cm.	Depth Cent. cm.	R cm.
10		31.15	
15		31.25	
20		31.48	
25		31.65	
27.5		31.64	
29.9		31.48	
30.3	16.43		18.0

Run 303

Sta. ft.	L cm.	Depth Cent. cm.	R cm.
10		28.90	
15		29.099	
20		29.18	
25		29.34	
27.5		29.17	
29.9		29.02	
30.3	21.12		21.99

Run 304

Sta. ft.	L cm.	Depth Cent. cm.	R cm.
10		29.98	
15		30.02	
20		30.05	
25		30.05	
27.5		30.02	
29.9		29.95	
30.3	26.95		26.98

Run 305

Ste. ft.	L cm.	Depth Cent. cm.	R cm.
10		32.18	
15		32.22	
20		32.25	
25		32.26	
27.5		32.18	
29.9		31.43	
30.3	24.67		25.61

Run 306

Sta. ft.	L cm.	Depth Cent. cm.	R cm.
10		38.83	
15		38.98	
20		39.02	
25		39.02	
27.5		38.98	
29.9		38.85	
30.3	34.84		34.48

Run 307

Sta. ft.	L cm.	Depth Cent. cm.	R cm.
10		43.49	
15		43.47	
20		43.44	
25		43.42	
27.5		43.41	
29.9		43.19	
30.3	40.57		40.22

TABLE 8-3 - RAW DATA - SUBMERGED TESTS

Run No. - 70
Geometry - Ia
n - 0.0110
Q - 3.75 cfs.
S - 0.001
M=b/B - 0.35
L/b - 0.0
Temp. - 66° F
Model Sta. - 16.8
Y_1 - 28.70 cm.
Y_2 - 8.00 cm.
N - 1.0
ϕ_2 - 0.0

HORIZONTAL DISTANCE FROM CENTER LINE (ft.)

VELOCITY READINGS (fps.)

Depth from Bottom ft.	.74	0.7	0.6	0.5	0.4	0.3	0.2	0.1	0.0	0.1	0.2	0.3	0.4	0.5	0.6	0.7	.74
0.664								4.03	4.03	4.03							
0.564				(.35)	4.76	4.68	4.46	4.36	4.32	4.36	4.54	4.76	4.85 (.35)				
0.498			(.45)	5.30	5.17	4.88	4.60	4.45	4.40	4.42	4.54	4.80	5.15	5.27 (.45)			
0.367			6.02	5.42	5.07	4.80	4.62	4.54	4.49	4.55	4.70	4.88	5.16	5.55	5.42		
0.236		6.24	6.02	5.50	5.14	4.85	4.68	4.58	4.55	4.58	4.71	4.91	5.17	5.50	5.50	6.24	
0.1045		6.24	5.93	5.50	5.10	4.85	4.70	4.60	4.56	4.64	4.76	4.93	5.18	5.68	5.50	6.24	6.24
0.0062	6.24	6.24	5.90	5.42	5.15	4.85	4.68	4.60	4.55	4.60	4.72	4.85	5.10	5.35	5.85	6.24	6.24

CROSS SECTION READINGS

Distance from Centerline (ft.)	.74	.70	.60	.50	.40	.30	.20	.10	.00	.10	.20	.30	.40	.50	.60	.70	.74
Water Depth (ft.)	0.0	.352	.480	.562	.605	.630	.700	.727	.727	.727	.698	.629	.605	.561	.480	.353	0.00

Run No. - 71
Geometry - Ia
n - 0.0110
Q - 2.62 cfs.
S - 0.001
M=b/B - 0.30
L/b - 0.0
Temp. - 64° F
Model Sta. - 17.07
Y_1 - 25.45 cm.
Y_2 - 1.75 cm.
N - 1.0
ϕ_2 - 0.0

HORIZONTAL DISTANCE FROM CENTER LINE (ft.)

VELOCITY READINGS (fps.)

Depth from Bottom (ft.)	.70	.60	.50	.40	.30	.20	.10	0.0	0.10	0.20	0.30	0.40	0.50	0.60	0.70
.564								4.05							
.511						4.40	4.20	4.10	4.10	4.40					
.498				(.35) 4.95	4.75	4.50	4.30	4.20	4.20	4.40	4.60				
.367			(.45) 5.45	5.15	4.75	4.50	4.35	4.25	4.30	4.40	4.60	5.00	5.25 (.45)		
.236		(.55) 6.40	5.65	5.10	4.75	4.50	4.35	4.30	4.30	4.40	4.60	5.00	5.50	5.85	
.105		6.10	5.55	5.05	4.75	4.50	4.40	4.30	4.35	4.45	4.65	5.05	5.65	6.10	
.0062		6.10	5.55	5.15	4.75	4.55	4.40	4.35	4.40	4.50	4.60	5.00	5.30	5.90	6.10

CROSS SECTION READINGS

Distance from Centerline (ft.)	.68	.60	.55	.50	.45	.40	.35	.30	.20	0.10	0.0	.05	.15	.25	.35	.45	.55	.65	.70
Water Depth (ft.)	0.0	.239	.321	.381	.439	.484	.512	.535	.574	.621	.633	.633	.627	.574	.524	.453	.353	.190	.00

TABLE 8-3 - RAW DATA - SUBMERGED TESTS

Run No. - 72
Geometry - Ia
n - 0.0110
Q - 3.575 cfs.
S - 0.001
Hmb/B - .325
L/b - 0.0
Temp. - 64° F
Model Sta. - 17.1
Y_1 - 29.82 cm.
Y_2 - 1.69 cm.
N^2 - 1.0
2 - 0.0

HORIZONTAL DISTANCE FROM CENTERLINE (ft.)

Depth from Bottom (ft.)	.75	.70	.60	.50	.40	.30	.20	.10	0.0	.10	.20
	VELOCITY READINGS (fps.)										
.649								4.37	4.29		
.616							(.15) 4.61	4.61	4.45		
.564						5.03	4.73	4.61	4.53	4.61	4.80
.498				(.45) 5.63	5.42	5.13	4.82	4.65	4.61	4.69	4.82
.367			(.55) 6.16	5.75	5.39	5.13	4.91	4.80	4.76	4.80	4.91
.236		(.65) 6.17	6.17	5.79	5.49	5.17	4.92	4.84	4.77	4.82	4.91
.1045		6.19	6.17	6.85	5.45	5.13	4.97	4.87	4.84	4.87	
.0062	(.75) 6.21	6.21	6.21	5.75	5.42	5.20	5.03	4.91	4.87	4.91	4.99

CROSS SECTION READINGS

Distance from Centerline (ft.)	.74	.70	.65	.55	.45	.35	.25	.15	.05	0.0
Depth (ft.)	.089	.213	.325	.460	.544	.597	.641	.681	.708	.713

Run No. - 73
Geometry - Ia
n - 0.0110
Q - 3.75 cfs.
S - 0.001
Hmb/B - 0.30
L/b - 0.0
Temp. - 66° F
Model Sta. - 17.0
Y_1 - 37.3 cm.
Y_2 - 0.0 cm.
N^2 - 1.0
2 - 0.0

HORIZONTAL DISTANCE FROM CENTERLINE (ft.)

Depth From Bottom (ft)	.80	.75	.70	.65	.60	.55	.50	.45	.40	.35	.30	.25	.20	.15	.10	.05	0.0	.025	.075	.125	.175	.225	.275	.325	.375	.425	.475	.525	.575	.625	.675	725
	VELOCITY READINGS (fps.)																															
.458														4.79	4.70	4.68	4.7		4.72	4.72		4.99										
.416											4.98	4.90	4.80	4.80	4.72	4.72	4.74		4.72	4.79	4.80	4.97	4.96	5.10								
.375									5.29	5.17			4.87		4.70		4.74			4.82	4.85	4.98		5.17	5.25	5.37	5.60					
.333							5.65		5.29	5.16	5.04	4.90	4.87	4.82	4.72	4.77	4.75		4.74	4.82	4.87	5.02	4.98	4.96	5.26	5.43	5.59	5.79				
.291							5.62								4.74		4.77			4.82	4.89	4.91				5.42		5.85	6.03			
.250					6.18		5.65		5.29	5.17	5.05	4.91	4.85	4.82	4.77	4.77	4.77		4.74	4.87	4.90	4.88	5.02	5.14	5.25	5.42	5.59	5.85	6.08	6.33		
.208			6.64		6.19										4.77		4.77			4.85	4.90	4.94				5.42		5.80		6.33		
.167			6.73		6.18		5.68		5.29	5.19	5.04	4.91	4.87	4.82	4.79	4.79	4.78		4.72	4.87	4.88	4.91	4.99	5.14	5.24	5.42	5.57	5.85	6.06	6.33	6.62	
.125			6.72		6.10						5.05				4.79		4.78			4.87	4.90	4.91				5.44		5.80		6.32	6.58	
.0833			6.68		6.03		5.70		5.25	5.19	4.98	4.91	4.87	4.82	4.79	4.77	4.79		4.77	4.89	4.90	4.90	4.99	5.14	5.19	5.35	5.54	5.78	5.97	6.25	6.58	6.82
.0417			6.59	6.36	6.05		5.54		5.31	5.24	5.02	4.96	4.87	4.80	4.79	4.79	4.78		4.77	4.90	4.83	4.90				5.28	5.40	5.58	5.82	6.03	6.43	6.81
.010			6.48		6.05		5.42		5.11		4.99	4.96	4.87	4.80	4.77	4.74	4.77		4.79	4.85	4.85	4.88	4.99	5.10	5.18	5.25	5.29	5.47	5.68	6.12	6.27	6.70

CROSS SECTION READINGS

Distance From Centerline (ft)	.80	.75	.70	.65	.60	.55	.50	.45	.40	.35	.30	.25	.20	.15	.10	.05	0.0	.025	.075	.125	.175	.225	.275	.325	.375	.425	.475	.525	.575	.625	.675	725	.775
Water Depth (ft)	0.0	.142	.250	.344	.406	4.60	.506	.536	.566	.598	.616	.645	.674	.695	.712	.736	.737	.736	.730	.700	.683	.604	.638	.604	.584	.549	.516	.465	.418	.350	.271	.167	0.0

TABLE 8-4 CALCULATED VALUES - RUN NO. 2 - 140

Run No.	A_r	Q_t	C_c	C_d	C_v	$\frac{b}{Y_1}$	Y_n	F_n
2	.635	8.317	.718	.570	.842	.901	.435	.587
3	.632	7.291	.715	.554	.812	1.120	.393	.583
4	.628	6.737	.710	.552	.798	1.257	.372	.580
5	.617	6.585	.698	.544	.785	1.293	.364	.579
6	.624	6.229	.705	.542	.775	1.400	.352	.578
7	.614	5.897	.694	.540	.771	1.500	.338	.576
8	.629	5.493	.711	.526	.752	1.640	.318	.573
9	.654	5.198	.740	.520	.744	1.759	.305	.570
10	.641	4.917	.726	.515	.736	1.870	.293	.569
11	.594	8.265	.671	.570	.842	.919	.433	.587
12	.604	7.315	.682	.550	.806	1.110	.392	.583
13	.614	6.687	.694	.556	.800	1.267	.374	.580
14	.622	6.163	.704	.540	.771	1.418	.348	.577
15	.623	5.450	.705	.529	.756	1.657	.317	.572
16	.515	7.232	.711	.256	.385	.800	.401	.584
17	.488	6.475	.674	.370	.518	.956	.372	.580
18	.490	6.371	.676	.394	.546	.980	.367	.580
19	.491	6.148	.677	.440	.613	1.025	.357	.578
20	.500	5.563	.690	.623	.902	1.208	.332	.575
21	.505	5.291	.697	.747	1.040	1.297	.321	.573
22	.506	5.000	.700	.917	1.274	1.400	.307	.571
23	.510	4.950	.705	.960	1.371	1.420	.306	.571
24	.522	4.668	.721	1.240	1.671	1.530	.291	.568
25	.524	4.488	.723	1.386	1.915	1.610	.282	.567
26	.525	4.133	.725	1.949	2.780	1.780	.267	.560
27	.511	4.626	.706	1.257	1.793	1.550	.293	.569
28	.508	4.920	.701	1.060	1.435	1.430	.309	.571
29	.501	5.252	.692	.784	1.162	1.310	.323	.573
30	.496	5.701	.685	.578	0.843	1.165	.341	.576
31	.488	6.283	.674	.408	0.605	1.010	.363	.579
32	.411	6.240	.670	.591	.883	.690	.371	.580
33	.410	5.939	.669	.589	.879	.750	.358	.578
34	.417	5.729	.679	.595	.889	.797	.353	.578
35	.425	5.308	.693	.584	.872	.900	.332	.575
36	.413	5.145	.672	.588	.878	.945	.327	.574
37	.421	4.968	.685	.587	.876	1.000	.320	.573
38	.422	4.716	.686	.590	.872	1.082	.310	.571
39	.427	4.445	.695	.567	.845	1.182	.291	.568
40	.429	4.221	.699	.565	.816	1.273	.282	.566
41	.435	3.899	.709	.560	.804	1.420	.266	.563
42	.434	3.653	.707	.555	.794	1.549	.255	.561
43	.433	3.511	.705	.549	.784	1.628	.246	.558
44	.432	3.188	.704	.546	.768	1.825	.232	.555
45	.412	6.256	.670	.591	.883	.686	.371	.580
46	.414	4.842	.674	.585	.858	1.040	.314	.572
47	.415	4.374	.676	.575	.839	1.210	.291	.568
48	.430	3.741	.700	.565	.807	1.500	.261	.562
49	.434	3.273	.706	.556	.795	1.773	.230	.586
51	.261	4.256	.664	.600	.896	.518	.294	.569
52	.262	4.097	.665	.598	.893	.545	.286	.567
53	.262	3.868	.666	.592	.884	.601	.275	.565
54	.263	3.700	.667	.587	.875	.650	.266	.563
55	.263	3.560	.667	.595	.889	.695	.262	.562
56	.267	3.388	.678	.583	.870	.755	.251	.559
57	.263	3.286	.668	.587	.875	.792	.247	.558
58	.263	3.088	.668	.583	.869	.879	.236	.556
59.	.263	2.964	.668	.590	.881	.937	.232	.555
60	.263	2.792	.668	.580	.866	1.030	.221	.551
61	.264	2.706	.670	.580	.861	1.080	.212	.550
62	.273	2.654	.693	.578	.843	1.112	.214	.550
63	.276	2.502	.702	.580	.841	1.215	.207	.548
64	.252	2.282	.639	.575	.826	1.380	.194	.544
65	.275	2.204	.698	.575	.821	1.448	.228	.554
66	.277	2.093	.705	.574	.820	1.548	.184	.540
67	.277	1.929	.705	.560	.801	1.710	.172	.536

Run No.	K	M'	$\frac{h_1^*}{Y_n}$	$(\frac{F_n}{M'})^2$	$\frac{Q}{g^{1/2}b^{5/2}}$	$\frac{Y_1}{b}$	$\frac{Y_1}{b/2}$	$\frac{Y_n}{b/2}$	Q_t	C_d
102	2.132	.141	.637	.594	.253	1.145	2.290	1.395	5.404	.462
103	1.886	.171	.385	.405	.199	.878	1.762	1.272	5.789	.431
104	1.955	.203	.282	.286	.160	.745	1.480	1.166	6.417	.389
105	2.232	.104	1.191	1.062	.353	1.670	3.330	1.521	3.874	.516
106	2.210	.162	.485	.436	.202	.905	1.820	1.219	4.647	.430
107	2.230	.196	.335	.297	.159	.737	1.479	1.109	5.124	.390
108	1.960	.234	.208	.210	.128	.612	1.227	1.030	5.522	.362
109	2.201	.141	.657	.593	.202	1.160	2.308	1.400	5.447	.458
110	3.004	.171	.612	.405	.159	1.020	2.050	1.274	6.397	.390
111	2.146	.203	.310	.286	.128	.764	1.527	1.168	6.517	.383
112	2.020	.120	1.957	1.923	.441	1.940	3.882	1.321	4.226	.591
113	2.095	.188	.838	.789	.253	.966	1.934	1.067	4.854	.515
114	1.862	.227	.510	.538	.199	.720	1.443	.969	5.038	.496
115	1.907	.271	.370	.380	.160	.600	1.201	.888	5.428	.461
116	2.188	.159	1.062	.961	.303	1.280	2.562	1.242	5.795	.517
117	2.283	.192	.758	.655	.238	.992	1.989	1.131	6.272	.478
118	2.190	.229	.515	.463	.192	.785	1.771	1.037	6.649	.451
119	2.066	.174	.844	.807	.278	1.150	2.300	1.250	6.889	.508
120	2.807	.207	.594	.418	.224	.912	1.825	1.146	7.375	.474
121	2.045	.120	1.981	1.923	.441	1.960	3.920	1.321	4.246	.588
122	2.171	.188	.869	.789	.253	.982	1.965	1.067	4.906	.509
123	2.239	.227	.613	.538	.199	.769	1.542	.969	5.282	.473
124	2.040	.271	.396	.380	.160	.610	1.222	.888	5.510	.453
125		.156			.441	1.930	3.860	1.080	4.214	.593
126		.228			.253	.960	1.925	.864	4.840	.516
127		.277			.199	.734	1.471	.786	5.106	.489
128		.329			.160	.573	1.148	.720	5.225	.478
129	2.121	.194	1.263	1.171	.303	1.156	2.301	1.020	5.434	.551
130	2.178	.234	.889	.799	.238	.874	1.755	.928	5.771	.519
131	2.097	.279	.607	.564	.192	.684	1.367	.849	6.010	.499
132	2.040	.173	1.479	1.429	.354	1.410	2.820	1.138	6.136	.570
133	2.141	.210	1.063	.974	.278	1.065	2.135	1.035	6.565	.533
134	2.065	.250	.727	.688	.224	.820	1.639	.949	6.852	.510
171	1.886	.140	1.100	1.154	.354	1.480				
180	2.211	.356	1.494	1.277	256	.830				
191	2.204	.170	1.565	1.401	.354	1.490				
135	1.878	.100	.953	1.011	.353	1.560				
136	1.617	.100	.821	1.011	.353	1.455				
137	1.555	.100	.790	1.011	.353	1.430				
138	1.347	.100	.684	1.011	.353	1.348				
139	2.606	.154	.544	.415	.202	.988				
140	1.865	.154	.390	.415	.202	.890				

TABLE 8-5- CALCULATED VALUES - RUN NO. 141 - 306

Run No.	K	M'	$\frac{h_1^*}{Y_n}$	$(\frac{F_n}{M'})^2$	$g^{1/2} b^{5/2}$	$\frac{Y_1}{b}$
141	1.527	.154	.390	.415	.202	.843
142	1.466	.154	.306	.415	.202	.835
143	1.431	.223	.144	.200	.128	.610
144	1.333	.223	.134	.200	.128	.606
145	1.227	.223	.123	.200	.128	.600
146	.893	.223	.090	.200	.128	.588
147	2.430	.134	.688	.563	.253	1.100
148	1.577	.134	.447	.563	.253	1.065
149	1.503	.134	.427	.563	.253	1.050
150	1.403	.134	.398	.563	.253	1.030
151	1.891	.113	1.719	1.804	.441	1.900
152	1.788	.113	1.625	1.804	.441	1.839
153	1.684	.113	1.531	1.804	.441	1.771
154	1.602	.113	1.457	1.804	.441	1.718
155	1.941	.176	.728	.740	.253	.968
156	1.672	.176	.627	.740	.253	.910
157	1.523	.176	.572	.740	.253	.880
158	1.283	.176	.483	.740	.253	.823
159	1.440	.254	.262	.356	.160	.589
160	1.000	.254	.182	.356	.160	.553
161	.922	.254	.168	.356	.160	.545
162	.746	.254	.136	.356	.160	.531
163	1.807	.154	.852	.933	.303	1.187
164	1.488	.154	.703	.933	.303	1.091
165	1.474	.154	.696	.933	.303	1.086
166	1.109	.154	.525	.933	.303	.980
167	1.487	.223	.340	.449	.192	.711
168	1.375	.223	.314	.449	.192	.702
169	1.164	.223	.256	.449	.192	.680
170	.959	.223	.220	.449	.192	.650
171	1.886	.140	1.100	1.154	.354	1.480
172	1.706	.140	.995	1.154	.354	1.400
173	1.500	.140	.875	1.154	.354	1.320
174	1.442	.140	.842	1.154	.354	1.300
175	1.104	.140	.646	1.154	.354	1.160
176	1.499	.202	.424	.556	.224	.835
177	1.455	.202	.411	.556	.224	.828
178	1.256	.202	.355	.556	.224	.795
179	1.077	.202	.305	.556	.224	.765
180	2.211	.356	1.494	1.277	.256	.830
181	1.247	.184	.420	.662	.256	.912
182	.919	.284	.310	.662	.256	.840
183	1.993	.135	2.173	2.160	.441	1.856
184	2.197	.211	.991	.886	.253	.930
185	2.009	.211	.907	.886	.253	.292
186	1.681	.304	.370	.427	.160	.578
187	1.375	.223	.314	.450	.160	.557
188	1.555	.100	.790	1.011	.160	.550
189	1.728	.304	.380	.427	.160	.538
190	1.899	.187	1.092	1.131	.303	1.104
191	2.204	.170	1.565	1.401	.354	1.490
192	1.805	.170	1.284	1.401	.354	1.324
193	2.202	.100	1.117	1.011	.354	1.590
194	2.618	.154	.546	.415	.204	.990
195	2.749	.187	.392	.283	.159	.807
196	2.500	.223	.252	.200	.128	.669
197	1.500	.112	1.352	1.789	.441	1.650
198	1.949	.175	.724	.735	.253	.974
199	2.082	.212	.529	.501	.199	.784
200	1.650	.252	.297	.353	.160	.610
201	1.599	.158	1.312	1.617	.353	1.155
202	1.370	.135	1.499	2.159	.441	1.463
203	1.515	.211	.686	.886	.253	.3[illegible]5
204	1.603	.256	.497	.604	.199	.635
205	1.448	.140	.846	1.154	.354	1.300
206	1.646	.100	.836	1.011	.353	1.470
207	1.398	.100	.710	1.011	.353	1.370
208	2.589	.154	.540	.415	.202	.980
209	1.471	.154	.307	.415	.202	.837
210	1.199	.223	.121	.200	.128	.597
211	1.398	.158	1.150	1.617	.441	1.465
212	1.199	.223	.121	.200	.441	1.330
213	.960	.112	.868	1.789	.441	1.320
214	1.939	.175	.720	.734	.253	.970
215	1.336	.175	.498	.734	.253	.845
216	1.119	.175	.417	.734	.253	.801
218	1.419	.211	.643	.886	.354	1.250
219	.941	.140	.551	1.154	.354	1.095
220	.723	.140	.424	1.154	.354	1.003
221	1.674	.252	.302	.353	.160	.613

Run No.	K	M'	$\frac{h_1^*}{Y_n}$	$(\frac{F_n}{M'})^2$	$g^{1/2} b^{5/2}$	$\frac{Y_1}{b}$
222	1.580	.252	.285	.353	.253	.605
223	1.085	.252	.196	.353	.160	.562
224	1.398	.158	1.149	1.617	.353	1.075
225	1.240	.158	1.021	1.617	.353	1.010
226	1.079	.158	.890	1.617	.353	.943
227	1.073	.135	1.177	2.159	.441	1.270
228	1.036	.135	1.137	2.159	.441	1.250
229	1.419	.211	.643	.886	.253	.770
230	1.011	.211	.460	.886	.253	.684
231	1.059	.304	.234	.427	.160	.480
232	.654	.100	.333	1.011	.353	1.067
233	.251	.223	.025	.200	.128	.504
234	.694	.100	.353	1.011	.353	1.082
235	.169	.223	.017	.200	.128	.512
236	.786	.100	.400	1.011	.353	1.120
237	.222	.223	.022	.200	.128	.524
238	.458	.076	.404	1.749	.529	1.460
239	.226	.171	.040	.345	.192	.721
240	.537	.076	.473	1.749	.529	1.530
241	.307	.171	.054	.345	.192	.730
242	.391	.130	.264	1.325	.353	.770
243	.442	.130	.298	1.325	.353	.790
244	.463	.130	.312	1.325	.353	.800
245	.592	.100	.682	2.274	.529	1.344
246	1.024	.223	.234	.449	.192	.635
247	.504	.100	.696	2.274	.529	1.354
248	1.258	.223	.288	.449	.192	.665
249	.557	.158	.403	1.617	.353	.731
250	.541	.158	.450	1.617	.353	.723
251	.573	.158	.476	1.617	.353-	.738
252	.627	.120	.882	2.756	.529	1.242
253	1.362	.270	.382	.544	.192	.587
254	.6[illegible]7	.120	.964	2.756	.529	1.295
255	1.543	.270	.432	.544	.192	.609
256	.211	.056	.337	3.179	.710	1.430
257	.194	.100	.099	1.011	.353	.794
258	.082	.154	.017	.415	.202	.598
259	.186	.048	.405	4.320	.885	1.735
260	.139	.086	.397	1.373	.441	.993
261	.[illegible]	.134	.020	.563	.253	.724
262	.191	.043	.529	5.502	1.062	2.120
263	.179	.076	.158	1.749	.529	1.204
264	.061	.118	.022	.718	.303	.850
265	.235	.073	.497	4.170	.710	1.220
266	.050	.130	.034	1.325	.353	.627
267	.211	.063	.063	5.630	.885	1.510
268	.113	.112	.104	1.789	.441	.778
269	.045	.168	.016	.704	.253	.565
270	.203	.056	.734	7.153	1.062	1.806
271	.181	.099	.2 10	2.274	.529	.966
272	.065	.154	.031	.933	.303	.660
273	.231	.089	.601	5.097	.710	1.070
274	.106	.158	.089	1.617	.353	.544
275	.206	.076	.714	6.793	.885	1.340
276	.138	.135	.155	2.159	.441	.675
277	.202	.068	.894	8.071	1.062	1.668
278	.196	.120	.280	2.755	.529	.843
279	.116	.187	.069	1.131	.303	.565
285	1.855	.288	1.647	1.697	.045	.500
286	1.786	.257	1.401	1.513	.045	.508
287	1.568	.207	.978	1.217	.045	.520
288	1.366	.161	.658	.949	.045	.559
289	2.941	.190	.415	.280	.018	.404
290	3.045	.450	1.960	1.202	.120	.575
291	3.082	.413	1.486	.913	.109	.526
292	3.148	.392	.910	.554	.087	.425
293	3.093	.305	.684	.432	.087	.482
294	3.151	.191	.429	.270	.087	.654
300	1.919	.461	1.263	1.189	.069	.380
301	1.814	.395	.996	1.019	.069	.392
302	1.650	.323	.721	.832	.069	.413
303	1.810	.289	.421	.453	.054	.381
304	2.586	.242	.428	.168	.036	.392
305	2.523	.400	.322	.247	.168	.413
306	3.972	.300	.225	.113	.131	.510